Control of Constrained Nonlinear Systems: Applications in Aerospace and Robotics

Khoi Ba Ngo

A thesis submitted for the degree of

Doctor of Philosophy

of

THE AUSTRALIAN NATIONAL UNIVERSITY

April, 2007

Declaration

This thesis is an account of research undertaken at the Department of Engineering, Faculty of Engineering and Information Technology, Australian National University, Canberra, Australia, and is based upon work performed jointly with Dr. Robert Mahony and Prof. Zhong-Ping Jiang. The majority, approximately 85 percent, of the work is my own.

Except where acknowledged in the customary manner, the material presented in this thesis is, to the best of my knowledge, original and has not been published or submitted in whole or in part for a degree at any university or institute of higher learning.

Khoi Ba Ngo
April, 2007

Abstract

Saturation nonlinearities are ubiquitous to all physical systems. The two most common forms of saturation nonlinearities encountered in control engineering are actuator saturations and state constraints. Whilst the problem of actuator saturations has been extensively studied, there has been much less effort expended to study the problem of state constraints, particularly within the framework of constructive nonlinear control. This is despite the fact that state constraints are a major concern in many practical engineering systems.

The principal objective of this thesis is to develop constructive nonlinear control design procedures to address the stabilisation problem for nonlinear systems subject to state constraints. The general approach adopted, and indeed the central theme of this thesis, is to directly incorporate the constraints into the control design process by modifying the energy function of the system to include barrier function characteristics at the constraint boundaries. The design tools employed are backstepping and passivity-based control.

The thesis comprises of two parts. In Part I, the stabilisation problem for certain classes of non-affine, nonlinear systems subject to state constraints is considered. Two modified backstepping approaches are developed, providing trade-offs between complexity and applicability. The new controller designs are validated via application to flight control. Simulations on a fully nonlinear, 6-degree-of-freedom dynamic model of an aerial robotic drone demonstrate that the proposed controller designs produce excellent closed-loop performance, whilst strictly satisfying the imposed state constraints.

Part II of the thesis is dedicated to the control of constrained robot manipulators. Two controller designs are proposed, both utilizing ideas from the passivity-based control and artificial potential field literature to address the stabilisation problem for constrained robot manipulators. The first controller design considers the general problem of autonomous, or online, obstacle avoidance for robot manipulators subject to joint position and joint rate constraints. For arbitrary constraints, closed-loop asymptotic stability can not be guaranteed. However, in specific cases where the constraints possess certain convexity properties, then asymptotic stability of the closed-loop system is assured. The second controller design extends the literature in a different direction, and is geared towards solving the asymptotic stabilisation problem for robot manipulators subject to joint velocity and input torque limits. The resulting controllers are modified Proportional-Derivative controllers, which are simple, intuitive, and can easily be implemented in practice. The validity and effectiveness of the proposed controller designs are illustrated via closed-loop simulations on a 2-link planar manipulator.

Acknowledgments

First and foremost, I would like to express my gratitude to my supervisor, Dr. Robert Mahony. His unique perspective on control theory and rigorous mathematical approach have forever changed my perception of the fundamentals of control theory. I can never thank him enough for encouraging and allowing me great freedom in pursuing the research areas of my interest. Without his guidance, patience, and support, this thesis would not have come to fruition.

I would like to acknowledge the financial support from Aerosonde Pty Ltd. Special thanks to all the wonderful people at Aerosonde, particularly Gavin Brett, Andrew Glenk, Kate Wright, Brad Phillips, and Peter Kernebone, for making my visits to Aerosonde memorable experiences. I learned a great deal about UAVs and their operations there.

Many thanks go to Marius Niculescu for generously making his AeroSim blocket for Matlab/Simulink freely available for academic uses. His insider knowledge of the Aerosonde's autopilots had also been a great help.

I am indebted to Prof. Zhong-Ping Jiang and Prof. Laurent Praly for their contributions, direct and indirect, to this thesis. Moreover, their expert views, comments, and remarks on constructive nonlinear control theory have immensely enhanced my understanding of the subject.

I would like to thank Prof. John Baird, Prof. Matt James, and Andrew Glenk from Aerosonde for serving on my supervisory panel.

I consider myself to be tremendously fortunate to have met many wonderful friends during my years at the ANU, especially Dung, Van, Kien, Helmüt and Cynthia, Thao, Thanh, Nga, Thuy, Long, Hien, and Ha. Their friendships were the only few things that kept me "sane".

Lastly, I am extremely grateful to my parents and everyone in the extended clan for doing everything they could to help me complete this thesis. Their encouragement and unwavering support had always been a source of inspiration and motivation for me during the most stressful of times.

List of Abbreviations

AGL	Above ground level
cLf	control Lyapunov function
CPBC	Constrained passivity-based control
DGAS	Domain globally asymptotically stable
DOF	Degree of freedom
ISS	Input-to-state stability
LQ	Linear Quadratic
MPC	Model predictive control
ODE	Ordinary differential equation
PBC	Passivity-based control
PD	Proportional-Derivative
PLC	Piecewise-linear control
RWP	Reaction Wheel Pendulum
UAV	Uninhabited Aerial Vehicle

Contents

List of Figures

Chapter 1

Introduction

This introductory chapter aims to acquaint the readers with the background literature and the practical control problem that motivated our research. The chapter starts with a brief historical account of constructive nonlinear control and an overview of existing control design methods for constrained systems. This is followed by an outline of the research directions undertaken. A description of the flight control problem that provided the impetus behind our work along with a general review of traditional aircraft control design techniques are next presented. A brief literature review on passivity-based control of Euler-Lagrange systems is then given. The chapter ends with an outline of the thesis's structure and main contributions to the body of knowledge.

1.1 Constructive nonlinear control

Although linear control theory has a long and rich history of successful industrial applications, it is deemed to be inadequate for many practical engineering systems. The reasons are increasingly stringent performance requirements and vastly expanded operating envelopes, mainly due to safety considerations and technological advances. Inherent nonlinear phenomena such as finite escape time, multiple isolated equilibria, limit cycles, multiple modes of behaviour and other complex dynamic behaviours cannot be described nor predicted by linear models. In addition, many physical systems have hard-nonlinearities such as Coulomb friction, saturations, dead zones, backlash, and hysteresis [68]. These nonlinearities are non-smooth or discontinuous, thus precluding linear approximations. Furthermore, nonlinear systems do not follow the *superposition principle*, which states that the output response of a linear system to a combination of input signals is the sum of its responses to each individual input. The total effect of measurement noise, external disturbances, and reference inputs therefore cannot be simply determined by analysing the effect of each input signal separately. Other challenges include the facts that *internal* and *input-output stability* are generally not equivalent, and the *separation principle* does not hold for nonlinear systems. All of the above factors have made nonlinear control a both theoretically and practically challenging topic. As a result, considerable research efforts have been expended on studying nonlinear systems and tremendous progress has been made over the past twenty five years.

In the early 1980s, Jurdjevic, Isidori, Krener, Sussmann and many other pioneers

introduced differential geometric methods to express and extend notions from linear control theory such as *controllability* and *observability*. Differential geometric concepts, especially nonlinear *relative degree* and *zero dynamics*, have since become invaluable tools in the analysis of input-output structural properties of nonlinear systems. Following from the early seminal work is a number of nonlinear control design techniques generally grouped under the label of *feedback linearization*. (For a comprehensive treatment on the subject, see such texts as [52], [89], [106], and [127]). The central idea of these techniques is to algebraically transform nonlinear system dynamics into a fully, or partly, linear one. Linear theory is then applied to design the controller. The major drawback of feedback linearization methods is that useful nonlinearities, for example, inherently stabilising terms such as $-x^3$, are canceled indiscriminately and replaced by their dangerously destabilising positive counterparts. Another weakness of feedback linearization is that in the presence of modeling errors, the concepts of relative degree and zero dynamics may be non-robust. Sastry *et al.* [120] showed that regular perturbations in a system may lead to singularly perturbed unstable zero dynamics.

It was in the 1990's that nonlinear control theory really came of age with two exciting breakthroughs. The emergence of new analysis tools such as *input-to-state stability* (ISS), nonlinear *small-gain* theorems, and the idea of rendering a system *passive* by feedback have led to recursive design procedures, namely *backstepping* and *forwarding*. It is uncertain whether the idea of backstepping appeared in earlier literature but its use as a design tool was initiated in the early nineties [19, 71, 147, 148]. However, the true potential of backstepping was only discovered when this approach was developed for nonlinear systems with structured uncertainty. With *adaptive backstepping*, Kanellakopoulos *et al.* [59] achieved global stabilisation in the presence of unknown parameters, and with *robust backstepping*, Freeman and Kokotovic in [36, 37], and Marino and Tomei in [88], achieved global stabilisation in the presence of disturbances.

The ease with which backstepping incorporates uncertainties and unknown parameters contributed to its instant popularity and rapid acceptance. At the same time, its limitation to a class of pure feedback (lower-triangular) systems stimulated the development of *forwarding*, which is applicable to feedforward systems, by Teel [142, 143], Mazenc and Praly [93], and Jankovic, Sepulchre, and Kokotovic [53]. Interlacing the steps of these procedures further expanded the classes of systems these two recursive design techniques are applicable to [123].

1.2 Control of constrained systems

All physical systems are subject to constraints. In the mathematical model of a system, a constraint is expressed as a limit or bound on a system signal. Constraints can be *soft* or *hard*. A *soft* constraint is one that may be violated at certain times and for certain periods of time, whereas a *hard* constraint must be satisfied at all time. Only hard constraints are considered in this thesis. There are essentially three classes of signals within a system model: control input, state, and output. Constraints on control input signals are the most

commonly encountered constraints, and stem from magnitude and slew rate limits of all actuators. State constraints arise from *physical*, *performance*, and/or *safety* constraints. For example, all aircraft have to fly below a certain angle of attack. Should they exceed this aerodynamic performance constraint, stall ensues with possibly disastrous consequences. In robotics, manipulator arms operating on factory floors may have constraints imposed on their movement due to spatial restrictions and/or performance limitations to prevent material wear and tear. Constraints on the output signals can be further classified into two distinct subclasses. The first subclass of output constraints consists of those which arise as a direct consequence of constraints on the system states. These constraints can be treated as nonlinear or linear combinations of the state constraints, depending on the mathematical output model of the system. The second subclass of output constraints arises from sensors' measurement range saturations, and requires different analysis and control design strategies which are beyond the scope of this thesis and will not be considered herein.

1.2.1 Input constraints

The problem of actuator saturations has been extensively studied. There are many techniques available in the linear control literature for incorporating actuator saturations into the design process. The simplest but also most widely used in practice are *anti-windup compensation* schemes, see [3,42,60,72,115], and references therein. These approaches are however, *ad hoc* in nature which make their stability and robustness properties difficult to analyse. More sophisticated techniques include the use of l_1 analysis and synthesis techniques, which allow specification of the maximum output response as a function of the maximum size of noise and disturbances [26], and the use of convex optimisation to design controllers with a variety of input and performance constraints [15,16]. A major limitation of using a linear approach is the requirement that the system operates in a linear regime. For any nonlinear system with non-trivial transient response, this assumption is immediately invalid.

Another limitation associated with linear control techniques is that in general, no linear systems, even simple integrator cascades, of order greater than two which are subject to input saturations can be globally asymptotically stabilised by linear feedback control laws [136]. This negative result led to a number of semi-global approaches, including the low-gain designs by Lin and Saberi [82,84] and Teel [139], which achieve semi-global stabilisation of null-controllable systems, that is, systems with non-positive eigenvalues. The main drawback of these designs is poor performance and disturbance attenuation due to the use of low gains to achieve large domains of attraction. In an effort to improve the performance and disturbance rejection properties of the closed-loop system, high-and-low gain designs were proposed by Saberi *et al.* [117] and Lin [83]. Although these approaches allow for more effective use of the allowable input gains, they do not, in general, provide any significant improvements over the low-gain designs [44].

To improve the convergence performance and still achieve semi-global stabilisation of

linear input constrained systems, Wredenhagen and Belanger [157] proposed a piecewise-linear control (PLC) design method, which is based on Linear Quadratic (LQ) theory. PLC employs a very simple fact, and that is as the system approaches the origin, the control gains may be increased without affecting the stability of the system. The method involves deriving a succession of positively invariant sets of diminishing size (nested ellipsoids) and assigning each with the corresponding highest LQ gain possible in the presence of the input constraints. As a system trajectory moves from an outer ellipsoid into an inner one, the controller switches to the corresponding feedback law. Since each ellipsoid is invariant under the corresponding feedback law, the switch is safe, that is, no chattering, and the existence and uniqueness of the solution to the closed-loop differential equation is guaranteed [50]. Consequently, the convergence performance of the closed-loop system is progressively enhanced as the system approaches the origin.

In optimal control theory, the bang-bang control methodology, which optimises a performance index subject to control input constraint, has attracted numerous research efforts [64, 75, 99, 100, 145, 149, 156]. In practice however, this control technique is rarely implemented. The major disadvantage of bang-bang control is that it is generally impossible to characterise the switching surface. For discrete-time systems, online computation has been proposed in the literature, but the computational demand is substantial since dynamic programming has to be solved recursively with increasing time-horizon. This intensive online computation process increases the time delay and may lead to instability due to the accumulated error in the online evaluation of the control law, which is further exacerbated as the time-horizon is extended. In addition, the undesirable control chatter near the origin of state-space due to high frequency switching of the control signal often occurs which may lead to the excitation of undesirable high-frequency dynamics [49].

Several new nonlinear tools have been introduced in the last fifteen years for analysing and controlling linear and nonlinear systems with input saturations. One of the fundamental techniques is based on the thesis work of Teel [140,141], who showed how to stabilise a chain of integrators using nested saturation functions. This result is significant since it has been established that global asymptotic stabilisation of integrator chains of order greater than two cannot be achieved using bounded linear feedback laws. Thus, even simple linear systems with simple saturations can give rise to difficult nonlinear problems. Teel's approach generates nonlinear controllers which are locally linear, but become nonlinear as the inputs grow toward the saturation limits. This result was later generalised to null-controllable systems by Sussman *et al.* [137]. Teel and Kapoor [144] then extended Teel's earlier work by devising an algorithm to dynamically combine a local (performance) controller and a global (stability) controller to achieve local performance and global stability for a class of fully-actuated Euler-Lagrange systems with input saturation.

In 1996, Teel [143] added another nonlinear tool to deal with the problem of input constraints. He formalised a nonlinear small-gain theorem which can be used to derive iterative control design procedures for systems in the feedforward form subject to magnitude and rate saturations. Mazenc and Praly [93], and Jankovic *et al.* [123] then furthered Teel's idea by developing recursive design procedures, now known as *forwarding*, for such feedfor-

ward systems subject to input constraints. Another design technique was introduced by Megretski [95], who used a *gain-scheduling* approach to generate nonlinear stabilisers for saturated linear systems. In addition to stability, Megretski showed that for stable plants, the map from plant disturbances to control inputs is L_2 bounded. More recently, the control input saturation problem was studied by Freeman and Praly in [35], and Mazenc and Iggidr [92] in the *backstepping* framework. They showed that global stabilisation of certain classes of systems subject to bounded control and control rates can be achieved by imposing bounds on the stabilising functions and propagating those boundedness properties through each step of the backstepping technique.

1.2.2 State constraints

Although state constraints are a major concern in almost all practical control problems, they have not received as much attention as the problem of control input constraints. There have been efforts to solve state saturation control problems for linear systems using the concept of positive *invariant sets*, see [14,124] and references there within. These methods are based on the construction of a maximal controlled invariant set, that is, a subset of the state-space that will always contain the state under appropriate saturated state feedback. The available tools presented in this line of work, however, are computationally very demanding and yield highly complex controllers. *Model predictive control* (MPC), a popular control design technique for industrial processes, has also been employed to deal with constrained linear systems [86,91] as well as nonlinear systems [1,2,33]. The general MPC algorithm functions as follows. At each sampling instant, MPC solves an open-loop trajectory optimisation problem to compute an optimal control sequence over a finite horizon, using the current state of the plant as the initial condition and the plant model to predict future plant outputs. The first control in the optimal control sequence is applied to the plant. At the next sampling instant, the optimisation problem is reformulated with the horizon shifted forward by one unit of time and the control input is computed using new measurements of the states as the initial condition, and so on. The popularity of the approach stems from its inherent ability to explicitly handle state and input constraints, and the resulting control action is stable, and optimal with respect to the specified cost function [91]. However, the demanded online computation, that is, the solving of an optimal control problem at each sampling instant, is intensive and therefore, not suitable for systems with fast dynamics.

In contrast to the aforementioned numerical methods, Saberi *et al.* [116] adopted a structural approach to the problem. They established necessary and sufficient structural conditions for the solvability of linear systems subject to magnitude and rate constraints on both the state and control signals. They then proposed nonlinear time-varying control laws for systems that satisfy the imposed structural conditions. Although different types of constraints are allowed, the solvability conditions are restrictive, thus limiting the applicability of the method.

In what appears to be the only other published work that deals with the prob-

lem of state constraints in the framework of constructive nonlinear control, Wolff and Buss [154, 155] extended the concept of invariance control [87] to solve the problem of stabilisation for *control affine* nonlinear systems subject to state constraints. In their design, a nominal stabilising controller for the system, which does not take into account the constraints, is assumed to exist. Compliance with the constraints is enforced by constructing an invariance controller, through input-output linearization [121,127], to modify the nominal control signal such that a pointwise constraint admissible state space region becomes positively invariant. Switching from the nominal controller to the invariance controller is done every time the trajectory of the constrained system reaches the boundary of the invariance region. The construction of the invariance controller, however, requires solving a set of polynomials, one for each constraint, where the order of each polynomial is the relative degree of the constrained state it corresponds to. The design therefore becomes analytically complex for state constraints with relative degree greater than two. For systems subject to state constraints with relative degree greater than four, closed-form solutions do not exist and numerical solutions must be sought.

1.3 Research directions

Although the problem of state constraints has been addressed in the literature, it has not received the same focus and energy as had the input constraint problem. Furthermore, there have been very few attempts made to study the state constraint problem within the context of constructive nonlinear control.

The purpose of this thesis is two fold. The first is to develop backstepping-based control design procedures to address the stabilisation problem for specific classes of non-affine, nonlinear systems subject to state constraints. The proposed control design procedures are then applied to provide solutions to practical engineering problems. The second objective is to address the set-point regulation problem for constrained Euler-Lagrange mechanical systems in the framework of passivity-based control.

1.4 Practical motivation: longitude control of Uninhabited Aerial Vehicles

Due to recent advances in computing and sensor technologies, and the social pressure to reduce risks to human pilots, there has been an enthusiastic drive towards the use of small Uninhabited Aerial Vehicles (UAVs). An example is the Aerosonde UAV depicted in Figure 1.1. The Aerosonde is a long-range reconnaissance robotic drone which has been successfully deployed in a variety of meteorological sensing missions. Current research efforts now focus on improving and extending the operational capability of the aircraft. With its small size, approximately 2.9m $\times$ 2m in wingspan and length, respectively, and an endurance of more than 30 hours, the Aerosonde provides the ideal platform for a wide range of low-cost surveillance and sensing tasks. Apart from meteorological data

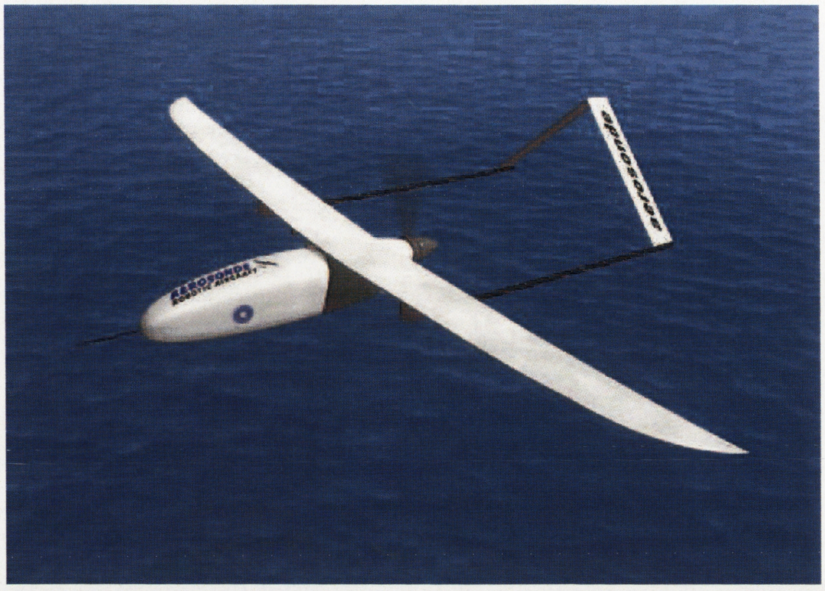

Figure 1.1: The Aerosonde UAV (Digital image by Jon Becker, Aerosonde Pty Ltd)

collection, which the aircraft was originally developed for, potential applications include coastal surveillance, landscape mapping, aerial photography, low-altitude mineral exploration, just to name a few.

Commercial operations of miniaturized, low-cost UAVs pose different control problems to those of manned aircraft or military UAVs. Aircraft and load configurations are more likely to change quickly to capture market opportunities. Although performance criteria are less stringent, the desire for enhanced functionality demands that the aircraft operates over an expanded flight envelope characterised by potentially hostile and highly nonlinear variations in dynamic pressure and aerodynamic phenomena [20]. At the same time, limited resources, cost effectiveness considerations, and the fact that these aircraft are disposable, mandate the use of simplified and incomplete dynamic models and inexpensive hardware in the implementation of the control system.

In addition, as with any other practical systems, aircraft control warrants the consideration of input and/or state constraints. Input constraints arise due to physical limitations on the range of operations of actuators. Aerodynamic phenomena such as stall and flutter impose magnitude constraints on the system states.

One of the main objectives of this thesis is to address these challenges and design a longitudinal flight controller that guarantees acceptable tracking and stabilising performance for the class of small commercially-operated flying robots such as the Aerosonde. The focus is firmly placed on the longitudinal dynamics due to the fact that the mission profiles of the UAVs under consideration do not require acrobatic nor evasive maneuvers. Consequently, these aircraft are normally built with a relatively high degree of lateral-directional stability. The Aerosonde, for example, is very stable in the roll mode.

1.4.1 Traditional aircraft control design methods

Traditional approaches to automatic flight control design, though highly successful in manned aircraft and military UAVs, are unsuitable as design tools for commercial UAVs. The popular, for its systematic divide-and-conquer framework, gain-scheduling methodology is tedious, relies heavily on the designer's experience, demands system information to be known *a priori*, and requires extensive flight tests to verify the final control law [77, 110]. Furthermore, small changes in aircraft dynamics require re-tuning of the controller since it does not intrinsically model nonlinear parameter variation in dynamic pressure [20]. Although automated gain-scheduling methods dramatically reduces the workload involved [98, 108, 111], automation does little to address the trial-and-error nature of the method and robustness issues. Moreover, there exists no simple or direct mechanism to incorporate actuator saturation and/or state constraints into the design process. The use of nonlinear actuation systems can also significantly increase the complexity of the control design [20]. Similarly inapplicable are feedback linearization techniques because they involve the inversion of the nonlinear plant dynamics that depend crucially on the quality of the flight dynamic model. The so called self-learning approaches, including fuzzy logic, neural network, and genetic algorithm, have significant problems. Although there have been various proposals which have produced encouraging simulation results [80, 97, 112, 132], the major shortcoming of these methodologies as flight control design tools is the lack of the analytical and practical means to examine the stability, performance, and robustness of the resulting controller.

1.4.2 Integrator backstepping

Integrator backstepping is a nonlinear control design technique that employs Lyapunov synthesis to recursively determine controllers for systems satisfying the *lower-triangular* cascaded structure, see Figure 1.2. The advantages of backstepping are numerous. In contrast to the feedback linearization technique which stipulates the cancellation of all nonlinearities including useful ones, backstepping affords the control engineer not only the choice of retaining all beneficial nonlinearities, but also great freedom in selecting the final control law [68]. Other strengths of backstepping include its ability to accommodate, by explicitly accounting for, large nonlinearities and uncertainties in the system's model, ignored dynamics, input and measurement disturbances [74], [38], [56], [159], [6], [28]. All of these factors, coupled with its constructive nature, and the fact that the aircraft longitudinal dynamics can be transformed into the strict-feedback cascaded structure, make backstepping very attractive as a design tool to solve the Aerosonde's control challenges described previously. However, direct application of traditional backstepping [74] tends to produce highly aggressive control laws. Such control laws are unsuitable for real systems due to actuator saturation and the possible presence of hard bounds on the physical system states.

Aircraft control requires the consideration of bounded states rather than bounded control inputs. Let us illustrate by considering the elevators-to-altitude dynamics which

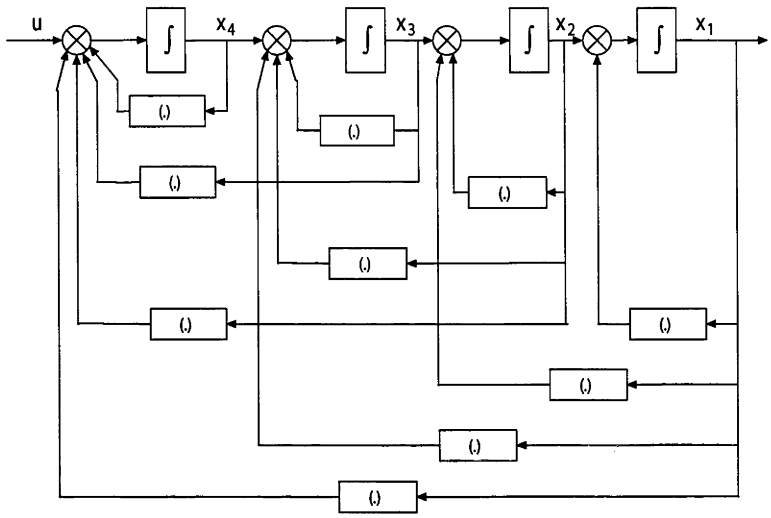

Figure 1.2: Lower-triangular cascaded structure

can be transformed into a 4^{th}-order system driven by the elevators, see Figure 1.3. The control margin provided by the elevators for a typical aircraft is more than adequate for all required manoeuvres. In fact, the control margin can be considered infinite with respect to the system in the sense that both the magnitude and the rate of the control inputs are sufficient to cause catastrophic system failure should they be applied too aggressively. For example, if the aircraft attempts to gain altitude at too quickly a rate, the resultant large elevator deflections will cause the aircraft to stall. Hard bounds on the states due to performance/physical limitations such as that of the aircraft example are very common in practice. To design a robust stabilising controller for such systems, it is more applicable to place hard bounds on the relevant state/s rather than the control inputs in the control design procedure.

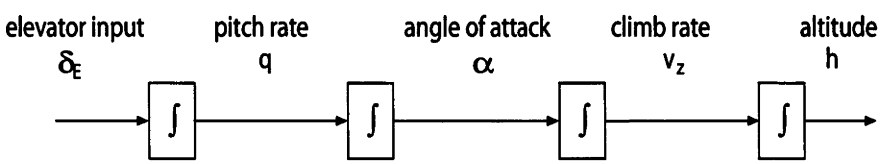

Figure 1.3: Schematic representation of aircraft longitudinal dynamics

Motivated by this control problem, we dedicate the first part of this thesis to developing backstepping-based design procedures to asymptotically stabilise general classes of non-affine, nonlinear systems subject to state constraints. The design procedures developed are then applied to design a longitudinal autopilot for the Aerosonde UAV which takes into account the state constraints imposed by aerodynamic phenomena and performance limitations.

1.5 Passivity-based control of Euler-Lagrange systems

Passivity-based control (PBC) is in essence a nonlinear, two-stage control design methodology whose objective is rendering the closed-loop system passive. The first stage, termed the *energy shaping* stage, involves the modification of the potential energy such that the modified potential energy function has a global and unique minimum in the desired equilibrium. The second stage, or *injection damping*, entails the modification of the dissipation function to ensure asymptotic stability. First introduced in the seminal paper by Takegaki and Arimoto [138] to solve the set-point regulation of robot manipulators, PBC has attracted enormous popularity because it generates computationally simple control laws that can accomplish complicated tasks with rigorously established stability, performance, and robustness properties. The final control laws are invariably Proportional-Derivative-like control laws, which are intuitively simple and can easily be implemented in practice. Numerous extensions of PBC have been made, most notably the research work described in [109] which is applicable to general Euler-Lagrange systems, that is, systems which admit an Euler-Lagrangian formulation. In [109], issues such as output feedback, disturbance attenuation, under-actuation, and adaptivity were addressed. This work also provided the motivation that led to the thesis work of Akmeliawati [4] where the author applied the concept of PBC to design longitudinal autopilots for aircraft. Akmeliawati's approach however, does not account for state or input constraints. Although PBC has been employed to address the bounded input control problem for robot manipulators [65, 66, 119], the problem of state constraints has never been considered in the literature. Motivated by this, in the second part of this thesis, we extend the PBC methodology to solve the set-point regulation problem for constrained Euler-Lagrange systems. Although the results presented in this thesis are explicitly developed for robot manipulators, which are an important class of Euler-Lagrange systems due to their pervasive presence in modern manufacturing processes, the proposed controller designs are applicable to general Euler-Lagrange systems.

1.6 Thesis contributions and outline

This thesis consists of two parts, preceded by a chapter of preliminaries. In Part I, modified backstepping design procedures are developed to solve the problem of stabilisation for general classes of non-affine, nonlinear systems subject to state constraints. These theoretical developments are then applied to mechanical and aerospace systems to demonstrate their validity, practicality, and performance. Part II of the thesis is devoted to studying the set-point regulation problem for constrained robot manipulators in the framework of passivity-based control.

Part I

Part I of the thesis is composed of three chapters and includes extensions of the following two papers:

- K. B. Ngo, R. Mahony, and Z.-P. Jiang, Integrator backstepping design for motion systems with velocity constraint, in *Proceedings of the 5^{th} Asian Control Conference 2004*, pages 141-146, Melbourne, Australia, July 2004.

- K. B. Ngo, R. Mahony, and Z.-P. Jiang, Integrator backstepping using barrier functions for systems with multiple state constraints, in *Proceedings of the 44^{th} IEEE Conference on Decision and Control and European Control Conference 2005*, Seville, Spain, December 2005.

In Chapter 3, two modified backstepping-based control designs are proposed to asymptotically stabilise a class of non-affine, nonlinear systems subject to a single or two consecutively constrained states. The first design, or the "non-strict" approach, only requires the construction of non-strict control Lyapunov functions but yields long and algebraically complicated control laws. The second design, or the "ISS" approach, generates simpler control laws but at the cost of having to construct input-to-state control Lyapunov functions, which are not always possible, and are generally much more difficult than the determination of non-strict control Lyapunov functions. The validity and effectiveness of the proposed control designs are illustrated via closed-loop simulations of two mechanical systems: the active car suspension system subject to suspension travel limits and the Reaction Wheel Pendulum system subject to torque and pendulum's velocity constraints.

In Chapter 4, the results of Chapter 3 are extended to asymptotically stabilise a class of nonlinear systems subject to multiple state constraints. The adaptation of the "ISS" approach to accommodate multiple state constraints is straightforward, requiring only one additional assumption on the nonlinear terms in the system's dynamic model. For the "non-strict" approach, the extension is more complicated. To achieve boundedness of the states, the cross-terms of the traditional backstepping method have to be dominated instead of being directly cancelled. The outcome of the proposed design procedure is a set of constraints on the controller parameters. From these constraints, nonlinear bounds for the stabilising functions and error variables, and ultimately, for the system states, in terms of the controller parameters can be computed. Together, the constraints on the controller parameters, the computed bounds on the system states, and the prescribed state bounds provide the ingredients for a multi-criteria constrained optimisation routine to tuning the controller parameters. The result is a set of controller parameters that guarantees that the closed-loop system is asymptotically stable, and yields the maximum possible constraint admissible region given the prescribed state bounds and the constraints imposed by the proposed design procedure.

Chapter 5 is dedicated to designing a longitudinal autopilot, based on the backstepping method, to regulate the altitude of the Aerosonde UAV. Application of traditional backstepping however, leads to an aggressive controller that causes the aircraft to stall by commanding excessively large elevator deflections. To solve this "large effector commands" problem, and hence prevent the onset of stall, a hard bound on the climb rate of the aircraft is imposed. This state constraint is directly incorporated into the controller design by utilizing the results developed in Chapter 3. Closed-loop simulations on a fully

nonlinear, 6-degree-of-freedom dynamic model of the Aerosonde UAV are presented to demonstrate the validity and performance of the proposed controller design.

Part II

Part II of the thesis is devoted to studying robot manipulators subject to constraints in the framework of passivity-based control, and is a composition of the following two papers:

- K. B. Ngo and R. Mahony, Passivity-based control of robot manipulators subject to constraints, in *Proceedings of the 2005 Australasian Conference on Robotics and Automation*, Sydney, Australia, December 2005.

- K. B. Ngo and R. Mahony, Bounded torque control for robot manipulators subject to joint velocity constraints, in *Proceedings of the 2006 IEEE International Conference on Robotics and Automation*, Florida, USA, May 2006.

In Chapter 6, a control design procedure is developed which utilizes ideas from passivity-based control and artificial potential field methods to address the general problem of autonomous obstacle avoidance for constrained robot manipulators subject to joint position and joint rate constraints. The control objectives are achieved by incorporating barrier-function characteristics into the control Lyapunov function. In common with the artificial potential field method, for arbitrary constraints, the asymptotic stability of the closed-loop system is not guaranteed due to the possible presence of local minima in the structure of the proposed control Lyapunov function. However, for systems with state constraints that possess certain convexity properties, asymptotic stability of the closed-loop system is assured.

In Chapter 7, the ideas of passivity-based control and artificial potential field methods are extended in a different direction to solve the stabilisation problem for robot manipulators with torque limits and joint velocity constraints. The key advantage of the control design procedure derived in this chapter is that the resulting controllers are invariably modified PD-controllers, which are structurally simple, robust, and immensely practical.

The attractiveness of the control design procedures developed in this part is that although the focus is principally on robot manipulator dynamics, the proposed design procedures are equally applicable to general Euler-Lagrange systems. Closed-loop simulation results on a 2-link planar robot manipulator are provided to illustrate the validity and effectiveness of the proposed controller designs.

The thesis concludes with Chapter 8 which is a summary of the main contributions of this thesis, and contains a discussion of recommended future research.

Chapter 2

Preliminaries

This chapter provides a brief review of the ideas and concepts used in this thesis. In Section 2.1, we lay the foundation for the thesis by defining the necessary notation and terminology. Section 2.2 contains the definitions of barrier functions and re-centred barrier functions. The concept of relative degree is outlined in Section 2.3. Notions of stability are given in Section 2.4. The definitions of control Lyapunov functions are presented next in Section 2.5. The chapter then ends with Section 2.6 where the integrator backstepping method is briefly recapitulated. Since the materials presented in Sections 2.4 and 2.6 are well-established, no proofs are offered. For more detailed treatments of those materials, the interested reader is referred to such excellent texts as [52, 68, 74, 127].

2.1 Notation and Terminology

- A function f: $\mathbb{R}^n \to \mathbb{R}^q$ is C^k if its partial derivatives exist and are continuous up to order k, $1 \leq \mathrm{k} \leq \infty$. A C^0 function is continuous. A C^∞ function is smooth, that is, it has continuous partial derivatives of any order.

- Given a vector field $f : \mathbb{R}^n \to \mathbb{R}^n$ and a differentiable scalar function $\lambda : \mathbb{R}^n \to \mathbb{R}$, $L_f\lambda$ denotes the Lie derivative (directional derivative) of λ along f

$$L_f\lambda(x) = \frac{\partial \lambda}{\partial x} f(x)$$

  Higher order Lie derivatives can be defined recursively as

$$L_f^2\lambda(x) = L_f L_f \lambda(x)$$
$$L_f^i\lambda(x) = L_f L_f^{i-1}\lambda(x)$$

  for $i = 1, 2, \ldots$ with $L_f^0\lambda(x) = \lambda(x)$.

- A continuous function $\alpha : [0, a) \to [0, \infty)$ is said to belong to class $\mathcal{K}$, that is, $\alpha \in \mathcal{K}$, if it is strictly increasing and $\alpha(0) = 0$. It is said to belong to class $\mathcal{K}_\infty$ if $a = \infty$ and $\alpha(r) \to \infty$ as $r \to \infty$.

- A continuous function $\beta : [0, a) \times [0, \infty) \to [0, \infty)$ is said to belong to class $\mathcal{KL}$ if, for each fixed s, the mapping $\beta(r, s)$ belongs to class $\mathcal{K}$ with respect to r and, for

each fixed r, the mapping $\beta(r,s)$ is decreasing with respect to s and $\beta(r,s) \to 0$ as $s \to \infty$.

- The notations $\lambda_{max}\{B\}$ and $\lambda_{min}\{B\}$ denote the largest and smallest eigenvalues of matrix B, respectively. The norm of vector x is defined as $||x|| = \sqrt{x^T x}$, and that of matrix A is defined as $||A||_2 = \sqrt{\lambda_{max}\{A^T A\}}$.
- Throughout this thesis, $|\ .\ |$ denotes the Euclidean norm.

2.2 Barrier functions and re-centred barrier functions

Definition 2.1 (Barrier function and re-centred barrier function [152], pg. 90). *Let $\mathcal{S}$ be an open, non-empty, and convex subset of $\mathbb{R}^n$. A function f is called a barrier function in $\mathcal{S}$ if it satisfies the following conditions.*

- *The function $f : \mathcal{S} \to \mathbb{R}$ is continuously differentiable and strictly convex in $\mathcal{S}$.*
- *$f(x_k) \to \infty$ for every sequence $\{x_k \in \mathcal{S}\}$ approaching a boundary point of $\mathcal{S}$.*

Given a point $x_d \in \mathcal{S}$, a barrier function f is called a re-centred barrier function about x_d if

- *$f(x_d) = 0$, and $f(x) > 0$ for all $x \in \mathcal{S}$ with $x \neq x_d$.*

Lemma 2.2 (Re-centred barrier function [152], pg. 94). *Let $\mathcal{S}$ be an open, non-empty convex subset of $\mathbb{R}^n$, and f be a barrier function in $\mathcal{S}$. Given a point $x_d \in \mathcal{S}$, and define function $f_{x_d} : \mathcal{S} \to \mathbb{R}$ as*

$$f_{x_d}(x) = f(x) - f(x_d) - \nabla f(x_d)^T (x - x_d). \tag{2.1}$$

Then f_{x_d} is a re-centred barrier function about x_d.

Proof. Since the function f is strictly convex and continuously differentiable in $\mathcal{S}$, then

$$f(x) \geq f(x_d) + \nabla f(x_d)^T (x - x_d), \tag{2.2}$$

with equality only at $x = x_d$ [152]. □

2.3 Relative degree

Definition 2.3 (Relative degree of nonlinear systems [90]). *The nonlinear Single-Input-Single-Output (SISO) system*

$$\begin{aligned} \dot{x} &= f(x) + g(x)u \\ y &= h(x), \end{aligned} \tag{2.3}$$

where f, $g : \mathcal{D} \subset \mathbb{R}^n \to \mathbb{R}^n$, *and* $h : \mathcal{D} \subset \mathbb{R}^n \to \mathbb{R}$, *is said to have relative degree* r, $1 \leq r \leq n$, *in a region* $\mathcal{D}_0 \subset \mathcal{D}$ *if*

$$L_g L_f^i h(x) = 0, \quad i = 1, ..., r-1,$$
$$L_g L_f^{r-1} h(x) \neq 0$$

for all $x \in \mathcal{D}_0$.

2.4 Stability

Definition 2.4 (Lyapunov stability [74]). *The origin of the system*

$$\dot{x} = f(x), \tag{2.4}$$

where $x \in \mathbb{R}^n$ *and* $f(x)$ *is Lipschitz continuous, is said to be*

- *Stable if, for each* $\epsilon > 0$, *there exists* $\delta > 0$ *such that*

$$|x(0)| \leq \delta \Rightarrow |x(t)| \leq \epsilon, \forall t \geq 0.$$

- *Attractive if there exists* $\delta > 0$ *such that*

$$|x(0)| \leq \delta \Rightarrow \lim_{t \to \infty} x(t) = 0.$$

- *Asymptotically stable (AS) if it is stable and attractive.*

- *Globally asymptotically stable (GAS) if it is stable and*

$$\forall x(0) \in \mathbb{R}^n, \lim_{x \to \infty} x(t) = 0.$$

- *Locally exponentially stable (LES) if there exists* δ, k, $\beta > 0$ *such that*

$$|x(0)| \leq \delta \Rightarrow |x(t)| \leq k|x(0)|e^{-\beta t}.$$

A sufficient condition for stability at the origin of any system is established through Lyapunov's direct method.

Theorem 2.5 (Global asymptotic stability [74]). *Let* $x = 0$ *be an equilibrium of system (2.4). If there exists a continuously differentiable positive definite and radially unbounded function* $V(x)$: $\mathbb{R}^n \to \mathbb{R}_+$ *such that*

$$\dot{V}(x) = \frac{\partial V}{\partial x}(x) f(x) \leq 0, \quad \forall x \in \mathbb{R}^n,$$

then $x = 0$ is stable, and all solutions of (2.4) are bounded and converge to the set where $\dot{x} \equiv 0$. If $\dot{V}(x)$ is negative definite, the origin is globally asymptotically stable. The function $V(x)$ is called a Lyapunov function for system (2.4).

Theorem 2.6 (LaSalle's Invariance Principle [74]). *Let Ω be a positively invariant set of (2.4). Let $V : \Omega \to \mathbb{R}_+$ be a continuously differentiable function $V(x)$ such that $\dot{V}(x) \leq 0$, $\forall x \in \Omega$. Let $E = \{x \in \Omega \mid \dot{V}(x) = 0\}$, and let M be the largest invariant set contained in E. Then, every bounded solution $x(t)$ starting in Ω converges to M as $t \to \infty$.*

Another stability concept used in this thesis is the input-to-state stability (ISS). First introduced by Sontag in [129], ISS is used to establish boundedness of system's states with respect to bounded inputs.

Definition 2.7 (ISS [68]). *The time-invariant system*

$$\dot{x} = f(x, d) \tag{2.5}$$

where $x \in \mathbb{R}^n$ is the state, $d \in \mathbb{R}^r$ is the disturbance, and $f : \mathbb{R}^n \times \mathbb{R}^r$ is Lipschitz continuous, is said to be input-to-state stable if there exist a class $\mathcal{KL}$ function β and a class $\mathcal{K}$ function γ such that for any initial state x_0 and for any bounded disturbance $d(t)$, the solution $x(t)$ exists for all $t \geq 0$ and satisfies

$$|x(t)| \leq \beta(|x_0|, t) + \gamma\left(\sup_{0 \leq \tau \leq t} |d(\tau)|\right). \tag{2.6}$$

The following theorem establishes the connection between the existence of a Lyapunov-like function and ISS.

Theorem 2.8 (ISS Lyapunov function [74]). *Suppose that for the system (2.5) there exists a continuously differentiable function $V : \mathbb{R}^n \to \mathbb{R}_+$ such that for all $x \in \mathbb{R}^n$ and $d \in \mathbb{R}^r$,*

$$\gamma_1(|x|) \leq V(x) \leq \gamma_2(|x|) \tag{2.7}$$

and

$$|x| \geq \rho(|d|) \Longrightarrow \frac{\partial V}{\partial x} f(x, d) \leq -\gamma_3(|x|), \tag{2.8}$$

where γ_1, γ_2, and ρ are class $\mathcal{K}_\infty$ functions and γ_3 is a class $\mathcal{K}$ function. Then the system (2.5) is ISS with $\gamma = \gamma_1^{-1} \circ \gamma_2 \circ \rho$. The function V is said to be an ISS-Lyapunov function.

One useful application of ISS is the stability analysis of interconnected cascades. We are interested in the following result as we will be using it later in Chapters 3 and 4.

Corollary 2.9 (GAS of ISS-interconnected cascades [68]). *Given the cascade system*

$$\dot{x}_1 = f_1(x_1, x_2) \tag{2.9}$$

$$\dot{x}_2 = f_2(x_2), \tag{2.10}$$

where $f_1 : \mathbb{R}^{n_1} \times \mathbb{R}^{n_2} \to \mathbb{R}^{n_1}$, and $f_2 : \mathbb{R}^{n_2} \to \mathbb{R}^{n_2}$ are Lipschitz continuous. If the system (2.9), with x_2 as input, is input-to-state stable and the origin of (2.10) is globally asymptotically stable, then the origin of the interconnected system with state $x = [x_1 \; x_2]^T$ is globally asymptotically stable.

Definition 2.10 (Domain global asymptotic stability [104]). *A system*

$$\dot{x} = f(x, t), \quad f(x_0, t) = 0, \quad x_0 \in \mathbb{R}^n \tag{2.11}$$

with equilibrium point x_0 is termed domain globally asymptotically stable (DGAS) to x_0 with domain U if

1. *There exists a set $U \subseteq \mathbb{R}^n$ that is forward invariant under the dynamics of (2.11) and $x_0 \in U$.*
2. *The equilibrium point x_0 is Lyapunov stable under the dynamics of (2.11) restricted to U.*
3. *For any initial condition $x(0) \in U$, then the solution $x(t)$ of (2.11) satisfies*

$$\lim_{t \to \infty} x(t) = 0.$$

2.5 Control Lyapunov functions

In this section we present the definitions for control Lyapunov functions and ISS-control Lyapunov functions.

Definition 2.11 (Control Lyapunov functions [74]). *Given the system*

$$\dot{x} = f(x, u) \tag{2.12}$$

where $x \in \mathbb{R}^n$ is the state vector, $u \in \mathbb{R}^m$ is the control signal, and $f : \mathbb{R}^n \times \mathbb{R}^m \to \mathbb{R}^n$ is Lipschitz continuous. A smooth positive definite and radially unbounded function $V : \mathbb{R}^n \to \mathbb{R}_+$ is called a control Lyapunov function (cLf) for (2.12) if

$$\inf_{u \in \mathbb{R}^m} \left\{ \frac{\partial V}{\partial x}(x) f(x, u) \right\} \leq 0, \quad \forall x \in \mathbb{R}^n. \tag{2.13}$$

If in addition

$$\inf_{u\in\mathbb{R}^m}\left\{\frac{\partial V}{\partial x}(x)f(x,u)\right\}<0,\quad \forall x\neq 0, \tag{2.14}$$

then it is called a strict clf.

Definition 2.12 (ISS-control Lyapunov functions [68]). *Consider the system*

$$\dot{x}=f(x,d,u) \tag{2.15}$$

where $x\in\mathbb{R}^n$ is the state, $d\in\mathbb{R}^r$ is the disturbance, $u\in\mathbb{R}^m$ is the control signal, and $f:\mathbb{R}^n\times\mathbb{R}^r\times\mathbb{R}^m\to\mathbb{R}^n$ is Lipschitz continuous. A smooth positive definite and radially unbounded function $V:\mathbb{R}^n\to\mathbb{R}_+$ is called an ISS-control Lyapunov function (ISS-cLf) for (2.15) if there exists a class-$\mathcal{K}_\infty$ function ρ such that

$$|x|\geq\rho(|d|)\Longrightarrow\inf_{u\in\mathbb{R}^m}\left\{\frac{\partial V}{\partial x}(x)f(x,d,u)\right\}<0,\quad \forall x\neq 0,\ d\in\mathbb{R}^r. \tag{2.16}$$

2.6 Backstepping [74]

Backstepping is the main design tool in this thesis and in this section we give a brief description of the design procedure. Let us start with a simple nonlinear system cascaded by an integrator

$$\dot{x}=f(x)+g(x)\xi \tag{2.17a}$$

$$\dot{\xi}=u \tag{2.17b}$$

where $(x,\xi)\in\mathbb{R}^n\times\mathbb{R}$ is the state vector, and $u\in\mathbb{R}$ is the control. The functions $f,g:\mathbb{R}^n\to\mathbb{R}^n$ are assumed to be smooth, and $f(0)=0$. The objective is to find a state feedback control law such that the origin $x=0$, $\xi=0$ is globally asymptotically stable. The design procedure proceeds as follows. Suppose the the x-subsystem can be stabilised by a smooth state feedback *virtual control*, also *stabilising function*, $\xi=\alpha(x)$, with $\alpha(0)=0$ such that the origin of

$$\dot{x}=f(x)+g(x)\alpha(x)$$

is globally asymptotically stable. Assume that there exist a positive definite and radially unbounded Lyapunov function $V(x)$, and a positive definite function $W(x)$ such that the following inequality is satisfied

$$\frac{\partial V}{\partial x}\left[f(x)+g(x)\alpha(x)\right]\leq -W(x),\quad \forall x\in\mathbb{R}^n. \tag{2.18}$$

By adding and subtracting $g(x)\alpha(x)$ on the right hand side of (2.17a), we obtain the equivalent representation

$$\begin{aligned}\dot{x} &= [f(x) + g(x)\alpha(x)] + g(x)[\xi - \alpha(x)] \\ \dot{\xi} &= u.\end{aligned} \tag{2.19}$$

Define the change of variables

$$z = \xi - \alpha(x),$$

which yields

$$\dot{z} = u - \frac{d\alpha(x)}{dt}.$$

Since f, g and $\alpha(x)$ are known, the derivative $\frac{d\alpha(x)}{dt}$ can be computed analytically and is given by

$$\frac{d\alpha(x)}{dt} \triangleq \frac{\partial \alpha(x)}{\partial x}[f(x) + g(x)\xi].$$

This change of variables can be viewed as "backstepping" the virtual control $-\alpha(x)$ through the integrator, and results in the system

$$\dot{x} = [f(x) + g(x)\alpha(x)] + g(x)z \tag{2.20a}$$

$$\dot{z} = u - \frac{d\alpha(x)}{dt} \tag{2.20b}$$

which is exactly the same as the original system (2.17), except now the x-subsystem has a globally asymptotically stable origin when the input z is zero. This feature is now exploited in the design of a stabilising control law for the overall system (2.20). Consider the following positive definite and radially unbounded function as a candidate Lyapunov function

$$U(x, z) = V(x) + \frac{1}{2}z^2. \tag{2.21}$$

Differentiating $U(x, z)$ with respect to time yields

$$\begin{aligned}\dot{U} &= \frac{\partial V(x)}{\partial x}[f(x) + g(x)\alpha(x)] + z\left[u - \frac{\partial \alpha(x)}{\partial x}[f(x) + g(x)\xi] + \frac{\partial V(x)}{\partial x}g(x)\right] \\ &\leq -W(x) + z\left[u - \frac{\partial \alpha(x)}{\partial x}[f(x) + g(x)\xi] + \frac{\partial V(x)}{\partial x}g(x)\right].\end{aligned} \tag{2.22}$$

To render $\dot{U}$ negative definite, the simplest choice is

$$u = -cz + \frac{\partial \alpha(x)}{\partial x}[f(x) + g(x)\xi] - \frac{\partial V(x)}{\partial x}g(x), \tag{2.23}$$

where $c > 0$, which yields

$$\dot{U} \leq -W(x) - cz^2 \tag{2.24}$$

and is negative definite since $W(x)$ is positive definite. Since U is positive definite and radially unbounded, we can conclude that the origin $x = 0$, $z = 0$ is globally asymptotically stable. Since $\alpha(0) = 0$, then the origin of the original system $x = 0$, $\xi = 0$ is also globally asymptotically stable, and the control law u in the original coordinates is given by

$$u = -c[\xi - \alpha(x)] + \frac{\partial \alpha(x)}{\partial x}[f(x) + g(x)\xi] - \frac{\partial V(x)}{\partial x}g(x). \tag{2.25}$$

It is clear that the above design procedure can be employed to globally asymptotically stabilize systems of the following form [74]

$$\begin{aligned}
\dot{x} &= f(x) + g(x)\xi_1 \\
\dot{\xi}_2 &= f_1(x, \xi_1) + g_1(x, \xi_1)\xi_2 \\
&\vdots \\
\dot{\xi}_{m-1} &= f_{m-2}(x, \xi_1, ..., \xi_{m-1}) + g_{m-2}(x, \xi_1, ..., \xi_{m-1})\xi_m \\
\dot{\xi}_m &= f_{m-1}(x, \xi_1, ..., \xi_m) + g_{m-1}(x, \xi_1, ..., \xi_m)u
\end{aligned} \tag{2.26}$$

by recursively "backstepping" the control law from the x-subsystem through to the last subsystem ξ_m where the real control signal u appears.

Part I

Integrator Backstepping Control of Constrained Nonlinear Systems

Chapter 3

Stabilisation of nonlinear systems subject to state constraints

The problem of saturation nonlinearities is by far the most common challenge faced by control engineers as all practical control problems are constrained in one way or another [13,48]. There are two main types of saturation nonlinearities: actuator constraints and state constraints. Examples of constrained systems include mechanical systems with position and velocity limits, electrical systems with limited power supply to the actuators, chemical processes with magnitude restrictions on process variables due to safety issues etc. Control problems for constrained linear systems have been extensively studied in the literature due to the hitherto successful use of linear approximations to represent a restricted range of operating conditions of otherwise nonlinear processes. Key approaches include override control [43], set invariance and admissible set control [11,14], the reference governor approach [39], and Model Predictive Control (MPC) [10,21]. Many of the accepted linear techniques are numerical in nature, and rely heavily on computationally intensive algorithms to solve the control problems. It is only recently that insights into structural properties of stabilizable constrained linear systems, as well as control design methodologies for such systems, were provided in [116,118].

All real systems are, however, inherently nonlinear. In addition, factors such as higher product quality specifications, increasing productivity demands, tighter environmental regulations, and demanding economical considerations all require systems to operate over a wider range of operating conditions and often near the boundary of the admissible region. Under these conditions, linear models are no longer adequate to describe the system's dynamics and nonlinear models should be considered. A number of linear techniques has been extended to address the stabilisation problem of constrained nonlinear systems, most notably the MPC approach (see [1,2,33] and references therein). MPC, however, requires the solution of an optimal control problem at each time step, rendering it unsuitable for systems with fast dynamics.

In the constructive nonlinear control literature, despite significant advances in the development of analysis and design methodologies, the general stabilisation problem of nonlinear systems subject to saturation nonlinearities remains an open area of research. Previous work in the literature has mainly focused on the problem of actuator con-

straints for feedforward systems. This has led to the modern techniques of small gain designs [45, 55, 57, 141, 143] and forwarding [93, 123]. A criticism of small gain designs is that they generally have poor performance and are non-robust with respect to the presence of destabilising feedback terms [44]. Forwarding designs on the other hand, are mathematically involved. The major burden of the forwarding design proposed by Jankovic *et al.* [123] is the evaluation of the cross-terms which require the solving of partial differential equations, a difficult task in general. Similarly, the forwarding design devised by Mazenc and Praly [93] requires the determination of the coupling changes of coordinates which in many cases, lead to complicated calculations or cannot even be determined due to parameters inaccurately known or the presence of destabilising feedback terms. Motivated by the complexities associated with the forwarding control design methods, Freeman and Praly [35] showed that global stabilisation of the following class of control affine nonlinear systems

$$\begin{aligned} \dot{x} &= f(x) + g(x)\xi \\ \dot{\xi} &= u + f_1(x, \xi), \end{aligned} \tag{3.1}$$

where $(x, \xi) \in (\mathbb{R}^n \times \mathbb{R})$ is the state vector, $u \in \mathbb{R}$ is the control input, $f(0) = 0$, $h(0, 0) = 0$, subject to bounded controls and control rates can be achieved by imposing bounds on the stabilising functions and their derivatives, and propagating those boundedness properties through each step of the backstepping technique. This result was later extended by Mazenc and Iggidr [92] to the more general class of systems

$$\begin{aligned} \dot{x} &= f(x, \xi) \\ \dot{\xi} &= u + f_1(x, \xi), \end{aligned} \tag{3.2}$$

where $(x, \xi) \in (\mathbb{R}^n \times \mathbb{R})$ is the state vector, $u \in \mathbb{R}$ is the control input, $f(0) = 0$, $h(0, 0) = 0$, which includes feedforward systems that are not stabilisable by the forwarding techniques.

State constraints, which are a major concern in many practical control problems, have not received the same level of attention as the problem of actuator constraints has. Recently, Wolff and Buss [154, 155] employed the concept of invariance control [87] in conjunction with feedback linearization to solve the stabilisation problem for control affine nonlinear systems

$$\dot{x} = f(x) + g(x)u,$$

where $x \in \mathbb{R}^n$ is the state vector, $u \in \mathbb{R}$ is the control input, and $f, g : \mathbb{R}^n \to \mathbb{R}^n$ are smooth vector fields, subject to $m \in \mathbb{R}_+$ hard state constraints as defined by

$$y_i = h_i(x) \leq 0, \quad 1 \leq i \leq m,$$

where $h_i(x) : \mathbb{R}^n \to \mathbb{R}$ are smooth output functions. The main disadvantage of this approach is that it involves solving m polynomials, one for each state constraint, where

the order of each polynomial is the relative degree of the constrained state it corresponds to.

To tackle the problem of state saturation constraints, it appears more effective to employ the backstepping methodology which is capable of delivering the high input gain margins required to impose the state saturation constraints. Furthermore, high gains are necessary to drive the constrained states as close as possible to their limits, thus achieving better convergence properties. Another salient attribute of backstepping is that, in contrast to feedback linearization technique which stipulates the cancellation of all nonlinearities including useful ones, backstepping affords the control engineer not only the choice of retaining all beneficial nonlinearities, but also great freedom in selecting the final control law [74]. Other strengths of backstepping include its ability to accommodate, by explicitly accounting for, large and unmatched nonlinearities and parametric uncertainties in the system's model, ignored dynamics, input and measurement disturbances [6, 28, 38, 56, 74, 159].

The main objective of this chapter is to develop systematic design procedures to asymptotically stabilise a class of nonlinear systems subject to one or two constrained states as depicted in Figures 3.1 and 3.2. The control problems considered in this chapter are motivated by the problem of aircraft altitude control, which, due to such aerodynamic phenomena as stall, requires the consideration of state constraints rather than input constraints. To illustrate this point, let us examine the elevator-to-altitude dynamics of an aircraft, which resembles a 4^{th}-order integrator cascade driven by the elevators, see Figure 1.3. The control margin provided by the elevators for a typical aircraft is more than adequate for all required manoeuvres. In fact, the control margin can be considered infinite with respect to the system in the sense that both the magnitude and rate of the control inputs are sufficient to cause catastrophic system failure should they be applied too aggressively. For example, if the aircraft is made to climb or descend too quickly, that is, at too high an angle of attack, it will stall and fall from the sky due to the loss of lift. To design a controller for such systems, it is more applicable to place hard bounds on the relevant states rather than the control inputs in the control design procedure.

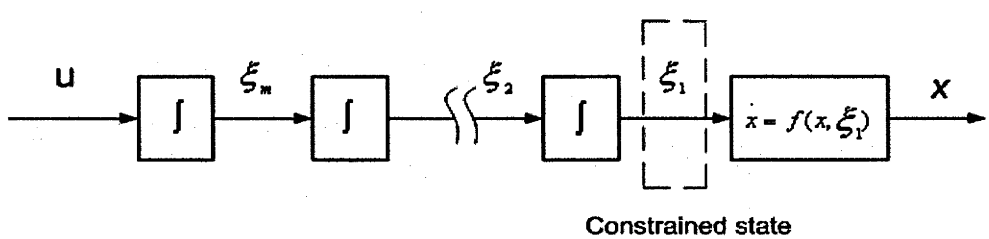

Figure 3.1: System subject to one constrained state

The principal contribution of this chapter is the introduction of two modified backstepping design procedures to solve the stabilisation problem of non-affine nonlinear systems subject to a single or two consecutive state constraints as depicted in Figures 3.1 and 3.2.

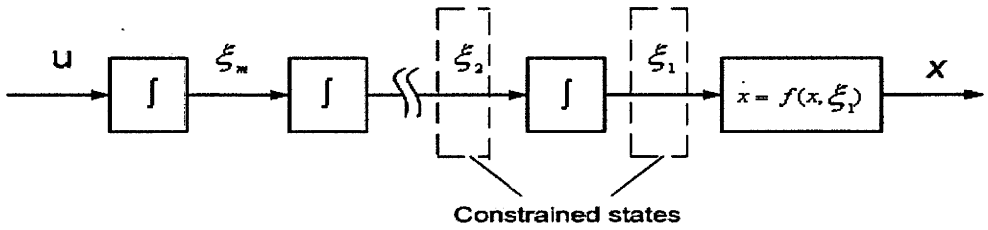

Figure 3.2: System subject to two consecutive constrained states

Observe that the x-subsystem is non-affine with respect to the state variable ξ_1. The class of systems considered includes those systems which are not locally exponentially stabilizable and thus are not conducive to the methods of forwarding. The results presented herein are extensions of our work in [54, 103], and complement the work of Wolff and Buss [154] in two ways. Firstly, we consider a more general class of systems than the control affine systems considered by Wolff and Buss. Secondly, the design procedure proposed by Wolff and Buss becomes mathematically involved for state constraints of relative degree greater than 2, and may not even yield a feasible solution for state constraints of relative degree greater than 4. In our proposed controller designs, closed-form analytic solutions exist for state constraints of any relative degree, provided that they are of the specified order in the cascade as shown in Figures 3.1 and 3.2.

The chapter is structured as follows. In Section 3.1, a control design procedure for systems subject to a single state constraint is proposed which is based on the assumption that no expression of a strict cLf is available. This approach, however, generates control laws which are algebraically complex for high-order systems, motivating us to seek a simpler design. The second design, presented in Section 3.2, yields considerably simpler control laws than the first. Nonetheless, the second design is based on a stronger set of assumptions which requires the determination of ISS-cLfs. To illustrate the validity and effectiveness of the proposed control designs, we apply the first design procedure, as exposed in Section 3.1, to solve the stabilisation problem for the active suspension system subject to suspension travel limits. The controller design and closed-loop simulations are presented in Section 3.3. In Section 3.4, we extend the first design procedure to solve the control problem where there exist magnitude constraints on two consecutive system states. Finally, the stabilisation problem of the Reaction Wheel Pendulum subject to magnitude constraints on the pendulum's velocity and applied torque is considered in Section 3.5 along with closed-loop simulation results.

3.1 The case of one constrained state: stabilisation with non-strict cLfs

In this section, we present an asymptotically stabilising controller design for a class of non-affine nonlinear systems subject to a single asymmetric state constraint, assuming

that no strict cLfs (cf. Definition 2.11) are available. Please note that some parts of the derivation and analysis of the main result, particularly the proof for asymptotic stability, are based on the work by Mazenc and Iggidr [92].

Given a class of nonlinear systems of the form

$$\begin{aligned}\dot{x} &= f(x,\xi_1)\\ \dot{\xi}_1 &= \xi_2 + f_1(x,\xi_1)\\ &\vdots\\ \dot{\xi}_m &= u + f_m(x,\xi_1,\ldots,\xi_m)\end{aligned} \tag{3.3}$$

where $(x,\xi) \in (\mathbb{R}^n \times \mathbb{R}^m)$ is the state vector, and $u \in \mathbb{R}$ is the control. The system (3.3) is non-affine in the sense that the x-subsystem is non-affine with respect to the state variable ξ_1. The functions $f, f_1, ..., f_m$ are assumed to be sufficiently smooth, and $f(0,0) = 0$, $f_1(0,0) = 0$, ..., $f_m(0,0,...,0) = 0$. In other words, the origin of (3.3) is an equilibrium point. There exist bounds on the state ξ_1 due to performance/physical limitations such that

$$-B_L < \xi_1(t) < B_U, \quad \forall t \geq 0, \tag{3.4}$$

where the constants B_L, $B_U \in \mathbb{R}_+$, B_L represents the lower limit and B_U represents the upper limit of the state ξ_1. The control objective is to develop a systematic design procedure to asymptotically stabilise system (3.3), whilst strictly respecting the constraints on ξ_1 as defined by (3.4).

3.1.1 Bounded state backstepping design

We make the following set of assumptions on system (3.3).

Assumption 3.1. *There exist*

- *A function $V(x)$ which is positive definite, radially unbounded, and of class C^1.*
- *A function $W(x)$ which is positive semi-definite and of class C^1.*
- *A sufficiently smooth control law $\alpha_1(x)$ satisfying*

$$\begin{aligned}\alpha_1(0) &= 0\\ |\alpha_1(x)| &\leq \Delta\\ \frac{\partial V}{\partial x} f(x,\alpha_1(x)) &\leq -W(x)\end{aligned} \tag{3.5}$$

  where $\Delta \in \mathbb{R}_+$ is a constant.

- *The solution $x(t) = 0$ is the unique function satisfying, for all t,*

$$\dot{x}(t) = f(x(t),\alpha_1(x(t))), \quad W(x(t)) = 0. \tag{3.6}$$

Assumption 3.1 concerns only the x-subsystem

$$\dot{x} = f(x, \xi_1),$$

with ξ_1 as the virtual input, and is a very natural assumption in the framework of backstepping. In essence, we require the construction of a bounded stabilising function $\alpha_1(x)$ such that with $\xi_1 = \alpha_1(x)$, the x-subsystem is globally asymptotically stable with the cLf $V(x)$, which can admit negative semi-definite derivatives along the trajectories of the closed-loop system $\dot{x} = f(x, \alpha_1(x))$. Naturally, Assumption 3.1 will lead us to invoke LaSalle's Invariance Principle (cf. Theorem 2.6) to prove asymptotic stability of the closed-loop system.

Note that Assumption 3.1 does not imply that system (3.3) is locally exponentially stabilisable. It follows that the design procedures developed in this chapter are applicable to those feedforward systems which cannot be stabilised through the forwarding designs exposed in [93] or [123]. An illustrative example is the three-dimensional feedforward system (adapted from [92])

$$\begin{cases} \dot{x}_1 &= x_2 \\ \dot{x}_2 &= -x_1^5 + \xi^5 \\ \dot{\xi} &= u \end{cases}$$

with $x = (x_1, x_2)^T$, which is not locally exponentially stabilisable.

To improve the clarity of the development of the result, we will first present the result for the reduced-order system

$$\begin{cases} \dot{x} &= f(x, \xi_1) \\ \dot{\xi}_1 &= v + f_1(x, \xi_1) \end{cases} \tag{3.7}$$

with $v \in \mathbb{R}$ as the control signal, then generalise the result to the full-order system (3.3) afterwards.

Proposition 3.2. *Consider system (3.7) subject to a single state constraint as defined by (3.4). Let $a_1 > \Delta$, $b_1 > \Delta$, and k_1, $c_1 \in \mathbb{R}_+$ be design constants, where Δ is as defined in Assumption 3.1. Define the error variable z_1 as*

$$z_1 = \xi_1 - \alpha_1(x) \tag{3.8}$$

and let the functions $T(x, \xi_1)$ and $\Gamma(z_1)$ denote

$$T(x, \xi_1) = \frac{\partial V}{\partial x}(x) \left[f(x, \xi_1) - f(x, \alpha_1(x)) \right] \tag{3.9}$$

$$\Gamma(z_1) = \frac{\left[(a_1 + z_1)(b_1 - z_1) \right]^2}{k_1 \left[2(a_1 + z_1)(b_1 - z_1) - z_1 \{ (b_1 - z_1) - (a_1 + z_1) \} \right]}, \tag{3.10}$$

respectively. Consider the following candidate cLf for system (3.7)

$$U(x, z_1) = V(x) + \frac{k_1 z_1^2}{(a_1 + z_1)(b_1 - z_1)}, \tag{3.11}$$

which is positive definite and radially unbounded in the domain

$$\mathcal{D} \triangleq \{(x, z_1) \in \mathbb{R}^n \times \mathbb{R} \mid z_1 \in (-a_1, b_1)\}.$$

Suppose that the system (3.7) satisfies Assumption 3.1, then the time derivative of (3.11) along the trajectories of system (3.7) in closed-loop with the control law

$$v(x, z_1) = -c_1 z_1 - f_1(x, \xi_1) + \frac{\partial \alpha_1}{\partial x}(x) f(x, \xi_1) - \frac{\Gamma(z_1) T(x, \xi_1)}{z_1} \tag{3.12}$$

is rendered non-positive, and negative definite if $W(x)$ is positive definite. Furthermore, for all initial conditions in $\mathcal{D}$, system (3.7) in closed-loop with feedback (3.12) is $\mathcal{D}$-domain globally asymptotically stable ($\mathcal{D}$-DGAS - cf. Definition 2.10) at the origin, the feedback (3.12) is continuous, and the state ξ_1 is bounded as defined by (3.4).

Before stating the proof of Proposition 3.2, the following lemma, which defines a continuous and strictly positive function in an open, non-empty, and convex set, is required.

Lemma 3.3. *Let*

$$y(s) = 2 - \frac{s}{\sigma + s} + \frac{s}{\beta - s}. \tag{3.13}$$

If $\sigma, \beta \in \mathbb{R}_+$, then $y(s)$ is continuous and strictly positive for all $s \in (-\sigma, \beta)$.

Proof of Lemma 3.3. See Appendix A. □

We are now ready to state the proof of Proposition 3.2.

Proof of Proposition 3.2. Let us consider the x-subsystem

$$\dot{x} = f(x, \xi_1). \tag{3.14}$$

From Assumption 3.1, one obtains

$$\begin{aligned} \dot{V}(x) &= \frac{\partial V}{\partial x}(x) f(x, \xi_1) \\ &\leq -W(x) + \frac{\partial V}{\partial x}(x) \left[f(x, \xi_1) - f(x, \alpha_1(x)) \right] \\ &\leq -W(x) + T(x, \xi_1). \end{aligned} \tag{3.15}$$

Differentiating (3.8) with respect to time yields

$$\dot{z}_1 = v + f_1(x, \xi_1) - \frac{\partial \alpha_1}{\partial x}(x) f(x, \xi_1). \tag{3.16}$$

It follows that the time derivative of the chosen cLf (3.11) satisfies the inequality

$$\dot{U} \leq -W(x) + z_1 \left\{ \frac{T(x,\xi_1)}{z_1} + \frac{1}{\Gamma(z_1)} \left[\xi_2 + f_1(x,\xi_1) - \frac{\partial \alpha_1}{\partial x}(x) f(x,\xi_1) \right] \right\}, \tag{3.17}$$

which in closed-loop with the control law (3.12) is rendered non-positive, negative definite if $W(x)$ is positive definite, in $\mathcal{D}$

$$\dot{U} \leq -W(x) - \frac{k_1 c_1 z_1^2}{(a_1 + z_1)(b_1 - z_1)} \left[2 - \frac{z_1}{a_1 + z_1} + \frac{z_1}{b_1 - z_1} \right] \leq 0 \tag{3.18}$$

since, according to Lemma (3.3), the function in the square brackets in (3.18) is strictly positive for all $z_1 \in (-a_1, b_1)$. To prove that the origin of system (3.7) is $\mathcal{D}$-domain globally asymptotically stabilised by the control law (3.12), we apply LaSalle's Invariance Principle. Using (3.8) and (3.18), and let $(x_p(t), \xi_{1p}(t))$ denote a solution of system (3.7) in closed-loop with control law (3.12) such that

$$\begin{aligned} &W(x_p(t)) \\ &+ \frac{k_1 c_1 \left[\xi_{1p}(t) - \alpha_1(x_p(t))\right]^2}{(a_1 + [\xi_{1p}(t) - \alpha_1(x_p(t))])(b_1 - [\xi_{1p}(t) - \alpha_1(x_p(t))])} \left[2 - \frac{[\xi_{1p}(t) - \alpha_1(x_p(t))]}{(a_1 + [\xi_{1p}(t) - \alpha_1(x_p(t))])} \right. \\ &\qquad \left. + \frac{[\xi_{1p}(t) - \alpha_1(x_p(t))]}{(b_1 - [\xi_{1p}(t) - \alpha_1(x_p(t))])} \right] = 0 \end{aligned} \tag{3.19}$$

for all $t \geq 0$. Then $x_p(t)$ and $\xi_{1p}(t)$ satisfy

$$W(x_p(t)) = 0, \quad \xi_{1p}(t) = \alpha_1(x_p(t)), \quad \forall t \geq 0 \tag{3.20}$$

and

$$\dot{x}_p(t) = f(x_p(t), \alpha_1(x_p(t))), \quad \forall t \geq 0. \tag{3.21}$$

According to Assumption (3.1), it follows that the function $x_p(.)$ satisfies

$$x_p(t) = 0, \quad \forall t \geq 0. \tag{3.22}$$

Combining (3.20) and (3.22) yields

$$x_p(t) = 0, \quad \xi_{1p}(t) = 0, \quad \forall t \geq 0, \tag{3.23}$$

which guarantees that the origin of (3.7) in closed-loop with the control law (3.12) is $\mathcal{D}$-DGAS according to LaSalle's Invariance Principle [92].

The control law $v(x, z_1)$ is continuous in $\mathcal{D}$ by composition. Since all the terms on the right hand side of (3.12) is continuous in $\mathcal{D}$, $v(x, z_1)$ is therefore continuous in $\mathcal{D}$.

What remains is the proof of the boundedness of the state ξ_1. From (3.11) and (3.18), one obtains

$$\frac{k_1 z_1(t)^2}{(a_1 + z_1(t))\,(b_1 - z_1(t))} \leq U(t) \leq U(0), \quad \forall t \geq 0. \tag{3.24}$$

By inspection, this proves that

$$-a_1 < z_1(t) < b_1, \quad \forall t \geq 0. \tag{3.25}$$

It follows from equations (3.8) and (3.25), and Assumption 3.1 which assumes that $|\alpha_1(x)| \leq \Delta$, that the state ξ_1 is bounded, and the explicit bounds on the state ξ_1 are

$$\begin{aligned} & -a_1 \;<\; \xi_1(t) - \alpha_1(x(t)) \;<\; b_1 \\ \Longrightarrow \quad & -|a_1 + \Delta| \;<\; \xi_1(t) \;<\; |b_1 + \Delta|, \quad \forall t \geq 0. \end{aligned} \tag{3.26}$$

The design constants a_1, b_1 must satisfy $a_1 > \Delta$ and $b_1 > \Delta$ because it follows from (3.8) that

$$z_1(0) \triangleq \xi_1(0) - \alpha_1(x(0)). \tag{3.27}$$

Consider the initial condition where $\xi_1(0) = 0$ and $\alpha_1(x(0)) = \pm\Delta$, then

$$\begin{aligned} z_1(0) &= 0 - \pm\Delta \\ &= \mp\Delta. \end{aligned} \tag{3.28}$$

Thus, to satisfy (3.25), the design constants a_1, b_1 must be chosen such that $a_1 > \Delta$ and $b_1 > \Delta$ to prevent z_1 from being ill-conditioned. □

Remark 3.4. *Note that the domain of attraction $\mathcal{D}$ is given in the error coordinates $(x,\ z)^T$. The domain of attraction in the original coordinates $(x,\ \xi_1)^T$ can easily be computed using the diffeomorphism (3.8), and necessarily depends on the values of the design constants a_1 and b_1.*

Remark 3.5. *It is straightforward to see that if the bound Δ on the norm of the stabilising function $\alpha_1(x)$ can be made arbitrarily small, then the achieved state bounds (3.26) can be made to satisfy arbitrary prescribed bounds.*

3.1.2 Control tuning

In the proof of Proposition 3.2, we have described how the design constants a_1 and b_1, which are the desired bounds on the error variable z_1, must be tuned. In this section, we explain how to tune the design constant k_1, which has a direct effect on how close the error

variable z_1 gets to its imposed bounds $(-a_1, b_1)$ during its evolution. It was established in (3.24) that

$$\frac{k_1 z_1(t)^2}{(a_1 + z_1(t))\,(b_1 - z_1(t))} \leq U(t), \quad \forall t \geq 0.$$

Expanding out the denominator on the left hand side of the above inequality yields

$$\frac{k_1 z_1(t)^2}{a_1 b_1 + (b_1 - a_1) z_1(t) - z_1(t)^2} \leq U(t). \tag{3.29}$$

For simplicity, let us consider the example where $a_1 = 1$, $b_1 = 1$, which means that $z_1 \in (-1, 1)$. Simple algebraic manipulations of (3.29) lead to the following over-bound on the evolution of z_1

$$z_1(t)^2 \leq \frac{1}{\frac{k_1}{U(t)} + 1}.$$

By inspection, it is obvious that for a given value of $U(t)$, the smaller k_1 is, the closer to its bounds, which is $(-1, 1)$ in this example, $z_1(t)$ gets. Consequently, the state ξ_1 will be pushed closer to its bounds by virtue of (3.8).

We are now ready to state the main result for the full-order system (3.3).

3.1.3 Main result

Theorem 3.6. *Consider system (3.3) subject to a single state constraint as defined by (3.4). Let $a_1 > \Delta$, $b_1 > \Delta$, and $k_i, c_i \in \mathbb{R}_+$ be design constants, where Δ is as defined in Assumption 3.1. Define the error variables z_i, for $i = 1, ..., m$, as follows*

$$z_i = \xi_i - \alpha_i, \tag{3.30}$$

where α_i denote the intermediate stabilising functions of the backstepping technique. Suppose that system (3.3) satisfies Assumption 3.1, then a continuous control law $u(x, z)$ can be constructed such that the time derivative of the following candidate cLf for (3.3), which is positive definite and radially unbounded in domain $\mathcal{D}$,

$$U(x, z) = V(x) + \frac{k_1 z_1^2}{(a_1 + z_1)\,(b_1 - z_1)} + \sum_{i=2}^{m} k_i z_i^2 \tag{3.31}$$

along the trajectories of system (3.3) in closed-loop with $u(x, z)$ is rendered non-positive, negative definite if $W(x)$ is negative definite, as follows

$$\dot{U} = -W(x) - \frac{k_1 c_1 z_1^2}{(a_1 + z_1)\,(b_1 - z_1)} \left[2 - \frac{z_1}{a_1 + z_1} + \frac{z_1}{b_1 - z_1}\right] - \sum_{i=2}^{m} k_i c_i z_i^2 \leq 0, \tag{3.32}$$

where domain $\mathcal{D} \triangleq \{(x,z) \in \mathbb{R}^n \times \mathbb{R}^m \mid z_1 \in (-a_1, b_1)\}$. *Furthermore, for all initial conditions in* $\mathcal{D}$, *the closed-loop system is* $\mathcal{D}$*-DGAS at the origin, and the state* ξ_1 *is bounded as defined by (3.4).*

Proof of Theorem 3.6. Following verbatim the proof of Proposition 3.2, we can readily establish that the reduced-order system

$$\begin{cases} \dot{x} &= f(x, \xi_1) \\ \dot{\xi}_1 &= \xi_2 + f_1(x, \xi_1) \end{cases} \tag{3.33}$$

with the candidate cLf

$$U_1(x, z_1) = V(x) + \frac{k_1 z_1^2}{(a_1 + z_1)(b_1 - z_1)}$$

in closed-loop with

$$\alpha_2(x, z_1) = -c_1 z_1 - f_1(x, \xi_1) + \frac{\partial \alpha_1}{\partial x}(x) f(x, \xi_1) - \frac{\Gamma(z_1) T(x, \xi_1)}{z_1} \tag{3.34}$$

is asymptotically stable in $\mathcal{D}_1 \subseteq \mathcal{D} = \{(x, z_1) \in \mathbb{R}^n \times \mathbb{R} \mid z_1 \in (-a, b)\}$, and that the state ξ_1 is bounded as defined by (3.26). Now that we have achieved our objective of bounding the state ξ_1, standard backstepping (cf. Section 2.6) is recursively applied to the remaining subsystems until the full system (3.3) is stabilised by the actual control u. At the final step of the design procedure, we end up with

$$z_m = \xi_m - \alpha_m \tag{3.35}$$

Differentiating (3.35) with respect to time yields

$$\dot{z}_m = u + f_m(x, \xi_1, ..., \xi_m) - \dot{\alpha}_m \tag{3.36}$$

It follows that the time derivative of the chosen cLf (3.31) satisfies the inequality

$$\begin{aligned} \dot{U} \leq -W(x) - \frac{k_1 c_1 z_1^2}{(a_1 + z_1)(b_1 - z_1)} \left[2 - \frac{z_1}{a_1 + z_1} + \frac{z_1}{b_1 - z_1} \right] - \sum_{i=2}^{m-1} k_i c_i z_i^2 \\ + z_m \left[k_{m-1} z_{m-1} + k_m \{ u + f_m(x, \xi_1, ..., \xi_m) - \dot{\alpha}_m \} \right] \end{aligned} \tag{3.37}$$

which, in closed-loop with the following continuous control law

$$u(x, z) = -c_m z_m - f_m(x, \xi_1, ..., \xi_m) + \dot{\alpha}_m - \frac{k_{m-1} z_{m-1}}{k_m} \tag{3.38}$$

is rendered non-positive, and negative definite if $W(x)$ is negative definite, in domain $\mathcal{D}$

as follows

$$\dot{U} = -W(x) - \frac{k_1 c_1 z_1^2}{(a_1 + z_1)(b_1 - z_1)} \left[2 - \frac{z_1}{a_1 + z_1} + \frac{z_1}{b_1 - z_1} \right] - \sum_{i=2}^{m} k_i c_i z_i^2 \leq 0. \tag{3.39}$$

Asymptotic stability of system (3.3) in closed-loop with feedback (3.38) in domain $\mathcal{D}$ is proved by invoking LaSalle's Invariance Principle and establishing that the set in which $\dot{U} = 0$ contains only the origin. See the proof of Proposition 3.2 for details. □

The cLf (3.31) constructed in Theorem 3.6 centres on the use of the barrier function (cf. Definition 2.1)

$$y(z) = \frac{kz^2}{(a+z)(b-z)}, \tag{3.40}$$

where a, $b \in \mathbb{R}_+$, to ensure that the state constraints are strictly satisfied. It works by imposing increasingly severe penalties on trajectories approaching the constraint boundary. Infinitesimally close to the boundary, the cLf (3.31) becomes infinite, thus guaranteeing that all trajectories starting inside the open, non-empty, convex set $\mathcal{Z} = \{z \in \mathbb{R} \mid z \in (-a, b)\}$ remain in $\mathcal{Z}$ for all future time. Trajectories close to the origin however, receive negligible penalty. Whilst this is good in the sense that softer control actions are demanded, in certain applications, it is often more desirable to have the system converge to the demanded position as quickly as possible. This is also consistent with the notion of time-optimal control. Maximal convergence rates require the constrained states to be pushed right up against their bounds until convergence, and in minimal time. These objectives can be achieved by choosing the design constant k small as explained in Section 3.1.2.

Note that the barrier function $y(z) = \frac{kz^2}{(a+z)(b-z)}$ is only one of many functions that satisfies our bounded state control objective. Indeed, any candidate cLf in z that tends to infinity as z tends to either $-a$ or b will satisfy our control objective. Interesting examples include gradient re-centred logarithmic functions [153]. It is worth emphasising that the the form of the barrier function has no impact on the effectiveness of the final control law.

As pointed out in [123], recursively applying backstepping in its standard form generates analytical expressions of increasing complexity, primarily due to the dependence of α_{i+1} on the time derivative of α_i. The complexity is further exacerbated by the inclusion of the barrier function $y(z) = \frac{kz^2}{(a+z)(b-z)}$ in the above design procedure. After a couple of recursive steps, the time derivative of $y(z)$ alone gets discouragingly long and complicated, thus providing the motivation to seek alternative designs. In the next section, we detail a different design approach which leads to simpler stabilising control laws for essentially the same problem, albeit with a stronger set of assumptions. We would like to emphasise here that the simplified control laws are achieved by adopting a different design route, and not by implementing approximate differentiating filters, that is to replace $\dot{\alpha}_{i-1}$ by $\frac{s}{\tau_1 s+1}$, where τ_i is a small time constant, or by using linear high-gain feedbacks as exposed in [123].

3.2 The case of one constrained state: stabilisation with ISS-cLfs

The result presented in this section is an extension of the work in [54]. The control problem considered herein is slightly different to that of Section 3.1, and for clarity and the reader's convenience, we shall state the control problem in full here.

Given nonlinear systems of the form

$$\dot{x} = f(x, \xi_1) \tag{3.41a}$$
$$\dot{\xi}_1 = \xi_2 + f_1(x, \xi_1)$$
$$\vdots$$
$$\dot{\xi}_m = u + f_m(x, \xi_1, ..., \xi_m), \tag{3.41b}$$

where $(x, \xi) \in \mathbb{R}^n \times \mathbb{R}^m$ is the state variable, and $u \in \mathbb{R}$ is the control. The functions $f, ..., f_m$ are assumed to be sufficiently smooth, and $f(0,0) = f_1(0,0) = ... = f_m(0,0,...,0) = 0$. There exists a magnitude constraint on the state ξ_1 due to performance/physical limitations such that

$$|\xi_1(t)| \leq B, \quad \forall t \geq 0, \tag{3.42}$$

where the bounding constant $B \in \mathbb{R}_+$. Observe that the symmetric bound defined by (3.42) is stricter than the asymmetric bound considered in Section 3.1. The control objective is to develop explicit feedback control laws which asymptotically stabilise system (3.41), whilst keeping the state ξ_1 bounded as defined by (3.42).

3.2.1 Bounded state backstepping: an ISS redesign

The following set of assumptions is made on system (3.41).

Assumption 3.7. *There exist*

- *A function $W(x)$ which is positive definite, of class C^1, and satisfies*

$$W(x) \geq \gamma_3(|x|), \quad \forall x \in \mathbb{R}^n, \tag{3.43}$$

  where γ_3 is a class $\mathcal{K}_\infty$ function.

- *A function $V(x)$ which is positive definite, radially unbounded, of class C^1, and such that*

$$\gamma_1(|x|) \leq V(x) \leq \gamma_2(|x|), \quad \forall x \in \mathbb{R}^n, \tag{3.44}$$

  where γ_1, γ_2 are class $\mathcal{K}_\infty$ functions.

- *A sufficiently smooth control law $\alpha_1(x)$, bounded in norm by a positive constant Δ,*

satisfying $\alpha_1(0) = 0$, *and such that*

$$\frac{\partial V}{\partial x} f(x, \alpha_1(x)) \leq -W(x). \tag{3.45}$$

- *A class* $\mathcal{K}_\infty$ *function* σ *such that*

$$T(x, \xi_1) \leq \sigma(|\xi_1 - \alpha_1(x)|), \quad \forall [\xi_1 - \alpha_1(x)] \in \mathbb{R}, \tag{3.46}$$

where $T(x, \xi_1)$ *denotes*

$$T(x, \xi_1) = \frac{\partial V}{\partial x}(x) \left[f(x, \xi_1) - f(x, \alpha_1(x)) \right]. \tag{3.47}$$

Assumption 3.7 essentially requires that an ISS-cLf (cf. Definition 2.12) for the x-subsystem, with respect to the input signal $[\xi_1 - \alpha_1]$, exists and can be constructed. This assumption allows us to asymptotically stabilise the ξ-subsystem independently of the x-subsystem, that is, without having to cancel the cross-terms. Asymptotic stability of the full system (3.41) is proved by applying the ISS argument for interconnected cascades (cf. Definition 2.9).

Theorem 3.8. *Consider system (3.41) subject to a single state constraint as defined by (3.42). Define*

$$z_1 = \xi_1 - \alpha_1 \tag{3.48a}$$

$$z_2 = \xi_2 + f_1(x, \xi_1) - \frac{d\alpha_1(x)}{dt} \tag{3.48b}$$

$$z_3 = \xi_3 + f_2(x, \xi_1, \xi_2) + \frac{df_1(x, \xi_1)}{dt} - \frac{d^2\alpha_1(x)}{dt^2} \tag{3.48c}$$

$$\vdots$$

$$z_m = \xi_m + f_{m-1}(x, \xi_1, ..., \xi_m) + \frac{df_{m-2}}{dt} + \frac{d^2 f_{m-3}}{dt^2} + ... - \frac{d^{m-1}\alpha_1(x)}{dt^{m-1}}. \tag{3.48m}$$

Suppose that system (3.41) satisfies Assumption 3.7. If the following control law is chosen

$$u(x, z) = -\sum_{i=1}^{m} c_i z_i - f_m(x, \xi_1, ..., \xi_m) - \frac{df_{m-1}}{dt} - \frac{d^2 f_{m-2}}{dt^2} - ... + \frac{d^m \alpha_1}{dt^m}, \tag{3.49}$$

where $c_i \in \mathbb{R}_+$ *are design constants,* $i = 1, ..., m$, *then the system (3.41) in closed-loop with (3.49) is rendered globally asymptotically stable. Furthermore, given an initial condition* $z_1(0) \in [-b_1, b_1], z_2(0) \in [-b_2, b_2], ..., z_m(0) \in [-b_m, b_m]$, *where* $b_1, b_2, ..., b_m \in \mathbb{R}_+$, *there exists a constant* $\epsilon > 0$ *such that the state* ξ_1 *is bounded as follows*

$$|\xi_1(t)| \leq b_1 + \epsilon + \Delta, \quad \forall t \geq 0, \tag{3.50}$$

where Δ *is as defined in Assumption 3.7.*

Proof of Theorem 3.8. Let us consider the x-subsystem

$$\dot{x} = f(x, \xi_1) \tag{3.51}$$

From Assumption 3.7, one obtains

$$\begin{aligned}\dot{V}(x) &= \frac{\partial V(x)}{\partial x} f(x, \xi_1) \\ &\leq -W(x) + \frac{\partial V(x)}{\partial x} [f(x, \xi_1) - f(x, \alpha_1(x))] \\ &\leq -\gamma_3(|x|) + \sigma(|z_1|), \quad \forall x \in \mathbb{R}^n, \quad \forall z_1 \in \mathbb{R}. \end{aligned} \tag{3.52}$$

Thus, the x-subsystem is globally input-to-state stable with respect to the input z_1.

We will now describe the design procedure to globally asymptotically stabilise the ξ-subsystem. By applying the diffeomorphism (3.48), the ξ-subsystem can be expressed in the new z-coordinates as

$$\begin{aligned}\dot{z}_1 &= z_2 \\ \dot{z}_2 &= z_3 \\ &\vdots \\ \dot{z}_m &= u + f_m(x, \xi_1, ..., \xi_m) + \frac{df_{m-1}}{dt} + \frac{d^2 f_{m-2}}{dt^2} + ... - \frac{d^m \alpha_1(x)}{dt^m}, \end{aligned} \tag{3.53}$$

which in closed-loop with feedback (3.49) is rendered

$$\begin{aligned}\dot{z} &= \begin{bmatrix} 0 & 1 & \dots & 0 \\ \vdots & \ddots & \ddots & \vdots \\ 0 & 0 & \ddots & 1 \\ -c_1 & -c_2 & \dots & -c_m \end{bmatrix} z \\ &= Az. \end{aligned} \tag{3.54}$$

The design constants c_i can be chosen such that A is diagonalisable and Hurwitz, that is, all the eigenvalues of A are distinct and negative real. From Lyapunov's direct method for time-invariant linear systems [68], if A is Hurwitz, then for any symmetric, positive definite matrix $Q \in \mathbb{R}^{m \times m}$, there exists a symmetric, positive definite matrix $P \in \mathbb{R}^{m \times m}$ such that

$$-Q = A^T P + PA. \tag{3.55}$$

Let us choose the following positive definite and radially unbounded function as the candidate cLf for (3.54)

$$S(z) = z^T P z. \tag{3.56}$$

The time derivative of (3.56) is given by

$$\begin{aligned}\dot{S}(z) &= z^T(A^TP + PA)z \\ &= -z^TQz \end{aligned} \tag{3.57}$$

and is negative definite as the matrix Q is selected to be positive definite. Since $S(x)$ is positive definite and radially unbounded, and $\dot{S}(x)$ is negative definite, the system (3.53) is therefore globally asymptotically stable. The original system (3.41) can be re-written in the new coordinates $(x, z)^T$ as follows

$$\begin{aligned}\dot{x} &= f(x, z_1) \\ \begin{bmatrix} \dot{z}_1 \\ \vdots \\ \dot{z}_{m-1} \\ \dot{z}_m \end{bmatrix} &= \begin{bmatrix} 0 & 1 & \dots & 0 \\ \vdots & \ddots & \ddots & \vdots \\ 0 & 0 & \ddots & 1 \\ -c_1 & -c_2 & \dots & -c_m \end{bmatrix} \begin{bmatrix} z_1 \\ \vdots \\ z_{m-1} \\ z_m \end{bmatrix} = Az. \end{aligned} \tag{3.58}$$

According to Assumption 3.7, the x-subsystem is input-to-state stable with respect to the input z_1, and we have just proved that the z-subsystem is globally asymptotically stable. It follows from Corollary 2.9 that the interconnected system (3.58) is globally asymptotically stable at the origin. Consequently, the original system (3.41) in closed-loop with feedback (3.49) is globally asymptotically stable.

The remaining task is to prove the boundedness of the state ξ_1. Given that A is diagonalisable, solving the system of linear differential equations (3.54) yields the following explicit solution for z_1

$$z_1(t) = d_1e^{s_1t} + d_2e^{s_2t} + ... + d_me^{s_mt}, \tag{3.59}$$

where s_i, $i = 1, ..., m$, denote the eigenvalues of the matrix A and depend on the design constants c_i, and the constants $d_i \in \mathbb{R}$ depend on the eigenvectors of A as well as the initial condition $z(0) = [z_1(0), ..., z_m(0)]^T$ [25]. Furthermore,

$$d_1 + d_2 + ... + d_m = z_1(0). \tag{3.60}$$

By inspecting (3.59) and (3.60), it is evident that given the initial condition $z_1(0) \in [-b_1, b_1]$, $z_2(0) \in [-b_2, b_2]$, ..., $z_m(0) \in [-b_m, b_m]$, the design constants c_i can be tuned such that the evolution of z_1 is bounded by

$$|z_1(t)| \leq b_1 + \epsilon, \quad \forall t \geq 0. \tag{3.61}$$

From (3.48a) and Assumption 3.7, it follows that the state ξ_1 is bounded in norm, and

the explicit bound is given by

$$\begin{aligned} |\xi_1(t)| &= |z_1(t) + \alpha_1(t)| \\ &\leq b_1 + \epsilon + \Delta, \quad \forall t \geq 0. \end{aligned}$$

This concludes the proof. □

The control law (3.49) is simpler than (3.38) since it does not contain the cross-term $\frac{\Gamma(z_1)T(x,\xi_1)}{z_1}$ and its derivatives, which significantly reduces the design time for high-order systems. However, the simplicity of the design comes at a cost, and that is the determination of ISS-cLfs, which from a practical point of view, cannot always be carried out and in the majority of cases, far more complicated than the construction of non-ISS, non-strict cLfs. As a result, the applicability of the design proposed in this section is severely limited. Other drawbacks of the above design procedure are that the method only guarantees a domain semi-global result, and requires the explicit solution of the z-subsystem.

Note that although in the above proof, we employ backstepping-based feedback linearization to compute the control law (3.49), which obviates the need to cancel the cross-terms, other control laws can as easily be derived through the standard backstepping approach, which offers greater flexibility and design freedom, hence robustness, than feedback linearization. On the other hand, not cancelling the cross-terms has other advantages besides yielding simpler control laws. With additional assumptions, the design procedure detailed in this section can readily be extended to solve the problem of multiple state constraints, as will be shown in Chapter 4.

3.3 Application: active suspension system subject to suspension travel limits

We will now illustrate the validity and effectiveness of the proposed design procedures by applying Theorem 3.6 to the active suspension system for cars subject to suspension travel limits.

When designing active suspensions, the main objective is to achieve a high degree of ride comfort, and at the same time, maintain a good level of handling performance. To improve ride quality, hence passenger comfort, the objective is to minimize the vertical acceleration of the car's body. For good handling performance, the tire deformation must be kept as small as possible to minimize wheel hop, whilst simultaneously maximizing traction with the road. In addition, an important trade-off which must be factored into the overall design process is the ride quality versus the suspension travel. By suspension travel we mean the space variation between the car body and the tire. To improve passenger comfort, it is necessary to use more suspension travel. However, this increases the likelihood of hitting the suspension travel limits, which not only creates considerable passenger discomfort but also increases wear and tear of vehicle components. Thus, a robust active suspension design must behave differently on smooth and rough roads. On smooth

roads, the emphasis is on a soft response to ensure a high degree of passenger comfort. On rough roads, the suspension must stiffen up to avoid bottoming out. Simultaneously, tire deformations must be kept small at all time for handling and safety reasons. Such an amplitude-dependent response is not achievable with linear control as the response of a linear controller is invariably proportional to the amplitude of the error signal. Thus, if one chooses the gains such that the suspension limits are not violated when driving over rough roads, the design will then become too conservative, resulting in the ride quality on smooth roads being greatly compromised [81].

In this section, we apply the control design procedure presented in Section 3.1 to address the problem of suspension travel limits in active suspension designs. The problem has been considered previously by Lin and Kanellakopoulos [81], and Karlsson et al. [62] in the backstepping framework. In [81], the authors introduced a filter design whose effective bandwidth is dependent on the magnitude of the suspension travel. In [62], the authors intentionally introduced saturation nonlinearities into the controller to stiffen up the suspension near its travel limits. However, neither of the mentioned controller designs actually guarantees that the suspension travel will stay within its limits. The contribution of this section is a controller design for the active suspension system which guarantees that the suspension will never bottom out, that is, the suspension travel will never reach its limits.

3.3.1 Dynamical model and problem statement

We adopt the dynamic model given in [62] and use the quarter-car model to represent the suspension system, see Figure 3.3. In this model, the suspension actuator is taken to be a force actuator acting between the car body (the *sprung mass*) and the axle of the car. The tire is represented as an ideal, undamped spring between the axle and the ground. The axle and wheel assembly are represented as a mass (the *unsprung mass*) connected

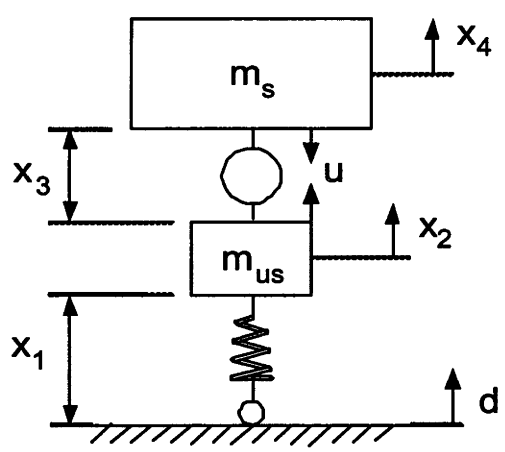

Figure 3.3: Quarter-car suspension model

to the ground via the spring which represents the tire. The suspension force also reacts against the unsprung mass. The system's dynamics is described by the following set of differential equations

$$\begin{aligned}\dot{x}_1 &= x_2 - d \\ \dot{x}_2 &= -\omega^2 x_1 + \rho u \\ \dot{x}_3 &= -x_2 + x_4 \\ \dot{x}_4 &= -u\end{aligned} \tag{3.62}$$

where we use the following notation

x_1	the deformation of the tire,
x_2	the unsprung mass (tire) velocity,
x_3	the suspension deflection,
x_4	the sprung mass (car body) velocity,
u	control force produced by the actuator,
d	the vertical ground velocity, which acts as a disturbance,
ω	the natural frequency of the unsprung mass,
ρ	the sprung to unsprung mass ratio.

The suspension travel limit is denoted by Ξ. That is,

$$|x_3(t)| < \Xi, \quad \forall t \geq 0. \tag{3.63}$$

The control objective is to construct an asymptotically stabilising control law for (3.62) such that the hard constraint on the suspension travel x_3 as defined by (3.63) is satisfied.

3.3.2 Controller design

Firstly, we need to transform system (3.62) into the form as described by (3.3). This is achieved with the following diffeomorphism [62]

$$\begin{aligned}\eta_1 &= x_1 + \frac{\rho}{\rho+1} x_3 \\ \eta_2 &= \frac{1}{\rho+1} x_2 + \frac{\rho}{\rho+1} x_4 \\ \xi_1 &= x_3 \\ \xi_2 &= -x_2 + x_4\end{aligned}$$

which yields

$$\begin{aligned}\dot{\eta}_1 &= \eta_2 - d \\ \dot{\eta}_2 &= -A\eta_1 + B\xi_1 \\ \dot{\xi}_1 &= \xi_2 \\ \dot{\xi}_2 &= C\eta_1 - D\xi_1 - Eu\end{aligned} \tag{3.64}$$

where

$$A = \frac{\omega^2}{\rho+1}, \quad B = \frac{\rho\omega^2}{(\rho+1)^2}, \quad C = \omega^2, \quad D = \frac{\rho\omega^2}{\rho+1}, \quad E = 1+\rho.$$

The system (3.64), which contains the η-subsystem driven by the constrained variable ξ_1, is exactly in the form as described by (3.3). Furthermore, the subsystem $\eta = (\eta_1, \eta_2)^T$ satisfies Assumption 3.1 with

$$V(\eta) = \frac{1}{2}A\eta_1^2 + \frac{1}{2}\eta_2^2, \tag{3.65}$$

and

$$\alpha_1(\eta) = -c_1 \tanh(k_1\eta_2). \tag{3.66}$$

Thus, according to Theorem 3.6, a continuous control law u can be constructed to asymptotically stabilise the system (3.64), whilst strictly satisfying the state constraint as defined by (3.63). It must also be noted that the controller design detailed in this section solves a stablisation problem and not a disturbance attenuation problem. Therefore, the design does not depend on where the disturbance enters the dynamic system. In addition, observe that it is impossible to solve a global L_∞ disturbance attenuation problem while keeping the state $\xi_1 \triangleq x_3$ bounded. We therefore take $d \equiv 0$ in the controller design process, which is reasonable since we only deal with disturbances that are almost impulsive in nature, and thus correspond to non-zero initial conditions [62]. The derivation of the control law u is presented in full below.

Step 1

Let us consider the η-subsystem

$$\begin{aligned} \dot{\eta}_1 &= \eta_2 \\ \dot{\eta}_2 &= -A\eta_1 + B\xi_1. \end{aligned} \tag{3.67}$$

The time-derivative of $V(\eta)$ is given by

$$\begin{aligned} \dot{V} &= A\eta_1\dot{\eta}_1 + \eta_2\dot{\eta}_2 \\ &= \eta_2\Big[A\eta_1 - A\eta_1 + B\xi_1\Big] \\ &= B\eta_2\xi_1, \end{aligned} \tag{3.68}$$

which in closed-loop with the stabilising function $\alpha_1(\eta)$ is rendered

$$\begin{aligned} \dot{V} &= -c_1 B\eta_2 \tanh(k_1\eta_2) + B\eta_2 z_1 \\ &\leq -W(\eta) + B\eta_2 z_1, \end{aligned} \tag{3.69}$$

where $c_1, k_1 \in \mathbb{R}_+$ are design constants. The error variable z_1 and the function $W(\eta)$ are given by

$$z_1 = \xi_1 - \alpha_1 \tag{3.70}$$

$$W = c_1 B \eta_2 \tanh(k_1 \eta_2), \tag{3.71}$$

respectively. Since the function $W(\eta)$ is positive semi-definite in $(\eta_1, \eta_2) \in \mathbb{R}^2$, it is obvious from (3.69) that $\dot{V}(\eta)$ is rendered negative semi-definite once z_1 is driven to zero. Application of Lasalle's Invariance Principle proves that the origin of the η-subsystem is indeed globally asymptotically stable when z_1 is driven to 0.

From (3.66), it follows that the stabilising function α_1 is bounded, and the bound on α_1 is

$$|\alpha_1(\eta(t))| \leq c_1, \quad \forall t \geq 0, \tag{3.72}$$

since $|\tanh(.)| \leq 1$.

Step 2

Consider the augmented subsystem for the η-subsystem

$$\dot{z}_1 = \xi_2 + c_1 k_1 \Big[1 - \tanh^2(k_1 \eta_2)\Big] \Big[-A\eta_1 + B\xi_1\Big], \tag{3.73}$$

and define the error variable for this design step z_2 as

$$z_2 = \xi_2 - \alpha_2. \tag{3.74}$$

Note that the stabilising function α_1 is bounded, see (3.72). We now require that the error variable z_1 to also be bounded in order to bound the state ξ_1. One candidate cLf that achieves this is

$$U_1(\eta, z_1) = V(\eta) + \frac{1}{2} k_3 \log\left(\frac{k_2^2}{k_2^2 - z_1^2}\right), \tag{3.75}$$

where $k_3 \in \mathbb{R}_+$, and $k_2 > c_1$ are design constants. The barrier function $\log\left(\frac{k_2^2}{k_2^2 - z_1^2}\right)$ is preferred over the barrier function $\frac{z_1^2}{(a+z_1)(b-z_1)}$ proposed in Theorem 3.6 because its time derivatives are simpler than the latter. In addition, since the state constraint in this problem is symmetric, the logarithmic barrier function suffices. This freedom to choose different candidate cLfs, hence the final control laws, exemplifies the flexibility of the backstepping method. The constant k_2 is the imposed bound on z_1. That is

$$|z_1(t)| < k_2, \quad \forall t \geq 0, \quad \forall |z_1(0)| < k_2, \tag{3.76}$$

and must satisfy the condition $k_2 > c_1$ because from (3.70), one obtains

$$z_1(0) = \xi_1(0) - \alpha_1(\eta(0)). \tag{3.77}$$

Consider the initial condition where $\xi_1(0) = 0$, and $\alpha_1(\eta(0)) = \pm c_1$, see (3.72), which yields

$$z_1(0) = 0 - \pm c_1 = \mp c_1. \tag{3.78}$$

Thus, k_2 must be tuned such that $k_2 > c_1$ to prevent z_1 from being ill-conditioned.

Differentiating $U_1(\eta, z_1)$ with respect to time yields

$$\begin{aligned}\dot{U}_1 &= \dot{V} + \frac{k_3 z_1 \dot{z}_1}{k_2^2 - z_1^2} \\ &= -W(\eta) + z_1\left\{B\eta_2 + \frac{k_3}{k_2^2 - z_1^2}\left(\xi_2 + c_1 k_1\left[1 - \tanh^2(k_1\eta_2)\right]\left[-A\eta_1 + B\xi_1\right]\right)\right\}.\end{aligned} \tag{3.79}$$

To render $\dot{U}_1$ negative semi-definite, the stabilising function for this design step, $\alpha_2(\eta, z_1)$, is chosen as

$$\alpha_2(\eta, z_1) = -c_2 z_1 - c_1 k_1\left[1 - \tanh^2(k_1\eta_2)\right]\left[-A\eta_1 + B\xi_1\right] - \frac{k_2^2 - z_1^2}{k_3} B\eta_2, \tag{3.80}$$

where $c_2 \in \mathbb{R}_+$ is a design constant. Such a choice for $\alpha_2(\eta, z_1)$ yields

$$\dot{U}_1 = -W - \frac{c_2 k_3 z_1^2}{k_2^2 - z_1^2} + \frac{k_3 z_1 z_2}{k_2^2 - z_1^2} \leq -W_1 + \frac{k_3 z_1 z_2}{k_2^2 - z_1^2} \tag{3.81}$$

and

$$\dot{z}_1 = -\frac{k_2^2 - z_1^2}{k_3} B\eta_2 - c_2 z_1 + z_2, \tag{3.82}$$

where

$$W_1 = W + \frac{c_2 k_3 z_1^2}{k_2^2 - z_1^2}, \tag{3.83}$$

and is semi-positive definite in the domain $\mathcal{D} = \{(\eta, z_1) \in \mathbb{R}^2 \times \mathbb{R} \mid z_1 \in (-k_2, k_2)\}$. It is clear from (3.81) that $\dot{U}_1$ is rendered positive semi-definite once z_2 is driven to zero. Application of Lasalle's Invariance Principle yields the conclusion that the subsystem (η, z_1) is $\mathcal{D}$-DGAS at the origin when z_2 is driven to 0.

Observe that the error signal z_1 is now bounded due to the hard-bound coded into the cLf (3.75). Since α_1 is bounded from (3.72), the suspension travel, $\xi_1 \triangleq x_3$, is bounded as

a direct result of (3.70). The explicit overbound on the suspension travel x_3 is

$$\begin{aligned} |x_3(t)| &\leq |z_1(t)| + |\alpha_1(t)| \\ &< k_2 + c_1. \end{aligned} \tag{3.84}$$

Step 3

Consider the last augmented subsystem

$$\dot{z}_2 = C\eta_1 - D\xi_1 - Eu - \dot{\alpha}_2. \tag{3.85}$$

The cLf for this design step is chosen as

$$U = U_1 + \frac{1}{2}k_4 z_2^2, \tag{3.86}$$

where $k_4 \in \mathbb{R}_+$ is a design constant, whose time derivative is given by

$$\dot{U} = -W_1 + z_2\left\{\frac{k_3 z_1}{k_2^2 - z_1^2} + k_4\left[C\eta_1 - D\xi_1 - Eu - \dot{\alpha}_2\right]\right\}. \tag{3.87}$$

The following final control law u is selected

$$u = -\frac{1}{E}\left\{-c_3 z_2 - C\eta_1 + D\xi_1 + \dot{\alpha}_2 - \frac{1}{k_4}\left[\frac{k_3 z_1}{k_2^2 - z_1^2}\right]\right\}, \tag{3.88}$$

where the design constant $c_3 \in \mathbb{R}_+$, and

$$\begin{aligned} \dot{\alpha}_2 = &-c_2\dot{z}_1 + 2c_1 k_1^2 \tanh(k_1\eta_2)\left[1 - \tanh^2(k_1\eta_2)\right]\dot{\eta}_2^2 \\ &- c_1 k_1\left[1 - \tanh^2(k_1\eta_2)\right]\left[-A\dot{\eta}_1 + B\dot{\xi}_1\right] \\ &+ \frac{2B}{k_3} z_1 \dot{z}_1 \eta_2 - \frac{k_2^2 - z_1^2}{k_3} B\dot{\eta}_2. \end{aligned} \tag{3.89}$$

Such a choice for u yields

$$\begin{aligned} \dot{z}_2 &= -c_3 z_2 - \frac{k_3 z_1}{k_4(k_2^2 - z_1^2)} \\ \dot{U} &= -W_1 - c_3 k_4 z_2^2 \leq -W_2 \end{aligned} \tag{3.90}$$

where

$$W_2 = W_1 + c_3 k_4 z_2^2,$$

and is positive semi-definite in the domain

$$\mathcal{D} = \{(\eta, z) \in \mathbb{R}^2 \times \mathbb{R}^2 \mid z_1 \in (-k_2, k_2)\}.$$

Consequently, the function $\dot{U}$ is positive semi-definite in the same domain and application of Lasalle's Invariance Principle proves that the system (η, z_1, z_2) is $\mathcal{D}$-DGAS at the origin. The control law (3.88) guarantees that the suspension will never bottom out, provided that the design constants are tuned appropriately, and that the initial condition for the error variable z_1 is proper. The closed-loop system in the error-coordinates is given by

$$\begin{aligned}
\dot{\eta}_1 &= \eta_2 \\
\dot{\eta}_2 &= -A\eta_1 - c_1 B \tanh(k_1\eta_2) + Bz_1 \\
\dot{z}_1 &= -\frac{k_2^2 - z_1^2}{k_3} B\eta_2 - c_2 z_1 + z_2 \\
\dot{z}_2 &= -c_3 z_2 - \frac{k_3 z_1}{k_4(k_2^2 - z_1^2)}
\end{aligned} \tag{3.91}$$

3.3.3 Simulation results

The closed-loop system is simulated in Matlab/Simulink. We simulate the situation when the car goes over an isolated bump of length $l = 2\text{m}$ and height A, on an otherwise flat road at a speed of $v = 25\text{m/s}$. The shape of the isolated bump is taken to be that of a haversine, which gives rise to the following road height function $r(t)$ [62]

$$r(t) = \begin{cases} 0, & t \leq 0, \\ \frac{A}{2}\left[1 - \cos\left(\frac{2\pi v}{l} t\right)\right], & 0 < t \leq \frac{l}{v}, \\ 0, & t > \frac{l}{v} \end{cases}$$

The above road height function $r(t)$ in turn gives rise to the following vertical ground velocity $d(t)$ [62]

$$d(t) = \begin{cases} 0, & t \leq 0, \\ 12.5\pi A \sin(25\pi t), & 0 < t \leq 0.08, \\ 0, & t > 0.08 \end{cases}$$

We run four sets of simulations. For the first three sets of simulations, the bump height A being set at 0.015m, 0.075m, and 0.11m with the system starting at zero initial condition. In the last set of simulations, the bump height is set to 0.11m. However, in this scenario, non-zero initial condition is imposed on the system. The following parameter values are used in the simulations: $\omega = 20\pi$ rad/s, and $\rho = 10$. The suspension travel limit, Ξ, is taken to be 0.1m, and the design constants are tuned as follows

$$k_1 = 3.5, \quad k_2 = 0.051, \quad k_3 = 0.07, \quad k_4 = 50, \quad c_1 = 0.049, \quad c_2 = 300, \quad c_3 = 500$$

For each bump response, we show plots of suspension travel, vertical body acceleration, and tire deformation. To obtain a qualitative measure of the performance of the pro-

posed controller design, we compare its responses (solid lines) against those of Karlsson's backstepping controller design (dashed lines).[1]

Figure 3.4 shows the response of the closed-loop system when going through a bump of height $A = 0.015$m. For bumps of this size, which are quite common on road surfaces, we require tire deflections to be small to ensure good road traction. In addition, small body acceleration is a must for passenger comfort [41,61]. It is clear from Figure 3.4 that these objectives are achieved with both controller designs. Comparing with Karlsson's controller design, we can see that our proposed controller design gives rise to slightly higher vertical body acceleration and suspension travel. Our proposed controller design however, achieves superior tire deformations and a shorter settling time, resulting in better handling performance.

From Figures 3.5 and 3.6, which depict the responses of the closed-loop system to bump heights of $A = 0.075$m and $A = 0.11$m, respectively, we can once again see that our proposed controller design produces slightly higher vertical body accelerations and suspension travels. On the other hand, smaller tire deformations and much shorter settling times are achieved, guaranteeing better grip on the road and improved handling.

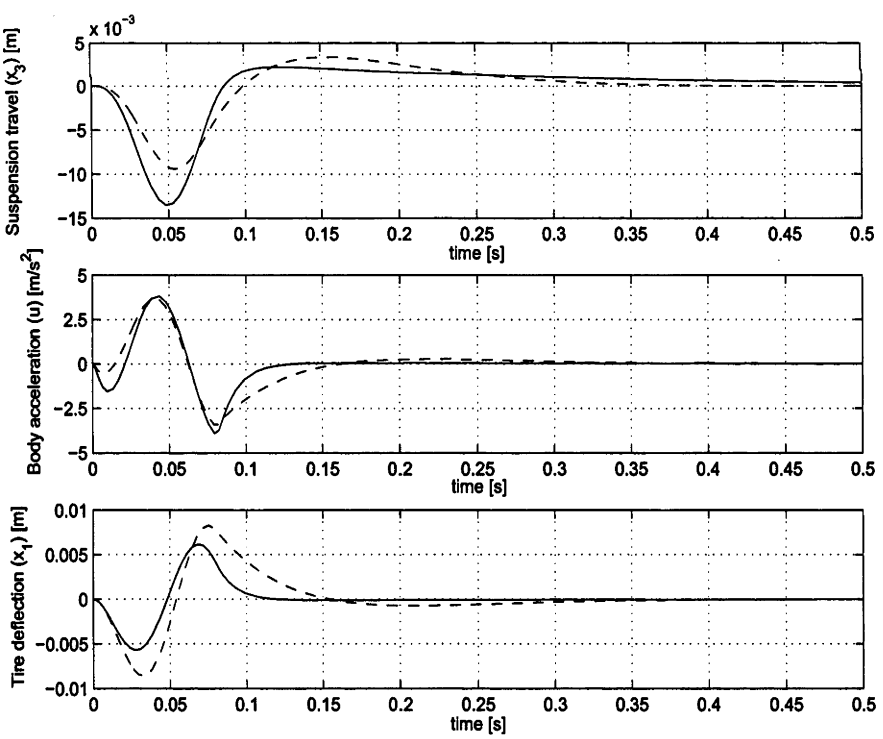

Figure 3.4: Closed-loop response to bump height $A = 0.015$m

[1]Karlsson's controller is obtained from his PhD thesis [61].

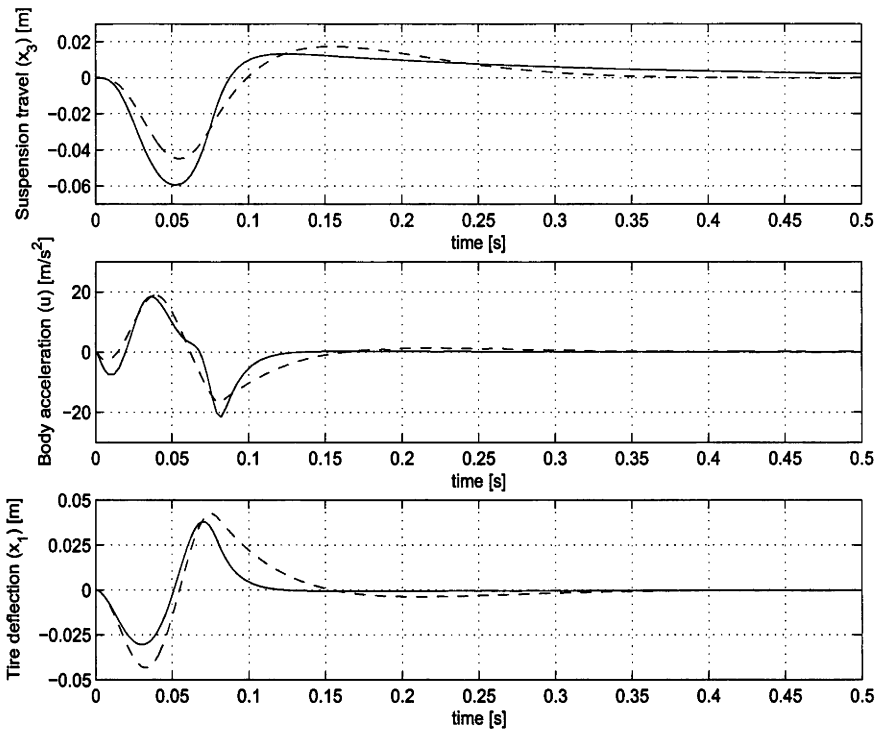

Figure 3.5: Closed-loop response to bump height $A = 0.075$m

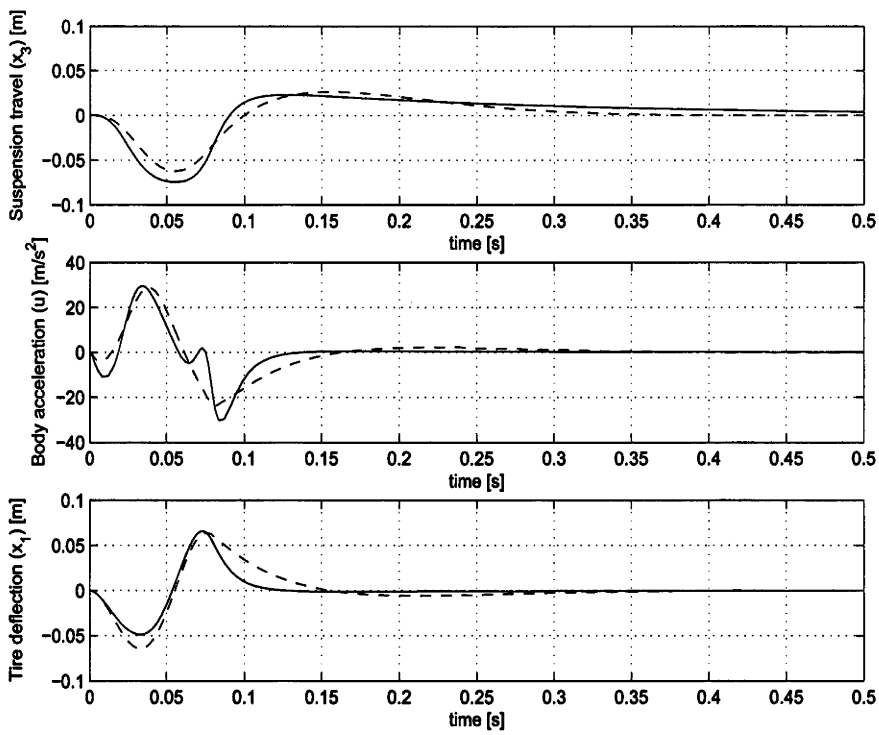

Figure 3.6: Closed-loop response to bump height $A = 0.11$m

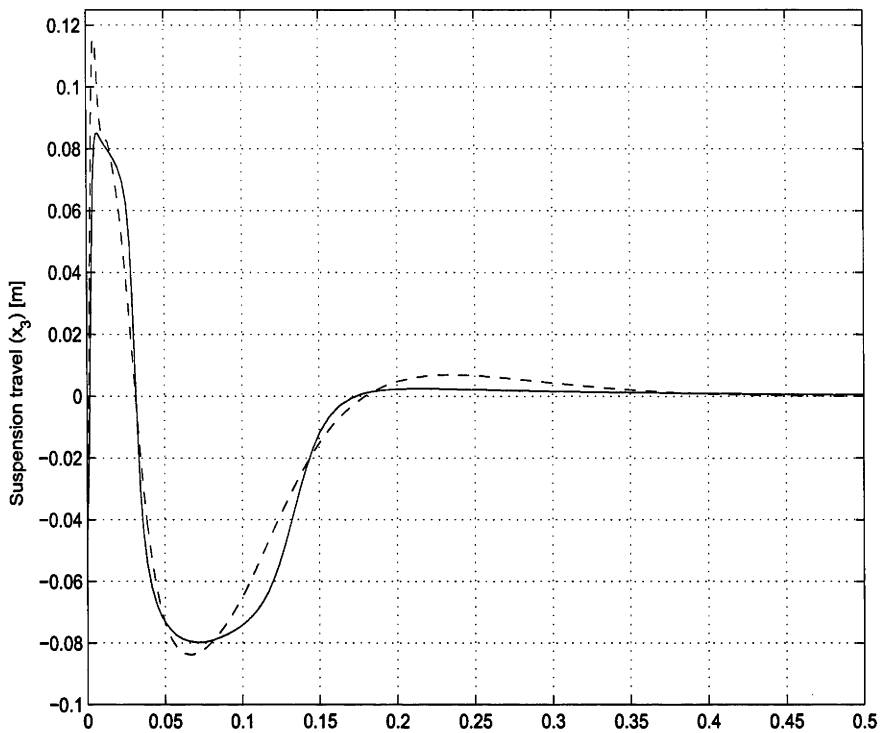

Figure 3.7: Closed-loop response to bump height $A = 0.1$m - non-zero initial condition

Figure 3.7 plots the suspension travel for both controllers. The bump height is set at $A = 0.11$m with the system starting at non-zero initial condition. The initial suspension travel (x_3) is set at -0.05m and the initial vertical velocity of the unsprung mass (x_2) is set at -20m/s. The figure shows that for this scenario, the suspension travel produced by Karlsson's controller exceeds the limits of $\pm$ 0.1m whereas the response produced by our proposed controller remains within the imposed limits.

3.4 The case of two state constraints

In this section, we extend the design procedure presented in Section 3.1 to asymptotically stabilise nonlinear systems subject to two consecutively constrained states. The class of systems considered remains the same as that of (3.3). All we require are additional conditions governing the growth properties of $V(x)$, $\alpha_1(x)$, and $f(x, \xi_1)$, as well as the boundedness of the function $f_1(x, \xi_1)$.

3.4.1 Problem statement

Consider system (3.3) subject to constraints on the states ξ_1 and ξ_2 as follows

$$-B_{1L} < \xi_1(t) < B_{1U}, \quad -B_{2L} < \xi_2(t) < B_{2U}, \quad \forall t \geq 0, \tag{3.92}$$

where B_{1L}, B_{1U}, B_{2L}, $B_{2U} \in \mathbb{R}_+$, B_{1L} and B_{2L} represent the lower limits, B_{1U} and B_{2U} represent the upper limits of the states ξ_1 and ξ_2, respectively. The control objective is to develop a systematic design procedure to asymptotically stabilise system (3.3), whilst strictly satisfying the state constraints as defined by (3.92) at all time.

3.4.2 Bounded states backstepping design

In addition to Assumption 3.1, the following assumptions are made on system (3.3).

Assumption 3.9. *There exist two positive constants Ψ_1 and Ψ_2 such that*

$$\left|\frac{\partial \alpha_1}{\partial x} f(x, \xi_1)\right| \leq \Psi_1, \tag{3.93}$$

and

$$\left|\frac{T(x, \xi_1)}{\xi - \alpha_1(x)}\right| \leq \Psi_2, \tag{3.94}$$

with

$$T(x, \xi_1) \triangleq \frac{\partial V}{\partial x}(x)\left[f(x, \xi_1) - f(x, \alpha_1(x))\right].$$

Assumption 3.10. *The function $f_1(x, \xi_1)$ is bounded in norm by a positive constant Ω, that is,*

$$|f_1(x, \xi_1)| \leq \Omega.$$

Assumption 3.9 governs the growth properties of the functions $V(x)$, $\alpha_1(x)$, and $f(x, \xi_1)$. Note that all the growth conditions are with respect to x, and not ξ_1 due to the fact that ξ_1 is bounded. Assumption 3.9 is important because it allows the stabilising function $\alpha_2(x, \xi_1)$ to be bounded in norm as will be shown later, which is crucial to the bounding of the state ξ_2. Indeed, the two-dimensional system (adapted from [35])

$$\begin{cases} \dot{x} &= -x^3 + x^3\xi \\ \dot{\xi} &= u \end{cases} \tag{3.95}$$

which satisfies Assumptions 3.1 and 3.10, but not Assumption 3.9 and admits unbounded trajectories, leading to the so called "finite escape time" phenomenon whenever u is a function bounded in norm by a constant [35].

Note that Assumptions 3.1, 3.9, and 3.10 do not imply that system (3.3) is locally exponentially stabilisable. It follows that the design procedure presented in this chapter is applicable to feedforward systems which can not be stabilised by the forwarding methods

of [123] or [93]. The following four-dimensional example illustrates this point

$$\begin{cases} \dot{x}_1 &= x_2 \\ \dot{x}_2 &= -\frac{x_1^5}{1+x_1^6} + \xi_1^3 \\ \dot{\xi}_1 &= \xi_2 \\ \dot{\xi}_2 &= u \end{cases}$$

with $x = (x_1, x_2)^T$ which is not locally exponentially stabilisable.

Similar to the approach taken in Section 3.1, we first consider the reduced-order system

$$\begin{cases} \dot{x} &= f(x, \xi_1) \\ \dot{\xi}_1 &= v + f_1(x, \xi_1) \end{cases} \tag{3.96}$$

with $v \in \mathbb{R}$ being the control signal, which gives rise to the following interesting result.

Proposition 3.11. *Suppose that system (3.96) satisfies Assumptions 3.1, 3.9, and 3.10. Let $a_1 > \Delta$, $b_1 > \Delta$, and k_1, $c_1 \in \mathbb{R}_+$ be design constants. Define the error variable z_1 and the function $\Gamma(z_1)$ as follows*

$$z_1 = \xi_1 - \alpha_1 \tag{3.97}$$

$$\Gamma(z_1) = \frac{[(a_1 + z_1)(b_1 - z_1)]^2}{k_1[2(a_1 + z_1)(b_1 - z_1)] - z_1\{(b_1 - z_1) - (a_1 + z_1)\}}. \tag{3.98}$$

Choose the following function as the candidate cLf for system (3.96)

$$U(x, z_1) = V(x) + \frac{k_1 z_1^2}{(a_1 + z_1)(b_1 - z_1)}, \tag{3.99}$$

which is positive definite and radially unbounded in the domain

$$\mathcal{D} \triangleq \{(x, z_1) \in \mathbb{R}^n \times \mathbb{R} \mid z_1 \in (-a_1, b_1)\}.$$

For all initial conditions in $\mathcal{D}$, the control law

$$v(x, z_1) = -c_1 z_1 - f_1(x, \xi_1) + \frac{\partial \alpha_1(x)}{\partial x} f(x, \xi_1) - \frac{\Gamma(z_1) T(x, \xi_1)}{z_1}, \tag{3.100}$$

where the function $T(x, \xi_1)$ is as defined in Assumption 3.9, renders the system (3.96) $\mathcal{D}$-DGAS at the origin. Furthermore, the state ξ_1 is bounded as defined by (3.92), and the control law v is bounded in norm.

Before stating the proof for Proposition 3.11, we require the following lemma, which defines a continuous and norm-bounded function in an open, non-empty, convex set.

Lemma 3.12. *Let*

$$y(s) = \frac{(\sigma+s)(\beta-s)}{2-\frac{s}{\sigma+s}+\frac{s}{\beta-s}} = \frac{[(\sigma+s)(\beta-s)]^2}{2(\sigma+s)(\beta-s)-s\{(\beta-s)-(\sigma+s)\}}. \tag{3.101}$$

If σ, $\beta \in \mathbb{R}_+$, *then* $y(s)$ *is continuous, and bounded by*

$$0 < y(s) \leq Y, \tag{3.102}$$

where $Y = \frac{\frac{1}{4}(\sigma+\beta)^3}{\sigma+\beta+2\sqrt{\sigma\beta}}$, *for all* $s \in (-\sigma, \beta)$.

Proof of Lemma 3.12. See Appendix A. □

We are now ready to present the proof for Proposition 3.11.

Proof of Proposition 3.11. In Proposition 3.2, we have established that if the design constants are tuned as stated, then the system (3.96) in closed-loop with feedback (3.100) is rendered $\mathcal{D}$-DGAS for all initial conditions in $\mathcal{D}$. It has also been proved that

$$-a_1 < z_1(t) < b_1, \tag{3.103}$$

and that the state ξ_1 is bounded and the explicit bounds are given by

$$-|a_1+\Delta| < \xi_1(t) < |b_1+\Delta|, \quad t \geq 0. \tag{3.104}$$

The remaining task is to prove the boundedness of the control law (3.100). From (3.103), and using Assumptions 3.9, 3.10 and Lemma 3.12, it follows that every term on the right hand side of (3.100) is bounded. Consequently, the control law (3.100) is bounded and the over-bound can be obtained explicitly as follows

$$|v(t)| < c_1 \max(a_1, b_1) + \Omega + \Psi_1 + \frac{Y_v \Psi_2}{k_1}, \quad \forall t \geq 0, \tag{3.105}$$

where $Y_v = \frac{\frac{1}{4}(a_1+b_1)^3}{a_1+b_1+2\sqrt{a_1 b_1}}$, Ψ_1, Ψ_2 are as defined in Assumption 3.9, and Ω is as defined in Assumption 3.10. □

Proposition 3.11 is interesting for two reasons. Firstly, it provides an alternative to solving the bounded control problem considered by Mazenc and Iggidr [92], albeit for a smaller class of systems. In addition, Proposition 3.11 is capable of accommodating saturation constraints on the state ξ_1. Secondly, there is a number of motion systems subject to both state and control saturation constraints whose equations of motion can be transformed into the cascade form of (3.96) as illustrated by the Reaction Wheel Pendulum control problem considered later in Section 3.5.

We will now present the main result for the full-order system (3.3).

3.4.3 Main result

Theorem 3.13. *Consider system (3.3) subject to state constraints as defined by (3.92). Let a_1, b_1, a_2, b_2, k_i, $c_i \in \mathbb{R}_+$ be design constants, $i = 1, ..., m$. The constants a_1, b_1 must satisfy the conditions $a_1 > \Delta$, $b_1 > \Delta$, where Δ is as defined in Assumption 3.1, and a_2, b_2 must satisfy the following conditions*

$$a_2 \geq c_1 \max(a_1, b_1) + \Omega + \Psi_1 + \frac{Y_v \Psi_2}{k_1},$$

and

$$b_2 \geq c_1 \max(a_1, b_1) + \Omega + \Psi_1 + \frac{Y_v \Psi_2}{k_1},$$

where $Y_v = \frac{\frac{1}{4}(a_1+b_1)^3}{a_1+b_1+2\sqrt{a_1 b_1}}$, Ψ_1, Ψ_2 are as defined in Assumption 3.9, and Ω is as defined in Assumption 3.10. Define the error variables as follows

$$z_i = \xi_i - \alpha_i, \quad i = 1, ..., m.$$

Suppose that system (3.3) satisfies Assumptions 3.1, 3.9, and 3.10. Then one can construct a continuous control law $u(x, z)$ such that the time derivative of the following cLf, which is positive definite and radially unbounded in $\mathcal{D}$,

$$U(x, z) = V(x) + \frac{k_1 z_1^2}{(a_1 + z_1)(b_1 - z_1)} + \frac{k_2 z_2^2}{(a_2 + z_2)(b_2 - z_2)} + \sum_{i=2}^{m} k_i z_i^2 \tag{3.106}$$

along the trajectories of system (3.3) in closed-loop with $u(x, z)$ is rendered non-positive, and negative definite if $W(x)$ is negative definite, as follows

$$\begin{aligned} \dot{U} = -W(x) &- \frac{k_1 c_1 z_1^2}{(a_1 + z_1)(b_1 - z_1)} \left[2 - \frac{z_1}{a_1 + z_1} + \frac{z_1}{b_1 - z_1}\right] \\ &- \frac{k_2 c_2 z_2^2}{(a_2 + z_2)(b_2 - z_2)} \left[2 - \frac{z_2}{a_2 + z_2} + \frac{z_2}{b_2 - z_2}\right] - \sum_{i=3}^{m} k_i c_i z_1^2, \end{aligned} \tag{3.107}$$

where domain $\mathcal{D}$ is given by

$$\mathcal{D} \triangleq \{(x, z) \in \mathbb{R}^n \times \mathbb{R}^m \mid z_1 \in (-a_1, b_1),\ z_2 \in (-a_2, b_2)\}. \tag{3.108}$$

Furthermore, for all initial conditions in $\mathcal{D}$, the closed-loop system is $\mathcal{D}$-DGAS at the origin, and the states ξ_1 and ξ_2 are bounded as defined by (3.92).

Proof of Theorem 3.13. Following verbatim the proof of Proposition 3.11, we can read-

ily prove that the subsystem

$$\begin{cases} \dot{x} &= f(x,\xi_1) \\ \dot{\xi}_1 &= \xi_2 + f_1(x,\xi_1) \end{cases} \tag{3.109}$$

with the candidate cLf

$$U_1 = V(x) + \frac{k_1 z_1^2}{(a_1+z_1)(b_1-z_1)} \tag{3.110}$$

in closed-loop with

$$\alpha_2(x,z_1) = -c_1 z_1 - f_1(x,\xi_1) + \frac{\partial \alpha_1(x)}{\partial x} f(x,\xi_1) - \frac{\Gamma(z_1)T(x,\xi_1)}{z_1}, \tag{3.111}$$

where the error variable $z_1 = \xi_1 - \alpha_1$, the function $\Gamma(z_1)$ is given by (3.98), and the function $T(x,\xi_1)$ is as defined in Assumption 3.9, is asymptotically stable in $\mathcal{D}_1 \subseteq \mathcal{D} = \{(x,z_1) \in \mathbb{R}^n \times \mathbb{R} \mid z_1 \in (-a_1,b_1)\}$. In addition, the state ξ_1 is bounded and the bounds are given by (3.104), and the stabilising function α_2 is bounded in norm as follows

$$|\alpha_2(x(t),z_1(t))| < c_1 \max(a_1,b_1) + \Omega + \Psi_1 + \frac{Y_v \Psi_2}{k_1}, \quad \forall t \geq 0. \tag{3.112}$$

Such a choice for α_2 yields

$$\begin{aligned} \dot{U}_1 &= -W(x) - \frac{k_1 c_1 z_1^2}{(a_1+z_1)(b_1-z_1)} \left[2 - \frac{z_1}{a_1+z_1} + \frac{z_1}{b_1-z_1}\right] + \frac{1}{\Gamma(z_1)} z_1 z_2 \\ &\leq -W_1(x,z_1) + \frac{1}{\Gamma(z_1)} z_1 z_2, \end{aligned} \tag{3.113}$$

and

$$\dot{z}_1 = -c_1 z_1 - \frac{\Gamma(z_1)T(x,\xi_1)}{z_1} + z_2, \tag{3.114}$$

where the error variable z_2 and the function $W_1(x,z_1)$ denote

$$\begin{aligned} z_2 &= \xi_2 - \alpha_2 \\ W_1(x,z_1) &= W(x) + \frac{k_1 c_1 z_1^2}{(a_1+z_1)(b_1-z_1)} \left[2 - \frac{z_1}{a_1+z_1} + \frac{z_1}{b_1-z_1}\right]. \end{aligned} \tag{3.115}$$

The function $W_1(x,z_1)$ is non-negative, and is positive definite if $W(x)$ is positive definite. It is thus obvious from (3.113) that $\dot{U}_1$ is non-positive, and is positive definite if $W(x)$ is positive definite, once z_2 is driven to 0.

Consider the following augmented subsystem for (3.114)

$$\dot{z}_2 = \xi_3 + f_2(x, \xi_1, \xi_2) - \frac{d\alpha_2}{dt}, \tag{3.116}$$

and define the error variable z_3 as follows

$$z_3 = \xi_3 - \alpha_3. \tag{3.117}$$

Since the stabilising function α_2 is bounded, all we need to do now is bound z_2 in order to have ξ_2 bounded, see (3.115). To achieve this, we select the following candidate cLf

$$U_2(x, z_1, z_2) = U_1 + \frac{k_2 z_2^2}{(a_2 + z_2)(b_2 - z_2)}. \tag{3.118}$$

The chosen cLf (3.118) is positive definite and radially unbounded in the domain $\mathcal{D}_2 \triangleq \{(x, z) \in \mathbb{R}^n \times \mathbb{R}^2 \mid z_1 \in (-a_1, b_1),\ z_2 \in (-a_2, b_2)\}$. Differentiating (3.118) with respect to time yields

$$\begin{aligned} \dot{U}_2 &= \dot{U}_1 + \frac{1}{\Gamma_1(z_2)} z_2 \dot{z}_2 \\ &\leq -W_1(x, z_1) + z_2 \left[\frac{1}{\Gamma(z_1)} z_1 + \frac{1}{\Gamma_1(z_2)} \left\{ \xi_3 + f_2(x, \xi_1, \xi_2) - \frac{d\alpha_2}{dt} \right\} \right], \end{aligned} \tag{3.119}$$

where $\Gamma_1(z_2)$ denotes

$$\Gamma_1(z_2) = \frac{[(a_2 + z_2)(b_2 - z_2)]^2}{k_2 [2(a_2 + z_2)(b_2 - z_2) - z_2\{(b_2 - z_2) - (a_2 + z_2)\}]}$$

whenever $U_2(x, z_1, z_2)$ is well-defined and bounded at every $t \geq 0$. From (3.116) and (3.119), the choice of

$$\alpha_3 = -c_2 z_2 - f_2(x, \xi_1, \xi_2) + \frac{d\alpha_2}{dt} - \frac{\Gamma_1(z_2)}{\Gamma(z_1)} z_1, \tag{3.120}$$

where $c_2 > 0$ is a design constant, renders

$$\dot{z}_2 = -c_2 z_2 - \frac{\Gamma_1(z_2)}{\Gamma(z_1)} z_1 + z_3 \tag{3.121}$$

$$\begin{aligned} \dot{U}_2 &= -W_1 - \frac{k_2 c_2 z_2^2}{(a_2 + z_2)(b_2 - z_2)} \left[2 - \frac{z_2}{a_2 + z_2} + \frac{z_2}{b_2 - z_2} \right] + \frac{1}{\Gamma_1(z_2)} z_2 z_3 \\ &\leq -W_2(x, z_1, z_2) + \frac{1}{\Gamma_1(z_2)} z_2 z_3, \end{aligned} \tag{3.122}$$

where

$$W_2(x, z_1, z_2) = W_1 + \frac{k_2 c_2 z_2^2}{(a_2 + z_2)(b_2 - z_2)} \left[2 - \frac{z_2}{a_2 + z_2} + \frac{z_2}{b_2 - z_2} \right] \tag{3.123}$$

and is non-positive, positive definite if $W(x)$ is positive definite, in $\mathcal{D}_2$ since according to Lemma 3.3, the function in the square brackets on the right hand side of (3.123) is strictly positive for all $z_2 \in (-a_2, b_2)$. It follows from (3.122) that $\dot{U}_2$ is rendered non-positive, positive definite if $W(x)$ is positive definite, in $\mathcal{D}_2$ once z_3 is driven to 0.

Observe that the stabilising function α_3 contains the cross-term $\frac{\Gamma_1(z_2)}{\Gamma(z_1)} z_1$ whose magnitude goes to infinity as z_1 gets infinitesimally close to $-a_1$ or b_1. This prohibits further bounding of the remaining state variables in the cascade (3.3) using this design procedure. Consequently, a different approach must be adopted to address the case where more than two states are constrained.

When z_3 has been driven to 0, ie. when $\xi_3 = \alpha_3$, one obtains

$$\dot{U}_2 \leq -W_2(x, z_1, z_2) \leq 0. \tag{3.124}$$

Application of Lyapunov's direct method [68] to (3.118) and (3.124) gives rise to the following

$$\frac{k_2 z_2(t)^2}{(a_2 + z_2(t))(b_2 - z_2(t))} \leq U_2(t) \leq U_2(0), \quad \forall t \geq 0. \tag{3.125}$$

By inspection, this proves that

$$-a_2 < z_2(t) < b_2, \quad \forall t \geq 0. \tag{3.126}$$

From (3.112) and (3.115), it follows that the state ξ_2 is bounded and the explicit bounds are given by

$$-a_2 < \xi_2(t) - \alpha_2(t) < b_2 \tag{3.127}$$

$$-\left| a_2 + c_1 \max(a_1, b_1) + \Omega + \Psi_1 + \frac{Y_v \Psi_2}{k_1} \right| < \xi_2(t) < \left| b_2 + c_1 \max(a_1, b_1) + \Omega + \Psi_1 + \frac{Y_v \Psi_2}{k_1} \right| \tag{3.128}$$

Similar to the conditions that $a_1 > \Delta$ and $b_1 > \Delta$, see the proof of Proposition 3.2, the conditions on the constants a_2 and b_2 such that

$$a_2 \geq c_1 \max(a_1, b_1) + \Omega + \Psi_1 + \frac{Y_v \Psi_2}{k_1} \tag{3.129}$$

$$b_2 \geq c_1 \max(a_1, b_1) + \Omega + \Psi_1 + \frac{Y_v \Psi_2}{k_1} \tag{3.130}$$

must be satisfied in order to prevent z_2 from being ill-conditioned.

Now that we have achieved our objective of bounding both ξ_1 and ξ_2, standard backstepping can be applied to stabilise the remaining subsystems of (3.3). We skip to the final step of the design when the last augmented subsystem is considered

$$\dot{z}_m = u + f_m(x, \xi_1, ..., \xi_m) - \frac{d\alpha_m}{dt}. \tag{3.131}$$

It then follows that the time derivative of the chosen cLf (3.106) satisfies the following inequality

$$\dot{U} \leq -W_2(x, z_1, z_2) - \sum_{i=2}^{m-1} k_i c_i z_i^2 + z_m \left[k_{m-1} z_{m-1} + k_m \left\{ u + f_m(x, \xi_1, ..., \xi_m) - \frac{d\alpha_m}{dt} \right\} \right], \tag{3.132}$$

whenever (3.106) is well-defined and bounded at every $t \geq 0$. Choosing the final control law

$$u(x, z) = -c_m z_m - f_m(x, \xi_1, ..., \xi_m) + \frac{d\alpha_m}{dt} - \frac{k_{m-1} z_{m-1}}{k_m}, \tag{3.133}$$

where $c_m \in \mathbb{R}_+$ is a design constant, renders $\dot{U}$ non-positive, and negative definite if W_2 is negative definite, in $\mathcal{D}$ as follows

$$\dot{U} \leq -W_2(x, z_1, z_2) - \sum_{i=2}^{m} k_i c_i z_i^2 \leq 0. \tag{3.134}$$

Asymptotic stability of system (3.3) in closed-loop with feedback (3.133) in $\mathcal{D}$ at the origin is proved by applying Lasalle's Invariance Principle and using Assumption (3.1) to establish that the set in which $\dot{U}(x, z) = 0$ contains only the origin. See the proof of Proposition 3.2 for details. □

Remark 3.14. *Note that the bounds on the state ξ_2, given in (3.128), and the lower bound for a_2 and b_2, given in (3.129) and (3.130), are conservative. The actual bounds can be much smaller in practice.*

3.5 Application: the Reaction Wheel Pendulum

The RWP is a mechanical system consisting of a pendulum with a rotating disk attached to the end, which is free to rotate about an axis parallel to the axis of the pendulum, see Figure 3.8. The disk is actuated by a DC-motor and the coupling torque generated by the angular acceleration of the disk can be used to actively control the system. The control

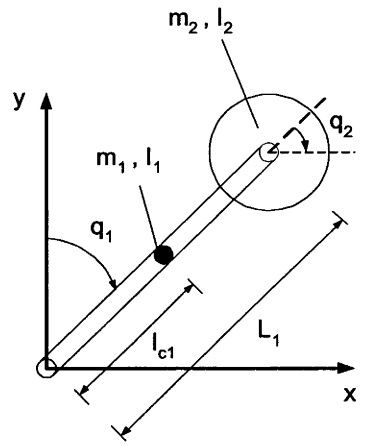

Figure 3.8: The Reaction Wheel Pendulum system

objective for the RWP is to asymptotically stabilise the system about the pendulum's upright position. The system was first introduced in [130] where a switching/hybrid control scheme was proposed. The swing-up problem was solved by a passivity-based controller, and a feedback linearization controller was employed to balance the pendulum about its its upright position. A switching schedule was then used to switch between the swing-up and the balance controllers. In [107], Olfati-Saber showed that the RWP's dynamics can be transformed into the nonlinear cascade form as described by (3.3), using a global change of coordinates in an explicit form. He then presented a standard backstepping-based controller design which globally asymptotically stabilises the RWP system about its upright position. His controller design, however, is highly aggressive and demands very high pendulum's velocities, which in turn impose severe loading at the pendulum's joint. Furthermore, the magnitude of the torque input is dependent on the state initial condition. In [30], Fantoni and Lozano proposed two passivity-based controller designs for the swinging-up problem. Although their controller designs allow the applied torque to be made to satisfy arbitrary bounds, the pendulum's velocities are excessively high, and the closed-loop system is not guaranteed to converge.

In this section, we apply the result from Proposition 3.11 to address the asymptotic stabilisation of the RWP system about its upright position subject to magnitude constraints on the pendulum's velocity and applied torque.

3.5.1 Dynamical model and problem statement

The dynamics of the RWP system can be described by the following Euler-Lagrangian equations [30]

$$\begin{aligned}(m_1 l_{c1}^2 + m_2 l_1^2 + I_1 + I_2)\ddot{q}_1 + I_2\ddot{q}_2 - (m_1 l_{c1} + m_2 l_1) g \sin(q_1) &= 0 \\ I_2\ddot{q}_1 + I_2\ddot{q}_2 &= \tau \end{aligned} \tag{3.135}$$

where the following notation is used

q_1	the position of pendulum with respect to the vertical,
q_2	the position of the rotating disk,
m_1	mass of the pendulum,
m_2	mass of the rotating disk,
L_1	length of the pendulum,
l_{c1}	distance from the joint to the centre of mass of the pendulum,
I_1	moment of inertia of the pendulum,
I_2	moment of inertia of the rotating disk,
g	gravity,
τ	motor torque applied on the rotating disk.

Let

$$\begin{aligned} d_{11} &= m_1 l_{c1}^2 + m_2 l_1^2 + I_1 + I_2 \\ d_{12} &= d_{21} = d_{22} = I_2 \\ d_0 &= (m_1 l_{c1} + m_2 l_1) g. \end{aligned} \tag{3.136}$$

Then the equations of motion can be re-written in a more compact form as follows

$$\begin{aligned} d_{11}\ddot{q}_1 + d_{12}\ddot{q}_2 - d_0 \sin(q_1) &= 0 \\ d_{21}\ddot{q}_1 + d_{22}\ddot{q}_2 &= \tau. \end{aligned} \tag{3.137}$$

Applying the following global change of coordinates [107]

$$\begin{aligned} \eta_1 &= m_{11}\dot{q}_1 + m_{12}\dot{q}_2 \\ \eta_2 &= q_1 \\ \eta_3 &= \dot{q}_2 \end{aligned} \tag{3.138}$$

yields

$$\begin{aligned} \dot{\eta}_1 &= d_0 \sin(\eta_2) \\ \dot{\eta}_2 &= \frac{\eta_1 - d_{12}\eta_3}{d_{11}} \\ \dot{\eta}_3 &= \frac{\tau - \frac{d_{21} d_0}{d_{11}} \sin(\eta_2)}{d_{22} - \frac{d_{21} d_{12}}{d_{11}}}. \end{aligned} \tag{3.139}$$

Since the position of the rotating disk, q_2, does not influence the dynamics of the RWP in any way, it is ignored as a state variable in the dynamic model [107]. Let us make a further change of variable. By defining $\xi = (\eta_1 - d_{12}\eta_3)/d_{11}$, the following dynamic model

is obtained

$$\begin{aligned}\dot{\eta}_1 &= d_0 \sin(\eta_2)\\ \dot{\eta}_2 &= \xi\\ \dot{\xi} &= A\sin(\eta_2) + C\sin(\eta_2) - B\tau,\end{aligned} \tag{3.140}$$

where

$$A = \frac{d_0}{d_{11}}, \quad B = \frac{d_{12}}{d_{11}d_{22} - d_{21}d_{12}}, \quad C = \frac{d_{12}d_{21}d_0/d_{11}}{d_{11}d_{22} - d_{21}d_{12}}.$$

Observe that the variable ξ now represents $\dot{q}_1$, ie. the angular velocity of the pendulum. Note also that system (3.140) is in the form described by (3.3). There exist limits on the angular velocity of the pendulum ξ and the applied torque τ as follows

$$|\xi(t)| \leq \Xi, \quad |\tau(t)| \leq \tau_{max}, \quad \forall t \geq 0, \tag{3.141}$$

where the constants Ξ, $\tau_{max} \in \mathbb{R}_+$.

The control objective is to explicitly construct a control law τ which asymptotically stabilises the Reaction Wheel Pendulum about its upright position, whilst strictly respect the constraints as defined by (3.141).

3.5.2 Controller design

Observe that the subsystem $\eta = (\eta_1, \eta_2)^T$ satisfies Assumptions 3.1, 3.9, and 3.10 with

$$V(\eta) = \frac{1}{2}k_1 \log\left(1 + \eta_1^2\right) + k_2 \log[2 - \cos(\eta_2)], \tag{3.142}$$

and

$$\alpha_1(\eta) = -c_1 \sin(\eta_2) - \frac{k_1 d_0 \eta_1 [2 - \cos(\eta_2)]}{k_2(1 + \eta_1^2)}, \tag{3.143}$$

where k_1, k_2, $c_1 \in \mathbb{R}_+$ are design constants. Thus, according to Proposition 3.11, a continuous control law τ can be constructed to asymptotically stabilise system (3.140) about its upright position whilst strictly satisfying the constraints as defined in (3.141). Note that the chosen cLf $V(\eta)$ is only valid in the set $\{(\eta_1, \eta_2) \in \mathbb{R}^2 \mid -\pi < \eta_2 \leq \pi\}$. This is physically intuitive since the pendulum can only move between $(-\pi, \pi]$. The full derivation of the control law τ is presented below.

Step 1

Let us consider the η-subsystem

$$\begin{aligned}\dot{\eta}_1 &= d_0 \sin(\eta_2)\\ \dot{\eta}_2 &= \xi\end{aligned} \tag{3.144}$$

The time derivative of $V(\eta)$ is given by

$$\dot{V}(\eta) = \sin(\eta_2)\left[\frac{k_1 d_0 \eta_1}{1+\eta_1^2} + \frac{k_2 \xi}{2-\cos(\eta_2)}\right] \tag{3.145}$$

which in closed-loop with the stabilising function $\alpha_1(\eta)$ satisfies the following inequality

$$\begin{aligned}\dot{V}(\eta) &= -\frac{c_1 k_2 \sin^2(\eta_2)}{2-\cos(\eta_2)} + \frac{k_2 \sin(\eta_2)}{2-\cos(\eta_2)} z\\ &\leq -W(\eta) + \frac{k_2 \sin(\eta_2)}{2-\cos(\eta_2)} z\end{aligned} \tag{3.146}$$

where $c_1 \in \mathbb{R}_+$ is a design constant, the error variable z and the function $W(\eta)$ denote

$$\begin{aligned}z &= \xi - \alpha_1\\ W(\eta) &= \frac{c_1 k_2 \sin^2(\eta_2)}{2-\cos(\eta_2)}.\end{aligned} \tag{3.147}$$

Observe that $W(\eta)$ is positive semi-definite in the set $\{(\eta_1, \eta_2) \in \mathbb{R}^2 \mid -\pi < \eta_2 \leq \pi\}$. Thus, $\dot{V}(\eta)$ is negative semi-definite in the same set once z is driven to 0. Asymptotic stability of the η-subsystem at the origin when z has been driven to 0 is proved by applying Lasalle's Invariance Principle [68].

From (3.143), it follows that the stabilising function $\alpha_1(\eta)$ is bounded by

$$|\alpha_1(t)| \leq c_1 + \frac{k_1 d_0}{k_2}, \quad \forall t \geq 0. \tag{3.148}$$

Step 2

Consider the augmented subsystem for the η-subystem

$$\dot{z} = A\sin(\eta_2) + C\sin(\eta_2) - B\tau - \frac{d\alpha_1(\eta)}{dt}, \tag{3.149}$$

where

$$\frac{d\alpha_1(\eta)}{dt} = -c_1\cos(\eta_2)\xi - \frac{k_1 d_0 \eta_1 \sin(\eta_2)\xi}{k_2(1+\eta_1^2)} - \frac{k_1 d_0^2 (2-\cos(\eta_2))\sin(\eta_2)}{k_2(1+\eta_1^2)^2}\left(1-\eta_1^2\right). \tag{3.150}$$

Since $\alpha_1(\eta)$ is bounded, see (3.148), we now require that the error variable z to also be bounded in order to bound the state ξ. One candidate cLf that achieves this is

$$U(\eta, z) = V(\eta) + \frac{1}{2}k_3 \log\left(\frac{k_4^2}{k_4^2 - z^2}\right), \tag{3.151}$$

where k_3, $k_4 \in \mathbb{R}_+$ are design constants, and k_4 is the imposed bound on z. That is, $|z(t)| < k_4$, $\forall t \geq 0$. In addition, k_4 must be tuned such that $k_4 > c_1 + \frac{k_1 d_0}{k_2}$ is satisfied. (See the Proof of Proposition 3.2 for full details). The chosen cLf $U(\eta, z)$ is positive definite and radially unbounded in the domain $\mathcal{D} \triangleq \{(\eta, z) \in \mathbb{R}^2 \times \mathbb{R} \mid -\pi < \eta_2 \leq \pi,\ z \in (-k_4, k_4)\}$. Differentiating $U(\eta, z)$ with respect to time yields

$$\dot{U}(\eta, z) = -W(\eta) + z\left[\frac{k_2 \sin(\eta_2)}{2 - \cos(\eta_2)} + \frac{k_3}{k_4^2 - z^2}\left\{A\sin(\eta_2) + C\sin(\eta_2) - B\tau - \frac{d\alpha_1(\eta)}{dt}\right\}\right]. \tag{3.152}$$

The control τ is chosen as

$$\tau = \frac{1}{B}\left[c_2 z + A\sin(\eta_2) + C\sin(\eta_2) - \frac{d\alpha_1(\eta)}{dt} + \frac{k_2(k_4^2 - z^2)\sin(\eta_2)}{k_3(2 - \cos(\eta_2))}\right]. \tag{3.153}$$

The function $\dot{U}(\eta, z)$ in closed-loop with feedback (3.153) satisfies the following inequality

$$\begin{aligned} \dot{U}(\eta, z) &\leq -W(\eta) - \frac{k_3 c_2 z^2}{k_4^2 - z^2} \\ &\leq 0, \end{aligned} \tag{3.154}$$

and is negative semi-definite in $\mathcal{D}$. Asymptotic stability of the closed-loop system at the origin is proved by applying Lasalle's Invariance Principle. The closed-loop system in the error-coordinates is given by

$$\begin{aligned} \dot{\eta}_1 &= d_0 \sin(\eta_2) \\ \dot{\eta}_2 &= -c_1 \sin(\eta_2) - \frac{k_1 m_0 \eta_1 [2 - \cos(\eta_2)]}{k_2(1 + \eta_1^2)} + z \\ \dot{z} &= -c_2 z - \frac{k_2(k_4^2 - z^2)\sin(\eta_2)}{k_3(2 - \cos(\eta_2))} \end{aligned} \tag{3.155}$$

From (3.151) and (3.154), it follows that

$$\frac{1}{2}k_3 \log\left(\frac{k_4^2}{k_4^2 - z^2}\right) \leq U(t) \leq U(0).$$

Thus,

$$|z(t)| < k_4, \quad \forall t \geq 0. \tag{3.156}$$

From (3.147), the bound on the state ξ can be explicitly computed as follows

$$|\xi(t)| = |z(t) + \alpha_1(t)| < k_4 + c_1 + \frac{k_1 d_0}{k_2}, \quad \forall t \geq 0. \tag{3.157}$$

Now that we have obtained an over-bound on the state ξ, we can prove that the control τ is also bounded. From (3.150), it follows that $\frac{d\alpha_1}{dt}$ is bounded, and the over-bound is given by

$$\left|\frac{d\alpha_1(t)}{dt}\right| < c_1 \left[k_4 + c_1 + \frac{k_1 d_0}{k_2}\right] + \frac{k_1 d_0 \left[k_4 + c_1 + \frac{k_1 d_0}{k_0}\right]}{2k_2} + \frac{2k_1 d_0^2}{k_2}, \quad \forall t \geq 0. \tag{3.158}$$

By examining (3.153), the following explicit bound on τ can be obtained

$$|\tau(t)| < \frac{1}{B}\left[c_2 k_4 + A + C + \left|\frac{d\alpha_1(t)}{dt}\right| + \frac{k_2 k_4^2}{k_3}\right], \quad \forall t \geq 0. \tag{3.159}$$

3.5.3 Simulation results

The closed-loop system is simulated in Matlab/Simulink. The following parameter values are used, which are the true system parameters of the RWP at the University of Illinois at Urbana-Champaign [30],

$$m_1 = 0.02\text{kg}, \quad m_2 = 0.3\text{kg}, \quad l_1 = 0.125\text{m}, \quad l_{c1} = 0.063\text{m},$$
$$I_1 = 47 \times 10^{-6}\text{kg.m}^2, \quad I_2 = 32 \times 10^{-6}\text{kg.m}^2, \quad g = 9.8\text{m.s}^{-2}$$

which yield

$$d_{11} = 4.83 \times 10^{-3}, \quad d_{12} = d_{21} = d_{22} = 32 \times 10^{-6}, \quad d_0 = 379.3 \times 10^{-3},$$
$$A = 78.52, \quad B = 208.42, \quad C = 523.7 \times 10^{-3}.$$

We desire a limit of $\pm$ 1rad/s on the angular velocity of the pendulum, and that the maximum input torque does not exceed $|\tau_{max}| \leq 0.4$ Nm. The design constants are tuned as follows

$$k_1 = 57.5 \times 10^{-3}, \quad k_2 = 2.225, \quad k_3 = 0.25,$$
$$k_4 = 0.501, \quad c_1 = 0.5, \quad c_2 = 1.$$

We run two sets of simulations. One for the initial condition of $(q_1, \dot{q}_1, \dot{q}_2) = (\pi/2, 0, 0)$, and another for the initial condition of $(q_1, \dot{q}_1, \dot{q}_2) = (\pi, 0, 0)$. For each set of simulations, plots of the pendulum's position, velocity, applied torque versus time, and the closed-loop trajectory in the $(q_1, \dot{q}_1)$ plane, are shown.

Figures 3.9-3.12 demonstrate that asymptotic stabilisation of the pendulum about its upright position is achieved. In terms of the imposed constraints, it is clear from Figures

3.9 and 3.11 that the magnitude of the pendulum's angular velocity and the magnitude of the applied torque remain below 1rad/s and 0.4Nm, irrespective of the initial condition. An intriguing feature which is obvious in Figure 3.11 is the slow rate of convergence of q_1 for approximately the first 6 seconds. This is due to the shape of the chosen cLf (3.142) whose gradient is very flat when $\eta_2 \triangleq q_1$ is close to $\pm\pi$. If a different $V(\eta)$, that is, one which does not have this property, can be constructed, then the transient response will greatly improve.

3.6 Chapter summary

Mechanical systems subject to state constraints are very common in practice. An example is the active suspension system with suspension travel limits. In this chapter, we have introduced two modified backstepping design procedures to asymptotically stabilise particular classes of non-affine, nonlinear systems subject to a single or two consecutively constrained states. The first approach, or the "non-strict" approach, assumes that only non-strict cLfs are available. The approach entails incorporating barrier function characteristics into the cLf, and propagating hard-bounds imposed on the pertinent stabilising functions through the steps of the backstepping methodology. The result is a class of controllers that asymptotically stabilises the closed-loop system, and strictly satisfies the imposed state constraints for all time $t \geq 0$. The validity and effectiveness of the design procedure are verified through closed-loop simulations of the active suspension system and the Reaction Wheel Pendulum benchmark system.

The second approach, or the "ISS" approach, is based on the notion of ISS, and therefore requires the computation of ISS-cLfs. Comparing with the first approach, this second approach generally yields considerably simpler control laws. One disadvantage associated with the first design procedure is that it leads to algebraically complex control laws due to the presence of barrier function terms in the cLf. However, since ISS-cLfs cannot always be determined, and in the majority of cases, much more difficult to construct than non-strict, non-ISS-cLfs, the applicability of the second approach is consequently more limited.

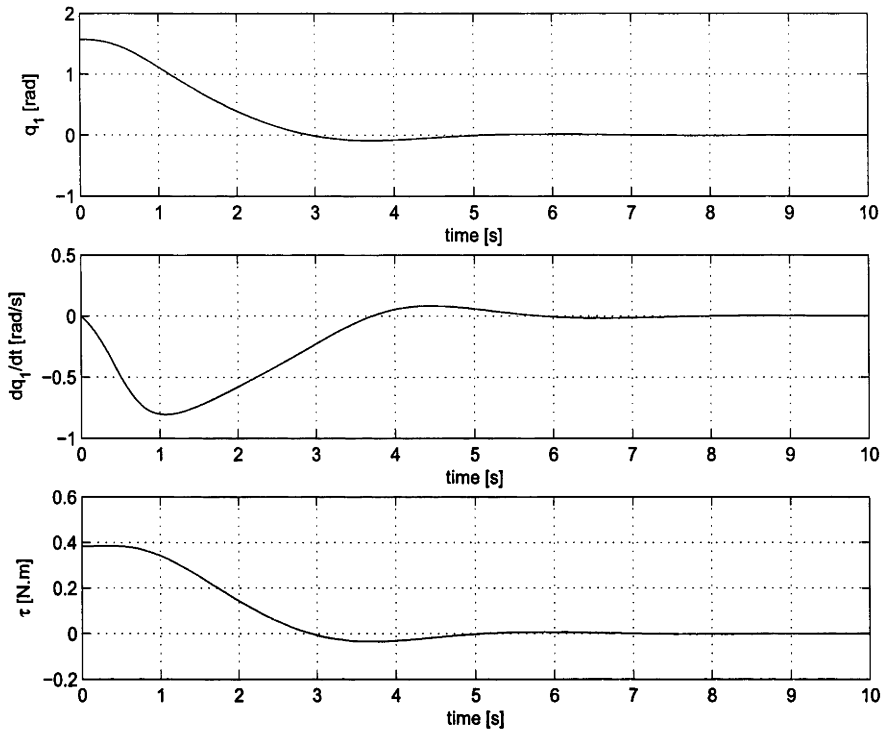

Figure 3.9: Closed-loop response to $(q_1, \dot{q}_1, \dot{q}_2) = (\pi/2, 0, 0)$

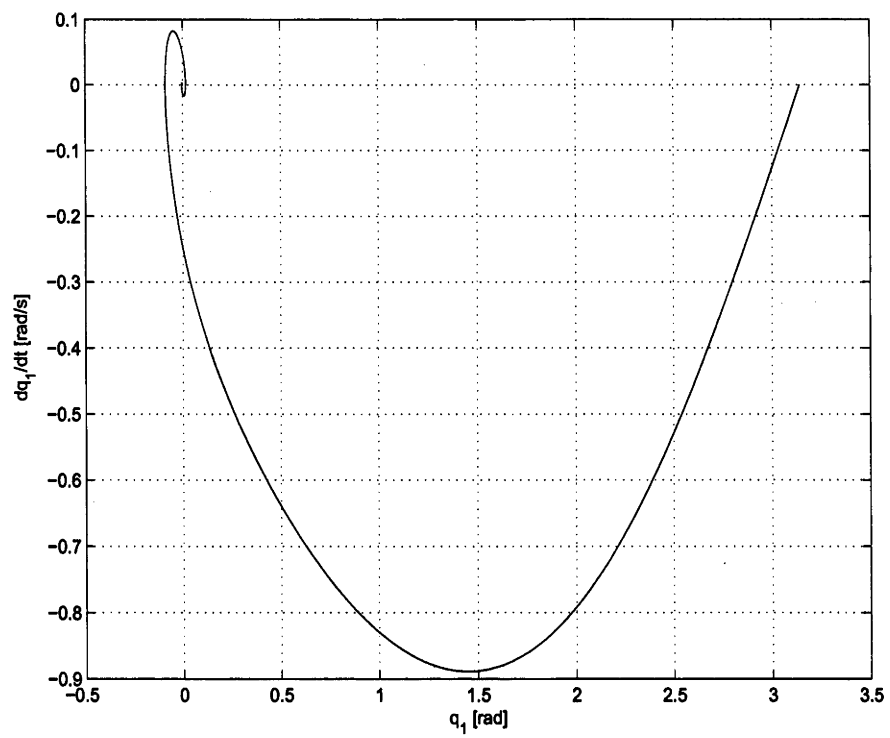

Figure 3.10: System trajectory in $(q_1, \dot{q}_1)$ plane with initial condition $(q_1, \dot{q}_1, \dot{q}_2) = (\pi/2, 0, 0)$

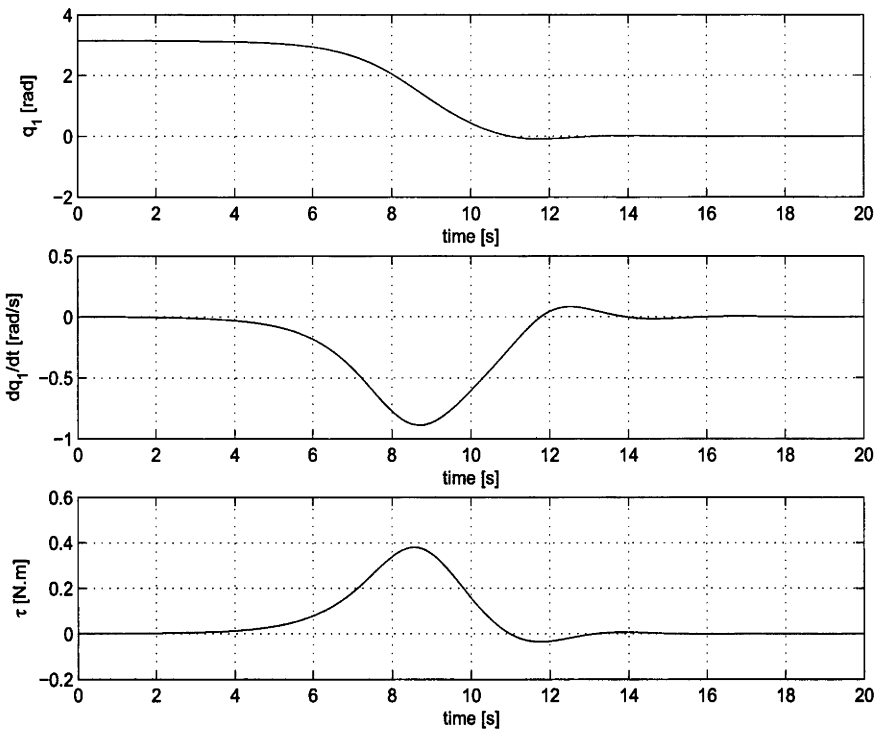

Figure 3.11: Closed-loop response to $(q_1, \dot{q}_1, \dot{q}_2) = (\pi, 0, 0)$

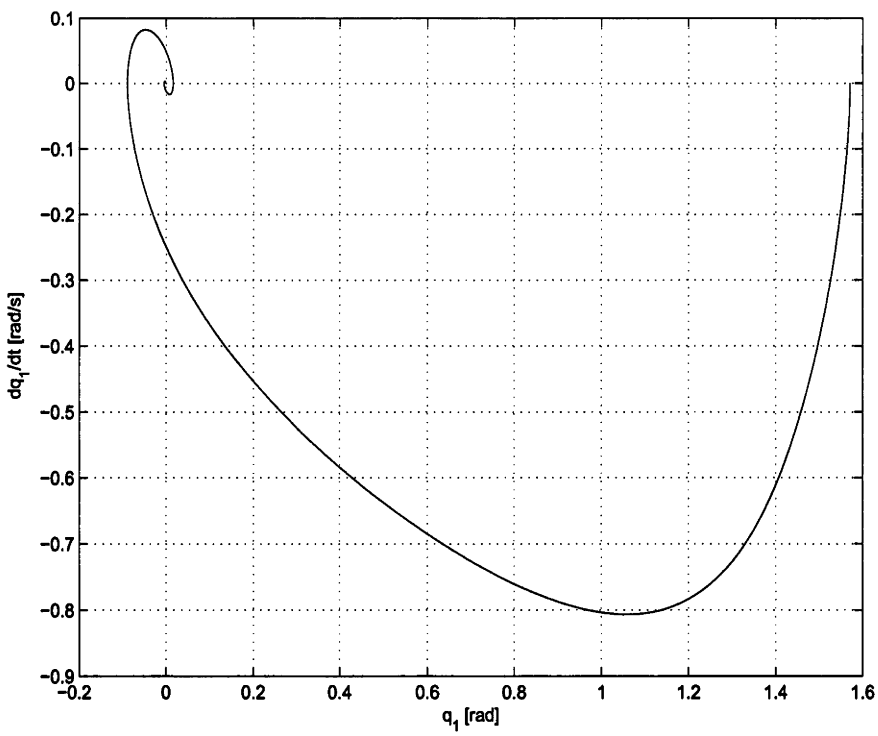

Figure 3.12: System trajectory in $(q_1, \dot{q}_1)$ plane with initial condition $(q_1, \dot{q}_1, \dot{q}_2) = (\pi, 0, 0)$

Chapter 4

Stabilisation of nonlinear systems subject to multiple state constraints

In the last chapter, we presented two systematic design procedures to asymptotically stabilise a class of nonlinear systems subject to a single or two consecutively constrained states. In this chapter, we extend both of those approaches to solve the stabilisation problem for a particular class of nonlinear systems subject to more than two consecutive state constraints. The problem is motivated by the consideration of physical motion systems where the nonlinear model of the system is only valid for a restricted band of velocities. We again use the 4^{th}-order longitudinal dynamics of a conventionally-configured aircraft, see Figure 1.3, as an example. The dynamic model comprises altitude, vertical velocity or climb rate, angle of attack, and pitch rate [134]. In this case, the vertical velocity, or climb rate, is proportional to the angle-of-attack of the aircraft. This internal state of the system model must be bounded below the stall angle-of-attack of the aircraft to avoid catastrophic failure of the closed-loop system. Structural strength of the airframe, and for commercial jet aircraft, the "passenger comfort" factor all impose magnitude constraints on both the aircraft's pitch attitude and pitch rate during manoeuvres which can be well below the actuator saturation limits.

The multiple state constraints control problem presents a significant increase in the level of complexity over the single or two consecutive state constraint cases considered in Chapter 3. The key difficulty of the problem lies in understanding the interactions between the state constraints without explicitly integrating the underlying ODEs in advance. Constraints on one system state variable of the system may lead to dynamic limitations on the evolution of the system which could cause another state variable to exceed its constraints, even though its initial conditions were well within the specified constraints. To account for these dependencies explicitly in the control design, one is naturally led towards industrially proven control techniques such as model predictive control (MPC). MPC, however, is computationally expensive and is therefore not suitable for systems possessing fast dynamics. The approach taken in this chapter is to impose a constructive nonlinear control design architecture on the problem and then deal with the complexities

of the problem as a nonlinear optimisation problem. That is, a constructive nonlinear design procedure is proposed, parameterised by a set of controller gains, that asymptotically stabilises the system and guarantees that the state constraints are satisfied at all time. Once the control architecture is fixed, a constrained nonlinear optimisation problem is formulated which characterises the correct choice of controller gains that achieves the required performance. If no feasible solution to the optimisation problem exists then this indicates that the nonlinear design architecture is incompatible with the specified state constraints. The design algorithm can be adjusted or re-formulated until a suitable or feasible solution is attained. The approach is motivated by the belief that the nonlinear design approach will provide a good structural representation of the constrained control problem. In practice, it may be convenient to partition the state-space and gain-schedule the final control law accordingly in order to enlarge the domain of validity of the control design. The proposed approach provides a purely algebraic process that can be performed off-line for complex systems.

The chapter is organised as follows. The problem statement is outlined in Section 4.1. In Section 4.2, the control design procedure which requires the construction of ISS-cLfs is presented. Section 4.3 details the design where only non-strict cLfs are assumed to be available. Simulation results are presented in Section 4.4 and Section 4.5 contains the concluding remarks.

4.1 Problem statement

Given nonlinear cascades of the form

$$\begin{aligned}
\dot{x} &= f(x, \xi_1) \\
\dot{\xi}_1 &= \xi_2 + f_1(x, \xi_1) \\
&\vdots \\
\dot{\xi}_m &= u + f_m(x, \xi_1, \ldots, \xi_m),
\end{aligned} \tag{4.1}$$

where $(x, \xi) \in \mathbb{R}^n \times \mathbb{R}^m$ is the state variable, and $u \in \mathbb{R}$ is the control input. The functions $f(x, \xi_1)$, $f_1(x, \xi_1)$, ..., $f_m(x, \xi_1, ..., x_m)$ are sufficiently smooth, and $f(0, 0) = 0$, $f_1(0, 0) = 0$, ..., $f_m(0, 0, ..., 0) = 0$. That is, the origin of (4.1) is an equilibrium point. There exist magnitude constraints on the system states due to physical/performance limits as follows

$$|\xi_i(t)| \leq \Xi_i, \quad i = 1, ..., m, \quad \forall t \geq 0. \tag{4.2}$$

The control objective is to develop a systematic procedure to design asymptotically stabilising controllers for system (4.1) subject to constraints as defined by (4.2).

4.2 Stabilisation with ISS-cLfs

In this section, we extend the result of Theorem 3.8 to solve the problem of multiple constraints as posed in the previous section. The design procedure presented herein is an extension of the work in [54].

We make the following assumptions on the system (4.1).

Assumption 4.1. *There exist*

- *A function $W(x)$ which is positive definite, of class C^1, and satisfies*

$$W(x) \geq \gamma_3(|x|), \quad \forall x \in \mathbb{R}^n, \tag{4.3}$$

where γ_3 is a class $\mathcal{K}_\infty$ function.

- *A function $V(x)$ which is positive definite, radially unbounded, of class C^1, and such that*

$$\gamma_1(|x|) \leq V(x) \leq \gamma_2(|x|), \quad \forall x \in \mathbb{R}^n, \tag{4.4}$$

where γ_1, γ_2 are class $\mathcal{K}_\infty$ functions.

- *A sufficiently smooth control law $\alpha_1(x)$ satisfying $\alpha_1(0) = 0$ and such that*

$$\frac{\partial V}{\partial x} f(x, \alpha_1(x)) \leq -W(x). \tag{4.5}$$

Furthermore, the norms of $\alpha_1(x)$ and its derivatives are bounded by positive constants.

- *A class $\mathcal{K}_\infty$ function σ such that*

$$T(x, \xi) \leq \sigma(|\xi_1 - \alpha_1(x)|), \quad \forall [\xi_1 - \alpha_1(x)] \in \mathbb{R}, \tag{4.6}$$

where $T(x, \xi)$ denotes

$$T(x, \xi_1) = \frac{\partial V}{\partial x}(x) \left[f(x, \xi_1) - f(x, \alpha_1(x)) \right]. \tag{4.7}$$

Assumption 4.2. *The functions $f_1(x, \xi_1)$, $f_2(x, \xi_1, \xi_2)$, ..., $f_{m-1}(x, \xi_1, ..., \xi_{m-1})$ and their derivatives are bounded in norm.*

Assumption 4.1 requires that an ISS-cLf for the x-subsystem with respect to the input signal $[\xi_1 - \alpha_1(x)]$ exists and can be constructed. This assumption affords us the freedom to asymptotically stabilise the ξ-subsystem independently of the x-subsystem. The advantage of this is that we do not have to cancel the cross-terms, resulting in simpler final control laws. Asymptotic stability of the full system (4.1) is proved by invoking the ISS argument for interconnected systems. The requirements that the stabilising function $\alpha_1(x)$ and its derivatives are bounded in norm and that Assumption 4.2 holds are necessary to bounding the states ξ_i, $i = 1, ..., m$.

Remark 4.3. *Note that in Assumption 4.2, we have placed no constraints on the function $f_m(x, \xi_1, ..., \xi_m)$. If f_m is also norm-bounded with bounded derivatives, then the design procedure outlined in this section will lead to control laws that are bounded in magnitude and rate as will be shown below.*

Theorem 4.4. *Consider the system (4.1) subject to state constraints as defined by (4.2). Define*

$$\begin{aligned} z_1 &= \xi_1 - \alpha_1 \\ z_2 &= \xi_2 + f_1 - \frac{d\alpha_1}{dt} \\ &\vdots \\ z_m &= \xi_m + f_{m-1} + \frac{df_{m-2}}{dt} + \frac{d^2 f_{m-3}}{dt^2} + ... - \frac{d^{m-1}\alpha_1}{dt^{m-1}}. \end{aligned} \tag{4.8}$$

Suppose that system (4.1) satisfies Assumptions 4.1 and 4.2. If the following control law is chosen

$$u(x, z) = -\sum_{i=1}^{m} c_i z_i - f_m - \frac{df_{m-1}}{dt} - \frac{d^2 f_{m-2}}{dt^2} - ... + \frac{d^m \alpha_1}{dt^m}, \tag{4.9}$$

where $c_i \in \mathbb{R}_+$ are design constants, then system (4.13) in closed-loop with (4.9) is rendered globally asymptotically stable. Consequently, given an initial condition in the set

$$\mathcal{IC} = \{(x, z) \in \mathbb{R}^n \times \mathbb{R}^m \mid z_1 \in [-Z_1, Z_1], z_2 \in [-Z_2, Z_2], ..., z_m \in [-Z_m, Z_m]\}, \tag{4.10}$$

where $Z_i \in \mathbb{R}_+$, there exist constants $b_i \in \mathbb{R}_+$ such that the evolution of the variables z_i is governed by

$$\begin{aligned} |z_1(t)| &\leq b_1, \\ |z_2(t)| &\leq b_2, \\ &\vdots \\ |z_m(t)| &\leq b_m, \quad \forall t \geq 0, \end{aligned}$$

and the states ξ_i are bounded in norm.

Proof of Theorem 4.4. Let us consider the x-subsystem

$$\dot{x} = f(x, \xi_1). \tag{4.11}$$

From Assumption 4.1, one obtains

$$\begin{aligned}\dot{V}(x) &= \frac{\partial V(x)}{\partial x} f(x, \xi_1) \\ &\leq -W(x) + \frac{\partial V(x)}{\partial x} [f(x, \xi_1) - f(x, \alpha_1(x))] \\ &\leq -\gamma_3(|x|) + \sigma(|z_1|), \quad \forall x \in \mathbb{R}^n, \quad \forall z_1 \in \mathbb{R}. \end{aligned} \tag{4.12}$$

Thus, the x-subsystem is globally input-to-state stable with respect to the input z_1.

Applying the diffeomorphism (4.8) to the ξ-subsystem yields

$$\begin{aligned}\dot{z}_1 &= z_2 \\ \dot{z}_2 &= z_3 \\ &\vdots \\ \dot{z}_m &= u + f_m + \frac{df_{m-1}}{dt} + \frac{d^2 f_{m-2}}{dt^2} + \ldots - \frac{d^m \alpha_1}{dt^m}. \end{aligned} \tag{4.13}$$

System (4.13) in closed-loop with control law (4.9) is rendered

$$\dot{z} = \begin{bmatrix} 0 & 1 & \ldots & 0 \\ \vdots & \ddots & \ddots & \vdots \\ 0 & 0 & \ddots & 1 \\ -c_1 & -c_2 & \ldots & -c_m \end{bmatrix} z = Az. \tag{4.14}$$

The original system (4.1) can now be re-written in the new coordinates $(x, z)^T$ as follows

$$\begin{aligned} \dot{x} &= f(x, z_1) \\ \begin{bmatrix} \dot{z}_1 \\ \vdots \\ \dot{z}_{m-1} \\ \dot{z}_m \end{bmatrix} &= \begin{bmatrix} 0 & 1 & \ldots & 0 \\ \vdots & \ddots & \ddots & \vdots \\ 0 & 0 & \ddots & 1 \\ -c_1 & -c_2 & \ldots & -c_m \end{bmatrix} \begin{bmatrix} z_1 \\ \vdots \\ z_{m-1} \\ z_m \end{bmatrix} = Az. \end{aligned} \tag{4.15}$$

Let us examine the z-subsystem (4.14). By inspection, it can be seen that the design constants c_i, $i = 1, \ldots, m$, can be tuned such that the matrix A is rendered diagonalisable and Hurwitz. If A is Hurwitz, then applying Lyapunov's direct method for time-invariant linear systems to (4.14), see the proof of Theorem 3.8, yields the conclusion that (4.14) is globally asymptotically stable. Since the x-subsystem is globally input-to-state stable with respect to the input z_1, and the z-subsystem is globally asymptotically stable, it then follows from Corollary 2.9 that the interconnected system (4.15) is globally asymptotically stable.

The remaining task is to prove the boundedness of the error variables z_i and the states

ξ_i. Given that A is diagonalisable, solving the system of linear differential equations (4.14) yields the following explicit solution [25]

$$\begin{aligned} z_1(t) &= d_{1,1}e^{s_1 t} + d_{1,2}e^{s_2 t} + ... + d_{1,m}e^{s_m t} \\ z_2(t) &= d_{2,1}e^{s_1 t} + d_{2,2}e^{s_2 t} + ... + d_{2,m}e^{s_m t} \\ &\vdots \\ z_m(t) &= d_{m,1}e^{s_1 t} + d_{m,2}e^{s_2 t} + ... + d_{m,m}e^{s_m t}, \end{aligned} \tag{4.16}$$

where s_i are the eigenvalues of (4.14), and the constants $d_{i,j}$ depend on the eigenvector of (4.14) and the initial condition of the error variables z_i. Furthermore,

$$\begin{aligned} d_{1,1} + d_{1,2} + ... + d_{1,m} &= z_1(0) \\ d_{2,1} + d_{2,2} + ... + d_{2,m} &= z_2(0) \\ &\vdots \\ d_{m,1} + d_{m,2} + ... + d_{m,m} &= z_m(0). \end{aligned} \tag{4.17}$$

By inspecting (4.16) and using (4.17), it is evident that given the initial condition $z_1(0) \in [-Z_1, Z_1]$, $z_2(0) \in [-Z_2, Z_2]$, ..., $z_m(0) \in [-Z_m, Z_m]$, the design constants c_i can be tuned such that the evolution of the variables z_i is governed by

$$\begin{aligned} |z_1(t)| &\leq b_1, \\ |z_2(t)| &\leq b_2, \\ &\vdots \\ |z_m(t)| &\leq b_m, \quad \forall t \geq 0, \end{aligned} \tag{4.18}$$

where the constants b_i can be computed explicitly from (4.16). From (4.8) and Assumptions 4.1 and 4.2, the states ξ_i are bounded and the explicit bounds are as follows

$$\begin{aligned} |\xi_1(t)| &= |z_1 + \alpha_1| \leq b_1 + |\alpha_1|, \\ |\xi_2(t)| &= \left| z_2 - f_1 + \frac{d\alpha_1}{dt} \right| \leq b_2 + |f_1| + \left| \frac{d\alpha_1}{dt} \right|, \\ &\vdots \\ |\xi_m(t)| &= \left| z_m - f_m - \frac{df_{m-1}}{dt} - \frac{d^2 f_{m-2}}{dt^2} - ... + \frac{d^m \alpha_1}{dt^m} \right| \\ &\leq b_m + |f_m| + \left| \frac{df_{m-1}}{dt} \right| + \left| \frac{d^2 f_{m-2}}{dt^2} \right| + ... + \left| \frac{d^m \alpha_1}{dt^m} \right|, \quad \forall t \geq 0. \end{aligned} \tag{4.19}$$

This concludes the proof. □

The above control design procedure is appealing in its systematic approach and sim-

plicity of the final control laws. These features have the potential to considerably reduce the design time for high-order systems. However, the major disadvantage associated with this design is that it relies on the construction of ISS-cLfs, which is practically difficult, and generally a far more mathematically involved task than the construction of non-ISS, non-strict cLfs.

Remark 4.5. *Inspection of the control law (4.9) reveals that if the function $f_m(x, \xi_1, ..., \xi_m)$ is bounded with bounded derivatives, then (4.9) is bounded in magnitude and rate. Consequently, the design procedure outlined in this section is equally apt in solving the problem of bounded controls and control rates as well as the problem of state constraints, or both.*

4.3 Stabilisation with non-strict cLfs

In this section, we extend the results of Theorems 3.6 and 3.8 to stabilise system (4.1) subject to multiple state constraints as defined by (4.2). The design procedure proposed in this section differs from the one outlined in the previous section in that only non-strict cLfs for the x-subsystem are assumed to be available. The main features of the design consist of shaping the cLfs to bound and suppress the propagation of the errors at each stage of the backstepping procedure, and introducing barrier-function-like terms to impose hard bound on the associated error signals. In addition, it was shown in the preceding chapter that if the cross-terms are cancelled, the method cannot be extended to address the problem of more than two consecutive state constraints due to the fact that the cross-terms escape to infinity at the constraint boundaries. To circumvent this problem, we will employ domination rather than direct cancellation of the cross-terms. The result presented in this chapter is an extension of the paper [104].

4.3.1 Control design procedure

We make the following assumptions on system (4.1).

Assumption 4.6. *There exist*

- *A function $V(x)$ which is positive definite, radially unbounded, and of class C^1.*
- *A function $W(x)$ which is non-negative and of class C^1.*
- *A sufficiently smooth control law $\alpha_1(x)$ satisfying*

$$\alpha_1(0) = 0$$
$$\frac{\partial V}{\partial x} f(x, \alpha_1(x)) \leq -W(x).$$

Furthermore, the norms of $\alpha_1(x)$ and its derivatives are bounded by positive constants.

- *The solution $x(t) = 0$ is the unique function satisfying, for all t,*

$$\dot{x}(t) = f(x(t), \alpha_1(x(t))), \quad W(x(t)) = 0.$$

Assumption 4.7. *The function*

$$\frac{T(x, \xi_1)}{\xi_1 - \alpha_1(x)} \tag{4.20}$$

with

$$T(x, \xi_1) \triangleq \frac{\partial V}{\partial x}(x) \left[f(x, \xi_1) - f(x, \alpha_1(x)) \right] \tag{4.21}$$

and its derivatives are bounded in norm by positive constants.

Assumption 4.8. *The functions $f_1(x, \xi_1)$, $f_2(x, \xi_1, \xi_2)$, ..., $f_{m-1}(x, \xi_1, ..., \xi_{m-1})$ and their derivatives are bounded by positive constants.*

Assumption 4.6 is essential to the global asymptotic stabilisation of the x-subsystem and to the bounding of the state ξ_1. Assumptions 4.7 and 4.8 are necessary to the bounding of the states ξ_i, $i = 2, ..., m$.

Remark 4.9. *Note that in Assumption 4.8, we have made no assumptions on the function $f_m(x, \xi_1, ..., \xi_m)$. As will be shown later, if $f_m(x, \xi_1, ..., \xi_m)$ and its derivatives are also bounded in norm by positive constants, then the design procedure outlined in this section has the potential to simultaneously solve the problem of multiple state constraints as well as the problem of bounded controls and control rates.*

The design procedure proceeds as follows.

Step 1

Consider the subsystem

$$\begin{aligned} \dot{x} &= f(x, \xi_1) \\ \dot{\xi}_1 &= \xi_2 + f_1(x, \xi_1) \end{aligned} \tag{4.22}$$

and introduce the error variables

$$z_1 = \xi_1 - \alpha_1. \tag{4.23}$$

From Assumption 4.6, one obtains

$$\begin{aligned} \dot{V}(x) = \frac{\partial V}{\partial x}(x) f(x, \xi_1) &\leq -W(x) + \frac{\partial V}{\partial x} \left[f(x, \xi_1) - f(x, \alpha_1(x)) \right] \\ &\leq -W(x) + T(x, \xi_1). \end{aligned} \tag{4.24}$$

Differentiate (4.23) with respect to time yields

$$\dot{z}_1 = \xi_2 + f_1(x, \xi_1) - \frac{d\alpha_1(x)}{dt}. \tag{4.25}$$

With the stabilising function $\alpha_1(x)$ being bounded in norm from Assumption 4.6, we are now only required to saturate the error variable z_1 in order to satisfy the bound on the state ξ_1 according to (4.23). This is achieved by defining the cLf for (4.25) with a barrier function structure such that the growth of the cLf is governed by

$$|z_1| \to \Delta_{z_1} \quad \Longrightarrow \quad U_1(z_1) \to +\infty \tag{4.26}$$

where the constant $\Delta_{z_1} \in \mathbb{R}_+$ denotes the desired hard-bound on z_1. A candidate cLf is

$$U_1(x, z_1) = V(x) + \frac{1}{2} k_1 \log\left(\frac{k_2^2}{k_2^2 - z_1^2}\right) \tag{4.27}$$

where $k_1 \in \mathbb{R}_+$ is a design constant, and the constant $k_2 \in \mathbb{R}_+$ is the desired hard-bound on the error variable z_1. The cLf (4.27) is positive definite and radially unbounded in the domain

$$\mathcal{D}_1 \triangleq \{(x, z_1) \in \mathbb{R}^n \times \mathbb{R} \mid z_1 \in (-k_2, k_2)\}.$$

Observe that (4.27) satisfies the required growth condition (4.26), that is, as $|z_1| \to k_2$, $U_1 \to +\infty$. Consequently, such a choice of cLf yields

$$|z_1(t)| < k_2, \quad \forall t \geq 0. \tag{4.28}$$

It follows that the time derivative of (4.27) satisfies the inequality

$$\dot{U}_1 \leq -W(x) + z_1 \left\{ \frac{T(x, \xi_1)}{z_1} + \frac{k_1}{k_2^2 - z_1^2} \left[\xi_2 + f_1(x, \xi_1) - \frac{d\alpha_1(x)}{dt} \right] \right\}, \tag{4.29}$$

whenever $U_1(x, z_1)$ is well-defined and bounded at every $t \geq 0$. The choice of

$$\alpha_2 = -c_1 z_1 - f_1(x, \xi_1) + \frac{d\alpha_1(x)}{dt} - \frac{(k_2^2 - z_1^2) T(x, \xi_1)}{k_1 z_1}, \tag{4.30}$$

where $c_1 \in \mathbb{R}_+$ is a design constant, renders

$$\dot{U}_1 \leq -W(x) - \frac{k_1 c_1}{k_2^2 - z_1^2} z_1^2 + \frac{k_1}{k_2^2 - z_1^2} z_1 z_2 \tag{4.31}$$

and

$$\dot{z}_1 = -c_1 z_1 - \frac{(k_2^2 - z_1^2) T(x, \xi_1)}{k_1 z_1} + z_2, \tag{4.32}$$

where the error variable z_2 is defined by

$$z_2 = \xi_2 - \alpha_2. \tag{4.33}$$

It is evident from (4.31) that $\dot{U}_1(x, z_1)$ is non-positive, and negative definite when $W(x)$ is positive definite, on domain $\mathcal{D}_1$ once z_2 is driven to 0.

Now that z_1 is bounded and from Assumption 4.6, $\alpha_1(x)$ is also bounded, the state ξ_1 is bounded as a direct result of (4.23). The over-bound on ξ_1 can be explicitly obtained by using (4.23), (4.28), and Assumption 4.6, as follows

$$\begin{aligned} |\xi_1(t)| &= |z_1(t) + \alpha_1(x(t))| \\ &< k_2 + |\alpha_1(x(t))|. \end{aligned} \tag{4.34}$$

The design constant k_2 must be tuned such that $k_2 > |\alpha_1(x(t))|$ because from (4.23), one obtains

$$z_1(0) \triangleq \xi_1(0) - \alpha_1(x(0)). \tag{4.35}$$

Consider the initial condition where $\xi_1(0) = 0$ and $\alpha_1(x(0)) = \pm|\alpha_1(x(t))|$, then

$$\begin{aligned} z_1(0) &= 0 - \pm|\alpha_1(x(t))| \\ &= \mp|\alpha_1(x(t))|. \end{aligned} \tag{4.36}$$

Thus, from (4.28), it follows that the condition

$$k_2 > |\alpha_1(x(t))| \tag{4.37}$$

must be satisfied in order to prevent z_1 from being ill-conditioned.

Note that the stabilising function α_2 is also bounded. Using Assumptions 4.7, 4.8, and Equation (4.28), the over-bound on α_2 can be obtained explicitly as follows

$$|\alpha_2(t)| < c_1 k_2 + |f_1(x, \xi_1)| + \left|\frac{d\alpha_1(x(t))}{dt}\right| + \frac{k_2^2}{k_1}\left|\frac{T(x, \xi_1)}{z_1}\right|. \tag{4.38}$$

Step 2

Consider the following augmented subsystem for (4.32)

$$\dot{z}_2 = \xi_3 + f_2(x, \xi_1, \xi_2) - \frac{d\alpha_2}{dt} \tag{4.39}$$

and define the error variable z_3 as follows

$$z_3 = \xi_3 - \alpha_3 \tag{4.40}$$

where the stabilising function α_3 is to be determined. With the stabilising function α_2 bounded, see (4.38), we are now only required to bound the error variable z_2 in order to bound the state ξ_2 according to (4.33). To achieve this, we proceed in a similar manner to Step 1 and impose a barrier function structure on the candidate cLf for (4.39) with a growth condition governed by

$$|z_2| \to \Delta_{z_2} \quad \Longrightarrow \quad U_2(z_2) \to +\infty \tag{4.41}$$

where $\Delta_{z_2} \in \mathbb{R}_+$ is a constant denoting the desired hard-bound on the error variable z_2. A valid candidate cLf is

$$U_2(x, z_1, z_2) = U_1 + \frac{1}{2} k_3 \log\left(\frac{k_4^2}{k_4^2 - z_2^2}\right) \tag{4.42}$$

where $k_3 \in \mathbb{R}_+$ is a design constant, and $k_4 \in \mathbb{R}_+$ is the desired hard-bound on z_2. The cLf (4.42) is positive definite and radially unbounded in the domain

$$\mathcal{D}_2 \triangleq \{(x, z_1, z_2) \in \mathbb{R}^n \times \mathbb{R}^2 \mid z_1 \in (-k_2, k_2), z_2 \in (-k_4, k_4)\}. \tag{4.43}$$

and yields

$$|z_2(t)| < k_4, \quad \forall t \geq 0. \tag{4.44}$$

It then follows that the time derivative of (4.42) satisfies the following inequality

$$\dot{U}_2 \leq -W(x) - \frac{k_1 c_1}{k_2^2 - z_1^2} z_1^2 + z_2 \left[\frac{k_1}{k_2^2 - z_1^2} z_1 + \frac{k_3}{k_4^2 - z_2^2}\left\{\xi_3 + f_2(x, \xi_1, \xi_2) - \frac{d\alpha_2}{dt}\right\}\right], \tag{4.45}$$

whenever $U_2(x, z_1, z_2)$ is well-defined, and bounded at every $t \geq 0$. To render $\dot{U}_2$ non-positive, or negative definite if $W(x)$ is positive definite, the simplest choice would be to choose the stabilising law α_3 as follows

$$\alpha_3 = -c_2 z_2 - f_2(x, \xi_1, \xi_2) + \frac{d\alpha_2}{dt} - \frac{k_1(k_4^2 - z_2^2)}{k_3(k_2^2 - z_1^2)} z_1.$$

Such a choice, however, means that α_3 is unbounded since the term $\frac{k_1(k_4^2 - z_2^2)}{k_3(k_2^2 - z_1^2)}$ escapes to infinity as $|z_1|$ approaches k_2, thus preventing the bounding of the remaining states. To yield a bounded α_3, we choose to not cancel the cross-term $\frac{k_1}{k_2^2 - z_1^2} z_1$, resulting in

$$\alpha_3 = -c_2 z_2 - f_2(x, \xi_1, \xi_2) + \frac{d\alpha_2}{dt}. \tag{4.46}$$

Let us now check that (4.46) is indeed bounded. We will first examine the boundedness of the third term on the RHS of (4.46) by differentiating (4.30)

$$\frac{d\alpha_2}{dt} = -c_1\dot{z}_1 - \frac{df_1}{dt} + \frac{d^2\alpha_1}{dt^2} + \frac{2z_1\dot{z}_1}{k_1}.\frac{T(x,\xi_1)}{z_1} + \frac{k_2^2 - z_1^2}{k_1}.\frac{d}{dt}\left[\frac{T(x,\xi_1)}{k_1}\right]. \tag{4.47}$$

Since z_2 is bounded as defined by (4.44), z_1 is bounded as defined by (4.28), and using Assumption 4.7, it immediately follows that the signal $\dot{z}_1$ is bounded. From (4.32), the explicit over-bound on $\dot{z}_1$ is given by

$$|\dot{z}_1(t)| < c_1k_2 + \frac{k_2^2}{k_1}\left|\frac{T(x,\xi_1)}{z_1}\right| + k_4. \tag{4.48}$$

Using Assumptions 4.6-4.8 and Equation (4.48), all terms on the RHS of (4.47) are bounded, $\frac{d\alpha_2}{dt}$ is therefore bounded. The over-bound on $\frac{d\alpha_2}{dt}$ is explicitly given by

$$\left|\frac{d\alpha_2}{dt}\right| < c_1|\dot{z}_1| + \left|\frac{df_1}{dt}\right| + \left|\frac{d^2\alpha_1}{dt^2}\right| + \frac{2k_2}{k_1}|\dot{z}_1|\left|\frac{T(x,\xi_1)}{z_1}\right| + \frac{k_2^2}{k_1}\left|\frac{d}{dt}\left[\frac{T(x,\xi_1)}{k_1}\right]\right|. \tag{4.49}$$

Consequently, α_3 is bounded and the over-bound is given by

$$|\alpha_3(t)| < c_2k_4 + |f_2(x,\xi_1,\xi_2)| + \left|\frac{d\alpha_2}{dt}\right|. \tag{4.50}$$

The choice of (4.46) for α_3 yields

$$\dot{z}_2 = -c_2z_2 + z_3 \tag{4.51}$$

and

$$\begin{aligned}\dot{U}_2 = -W(x) &- \frac{k_1c_1}{k_2^2 - z_1^2}z_1^2 + \frac{k_1}{k_2^2 - z_1^2}z_1z_2 \\ &- \frac{k_3c_2}{k_4^2 - z_2^2}z_2^2 + \frac{k_3}{k_4^2 - z_2^2}z_2z_3\end{aligned} \tag{4.52}$$

which is not guaranteed to be non-positive. To render $\dot{U}_2$ non-positive, and negative definite if $W(x)$ is positive definite, we dominate the cross-term by appropriately tuning the design constants. This is achieved by first manipulating (4.52) into the form

$$\begin{aligned}\dot{U}_2 = -W(x) &- \frac{k_1}{2(k_2^2 - z_1^2)}(z_1 - z_2)^2 - \frac{k_1c_1}{k_2^2 - z_1^2}z_1^2 + \frac{k_1}{2(k_2^2 - z_1^2)}z_1^2 + \frac{k_1}{2(k_2^2 - z_1^2)}z_2^2 \\ &- \frac{k_3c_2}{2(k_4^2 - z_2^2)}z_2^2 - \frac{k_3c_2}{2(k_4^2 - z_2^2)}z_2^2 + \frac{k_3}{k_4^2 - z_2^2}z_2z_3.\end{aligned} \tag{4.53}$$

What we have done is complete the squares for the cross-term $\frac{k_1}{k_2^2 - z_1^2}z_1z_2$, and add the terms $\frac{k_1}{2(k_2^2 - z_1^2)}z_1^2$ and $\frac{k_1}{2(k_2^2 - z_1^2)}z_2^2$, which come from the completion of the squares. These are the fourth and fifth terms on the RHS of (4.53), respectively. We then split the term

$-\frac{k_3c_2}{k_4^2-z_2^2}z_2^2$ in two parts to indicate our intention to use one part of the term to dominate the additional terms coming from the completion of the squares, and other part in the next step of the backstepping design procedure.

Let us now consider the sum of the third, fourth, fifth, and sixth term on the RHS of (4.53) separately

$$Y_1 = -\frac{k_1c_1}{k_2^2-z_1^2}z_1^2 + \frac{k_1}{2(k_2^2-z_1^2)}z_1^2 + \frac{k_1}{2(k_2^2-z_1^2)}z_2^2 - \frac{k_3c_2}{2(k_4^2-z_2^2)}z_2^2. \tag{4.54}$$

Our goal is to tune the design constants such that Y_1 is rendered negative-definite. If we choose

$$c_1 \geq \frac{k_4^2}{(k_2\alpha_{z_1})^2} + \frac{1}{2}, \tag{4.55}$$

where $\alpha_{z_1} \in (0, \sqrt{2})$ is a constant, then the following inequality is obtained

$$\begin{aligned} Y_1 &\leq -\frac{k_1}{k_2^2-z_1^2}\left[\frac{k_4^2}{(k_2\alpha_{z_1})^2} + \frac{1}{2}\right]z_1^2 + \frac{k_1}{2(k_2^2-z_1^2)}z_1^2 + \frac{k_1}{2(k_2^2-z_1^2)}z_2^2 - \frac{k_3c_2}{2(k_4^2-z_2^2)}z_2^2 \\ &\leq -\frac{k_1}{(k_2^2-z_1^2)(k_2\alpha_{z_1})^2}k_4^2z_1^2 + \frac{k_1}{2(k_2^2-z_1^2)}z_2^2 - \frac{k_3c_2}{2(k_4^2-z_2^2)}z_2^2. \end{aligned} \tag{4.56}$$

From (4.44), it follows that

$$\frac{k_1}{2(k_2^2-z_1^2)}z_2^2 < \frac{k_1}{2(k_2^2-z_1^2)}k_4^2. \tag{4.57}$$

Thus, when $|z_1| \geq k_2\alpha_{z_1}$, Y_1 is negative-definite if the design constant c_1 is tuned in accordance with (4.55).

When $|z_1| < k_2\alpha_{z_1}$, we employ the term $-\frac{k_3c_2}{2(k_4^2-z_2^2)}z_2^2$ to dominate $\frac{k_1}{2(k_2^2-z_1^2)}z_2^2$. By simple deduction, we can easily see that

$$\frac{k_3c_2}{2(k_4^2-z_2^2)}z_2^2 \geq \frac{k_3c_2}{2k_4^2}z_2^2. \tag{4.58}$$

In addition, when $|z_1| < k_2\alpha_{z_1}$, the following is true for the term $\frac{k_1}{2(k_2^2-z_1^2)}z_2^2$

$$\frac{k_1}{2(k_2^2-z_1^2)}z_2^2 < \frac{k_1}{2(k_2^2-[k_2\alpha_{z_1}]^2)}z_2^2. \tag{4.59}$$

Thus, if we choose

$$\frac{k_3c_2}{k_4^2} \geq \frac{k_1}{k_2^2-[k_2\alpha_{z_1}]^2} \tag{4.60}$$

then it follows that

$$\frac{k_3 c_2}{2(k_4^2 - z_2^2)} z_2^2 \geq \frac{k_1}{2(k_2^2 - z_1^2)} z_2^2, \quad \forall |z_1| < k_2 \alpha_{z_1}. \tag{4.61}$$

Consequently,

$$Y_1 = -\frac{k_1 c_1}{k_2^2 - z_1^2} z_1^2 + \frac{k_1}{2(k_2^2 - z_1^2)} z_1^2 + \frac{k_1}{2(k_2^2 - z_1^2)} z_2^2 - \frac{k_3 c_2}{2(k_4^2 - z_2^2)} z_2^2 \tag{4.62}$$

is negative-definite for $|z_1| < k_2$, $|z_2| < k_4$, if the design constants are tuned in accordance with (4.55) and (4.60). If (4.62) is negative-definite, then from (4.53), one obtains

$$\dot{U}_2 = -W(x) - W_{z_1 z_2} - \frac{k_3 c_2}{2(k_4^2 - z_2^2)} z_2^2 + \frac{k_3}{k_4^2 - z_2^2} z_2 z_3, \tag{4.63}$$

which is non-positive, and negative definite if $W(x)$ is negative definite, on domain $\mathcal{D}_2$ once z_3 is driven to 0. The function $W_{z_1 z_2}$ is defined as

$$W_{z_1 z_2} = \frac{k_1 c_1}{k_2^2 - z_1^2} z_1^2 - \frac{k_1}{k_2^2 - z_1^2} z_1 z_2 + \frac{k_3 c_2}{2(k_4^2 - z_2^2)} z_2^2 \tag{4.64}$$

and is positive definite in domain $\mathcal{D}_2$ provided that the design constants are tuned in accordance with (4.55) and (4.60).

Now that z_2 is bounded due to the barrier function structure imposed on the cLf (4.42) and α_2 is bounded as shown in (4.38), the state ξ_2 is bounded as a direct result of (4.33). The explicit bound on the state ξ_2 is given by

$$\begin{aligned} |\xi_2(t)| &\triangleq |z_2(t) + \alpha_2(t)| \\ &< k_4 + c_1 k_2 + |f_1(x, \xi_1)| + \left| \frac{d\alpha_1(x(t))}{dt} \right| + \frac{k_2^2}{k_1} \left| \frac{T(x, \xi_1)}{z_1} \right|. \end{aligned} \tag{4.65}$$

Similar to (4.37), k_4 must be chosen to satisfy

$$\begin{aligned} k_4 &> |\alpha_2(t)| \\ &\geq c_1 k_2 + |f_1(x, \xi_1)| + \left| \frac{d\alpha_1(x(t))}{dt} \right| + \frac{k_2^2}{k_1} \left| \frac{T(x, \xi_1)}{z_1} \right| \end{aligned} \tag{4.66}$$

in order to prevent z_2 from being ill-conditioned.

The procedure to bound each of the remaining states is recursive and is analogous to Step 2. The procedure involves not cancelling the cross-terms but dominating them and defining a barrier function structure on the cLfs to impose hard-bounds on the error variables. The recursion terminates when the system (4.1) is stabilised by the actual control signal u, which is at the m^{th} step of the proposed design procedure.

Step m

Define the error variable for this design step

$$z_m = \xi_m - \alpha_m \tag{4.67}$$

Differentiate (4.67) with respect to time yields the final augmented subsystem

$$\begin{aligned}\dot{z}_m &= \dot{\xi}_m - \dot{\alpha}_m \\ &= u + f_m(x, \xi_1, ..., \xi_m) - \dot{\alpha}_m.\end{aligned} \tag{4.68}$$

To bound ξ_m, we require the error variable z_m to be bounded. Similar to Step 2, this is achieved by imposing a barrier function structure on the cLf for (4.68) with a growth condition governed by

$$z_m \to \Delta_{z_m} \quad \Longrightarrow \quad U_m(z_m) \to +\infty, \tag{4.69}$$

where Δ_{z_m} denotes the desired hard-bound on the error variable z_m. A candidate cLf is

$$U_m(x, z_1, ..., z_m) = U_{m-1} + \frac{1}{2} k_{2m+1} \log\left(\frac{k_{2m}^2}{k_{2m}^2 - z_m^2}\right), \tag{4.70}$$

where $k_{2m+1} \in \mathbb{R}_+$ is a design constant, and the constant $k_{2m} \in \mathbb{R}_+$ is the desired bound on z_m. That is,

$$|z_m(t)| < k_{2m}, \quad \forall t \geq 0. \tag{4.71}$$

The cLf (4.70) is positive definite and radially unbounded in

$$\mathcal{D} = \{(x, z_1, ..., z_m) \in \mathbb{R}^n \times \mathbb{R}^m \mid z_i \in (-k_{2i}, k_{2i})\}, \quad i = 1, ..., m. \tag{4.72}$$

The time derivative of (4.70) is given by

$$\begin{aligned}\dot{U}_m = &-W(x) - W_{z_1 z_2} - \ldots - \frac{k_{2m-3} c_{m-1}}{2(k_{2m-2}^2 - z_{m-1}^2)} z_{m-1}^2 \\ &+ z_m \left[\frac{k_{2m-3}}{k_{2m-2}^2 - z_{m-1}^2} z_{m-1} + \frac{k_{2m-1}}{k_{2m}^2 - z_m^2} \{u + f_m(x, \xi_1, ..., \xi_m) - \dot{\alpha}_m\}\right],\end{aligned} \tag{4.73}$$

whenever $U_m(x, z_1, ..., z_m)$ is well-defined and bounded at every $t \geq 0$. As there is no prescribed constraint on the control u, one choice for u is

$$u = -c_m z_m - f_m(x, \xi_1, ..., \xi_m) + \dot{\alpha}_m \tag{4.74}$$

where $c_m \in \mathbb{R}_+$ is a design constant. Note that we have selected not to directly cancel the cross-term $\frac{k_{2m-3}}{k_{2m-2}^2 - z_{m-1}^2} z_{m-1} z_m$ in (4.73). This is because the presence of this term in

the final control law produces infinitely large effector commands as $|z_m| \to k_{2m}$. Such a choice of u yields

$$\dot{z}_m = -c_m z_m \tag{4.75}$$

and

$$\begin{aligned}\dot{U}_m = &-W(x) - W_{z_1 z_2} \\ &- \ldots - \frac{k_{2m-3} c_{m-1}}{2(k_{2m-2}^2 - z_{m-1}^2)} z_{m-1}^2 + \frac{k_{2m-3}}{k_{2m-2}^2 - z_{m-1}^2} z_{m-1} z_m - \frac{k_{2m-1} c_m}{k_{2m}^2 - z_m^2} z_m^2.\end{aligned} \tag{4.76}$$

The same trick to dominate the cross-term, as detailed in Step 2, is again required here in order to render $\dot{U}_m$ non-positive, and negative definite if $W(x)$ is positive definite. As this is the final design step, there is no need to split the term $-\frac{k_{2m-1} c_m}{k_{2m}^2 - z_m^2} z_m^2$. Thus, if we choose

$$c_{m-1} \geq \frac{k_{2m}^2}{(k_{2m-2}\alpha_{m-1})^2} + \frac{1}{2} \tag{4.77}$$

$$\frac{k_{2m-1} c_m}{k_{2m}^2} \geq \frac{k_{2m-3}}{2(k_{2m-2}^2 - [k_{2m-2}\alpha_{m-1}]^2)} \tag{4.78}$$

where $\alpha_{m-1} \in (0, \sqrt{2})$ is a constant. Then following the arguments outlined in Step 2, one obtains

$$\dot{U}_m \leq -W(x) - W_{z_1 z_2} - \ldots - W_{z_{m-1} z_m} \leq 0 \tag{4.79}$$

which is non-positive, and negative definite if $W(x)$ is positive definite, in domain $\mathcal{D}$. The function $W_{z_{m-1} z_m}$ is defined by

$$W_{z_{m-1} z_m} = \frac{k_{2m-3} c_{m-1}}{2(k_{2m-2}^2 - z_{m-1}^2)} z_{m-1}^2 + \frac{k_{2m-3}}{k_{2m-2}^2 - z_{m-1}^2} z_{m-1} z_m - \frac{k_{2m-1} c_m}{k_{2m}^2 - z_m^2} z_m^2 \tag{4.80}$$

and is positive definite on domain $\mathcal{D}$.

The last state ξ_m is now bounded by virtue of (4.67) since both z_m, as defined by (4.71), and α_m are bounded. The arguments to show the boundedness of α_m are similar to those used to demonstrate the boundedness of α_3 in Step 2. The bound on the state z_m is given by

$$\begin{aligned}|z_m(t)| &\triangleq |z_m + \alpha_m| \\ &< k_{2m} + |\alpha_m|\end{aligned} \tag{4.81}$$

Once again, the design constant k_{2m} must be chosen to satisfy

$$k_{2m} > |\alpha_m| \tag{4.82}$$

to prevent z_m from being ill-conditioned.

Remark 4.10. *The constraints on the design constants imposed by (4.55), (4.60), ..., (4.77), and (4.78), are analytically derived from the worst case scenario. Numerical determination of the design constants, based on the system's cLf and its derivative, reveals that the actual constraints on them are much less stringent. This can be observed in the simulation results presented later on.*

Remark 4.11. *It is interesting to note that if the function $f_m(x, \xi_1, ..., \xi_m)$ and its derivatives are norm bounded by positive constants, then the control u, as defined in (4.74), is bounded in both magnitude and rate. This means that the algorithm outlined in this section is potentially applicable to systems with bounded controls and control rates as well as those with state constraints, or both.*

4.3.2 Main result

Theorem 4.12. *Suppose that system (4.1) satisfies Assumptions 4.6, 4.7, and 4.8. Let $c_1, ..., c_m$, $k_1, ..., k_{2m} \in \mathbb{R}_+$ be design constants, and are tuned in accordance with (4.37), (4.55), (4.60), (4.66), ..., (4.77), (4.78), and (4.82). For all initial conditions in*

$$\mathcal{D} \triangleq \{(x, z) \in \mathbb{R}^n \times \mathbb{R}^m \mid x \in \mathbb{R}^n, z_i \in (-k_{2i}, k_{2i})\}, \quad i = 1, ..., m, \tag{4.83}$$

the system (4.1) in closed-loop with control law (4.74) is rendered $\mathcal{D}$-DGAS (cf. Definition 2.10) at the origin. Furthermore, the states ξ_i are bounded in norm.

Proof of Theorem 4.12. The cLf U_m, as defined by (4.70), is positive definite and radially unbounded in domain $\mathcal{D}$. Its time-derivative $\dot{U}_m$ is non-positive, and negative definite if $W(x)$ is positive definite, in the same domain $\mathcal{D}$ when (4.37), (4.55), (4.60), (4.66), ..., (4.77), (4.78), and (4.82) are satisfied, see (4.79). Using Assumption (3.1), it can readily be proved that the set in which $\dot{U}_m = 0$ contains only the origin. (See the proof of Proposition 3.2 for details). Application of Lasalle's Invariance Principle yields the conclusion that the closed-loop system is indeed asymptotically stable in $\mathcal{D}$.

The boundedness of the system states comes as a direct consequence of the proposed control design procedure. For example, to prove the boundedness of $z_1(t)$, application of Lyapunov's direct method to (4.70) and (4.79) gives rise to the following

$$\frac{1}{2} k_1 \log\left(\frac{k_2^2}{k_2^2 - z_1(t)^2}\right) \leq U_m(t) \leq U_m(0), \quad \forall t \geq 0. \tag{4.84}$$

By inspection, this proves that

$$|z_1(t)| < k_2, \quad \forall t \geq 0. \tag{4.85}$$

From Assumption 4.6 and Equation (4.23), it follows that the state ξ_1 is bounded, and the explicit bound is given by

$$|\xi_1(t)| < k_2 + |\alpha_1|. \tag{4.86}$$

The boundedness of the remaining states can be proved in a similar manner. □

4.3.3 Tuning the control gains

The goal of the control design is to obtain a controller that exploits the maximum allowable range of state variation whilst guaranteeing the satisfaction of the state constraints for all time. The first step in tuning the control gains is to restrict consideration to only those controller parameters $\{k_i, c_i\}$ that are self-consistent with respect to the proposed design procedure. By self-consistent, we mean controller parameters $\{k_i, c_i\}$ that satisfy the set of mutual constraints which is defined by (4.37), (4.55), (4.60), (4.66), ..., (4.77), (4.78), and (4.82). Self-consistency ensures that Theorem 4.12 holds. The design procedure provides a set of constraints on the controller parameters $\{k_i, c_i\}$, and a set of bounds on the stabilising functions and error variables. The remaining task required is to relate constraints on the stabilising functions and error variables back to constraints on the original state variables.

The domain constraints, obtained as a function of the proposed control design, yield a set of conditions on the error variables

$$|z_i| = |\xi_i - \alpha_i| < k_{2i}. \tag{4.87}$$

The stabilising functions, α_i are defined as algebraic functions of the error coordinates, system states and controller parameters. It is a simple exercise to obtain worst case overbounds for the norms of the reference trajectories. Following from these bounds, it is possible to obtain a set of nonlinear bounds $\{X_1, X_2, \ldots, X_n\}$ for the state evolution in terms of the control parameters

$$\begin{aligned}
|\xi_1(t)| &\leq |z_1(t) + \alpha_1(t)| \\
&< k_2 + |\alpha_1(t)| =: X_1 && \text{(4.88a)} \\
|\xi_2(t)| &\leq |z_2(t) + \alpha_2(t)| \\
&< k_4 + c_1 k_2 + |f_1| + \left|\frac{d\alpha_1}{dt}\right| + \frac{k_2^2}{k_1}\left|\frac{T(x,\xi_1)}{z_1}\right| =: X_2 && \text{(4.88b)} \\
&\vdots \\
|\xi_m(t)| &\leq |z_m(t) + \alpha_m(t)| \\
&< k_{2m} + |\alpha_m(t)| =: X_m && \text{(4.88m)}
\end{aligned}$$

These bounds are defined recursively in the sense that X_2 depends on X_1, X_3 depends on X_2 and X_1, etc. For a given set of controller parameters $\{k_i, c_i\}$, it is straight forward

to iteratively compute worst case bounds on the system states $\xi_i(t)| < X_i$. From the point of view of the control design we think of the worst case state constraints as a nonlinear function of the controller parameters

$$Z := (k_1, \ldots, k_{2i}, c_1, \ldots, c_m)$$
$$X := X(Z), \qquad X = (X_1, \ldots, X_m).$$

Next we introduce the set of constraints associated with the problem formulation

$$X_i \leq \Xi_i. \tag{4.89}$$

Satisfying (4.89) ensures that $|\xi_i(t)| < X_i \leq \Xi_i$. Thus, the state constraints specified for the problem are guaranteed to hold. The constraints (4.37), (4.55), (4.60), (4.66), ..., (4.77), (4.78), and (4.82), along with (4.89), define the feasible set for the controller parameters $\{k_i, c_i\}$.

Finally, introduce the cost functions

$$\Phi_i(Z) = \Xi_i - X_i, \quad i = 1, ..., m. \tag{4.90}$$

Note that $\Xi_i > X_i$ on the feasible set of $\Phi(Z) \in \mathbb{R}^m_+$. The goal of tuning the control parameters is a constrained multi-criteria optimisation problem:

> **Find controller parameters Z, subject to constraints (4.37), (4.55), (4.60), (4.66), ..., (4.77), (4.78), (4.82), and (4.89), that minimises the cost functions Φ_i.**

In general, the cost functions Φ_i are incompatible with each other, and can seldom be jointly minimised. That is, one set of controller parameters Z that optimises one cost function may be far from optimal for others.

To simplify the optimisation procedure, we introduce the following "utility function", which is a positively weighted sum of the cost functions Φ_i,

$$S(Z) = \sum w_i \Phi_i, \quad w_i \in \mathbb{R}_+, \quad i = 1, ..., m. \tag{4.91}$$

The resulting optimisation problem is a standard constrained single criterion problem. Although this constrained optimisation problem is difficult it is quite tractable using modern numerical optimisation algorithms [8]. (Consider trying to solve the original constrained nonlinear control problem using optimal control techniques.) The underlying philosophy in the overall approach is to use an algorithmic design procedure to impose structure on the nonlinear control problem and then exploit this structure to obtain a tractable optimisation problem. The resulting controller is conceptually the best sub-optimal controller that satisfies the constraints imposed by the design procedure. An important property of the proposed methodology is that it is relatively simple to find feasible values starting with

very small values for the controller parameters. The nice algebraic form of the constraints (4.37), (4.55), (4.60), (4.66), ..., (4.77), (4.78), and (4.82) is crucial in this process.

4.3.4 Finding feasible solutions for tuning the control gains

The approach proposed in Section 4.3.3 to tune the controller parameters guarantees that the actual state bounds obtained are optimised to ensure that they are tight worst-case bounds. A disadvantage associated with such an approach is that some of the arguments employed to estimate the bounds on the stabilising functions lead to sub-optimal bounds on the system states, ultimately resulting in reduced performance of the closed-loop system. Another disadvantage is the possibility that the introduction of the worst-case bounding arguments, which gave rise to the constraints on the design constants (4.55), (4.60), ..., (4.77), and (4.78), will lead to an infeasible optimisation problem. In this scenario the problem formulation can be adjusted to reduce the influence of the state bounds until a feasible solution is attained. However, it is possible that this will lead to a control design with such restrictive bounds that there is a distinct danger in it becoming little more than a low-gain argument and the performance advantages of the backstepping approach will be lost. This problem arises due to the limitations inherent in imposing a fixed design algorithm on a highly nonlinear system. The optimisation process can only do the best possible given the imposed structure. For certain systems, the imposed structure can be so restrictive that it precludes any solution.

Unfortunately, due to time limitations, a detailed analysis of the problem of finding feasible solutions for the controller parameters when the optimisation problem proposed in Section 4.3.3 fails can not be undertaken. The simulations presented in Section 4.4 considers a system for which the approach proposed in Section 4.3.3 can be applied. Even in this case some freedom in the controller parameter choice was required. It is instructive to briefly discuss how the controller parameters could be found for a larger class of systems.

4.3.5 Gain-scheduling

The control architecture proposed in Section 4.3 provides a local control design. That is, the control law u is a direct function of the system states and guarantees the decrease of a Lyapunov function which is also a function of the system states. Consider partitioning the constraint admissible state-space into small regions. On each of these regions the control architecture proposed in Section 4.3 may be applied. For each local region it is possible to compute the constraints imposed on the design constants, which are defined by (4.37), (4.55), (4.60), (4.66), ..., (4.77), (4.78), (4.82), and a subset of (4.89) depending on the local region. On each small subset it is no longer necessary to use a worst-case analysis to convert these bounds into constraint equations for the optimisation procedure since the system states need only be considered within each local region. As a result, within each region the sub-optimal bounds employed in Section 4.3.3 can be rewritten as explicit state bounds depending directly on the actual state values, at least to first-order approximations. It is natural to expect that the resulting optimisation problems will

mostly be feasible on the interior of the constraint admissible domain. It is interesting to note that each independent optimisation procedure will choose slightly different control parameters. Thus, far away from the boundaries of the individual region the influence of the constraints will be small and the design will focus on the asymptotic stability of the system. Close to the boundaries, however, the effect of the boundary constraints will dominate and the resulting controller parameters will be tuned to ensure that the barrier terms in the cLf are decreasing, thus guaranteeing the preservation of the state constraints.

There may be regions in the full constraint admissible state-space where the optimisation problem remains infeasible. These cases will tend to correspond to situations where the dynamics of the system prevent the system from exploiting the full constraint admissible domain that was arbitrarily specified in the problem specification. These regions of the constraint admissible state-space cannot be accessed by the system and are therefore not considered.

At the end of this process the designer will obtain, after some considerable expenditure of effort, a partition of the full constraint admissible domain in state-space into a union of local regions each of which has a local cLf and controller u. The final controller is obtained by combining these local controllers into a controller for the full constraint admissible state-space. The simplest design concept for a global control design is to introduce a gain-schedule based on which local region the system is contained within. The stability analysis of this approach will depend on how the cLfs interact at the boundaries of the partitioned regions. We believe that this approach will provide good performance in practice, even though it has not been possible to comprehensively investigate this issue in the present thesis. It is also possible to consider other schemes whereby the independent control laws are smoothly combined in some manner to obtain averaged control where the local regions intersect. The study of this topic is beyond the scope of the present thesis and will not be considered further.

4.3.6 Manual tuning of control gains

In this approach, the constraints imposed by (4.55), (4.60), ..., (4.77), and (4.78) are not considered in the determination of the controller parameters $\{k_i, c_i\}$. The rationale behind their omission is that, as mentioned previously, worst-case arguments were used in deriving those conditions which mean that they are necessarily conservative.

The controller parameters $\{k_i, c_i\}$ are computed in accordance with the nonlinear bounds on the system states given by (4.88), and the conditions (4.37), (4.66), ..., and (4.82). This ensures that the specified state constraints are satisfied and that the zero initial condition is proper. However, since the conditions (4.55), (4.60), ..., (4.77), and (4.78) have not been accounted for in determining the control gains, the stability of the closed-loop system is not assured. Thus, the set of allowable initial conditions cannot be directly calculated by using the expressions for the error variables (4.23), (4.33), (4.40), ..., and (4.67). Rather, the set of allowable initial conditions is determined by simulating the closed-loop system at various initial conditions and examining the evolution of the

candidate cLf and its time derivative. This method of tuning the design constants is simple, non-conservative, and guarantees to generate a set of feasible control gains as will be demonstrated via simulations of a 4^{th}-order integrator system in Section 4.4. The drawbacks of the method include its trial-and-error nature, which could lead to many iterations before the right set of controller gains, which satisfies the prescribed state bounds, and the maximum possible allowable set of initial conditions are obtained. The process could, however, be sped up considerably by using automated software testing, and is not dissimilar in concept to validation of current industry standard gain-scheduled linear control designs for flight control.

4.4 Simulation results

Simulations for a simple 4^{th}-order integrator cascade are presented to support our results. The system's equations of motion are given by

$$\begin{aligned} \dot{\xi}_1 &= \xi_2 \\ &\vdots \\ \dot{\xi}_4 &= u \end{aligned} \tag{4.92}$$

The constraints on the system's states are as follows

$$\xi_2 \leq 2.5, \quad \xi_3 \leq 12, \quad \xi_4 \leq 700 \tag{4.93}$$

The design constants are numerically tuned as follows

$$\begin{aligned} &c_1 = \frac{0.5}{\pi}, c_2 = 1, c_3 = 50, c_4 = 1, k_1 = 1, k_2 = 2, \\ &k_3 = 3, k_4 = 5.61, k_5 = 1, k_6 = 354.5, k_7 = 10 \end{aligned}$$

The closed-loop system is simulated in Matlab/Simulink using the fixed step Dormand-Prince solver option with a step size of 0.005.

Figures 1 and 2 clearly show that ξ_2, ξ_3, and ξ_4 all remain within the constraints expressed by (4.93), irrespective of the initial condition. Note the ramp-like response of the system which provides a perfect example of how a system with velocity constraints, such as that of non-acrobatic and non-fighter types of aircraft, should respond to a change-in-position command. Also note the near optimal velocity obtained, ξ_2, which can be pushed closer to its true bound by further tweaking the design constants. This is where backstepping is most proficient as it can provide the high gains required to push the system states as close to their maximum limits as possible to approximate optimal trajectories.

4.5 Chapter summary

This chapter extends the results presented in the previous chapter to address the problem of multiple state constraints. The main contribution of this chapter is the extending of the backstepping methodology to asymptotically stabilise a class of nonlinear systems subject to multiple state constraints. The adaptation of the design procedure which requires the construction of ISS-cLfs to accommodate multiple state constraints is straight forward as outlined in Section 4.2. All that is needed is the additional assumption that all nonlinearities in the system's dynamic model and their time derivatives are bounded in norm.

For the design procedure which assumes that no strict cLfs are available, the extension is not as straightforward. The standard approach of cancelling the cross-terms does not work because of the cross-terms escaping to infinity infinitesimally close to the constraint boundaries. Consequently, rather than cancellation of the cross-terms, we have adopted domination instead. The outcome of the proposed design procedure is a set of constraints on the controller parameters. Satisfying these constraints ensures that the closed-loop system is asymptotically stable, and the states are bounded in norm. From these constraints, nonlinear bounds for the stabilising functions and error variables, and ultimately, for the system states, in terms of the controller parameters were computed. Together, the constraints on the controller parameters, the computed bounds on the system states, and the prescribed state bounds provide the ingredients for a multi-criteria constrained optimisation routine to tuning the controller parameters. The result is a set of controller parameters which guarantees that the closed-loop system is asymptotically stable, and yields the maximum possible constraint admissible region given the prescribed state bounds and the constraints imposed by the proposed design procedure. There however, exists a distinct possibility, due to the worst-case arguments employed in deriving some of the constraints on the controller parameters, that in certain cases, the optimisation routine is ill-conditioned. Unfortunately, there was insufficient time to undertake a detailed analysis into the problem of finding feasible solutions for the controller parameters when the optimisation routine proposed in Section 4.3.3 fails. Two alternative methods were proposed including gain-scheduling and manually tuning the controller parameters. The validity of the manual tuning approach was demonstrated in Section 4.4 via simulations of a 4^{th}-order integrator cascade. The issue of whether the gain-scheduling approach provides better performance and robustness than the "global" approach and manual tuning is unresolved due to time limitations.

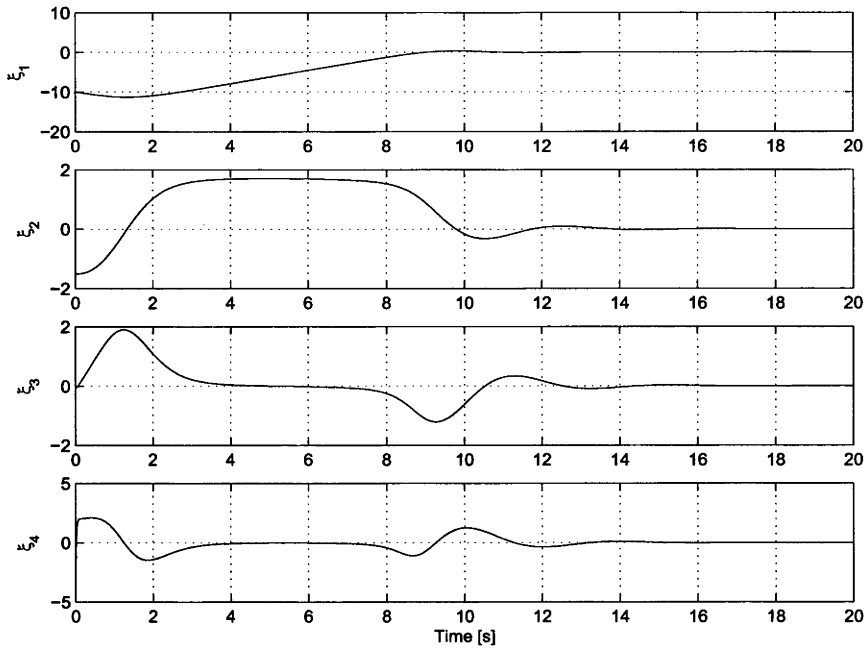

Figure 4.1: Closed-loop response with initial condition: $\xi_1(0) = -10, \xi_2(0) = -1.5, \xi_3(0) = -0.05, \xi_4(0) = -2.5$

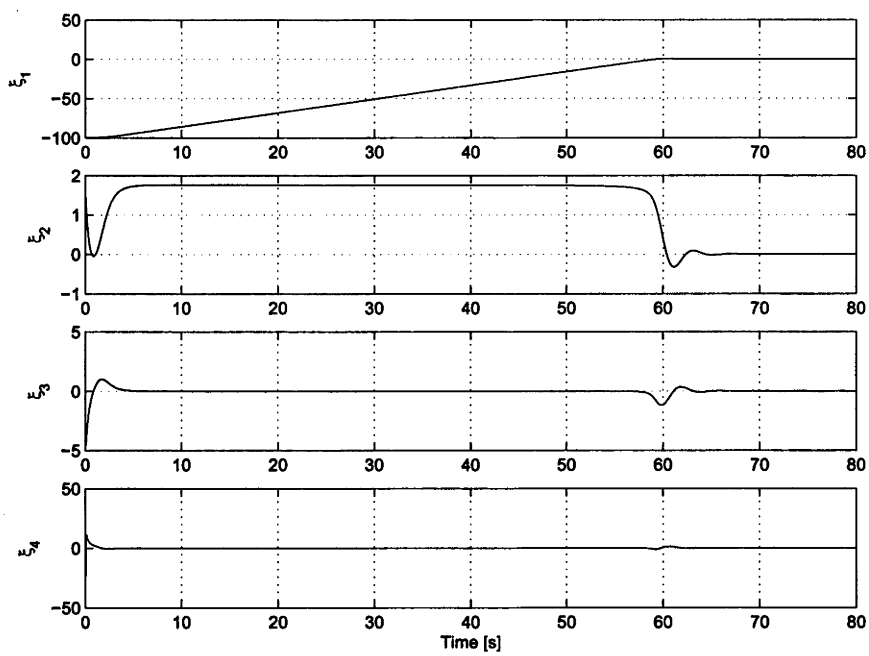

Figure 4.2: Closed-loop response with initial condition: $\xi_1(0) = -100, \xi_2(0) = 1.5, \xi_3(0) = -4, \xi_4(0) = -50$

Chapter 5

Constrained longitude control for the Aerosonde UAV

Nomenclature

$\bar{c}$	=	mean aerodynamic chord
C_{L_α}	=	lift curve slope
C_{L_0}	=	lift coefficient at zero angle of attack
C_{M_α}	=	pitching moment coefficient due to angle of attack
C_{M_0}	=	pitching moment coefficient at zero angle-of-attack
C_{M_q}	=	pitching moment coefficient due to pitch rate
$C_{M_{\delta_E}}$	=	pitching moment coefficient due to elevator deflections
F_T	=	thrust
g	=	gravity
h	=	altitude
I_{yy}	=	moment of inertia about the y-axis
L	=	aerodynamic lift force
M	=	aerodynamic pitching moment
m	=	aircraft's mass
p, q, r	=	roll, pitch, and yaw rate about the aircraft-body frame of reference
$\bar{q}$	=	dynamic pressure
S	=	wing planform area
v_T	=	true airspeed
v_z	=	climb rate
α	=	angle of attack
β	=	angle of sideslip
δ_E	=	elevators deflection

ϕ, θ, ψ = roll, pitch, and yaw angle

5.1 Introduction

The Aerosonde is a small-scale UAV developed specifically for long-range meteorological reconnaissance over oceanic and remote areas, and in hazardous conditions (see Figure 1.1). However, with a low-cost design, small footprint, and an aerodynamically efficient airframe, the Aerosonde is capable of performing a much wider range of surveillance and sensing tasks than what it was originally designed for. Potential applications include coastal surveillance, landscape mapping, aerial photography, low-altitude mineral exploration, just to name a few.

Presently, there is an on-going research and development (R&D) effort to extend and enhance the operational capability of the Aerosonde to capture new and emerging market opportunities. An integral part of this R&D initiative is the focus on developing a new flight controller for the Aerosonde that is capable of providing better stability and tracking performance over a much wider range of operating conditions and trajectories than the existing control algorithm. At the same time, limited resources, cost effectiveness considerations, and the fact that these aircraft are disposable, mandate the use of simplified and incomplete dynamic models and inexpensive hardware in the control implementation.

Motivated by the above challenges, we dedicate this chapter to designing a longitudinal flight controller to regulate the altitude of the Aerosonde UAV. We focus on the longitudinal dynamics because the Aerosonde is built with a relatively high degree of lateral/directional stability. Moreover, the mission profiles of the Aerosonde typically require the aircraft to fly straight and level whilst accurately tracking altitude change commands.

Traditional aircraft flight control designs are dominated by classical design techniques. The most popular design methodology, due largely to its systematic "divide-and-conquer" framework, involves linearizing the vehicle's dynamics about a number of operating conditions throughout the flight envelope, designing linear controllers for each of these operating condition, and blending these point designs with an interpolation scheme. This gain-scheduling approach, however, may produce a control law that does not globally possess the desirable properties exhibited locally by its constituent point designs. In addition, there exists no simple or direct mechanism to incorporate actuator saturation and/or state constraints into the design process. The use of nonlinear actuation systems can also add significant complexity to the controller design [20].

In the past few decades, a number of nonlinear control methodologies has been developed for application to advanced flight vehicles. These nonlinear design techniques, by dealing directly with the vehicle's complete dynamics rather than point designs, offer significant increases in performance as well as greatly reduce the development time. The most popular and widely employed nonlinear design methodology is feedback lineariza-

tion. A common approach to designing flight control laws with feedback linearization is to separate the vehicle's dynamics into fast and slow states using time-scale separation arguments with the fast states utilized as virtual controls to drive the slow states [17, 96, 128]. Although this approach greatly simplifies the state inversion transformations due to the now simpler dynamical equations, closed-loop stability is not guaranteed [78, 113].

Another drawback of feedback linearization techniques is that their performance and applicability rely crucially upon accurate knowledge of the vehicle's dynamics. Unfortunately, a high-fidelity aircraft model is expensive, and often not possible to obtain because most aerodynamic phenomena are highly nonlinear functions of several variables and therefore, very difficult to model exactly.

One nonlinear control technique that can provide solutions to the above issues is integrator backstepping. Rather than indiscriminately cancelling all nonlinearities including useful ones as stipulated by feedback linearization techniques, backstepping affords the control engineer not only the choice of retaining all beneficial nonlinearities, but also great freedom in selecting the final control law [68]. This flexibility means that not only the form of the resulting control law can be much simpler than those derived using feedback linearization, the dynamical model used need not be exact. In addition, as backstepping includes the transients in the virtual control signals explicitly in the derivation of the final control law, the time-scale separation assumption is therefore, no longer required.

Despite possessing many attractive features and holding numerous advantages over feedback linearization techniques, applications of backstepping to flight control have been few. The majority of those focus on the control of the aerodynamic angles (α, β) and/or Euler angles (ϕ, θ, ψ), which are essentially second-order systems [78, 126, 133]. Härkegård and Glad [46], and more recently, Sharma and Ward [125] employ backstepping to address the control problem of the flight-path angle (γ), which is a third-order system. Both of these work however, do not address the problem of actuator and/or state constraints. To the best of the author's knowledge, only the work in [31] considers the problem of state and actuator magnitude, rate, and bandwidth constraints in flight control using backstepping. To address these constraints, the authors in [31] implement limiting filters to bound the magnitude, rate, and bandwidth of the virtual control signals at each step of the backstepping design procedure, and correct the error signals to compensate for the periods during which the nominal virtual control signals exceed the constraints. However, this approach does not guarantee that the actual states remain within their specified hard bounds, nor does it guarantee the convergence of the error signals to the origin when saturations of the states and/or actuators are in effect.

Perhaps the main criticism being leveled at backstepping is that direct application of traditional backstepping produces highly aggressive controllers that require unbounded inputs. This is unsuitable for real dynamical systems because of actuator saturations and/or the possibility of hard bounds on the physical system states. Due to aerodynamic

phenomena such as stall and flutter, aircraft control requires the consideration of state constraints in the control design process rather than actuator saturations. For example, the control margin provided by the elevators for a typical aircraft is more than adequate for all required manoeuvres in the longitudinal plane. If the elevators are applied too aggressively, the aircraft will be subjected to excessive pitching moments which can lead to stall if the resulting angles of attack exceed the stall angle. Although this problem can readily be circumvented by implementing a guidance algorithm based on switching decision logics, such an approach can add significant complexity to the controller design, and is less robust than a base level controller design that reflects the state constraints. and can add significant complexity to the controller design. A more elegant, simple, and robust solution is to directly incorporate the state constraints into the controller design process in a natural manner.

In this chapter, we propose a backstepping controller to regulate the altitude of the Aerosonde UAV. The dynamic model considered is a fourth-order system. To prevent the controller from demanding excessive elevator deflections, hence causing the aircraft to stall, a hard constraint on the aircraft's climb rate is imposed. The rationale is that if the climb rate is bounded, then the angles of attack will also be bounded, which in turn will place limits on the pitch rates, and ultimately, the elevator deflections. The imposed state constraint is incorporated directly into the controller design by applying the results developed in Chapter 3.

The chapter is organised as follows. In Section 5.2, the aircraft altitude dynamics is described and cast into the requisite strict-feedback form. In Section 5.3, a controller design based on the traditional backstepping methodology is presented. This exercise serves to validate our argument that application of traditional backstepping leads to an overly aggressive controller which will cause stall if a sufficiently large altitude change is commanded. In Section 5.4, the controller is re-designed to take into account the hard constraint on the vertical velocity. The performance and stability of both controller designs are demonstrated via closed-loop simulations on a full 6-DOF, nonlinear model of the Aerosonde UAV.

5.2 System model

The altitude dynamics of an aircraft can be described by [134]

$$\dot{h} = v_T \sin(\gamma) \tag{5.1a}$$

$$\dot{\gamma} = \frac{1}{mv_T}\left[F_T \sin(\alpha) + L - mg\cos(\gamma)\right] \tag{5.1b}$$

$$\dot{\alpha} = \frac{1}{mv_T}\left[-F_T \sin(\alpha) - L + mg\cos(\gamma)\right] + q \tag{5.1c}$$

$$\dot{q} = \frac{M}{I_{yy}}. \tag{5.1d}$$

Before backstepping can be applied, we first need to transform system (5.1) into the strict-feedback form. To achieve this, we make the following assumptions.

Assumption 5.1. *The flight-path angle, γ, is small throughout the flight envelope and therefore can be approximated by*

$$\sin(\gamma) \approx \gamma, \quad \cos(\gamma) \approx 1 - \frac{\gamma^2}{2}.$$

Assumption 5.2. *The true airspeed, v_T, is controlled by a separate control loop and can be treated as a constant in (5.1) [46, 113, 125].*

Assumption 5.3. *The component of the thrust force, $F_T \sin(\alpha)$ is negligible as it is generally much smaller than the lift force, L [125].*

Assumption 5.4. *The aerodynamic lift force, L, can be approximated by the following linear relationship*

$$L = L_0 + L_\alpha \alpha,$$

where $L_\alpha = \bar{q}SC_{L_\alpha}$ represents the lift force due to the angle of attack, $L_0 = \bar{q}SC_{L_0}$ represents the lift force at zero angle of attack, and $C_{L_\alpha}, C_{L_0} \in \mathbb{R}$. Note that the lift component due to control surfaces is negligible compared to the principal components and is not modeled. Furthermore, its inclusion would prevent the transformation of the flight-path angle, γ, dynamics into the strict-feedback form. The above linear approximation of the aerodynamic lift force is valid up to the stall angle of attack.

The pitching moment, M, can be approximated by

$$M = M_0 + M_\alpha \alpha + M_q q + M_{\delta_E} \delta_E,$$

where $M_0 = \bar{q}S\bar{c}C_{M_0}$ represents the pitching moment at zero angle of attack, $M_\alpha = \bar{q}S\bar{c}C_{M_\alpha}$ represents the pitching moment due to the angle of attack, $M_q = \frac{1}{2v_T}\bar{q}S\bar{c}^2C_{M_q}$ is the pitching moment due to pitch rate, $M_{\delta_E} = \bar{q}S\bar{c}C_{M_{\delta_E}}$ is the pitching moment due to elevator deflections, and $C_{M_0}, C_{M_\alpha}, C_{M_q}, C_{M_{\delta_E}} \in \mathbb{R}$. (For a more detailed discussion on aerodynamic forces and moments, please refer to such excellent texts as [51, 134].)

Assuming that Assumptions 5.1-5.4 hold, equations (5.1) can be expressed as follows

$$\dot{h} = v_T \gamma \tag{5.2a}$$

$$\dot{\gamma} = \frac{1}{mv_T}\left[L_0 + L_\alpha \alpha - g + \frac{g\gamma^2}{2}\right] \tag{5.2b}$$

$$\dot{\alpha} = \frac{1}{mv_T}\left[-L_0 - L_\alpha \alpha + g - \frac{g\gamma^2}{2}\right] + q \tag{5.2c}$$

$$\dot{q} = \frac{1}{I_{yy}}\left[M_0 + M_\alpha \alpha + M_q q + M_{\delta_E}\delta_E\right]. \tag{5.2d}$$

Let us introduce the following change of variables

$$v_T\gamma = v_z \iff \gamma = \frac{v_z}{v_T},$$

and define

$$L_0' = \frac{L_0}{mv_T}, \quad L_\alpha' = \frac{L_\alpha}{mv_T}, \quad L_0^* = \frac{L_0}{m}, \quad L_\alpha^* = \frac{L_\alpha}{m}$$
$$M_0' = \frac{M_0}{I_{yy}}, \quad M_\alpha' = \frac{M_\alpha}{I_{yy}}, \quad M_q' = \frac{M_q}{I_{yy}}, \quad M_\delta' = \frac{M_\delta}{I_{yy}}$$

System (5.2) now becomes

$$\dot{h} = v_z \tag{5.3a}$$
$$\dot{v}_z = -g + \frac{g}{2v_T^2}v_z^2 + L_0^* + L_\alpha^*\alpha \tag{5.3b}$$
$$\dot{\alpha} = \frac{g}{v_T} - \frac{2}{2v_T^3}v_z^2 - L_0' - L_\alpha'\alpha + q \tag{5.3c}$$
$$\dot{q} = M_0' + M_\alpha'\alpha + M_q'q + M_{\delta_E}'\delta_E, \tag{5.3d}$$

which is in the requisite strict-feedback form.

5.3 Altitude controller: a backstepping design

In this section, we apply traditional backstepping, as developed in [74], to design a controller to regulate the altitude of the Aerosonde UAV. The system considered is described by (5.3). The controller design is detailed below.

Step 1

Introduce the error variable

$$z_1 = h - h_d, \tag{5.4}$$

where the constant $h_d \in \mathbb{R}$ denotes the desired (or commanded) altitude. Taking the time derivative of z_1 yields

$$\dot{z}_1 = v_z. \tag{5.5}$$

Let us select the following cLf for (5.5)

$$V_1(z_1) = \frac{1}{2}z_1^2, \tag{5.6}$$

whose time derivative is given by

$$\dot{V}_1 = z_1 v_z. \tag{5.7}$$

Choosing the stabilising function $v_{z_{ref}}$ to be

$$v_{z_{ref}} = -c_1 z_1, \tag{5.8}$$

and defining the error signal z_2 as follows

$$z_2 = v_z - v_{z_{ref}}, \tag{5.9}$$

one obtains

$$\dot{z}_1 = -c_1 z_1 + z_2 \tag{5.10}$$

$$\begin{aligned} \dot{V}_1 &= -c_1 z_1^2 + z_2 z_1 \\ &= -W_1(z_1) + z_2 z_1, \end{aligned} \tag{5.11}$$

where $c_1 \in \mathbb{R}_+$ is a design constant, and $W_1(z_1) = c_1 z_1^2$ which is positive definite. It is clear that once z_2 is driven to 0, $\dot{V}_1$ is negative definite which implies that $z_1 \to 0$, and the h dynamics becomes asymptotically stable at the desired altitude h_d.

Step 2

Consider the augmented subsystem for (5.10)

$$\dot{z}_2 = -g + \frac{g}{2v_T^2} v_z^2 + L_0^* + L_\alpha^* \alpha + c_1 \dot{z}_1. \tag{5.12}$$

The cLf for this step is chosen to be

$$V_2 = V_1 + \frac{1}{2} z_2^2. \tag{5.13}$$

Differentiating V_2 yields

$$\dot{V}_2 = -W_1(z_1) + z_2 \left[z_1 - g + \frac{g}{2v_T^2} v_z^2 + L_0^* + L_\alpha^* \alpha + c_1 \dot{z}_1 \right]. \tag{5.14}$$

Let

$$\alpha_{ref} = \frac{1}{L_\alpha^*} \left[-c_2 z_2 - z_1 + g - \frac{g}{2v_T^2} v_z^2 - L_0^* - c_1 \dot{z}_1 \right], \tag{5.15}$$

and define

$$z_3 = \alpha - \alpha_{ref}, \tag{5.16}$$

where $c_2 \in \mathbb{R}_+$ is a design constant. By substituting (5.15) and (5.16) into (5.12) and (5.14), one obtains

$$\dot{z}_2 = -c_2 z_2 - z_1 + L_\alpha^* z_3 \tag{5.17}$$

$$\begin{aligned}\dot{V}_2 &= -W_1(z_1) - c_2 z_2^2 + L_\alpha^* z_2 z_3 \\ &= -W_2(z_1, z_2) + L_\alpha^* z_2 z_3,\end{aligned} \tag{5.18}$$

where $W_2 = W_1 + c_2 z_2^2$ and is positive definite. Since $\dot{V}_2$ is negative definite once z_3 is driven to 0, $z_2 \to 0$, and the v_z dynamics becomes asymptotically stable at the origin.

Step 3

Consider the augmented subsystem for (5.17)

$$\begin{aligned}\dot{z}_3 = \frac{g}{v_T} - \frac{g}{2v_T^3} v_z^2 - L_0' - L_\alpha' \alpha + q \\ - \frac{1}{L_\alpha^*}\left[-c_2 \dot{z}_2 - \dot{z}_1 - \frac{g}{v_T^2} v_z \dot{v}_z - c_1 \ddot{z}_1\right].\end{aligned} \tag{5.19}$$

Let the cLf for this step be defined by

$$V_3 = V_2 + \frac{1}{2} z_3^2 \tag{5.20}$$

whose time derivative is given below

$$\begin{aligned}\dot{V}_3 = -W_2(z_1, z_2) + z_3 \Bigg\{ L_\alpha^* z_2 + \frac{g}{v_T} - \frac{g}{2v_T^3} v_z^2 - L_0' - L_\alpha' \alpha + q \\ - \frac{1}{L_\alpha^*}\left[-c_2 \dot{z}_2 - \dot{z}_1 - \frac{g}{v_T^2} v_z \dot{v}_z - c_1 \ddot{z}_1\right]\Bigg\}.\end{aligned} \tag{5.21}$$

Choosing the stabilising function q_{ref} to be

$$\begin{aligned}q_{ref} = -c_3 z_3 - L_\alpha^* z_2 - \frac{g}{v_T} + \frac{g}{2v_T^3} v_z^2 + L_0' + L_\alpha' \alpha \\ + \frac{1}{L_\alpha^*}\left[-c_2 \dot{z}_2 - \dot{z}_1 - \frac{g}{v_T^2} v_z \dot{v}_z - c_1 \ddot{z}_1\right],\end{aligned} \tag{5.22}$$

and defining

$$z_4 = q - q_{ref} \tag{5.23}$$

renders

$$\dot{z}_3 = -c_3 z_3 - L_\alpha^* z_2 + z_4 \tag{5.24}$$

$$\begin{aligned}\dot{V}_3 &= -W_2(z_1, z_2) - c_3 z_3^2 + z_3 z_4 \\ &= -W_3(z_1, z_2, z_3) + z_3 z_4,\end{aligned} \tag{5.25}$$

where $c_3 \in \mathbb{R}_+$ is a design constant, and

$$W_3 = W_2 + c_3 z_3^2,$$

which is positive definite. The function $\dot{V}_3$ is negative definite once z_4 is driven to 0. This guarantees that $z_3 \to 0$, and the α dynamics will asymptotically converge to a steady-state value α_0 which represents the angle of attack when $\gamma = \dot{\gamma} = 0$, or equivalently, $v_z = \dot{v}_z = 0$. That is, the steady-state angle of attack is defined by, see (5.3b) and (5.15),

$$\alpha_0 = \frac{1}{L_\alpha^*}\left[g - L_0^*\right]. \tag{5.26}$$

Step 4

Consider the final augmented subsystem

$$\begin{aligned}\dot{z}_4 = M_0' + M_\alpha' \alpha + M_q' q + M_{\delta_E}' \delta_E - \Bigg\{ &-c_3 \dot{z}_3 - L_\alpha^* \dot{z}_2 + \frac{g}{v_T^3} v_z \dot{v}_z + L_\alpha' \dot{\alpha} \\ &+ \frac{1}{L_\alpha^*}\left[-c_2 \ddot{z}_2 - \dddot{z}_1 - \frac{g}{v_T^2}\dot{v}_z^2 - \frac{g}{v_T^2} v_z \ddot{v}_z - c_1 \ddddot{z}_1\right]\Bigg\},\end{aligned} \tag{5.27}$$

where

$$\ddot{v}_z = \frac{g}{v_T^2} v_z \dot{v}_z + L_\alpha^* \dot{\alpha}.$$

The cLf for this step is selected by adding a term penalizing the error variable z_4

$$V = V_3 + \frac{1}{2} z_4^2. \tag{5.28}$$

The time derivative of (5.28) is defined by

$$\begin{aligned}\dot{V} = &-W_3(z_1, z_2, z_3) \\ &+ z_4 \Bigg[z_3 + M_0' + M_\alpha' \alpha + M_q' q + M_{\delta_E}' \delta_E - \Bigg\{ -c_3 \dot{z}_3 - L_\alpha^* \dot{z}_2 + \frac{g}{v_T^3} v_z \dot{v}_z + L_\alpha' \dot{\alpha} \\ &\qquad + \frac{1}{L_\alpha^*}\left[-c_2 \ddot{z}_2 - \dddot{z}_1 - \frac{g}{v_T^2}\dot{v}_z^2 - \frac{g}{v_T^2} v_z \ddot{v}_z - c_1 \ddddot{z}_1\right]\Bigg\}\Bigg].\end{aligned} \tag{5.29}$$

Selecting the following as the final control law

$$\delta_E = \frac{1}{M'_{\delta_E}}\Bigg[-c_4 z_4 - z_3 - M'_q q - M'_\alpha \alpha - M'_0 - z_3 + \Bigg\{-c_3 \dot{z}_3 - L^*_\alpha \dot{z}_2 + \frac{g}{v_T^3} v_z \dot{v}_z + L'_\alpha \dot{\alpha} + \frac{1}{L^*_\alpha}\left[-c_2 \ddot{z}_2 - \dddot{z}_1 - \frac{g}{v_T^2}\dot{v}_z^2 - \frac{g}{v_T^2} v_z \ddot{v}_z - c_1 \dddot{z}_1\right]\Bigg\}\Bigg] \tag{5.30}$$

renders

$$\dot{z}_4 = -c_4 z_4 - z_3 \tag{5.31}$$

$$\begin{aligned}\dot{V} &= -W_3(z_1, z_2, z_3) - c_4 z_4^2 \\ &= -W(z_1, z_2, z_3, z_4),\end{aligned} \tag{5.32}$$

where $c_4 \in \mathbb{R}_+$ is a design constant, and $W = W_3 + c_4 z_4^2$ which is positive definite. Consequently, the function $\dot{V}$ is negative definite. Application of Lyapunov's direct method yields the conclusion that the system $(z_1, z_2, z_3, z_4)^T$ is asymptotically stable at the origin and the original system (5.3) is asymptotically stable at $[h_d, 0, \alpha_0, 0]^T$. Note that asymptotic stability is not guaranteed beyond the stall angle of attack as our model of the aerodynamic lift force becomes invalid in the stall region.

5.3.1 Simulation results

In this section, we apply the control law (5.30) to the fully nonlinear, 6-DOF model of the Aerosonde UAV. The model is a part of the AeroSim blockset for Matlab/Simulink [105]. (The aerodynamic coefficients, which are based on wind-tunnel test data, are subjected to commercial-in-confidence restrictions and therefore cannot be listed.) The closed-loop system is implemented entirely in Matlab and Simulink. In the simulations that follow, the airspeed and the lateral dynamics are controlled by separate control loops.

To demonstrate the performance of the the control law (5.30), two scenarios are simulated. Both start at 100m above ground level (AGL) and with an airspeed of 23m/s. The effective range of the control input signal, in this case the elevators, is $\delta_E = [-57.3^o,\ 57.3^o]$. The design constants are tuned as follows

$$c_1 = 1.5, \qquad c_2 = 10, \qquad c_3 = 5, \qquad c_4 = 0.1$$

Figures 5.1 and 5.2 summarise the results of our first simulation scenario. The objective of this simulation is to track two altitude change commands. The first is a command to climb to 150m, applied at time $t = 10s$, and the second is a command to descend to 130m, applied at time $t = 100s$. The figures show that the controller provides good command

tracking, and a well-damped response with virtually no over-shoot. Such a good tracking performance from the controller justifies the use of a simplified aerodynamic model in the design process. The downside is that the simulated response has very long rise times. Let us examine the simulated response to the +50m step input commanded at 10s. Despite achieving a maximum climb rate of 4m/s at 12s, the rise time is approximately 40s. What we desire is that the aircraft attains the maximum possible vertical speed and maintains that speed until the aircraft has reached the commanded altitude. This however, is not possible with traditional backstepping because the control signals are proportional to the magnitude of the output error, see Figures 5.1 and 5.2.

Figures 5.3 and 5.4 summarise the results of the second simulation. In this case scenario, a step input of +100m is commanded at 10s. The figures show that due to the large size of the step input, the controller produces aggressive elevator deflections to try and drive the aircraft to the new altitude quickly, ultimately causing the aircraft to stall and enter into an irrecoverable dive. The stall occurs just before the 20s mark when the angle of attack goes beyond the stall angle of 17^o. This simulation exposes the main weakness of traditional backstepping. That is, it tends to produce very large effector commands, which are unsuitable for real dynamical systems due to actuator saturations and/or state constraints as shown in this simulation scenario.

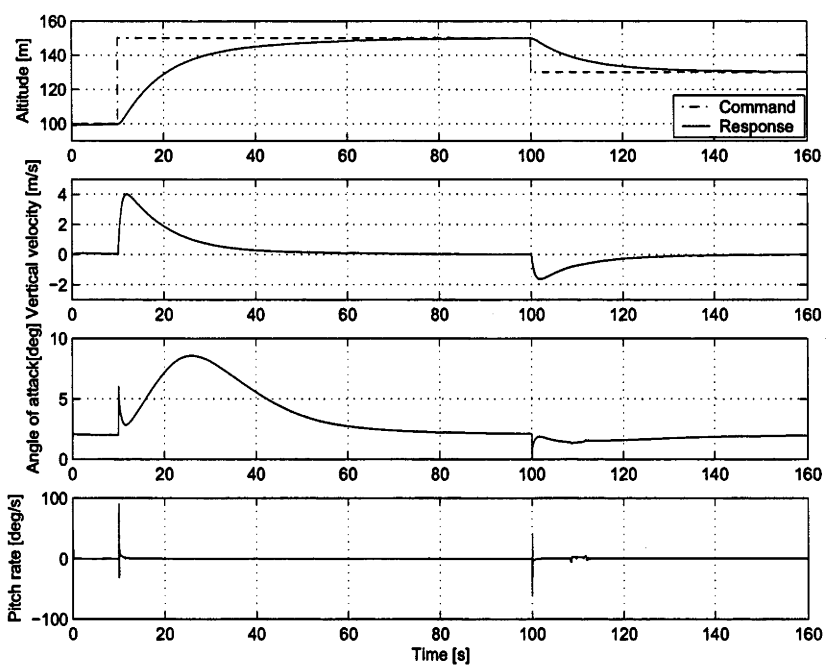

Figure 5.1: Aircraft response

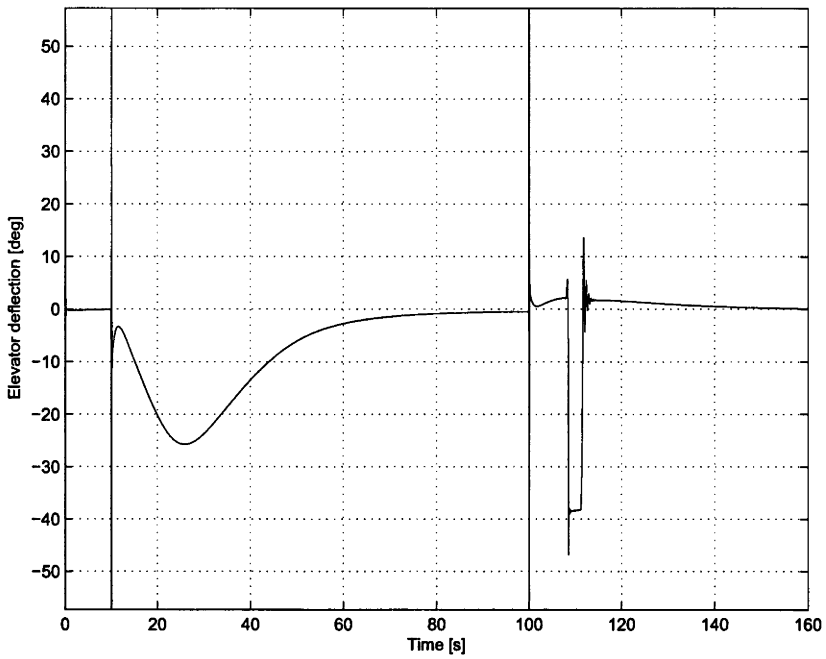

Figure 5.2: Elevator deflection

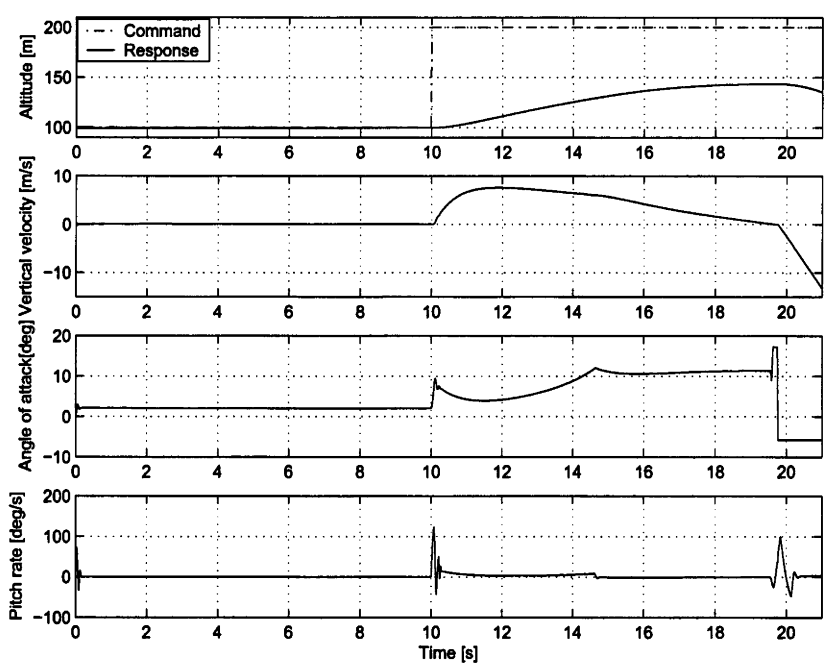

Figure 5.3: Aircraft response - stall case

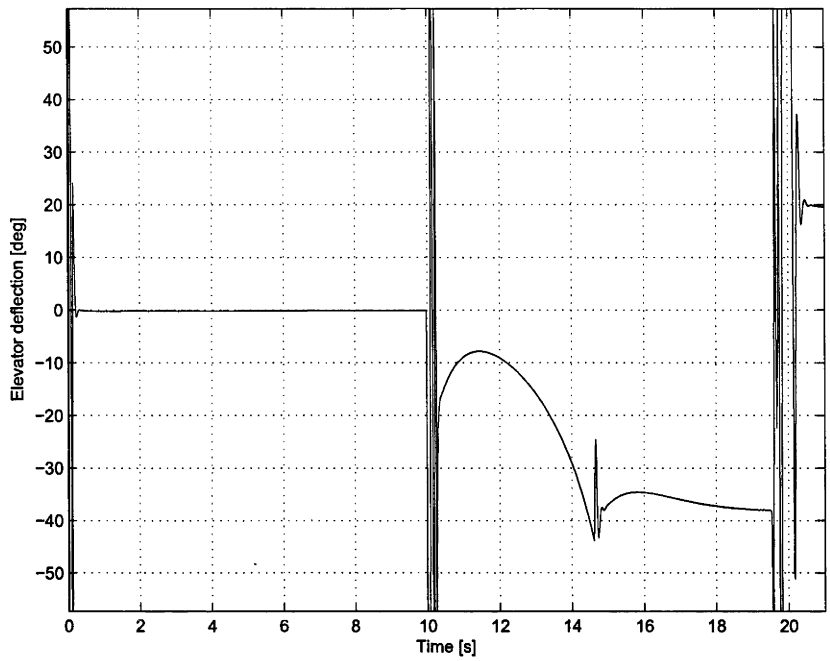

Figure 5.4: Elevator deflection - stall case

5.4 Constrained altitude controller: a backstepping re-design

In this section, we apply the results developed in Chapter 3 to re-design the altitude controller presented in the previous section. To prevent the controller from forcing the aircraft to attain altitude too quickly by commanding excessively large elevator deflections, hence causing the aircraft to stall, we impose a hard bound on the climb rate. That is,

$$|v_z(t)| \leq B, \quad \forall t \geq 0, \tag{5.33}$$

where $B \in \mathbb{R}_+$ is a constant. The design proceeds as follows.

Step 1

Let us go back to the first subsystem (5.4)

$$\dot{z}_1 = v_z, \tag{5.34}$$

where $z_1 = h - h_d$, and $h_d \in \mathbb{R}$ is the desired altitude. The following cLf is selected for this design step

$$V_1 = k_1 z_1 \tanh(z_1), \tag{5.35}$$

whose time derivative is given by

$$\begin{aligned} \dot{V}_1 &= k_1 \dot{z}_1 \left\{ \tanh(z_1) + z_1 - z_1 \tanh^2(z_1) \right\} \\ &= k_1 v_z \left\{ \tanh(z_1) + z_1 - z_1 \tanh^2(z_1) \right\}. \end{aligned} \tag{5.36}$$

Choosing the stabilising function $v_{z_{ref}}$ to be

$$v_{z_{ref}} = -c_1 \tanh(z_1), \tag{5.37}$$

and defining the error variable z_2 as follows

$$z_2 = v_z - v_{z_{ref}}, \tag{5.38}$$

one obtains

$$\dot{z}_1 = -c_1 \tanh(z_1) + z_2 \tag{5.39}$$

and

$$\begin{aligned} \dot{V}_1 &= -k_1 c_1 \tanh(z_1) \left\{ \tanh(z_1) + z_1 - z_1 \tanh^2(z_1) \right\} \\ &\quad + k_1 z_2 \left\{ \tanh(z_1) + z_1 - z_1 \tanh^2(z_1) \right\} \\ &= -W_1(z_1) + k_1 z_2 \left\{ \tanh(z_1) + z_1 - z_1 \tanh^2(z_1) \right\}, \end{aligned} \tag{5.40}$$

where

$$W_1 = k_1 c_1 \tanh(z_1) \left\{ \tanh(z_1) + z_1 - z_1 \tanh^2(z_1) \right\}. \tag{5.41}$$

Since the function W_1 is positive definite, $\dot{V}_1$ is negative definite once z_2 is driven to 0. This guarantees that $z_1 \to 0$ and the h dynamics becomes asymptotically stable at the desired altitude h_d. From (5.37), it follows that the selected stabilising function $v_{z_{ref}}$ is bounded in norm, that is,

$$|v_{z_{ref}}| \leq c_1. \tag{5.42}$$

The reason the cLf V_1 is chosen instead of the standard quadratic form is to limit the propagation of the error variable z_1 through to the next subsystem via the cross-term.

This would occur if the magnitude of z_1 is sufficiently large, due to a large step input in h_d for example, which may cause the next subsystem to become *stiff* and therefore harder to control.

Step 2

Consider the augmented subsystem for (5.39)

$$\dot{z}_2 = -g + \frac{g}{v_T^2} v_z^2 + L_0^* + L_\alpha^* \alpha + c_1 \dot{z}_1 - c_1 \dot{z}_1 \tanh^2(z_1). \tag{5.43}$$

To achieve the control objective of bounding the norm of the vertical velocity, v_z, the following cLf is selected for this design step

$$V_2 = V_1 + \frac{1}{2} k_3 \log\left(\frac{k_2^2}{k_2^2 - z_2^2}\right), \tag{5.44}$$

where k_2, $k_3 \in \mathbb{R}_+$ are design constants, and is positive definite and radially unbounded in the domain

$$\mathcal{D}_1 = \{(z_1, z_2) \in \mathbb{R}^2 \mid z_2 \in (-k_2, k_2)\}. \tag{5.45}$$

Differentiating V_2 yields

$$\dot{V}_2 = -W_1(z_1) + z_2 \left\{ k_1 \left[\tanh(z_1) + z_1 - z_1 \tanh^2(z_1) \right] + \frac{k_3}{k_2^2 - z_2^2} \dot{z}_2 \right\}, \tag{5.46}$$

whenever V_2 is well-defined and bounded at every $t \geq 0$. Selecting the stabilising function α_{ref} as follows

$$\begin{aligned} \alpha_{ref} = \frac{1}{L_\alpha^*} \Bigg\{ & -c_2 z_2 + g - \frac{g}{2v_T^2} v_z^2 - L_0^* - c_1 \dot{z}_1 + c_1 \dot{z}_1 \tanh(z_1)^2 \\ & - \frac{k_1}{k_3} \left(k_2^2 - z_2^2\right) \left[\tanh(z_1) + z_1 - z_1 \tanh^2(z_1) \right] \Bigg\}, \end{aligned} \tag{5.47}$$

and defining the error variable $z_3 = \alpha - \alpha_{ref}$ render

$$\dot{z}_2 = -c_2 z_2 - \frac{k_1}{k_3} \left(k_2^2 - z_2^2\right) \left[\tanh(z_1) + z_1 - z_1 \tanh^2(z_1) \right] + L_\alpha^* z_3 \tag{5.48}$$

$$\begin{aligned} \dot{V}_2 &= -W_1(z_1) - \frac{k_3 c_2 z_2^2}{k_2^2 - z_2^2} + \frac{k_3 L_\alpha^*}{k_2^2 - z_2^2} z_2 z_3 \\ &= -W_2(z_1, z_2) + \frac{k_3 L_\alpha^*}{k_2^2 - z_2^2} z_2 z_3, \end{aligned} \tag{5.49}$$

where $W_2 = W_1 + \frac{k_3 c_2 z_2^2}{k_2^2 - z_2^2}$ and is positive definite in $\mathcal{D}_1$. It then follows from (5.49) that $\dot{V}_2$ is rendered negative definite in the same domain $\mathcal{D}_1$ once z_3 is driven to 0. This guarantees

that the subsystem (z_1, z_2) is $\mathcal{D}_1$-domain asymptotically stable at the origin when z_3 is driven to 0.

Observe that the error signal z_2 is bounded due to the hard-bound coded into the cLf V_2. With the stability function $v_{z_{ref}}$ bounded in norm, the climb rate v_z is now bounded by virtue of (5.38). The explicit overbound on v_z is

$$\begin{aligned} |v_z(t)| &= |z_2(t)| + |v_{z_{ref}}(t)| \\ &< k_2 + c_1. \end{aligned} \tag{5.50}$$

We have now achieved our control objective. The remaining design steps mirror those of the traditional backstepping method.

Step 3

Consider the augmented subsystem for (5.48)

$$\dot{z}_3 = \frac{g}{v_T} - \frac{g}{2v_T^3} v_z^2 - L'_0 - L'_\alpha \alpha + q - \dot{\alpha}_{ref}. \tag{5.51}$$

The following cLf is selected for this design step

$$V_3 = V_2 + \frac{1}{2} z_3^2 \tag{5.52}$$

whose time derivative is given by

$$\dot{V}_3 = -W_2(z_1, z_2) + z_3 \left\{ \frac{k_3 L^*_\alpha}{k_2^2 - z_2^2} z_2 + \dot{z}_3 \right\}, \tag{5.53}$$

whenever V_3 is well-defined and bounded at every $t \geq 0$. The choice of

$$q_{ref} = -c_3 z_3 - \frac{k_3 L^*_\alpha}{k_2^2 - z_2^2} z_2 - \frac{g}{v_T} + \frac{g}{2v_T^3} v_z^2 + L'_0 + L'_\alpha \alpha + \dot{\alpha}_{ref}, \tag{5.54}$$

renders

$$\dot{z}_3 = -c_3 z_3 - \frac{k_3 L^*_\alpha}{k_2^2 - z_2^2} z_2 + z_4, \tag{5.55}$$

and

$$\begin{aligned} \dot{V}_3 &= -W_2 - c_3 z_3^2 + z_3 z_4 \\ &= -W_3 + z_3 z_4, \end{aligned} \tag{5.56}$$

where $z_4 = q - q_{ref}$, and $W_3 = W_2 + c_3 z_3^2$ which is positive definite in the domain

$$\mathcal{D}_2 = \{(z_1, z_2, z_3) \in \mathbb{R}^3 \mid z_2 \in (-k_2, k_2)\}. \tag{5.57}$$

This implies that $\dot{V}_3$ is negative definite in the same domain $\mathcal{D}_2$ once z_4 is driven to 0. Consequently, $z_3 \to 0$ and the α dynamics becomes asymptotically stable at the steady-state angle of attack α_0, which is defined by (5.26).

Step 4

Consider the final augmented subsystem

$$\dot{z}_4 = M'_0 + M'_\alpha \alpha + M'_q q + M'_{\delta_E} \delta_E - \dot{q}_{ref}. \tag{5.58}$$

The following cLf is chosen

$$V = V_3 + \frac{1}{2} z_4^2. \tag{5.59}$$

Differentiating V yields

$$\dot{V} = -W_3 + z_4 \{z_3 + \dot{z}_4\}, \tag{5.60}$$

whenever V is well-defined and bounded at every $t \geq 0$. If the following final control law δ_E is chosen

$$\delta_E = \frac{1}{M'_{\delta_E}} \left\{ -c_4 z_4 - z_3 - M'_q q - M'_\alpha \alpha - M'_0 + \dot{q}_{ref} \right\}, \tag{5.61}$$

we obtain

$$\dot{z}_4 = -c_4 z_4 - z_3 \tag{5.62}$$

$$\dot{V} = -W_3 - c_4 z_4^2 \leq -W_4, \tag{5.63}$$

where $W_4 = W_3 + c_4 z_4^2$ and is positive definite in the domain

$$\mathcal{D} = \{(z_1, z_2, z_3, z_4) \in \mathbb{R}^4 \mid z_2 \in (-k_2, k_2)\}. \tag{5.64}$$

Consequently, $\dot{V}$ is negative definite in the domain $\mathcal{D}$. Application of direct Lyapunov's method yields the conclusion that the system $(z_1, z_2, z_3, z_4)^T$ is asymptotically stable at the origin. This implies that the original system (5.3) is asymptotically stable at $[h_d, 0, \alpha_0, 0]^T$.

5.4.1 Main result

Theorem 5.5. *Consider the system (5.3) subject to constraints on the climb rate as follows*

$$|v_z(t)| \leq B, \quad B \in \mathbb{R}_+, \quad \forall t \geq 0. \tag{5.65}$$

Let $c_1 + k_2 \leq B$, $k_2 > c_1$, c_2, c_3, c_4, k_1, $k_3 \in \mathbb{R}_+$ *be design constants. For any initial condition such that* $|v_z(0)| < B$, *then system (5.3) in closed-loop with control law (5.61) is:*

i. asymptotically stable at the origin,

ii. $|v_z(t)| < B$, $\forall\, t \geq 0$, *and*

iii. the control $\delta_E(t)$ *is smooth.*

Proof. Part (i) follows from the application of Lyapunov's direct method to (5.59) and (5.63).

Part(ii) is a consequence of the proposed control design. From (5.44) and (5.59), it immediately follows that

$$\frac{1}{2}k_3 \log\left(\frac{k_2^2}{k_2^2 - z_2(t)^2}\right) \leq V(t) \leq V(0), \quad \forall t \geq 0. \tag{5.66}$$

By inspection, this proves that

$$|z_2(t)| < k_2, \quad \forall t \geq 0. \tag{5.67}$$

As a direct result of (5.37) and (5.38)

$$\begin{aligned} |v_z(t)| &\leq |z_2(t)| + |v_{z_{ref}}(t)| \\ &< k_2 + c_1 \end{aligned} \tag{5.68}$$

for all time $t \geq 0$. Since the constants c_1 and k_2 are chosen such that $c_1 + k_2 \leq B$,

$$|v_z(t)| < B, \quad \forall t \geq 0. \tag{5.69}$$

Lastly, part (iii) follows directly from the construction of the control law $\delta_E(t)$, see (5.61). □

5.4.2 Control tuning

In this section, we explain how the design parameter k_3 governs the evolution of the error variable z_2, and hence the vertical velocity v_z. From (5.66), we obtain

$$\frac{1}{2}k_3 \log\left(\frac{k_2^2}{k_2^2 - z_2(t)^2}\right) \leq V(t), \quad \forall t \geq 0. \tag{5.70}$$

Multiplying both sides by $\frac{2}{k_3}$ and exponentiating them yields

$$\left(\frac{k_2^2}{k_2^2 - z_2(t)^2}\right) \leq e^{\frac{2V(t)}{k_3}}. \tag{5.71}$$

For simplicity, let us consider the case where $k_2 = 1$ which means that $z_2 \in (-1, 1)$. Simple algebraic manipulations of (5.71) leads to the following bound on z_2

$$z_2^2(t) \leq 1 - \frac{1}{e^{\frac{2V(t)}{k_3}}}. \tag{5.72}$$

It is obvious from the above expression that for a given value of $V(t)$, the smaller k_3 is, the closer to its bounds, which is $(-1, 1)$ in this example, $z_2(t)$ gets. Consequently, the climb rate v_z will be pushed closer to its bounds by virtue of (5.38).

5.4.3 Simulation results

To illustrate the performance of the proposed controller design, the results of two simulation scenarios are presented in this section. In both cases, the aircraft starts out at 100m above ground level (AGL) with an airspeed of 23m/s. We demand that the climb rate of the Aerosonde UAV should never be allowed to exceed $\pm$ 3.5m/s. The design parameters are tuned accordingly as follows

$$c_1 = 1.5, \quad c_2 = 1, \quad c_3 = 5, \quad c_4 = 10, \quad k_1 = 1.5, \quad k_2 = 2, \quad k_3 = 0.5$$

Figures 5.5 and 5.6 plot the aircraft's response to a +100m step input commanded at 10s, and Figures 5.7 and 5.8 plot the aircraft's response to a +400m step input also commanded at 10s.

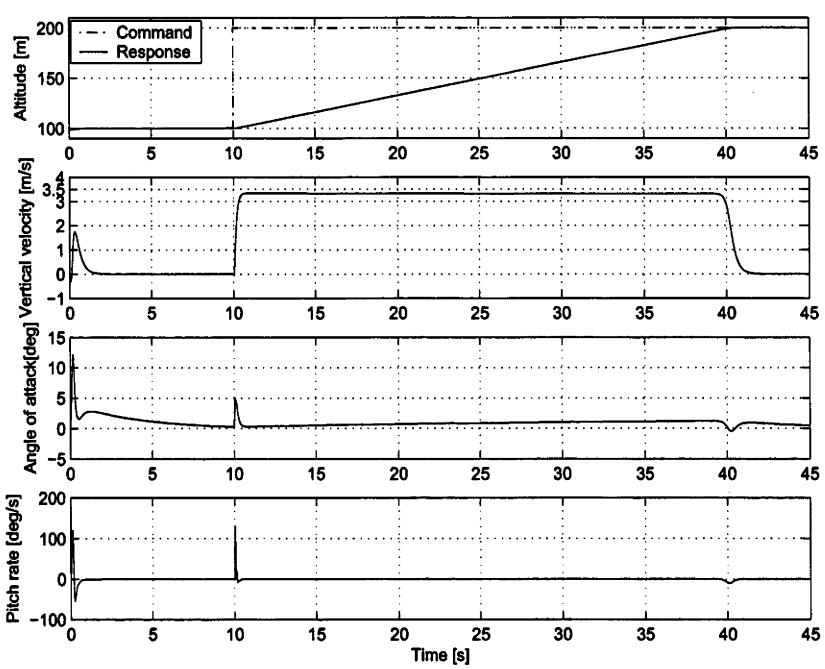

Figure 5.5: Constrained aircraft response to an altitude command of +100m at 10s

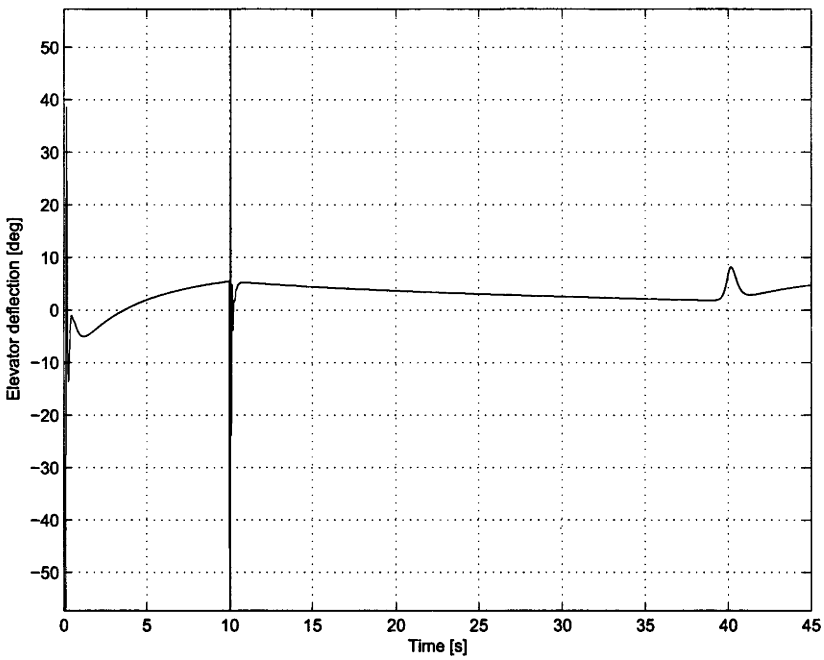

Figure 5.6: Elevator deflection for an altitude command of +100m at 10s

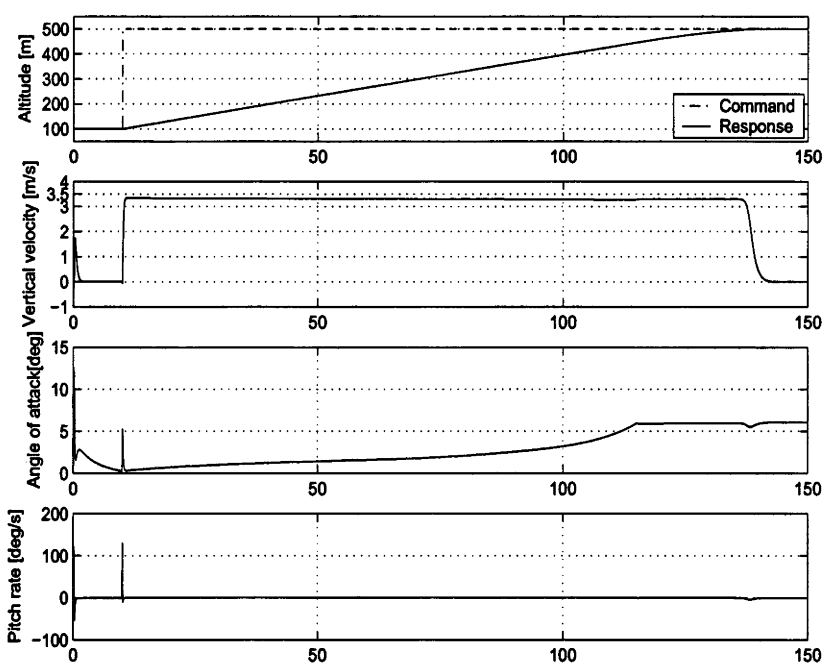

Figure 5.7: Constrained aircraft response to an altitude command of +400m at 10s

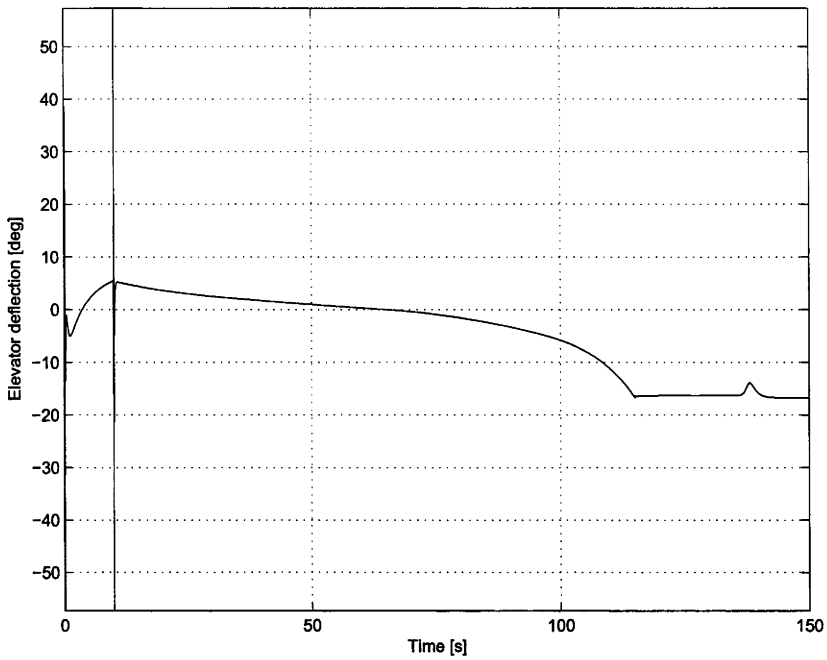

Figure 5.8: Elevator deflection for an altitude command of +400m at 10s

The simulation results clearly demonstrate that our objective of constraining the vertical velocity to below 3.5m/s at all time is achieved, irrespective of the magnitude of the commanded altitude changes. This imposed constraint on the climb rate means that the controller will never force the aircraft to climb or descend at too steeply a rate by commanding unnecessarily large elevator deflections. As a result, stall is no longer an issue. Performance wise, the response is exactly what is desired. That is, following an altitude change command, the aircraft reaches the maximum achievable climb rate in the shortest time possible, and maintains this speed until the commanded altitude has been attained. This type of response can be considered to be almost time-optimal and cannot be achieved with traditional backstepping.

5.5 Chapter summary

The contribution of this chapter is the introduction of two backstepping-based controller designs to regulate the altitude of the Aerosonde UAV. The first controller is designed based on the traditional backstepping approach. Closed-loop simulations of the controller on a fully nonlinear, 6-DOF aircraft model show that the the controller provides good tracking performance for small altitude commands. However, the controller becomes more aggressive for larger altitude commands, and eventually causes the aircraft to stall by commanding excessively large elevator deflections. To address this issue, we imposed a

hard bound on the aircraft's rate of climb and re-designed the controller using the results of Chapter 3. Closed-loop simulations for this controller demonstrate that the climb rate always remains within the specified bounds, irrespective of the size of the altitude change commands. This hard bound imposed on the climb rate means that the controller will never command the aircraft to attain altitude more quickly than is aerodynamically and physically achievable by the airframe, thus preventing stall. Furthermore, the re-designed controller provides excellent tracking performance, and the induced response can be regarded as almost time-optimal, given the constraints on the climb rate. That is, following an altitude change command, the aircraft reaches the maximum allowable climb rate in the shortest possible time, and maintains this velocity until the desired altitude is reached. Such performance is more robust than existing nonlinear control designs that do not consider state constraints. The use of a simplified aerodynamic model has also been justified as it causes no discernable degradation to the performance of either controller.

Part II

Passivity-based Control of Constrained Robot Manipulators

Chapter 6

Constrained stabilisation of robot manipulators

Robot manipulators have become an integral part in almost all modern manufacturing processes, performing tasks that are considered too dull, repetitive, and hazardous for humans, or that require strength, skill, and precision beyond the capability of humans. The control problem for robot manipulators is therefore a well-studied one. The recognised "classical" techniques for controlling a manipulator include: feedback linearization or dynamic inversion [52, 73], variable structure control [127], computed torque feedforward control [5, 70], and passivity-based control (PBC) [109, 138]. Although these early works solved the global asymptotic tracking and set-point regulation problems, they did not address the problems of obstacles in the workspace and/or hard constraints on the robot's joint positions and joint velocities.

The environments in which robot manipulators operate are often constrained and cluttered. Due to factors such as safety and economy of operations, it is imperative that the robots avoid collisions with obstacles while performing their work. There is a great amount of research devoted to the obstacle avoidance problem. Lozano-Perez [85], Brooks [18], and many others [32, 63, 76] proposed off-line algorithms using free-space to plan collision-free motions for general robot manipulators. However, these off-line methods are typically computationally expensive and thus unsuitable for real-time implementation except for very simple cases [9]. Online obstacle avoidance approaches on the other hand, are substantially faster and well-suited for real-time applications. Online obstacle avoidance can be achieved by employing the popular artificial potential field method [69, 114] where the robot is guided by potential fields that exert repulsive forces away from the obstacles and an attractive force toward the desired position. More recently, it has been shown in [135] that the extra freedom of the coordinate transformation in the feedback linearisation method can also be employed to solve the online obstacle avoidance problem. Biologically motivated, non-model-based methods have been considered, including fuzzy logic [27, 94], neural networks [158], and genetic algorithms [40, 146]. Although attempts to incorporate Lyapunov-like formalisms into such frameworks have been made in such works as [34, 58],

stability and convergence properties of these methods remain, in general, difficult to analyze.

Another important consideration in the controlling of robot manipulators is the hard constraints on the robot's joint positions and joint velocities. Ignoring these constraints will cause saturation as well as sustaining physical damage when a joint position or joint velocity is commanded beyond its physical bounds. Time-scaling [47] is a standard technique employed to avoid joint velocity saturation along pre-defined trajectories. An alternative approach is the "Windup Feedback Scheme" [102], where, whenever a joint position or joint velocity is saturated, the unmet control demands are redistributed among the remaining unsaturated joints. There have also been numerous studies of obstacle avoidance and/or joint position and joint velocity constraints for redundant manipulators [22–24, 151]. The applicability of these methods, however, is restricted to redundant manipulators only. For general manipulators, there are few works that address both obstacle constraints and joint limits in an integrated framework. In [135], Sugie et al. uses a two step process involving feedback linearisation with the extra degree of freedom to address the online obstacle avoidance problem along with a coupled time-scaling adjustment for bounded joint velocity control.

This chapter addresses the general problem of autonomous, or online, obstacle avoidance for robot manipulators subject to hard constraints on the robot's joint positions and joint velocities. The obstacles are assumed to be fixed and stationary, and we only consider set-point regulation. The proposed control design is based on the PBC framework, with modifications made to the cLf such that the constraints are strictly satisfied for all time. The structure of the modified cLf resembles those used in the artificial potential field method. We differ from the earlier developments by directly integrating the constraint equations into the cLf to derive a unified control law that achieves autonomous obstacle avoidance, respects joint position and joint velocity limits, and achieves local stabilisation of the closed-loop system. The modification of the cLf can be thought of as a form of energy shaping of both the kinetic and potential energy terms in the classical storage function obtained in PBC. The ideas presented in this chapter are similar to those of [150]. However, in [150], only joint position constraints of the form $q_L \leq q \leq q_U$, where q_L, q_U represent the upper and lower limits of the robot's joint position q, respectively, are considered. Furthermore, the cLf structure proposed in [150] is very different to ours, and cannot readily be extended to accommodate obstacle constraints and joint velocity constraints. For arbitrary constraints, the controller design proposed in this chapter suffers from the same limitations of the artificial potential field approach in regard to the possible presence of local minima in the cLf. However, there are certain cases for which asymptotic stability of the closed-loop system is guaranteed. Examples of such cases are covered in Section 6.3.1.

The chapter is organised as follows. Section 6.1 provides an overview of the robot dy-

namics. Section 6.2 briefly reviews the results of the "classical" PBC method. Section 6.3 details the main results. Simulation results are provided in Section 6.4 whilst concluding statements are contained in Section 6.6.

6.1 Robot dynamics

Consider a rigid and fully-actuated n-link robot manipulator with no external forces, that is, no end-effector contacts with the environment, and no external disturbances. The dynamics of such systems is described by [109]

$$\mathcal{D}(q)\ddot{q} + \mathcal{C}(q,\dot{q})\dot{q} + g(q) + \frac{\partial \mathcal{F}}{\partial \dot{q}}(\dot{q}) = \tau, \tag{6.1}$$

where we use the following notation

$q \in \mathbb{R}^n$	generalised joint coordinates,
$\mathcal{D}(q) \in \mathbb{R}^{n\times n}$	generalised inertia matrix,
$\mathcal{C}(q,\dot{q}) \in \mathbb{R}^{n\times n}$	Coriolis-centrifugal matrix,
$g(q) \in \mathbb{R}^n$	gravitational torques,
$\mathcal{F}(\dot{q})$	Rayleigh dissipation function,
$\tau \in \mathbb{R}^n$	applied input torques.

For all serial manipulators, the following properties hold for (6.1).

Property 6.1. *The inertial matrix $\mathcal{D}(q)$ is symmetric and positive definite. That is,*

$$\mathcal{D}(q)^T = \mathcal{D}(q) > 0, \quad \forall q \in \mathbb{R}^n. \tag{6.2}$$

Property 6.2. *The time derivative of the inertia matrix $\dot{\mathcal{D}}(q)$ and the Coriolis-centrifugal matrix $\mathcal{C}(q,\dot{q})$ satisfy the following "skew-symmetric" relationship*

$$\dot{q}^T[\dot{\mathcal{D}} - 2\mathcal{C}]\dot{q} = 0, \quad \forall q, \dot{q} \in \mathbb{R}^n, \tag{6.3}$$

Property 6.3. *The Rayleigh dissipation function $\mathcal{F}(\dot{q})$ satisfies*

$$\dot{q}^T \frac{\partial \mathcal{F}}{\partial \dot{q}}(\dot{q}) \geq 0, \quad \forall \dot{q} \in \mathbb{R}^n, \tag{6.4}$$

and

$$\frac{\partial \mathcal{F}}{\partial \dot{q}}(0) = 0. \tag{6.5}$$

6.2 Classical PBC for robot manipulators

In this section, we present a brief recapitulation of the classical theory of PBC of robot manipulators for the set-point regulation problem [67].

Let the vector $[\tilde{q}, \dot{q}]^T$ define the system state, where

$$\tilde{q} = q - q_d \tag{6.6}$$

represents the error between the actual, q, and the desired, q_d, link position. Select the following positive definite and radially unbounded function as the candidate cLf

$$\mathcal{L}(\tilde{q}, \dot{q}) = \frac{1}{2}\dot{q}^T\mathcal{D}(q)\dot{q} + \frac{1}{2}\tilde{q}^T K_P \tilde{q}, \tag{6.7}$$

which is derived from the kinetic energy of the system along with the "shaped" potential energy. The control gain matrix $K_P \in \mathbb{R}^{n\times n}$ is constant, diagonal, and positive definite. Note that the potential energy has been shaped such that the set-point $[q = q_d,\ \dot{q} = 0]^T$ is now the equilibrium of the system.

Differentiating (6.7) with respect to time yields

$$\dot{\mathcal{L}} = \dot{q}^T\mathcal{D}(q)\ddot{q} + \frac{1}{2}\dot{q}^T\dot{\mathcal{D}}(q)\dot{q} + \tilde{q}^T K_P \dot{q}. \tag{6.8}$$

Substituting the system dynamics (6.1) into (6.8) gives

$$\dot{\mathcal{L}} = \frac{1}{2}\dot{q}^T\left[\dot{\mathcal{D}}(q) - 2\mathcal{C}(q,\dot{q})\right]\dot{q} - \dot{q}^T\frac{\partial\mathcal{F}}{\partial\dot{q}}(\dot{q}) + \dot{q}^T\Big[\tau - g(q) + K_P\tilde{q}\Big]. \tag{6.9}$$

The first term on the right hand side (RHS) of (6.9) is null due to the passivity properties of mechanical systems [109], see Property 6.2. The second term is negative semi-definite (or dissipative) due to the properties of the Rayleigh dissipation function, see Property 6.3. To stabilise (6.1), the following input torque is chosen

$$\tau = g(q) - K_P\tilde{q} - K_D\dot{q}, \tag{6.10}$$

where the control gain matrix $K_D \in \mathbb{R}^{n\times n}$ is constant, diagonal, and positive definite. Such a choice for τ renders

$$\dot{\mathcal{L}} = -\dot{q}^T\frac{\partial\mathcal{F}}{\partial\dot{q}}(\dot{q}) - \dot{q}^T K_D\dot{q} \leq 0, \quad \forall\tilde{q},\dot{q} \in \mathbb{R}^n. \tag{6.11}$$

The resulting closed-loop dynamics is given by

$$\mathcal{D}(q)\ddot{q} = -K_P\tilde{q} - K_D\dot{q} - \mathcal{C}(q,\dot{q})\dot{q} - \frac{\partial\mathcal{F}}{\partial\dot{q}}(\dot{q}). \tag{6.12}$$

Application of Lyapunov's direct method [68] to (6.7) and (6.11) guarantees convergence to the invariant set characterised by $\mathcal{I} := \{(\tilde{q},\dot{q}) \in \mathbb{R}^n \times \mathbb{R}^n \mid \dot{q} = 0\}$. Note that since $\dot{q} = 0$, it must also hold that $\ddot{q} = 0$ in $\mathcal{I}$. Let us now evaluate the closed-loop dynamics

(6.12) in $\mathcal{I}$, that is, when $\dot{q} = \ddot{q} = 0$. Using Property 6.3, one obtains the following equality

$$0 = K_P \tilde{q}. \tag{6.13}$$

Since the control gain matrix K_P is chosen to be constant and positive definite, the above equality is true if and only if $\tilde{q} = 0$. According to LaSalle's Invariance Principle [68], the origin $[\tilde{q}, \dot{q}]^T = [0, 0]^T$ is therefore globally asymptotically stable. Thus, all closed-loop trajectories asymptotically converge to the set-point $[q = q_d,\ \dot{q} = 0]^T$. Detailed proof of this result can be found in such robotics text as [67,122].

6.3 Constrained PBC

This section proposes a modification to the "classical" PBC design for robot manipulators to incorporate obstacle constraints as well as hard constraints on joint positions and joint velocities.

In the following derivation, obstacle constraints and joint position constraints are represented mathematically by one-sided inequalities expressed in terms of the joint positions. Each constraint is represented by a separate constraint function.

Assumption 6.4. *For each obstacle or joint position constraint, there exists a differentiable function $h_i(q)$ and a constant $\Delta_i \in \mathbb{R}$ such that*

$$h_i(q) \geq \Delta_i \tag{6.14}$$

characterises the accessible workspace for that constraint.

Remark 6.5. *Non-smooth transitions such as edges and corners of an obstacle or singularities in joint positions can be accommodated by approximating the non-smooth constraint with a differentiable constraint. In practice, the function $h_i(q)$ is only required to be differentiable on the set $h_i(q) > \Delta_i$. It is acceptable to work with constraint functions $h_i(q)$ that are non-differentiable on the constraint boundary itself.*

Joint velocity constraints can be accommodated as long as they can be expressed as quadratic functions of joint velocities.

Assumption 6.6. *For each joint velocity constraint there exists a smoothly varying positive semi-definite matrix $Q_j(q) \geq 0$ and a smooth function $\Omega_j(q)$ such that the joint velocity constraint can be expressed as*

$$\frac{1}{2}\dot{q}^T Q_j(q)\dot{q} \leq \Omega_j(q).$$

Remark 6.7. *The simplest joint velocity constraints are those where each and every individual joint velocity is bounded as follows*

$$|\dot{q}_j(t)| \leq B_j, \quad t \geq 0, \quad j = 1, ..., n, \tag{6.15}$$

where $B_j \in \mathbb{R}_+$ is a constant. In this case, choosing $\Omega_j = B_j^2/2$, the velocity constraints can be re-written as

$$\frac{1}{2}\dot{q}_j(t)^2 = \frac{1}{2}\dot{q}^T e_j e_j^T \dot{q} = \frac{1}{2}\dot{q}^T Q_j \dot{q} \leq \Omega_j, \quad t \geq 0,$$

for $j = 1, ..., n$. Here e_j denotes the unit vector in the j'th direction and the matrix $Q_j = e_j e_j^T \geq 0$ is positive semi-definite. A limitation of Assumption 6.6 is that the velocity constraints have to be symmetric about the origin $\dot{q} = 0$. Thus, a velocity constraint $-a < \dot{q}_j(t) < b$ where $a, b \in \mathbb{R}_+$, $a \neq b$ cannot be accommodated using the proposed approach.

Denote the number of configuration constraints, that is, obstacle and joint position constraints, by N and the number of velocity constraints by M. To simplify the derivation that follows, we introduce the following notations

$$\Phi(q) = \prod_{i=1}^{N} \phi_i(q), \quad \phi_i(q) = h_i(q) - \Delta_i, \quad i = 1, \ldots, N, \tag{6.16}$$

and

$$\Psi(q, \dot{q}) = \prod_{j=1}^{M} \psi_j(q, \dot{q}), \quad \psi_j(q, \dot{q}) = \Omega_j(q) - \frac{1}{2}\dot{q}^T Q_j(q)\dot{q}, \quad j = 1, \ldots, M. \tag{6.17}$$

The admissible constraint set for the problem is the set of states contained in

$$\begin{aligned} S &= \{(q, \dot{q}) \in \mathbb{R}^n \times \mathbb{R}^n \mid \phi_i(q) > 0 \text{ and } \psi_j(q, \dot{q}) > 0, \quad i = 1, ..., N, \quad j = 1, ...M\} \\ &= \{(q, \dot{q}) \in \mathbb{R}^n \times \mathbb{R}^n \mid \Phi(q) > 0 \text{ and } \Psi(q, \dot{q}) > 0\}. \end{aligned} \tag{6.18}$$

The boundary of S is defined by

$$\partial S = \{(q, \dot{q}) \in \mathbb{R}^n \times \mathbb{R}^n \mid \Phi(q) = 0 \text{ or } \Psi(q, \dot{q}) = 0\}. \tag{6.19}$$

Let the vector $[\tilde{q}, \dot{q}]^T$ define the system state, where $\tilde{q} = q - q_d$ represents the error between the actual and the desired link position. The control problem considered is that of stabilisation to the target set-point $[q = q_d, \dot{q} = 0]^T$. It is desired to have control that behaves as do the PBC designs when distant from the constraints and is modified to ensure that the constraints are always respected. The underlying idea of the approach is similar to that of the artificial potential field method. We differ from the earlier developments in that we directly integrate the constraint equations into the cLf and use this cLf to derive a unified control law that fully respects the system's dynamics. To ensure a well-posed problem we make the following final assumption.

Assumption 6.8. *The initial condition* $[q_0, \dot{q}_0]^T \in \mathcal{S}$, *where* $q_0 \triangleq q(t=0)$, *and* $\dot{q}_0 \triangleq \dot{q}(t=0)$. *The desired link position* $q_d \in \mathcal{S}$, *and* q_d *and* q_0 *lie in the same path connected component of* $\mathcal{S}$.

Consider the following function, which is positive definite and radially unbounded in $\mathcal{S}$, as the candidate cLf for system (6.1)

$$V(\tilde{q}, \dot{q}) = \frac{\mathcal{L}(\tilde{q}, \dot{q})}{\Phi\Psi} = \frac{1}{2\Phi\Psi}\left[\dot{q}^T\mathcal{D}(q)\dot{q} + \tilde{q}^T K_P \tilde{q}\right], \tag{6.20}$$

where the function $\mathcal{L}(\tilde{q}, \dot{q})$ is given by (6.7). The constraint functions Φ and Ψ are identically zero on the boundary $\partial\mathcal{S}$. Consequently, $V(\tilde{q}, \dot{q})$ is asymptotically infinite on $\partial\mathcal{S}$. The proposed candidate cLf is similar to the barrier functions used in optimisation methods and the underlying idea is closely linked to the artificial potential field method. The advantage of the approach taken is that the function $V(\tilde{q}, \dot{q})$ can be thought of as a shaped energy function for the constrained system.

Theorem 6.9. *Consider the dynamics (6.1) for a serial manipulator. Given configuration and velocity constraints satisfying Assumptions 6.4 and 6.6, and functions* Φ *and* Ψ *as defined by (6.16) and (6.17). Define* $\mathcal{L}(\tilde{q}, \dot{q})$ *according to (6.7) and*

$$a_\phi(q) := \sum_{s=1}^{N}\left(\prod_{i\neq s}^{N}\phi_i(q)\right)\frac{\partial\phi_s}{\partial q}, \tag{6.21}$$

$$a_\psi(q, \dot{q}) := \sum_{s=1}^{M}\left(\prod_{j\neq s}^{M}\psi_j(q, \dot{q})\right)\left[\frac{\partial\Omega_s}{\partial q} - \frac{1}{2}\dot{q}^T\dot{Q}_j\dot{q}\right], \tag{6.22}$$

$$P(q, \dot{q}) := \sum_{s=1}^{M}\left(\prod_{j\neq s}^{M}\psi_j(q, \dot{q})\right)Q_s. \tag{6.23}$$

Choose the torque input to be

$$\begin{aligned}\tau(\tilde{q}, \dot{q}) = g(q) + \mathcal{D}(q)&\left[\Phi\Psi\mathcal{D}(q) + \mathcal{L}\Phi P\right]^{-1} \\ &\left[-\Phi\Psi\left\{K_P\tilde{q} + K_D\dot{q}\right\} + \mathcal{L}\left\{\Psi a_\phi + \Phi a_\psi\right\} + \mathcal{L}\Phi P\mathcal{D}^{-1}(q)\left\{C\dot{q} + \frac{\partial\mathcal{F}}{\partial\dot{q}}(\dot{q})\right\}\right],\end{aligned} \tag{6.24}$$

where the control gain matrices $K_P, K_D \in \mathbb{R}^{n\times n}$ *are constant, diagonal, and positive definite. Then for any initial condition* $[q_0, \dot{q}_0]^T$ *and desired link position* q_d *satisfying Assumption 6.8, all trajectories of the closed-loop system remain inside the admissible constraint set* $\mathcal{S}$ *for all time, and converge to the invariant set characterised by the following equality*

$$\Phi(q)\Psi(q, 0)K_P\tilde{q} = \mathcal{L}(\tilde{q}, 0)\left[\Psi(q, 0)a_\phi(q) + \Phi(q)a_\psi(q, 0)\right], \tag{6.25}$$

which contains the set-point $[q = q_d, \dot{q} = 0]^T$.

To simplify the notation, in the following development, functions are written without their arguments except where confusion may arise.

Proof. Consider the cLf given by (6.20). Differentiating with respect to time yields

$$\dot{V} = \frac{\dot{\mathcal{L}}\Phi\Psi - \mathcal{L}(\dot{\Phi}\Psi + \Phi\dot{\Psi})}{(\Phi\Psi)^2}. \tag{6.26}$$

whenever $V(\tilde{q}, \dot{q})$ is well-defined, and bounded at every $t \geq 0$. Taking the time-derivatives of $\mathcal{L}$, Φ, and Ψ gives

$$\dot{\mathcal{L}} = \frac{1}{2}\dot{q}^T\left[\dot{\mathcal{D}} - 2\mathcal{C}\right]\dot{q} - \dot{q}^T\frac{\partial\mathcal{F}}{\partial\dot{q}} + \dot{q}^T\left[\tau - g + K_P\tilde{q}\right] \tag{6.27}$$

$$\dot{\Phi} = \langle a_\phi, \dot{q}\rangle \tag{6.28}$$

$$\dot{\Psi} = \langle a_\psi, \dot{q}\rangle - \langle P\mathcal{D}^{-1}\left[\tau - \mathcal{C}\dot{q} - g - \frac{\partial\mathcal{F}}{\partial\dot{q}}\right], \dot{q}\rangle, \tag{6.29}$$

respectively, where $\langle\cdot,\cdot\rangle$ denotes the inner product. Substituting $\dot{\mathcal{L}}$, $\dot{\Phi}$, and $\dot{\Psi}$ into the expression for $\dot{V}$ yields

$$\begin{aligned}\dot{V} = {} & \frac{\Phi\Psi}{(\Phi\Psi)^2}\left\{\frac{1}{2}\dot{q}^T\left[\dot{\mathcal{D}} - 2\mathcal{C}\right]\dot{q} - \dot{q}^T\frac{\partial\mathcal{F}}{\partial\dot{q}} + \dot{q}^T\left[\tau - g + K_P\tilde{q}\right]\right\} \\ & - \frac{\mathcal{L}}{(\Phi\Psi)^2}\left\{\langle a_\phi, \dot{q}\rangle\Psi + \Phi\langle a_\psi, \dot{q}\rangle - \Phi\langle P\mathcal{D}^{-1}\left[\tau - \mathcal{C}\dot{q} - g - \frac{\partial\mathcal{F}}{\partial\dot{q}}\right], \dot{q}\rangle\right\}.\end{aligned} \tag{6.30}$$

Applying Properties 6.2 and 6.3, and collecting like terms together, one obtains

$$\begin{aligned}\dot{V} = \frac{\dot{q}^T}{(\Phi\Psi)^2}\Big\{ & \left[\Phi\Psi\mathcal{D} + \mathcal{L}\Phi P\right]\mathcal{D}^{-1}\tau + \Phi\Psi\left[K_P\tilde{q} - g\right] - \mathcal{L}\left[\Psi a_\phi + \Phi a_\psi\right] \\ & - \mathcal{L}\Phi P\mathcal{D}^{-1}\left[\mathcal{C}\dot{q} + g + \dot{q}^T\frac{\partial\mathcal{F}}{\partial\dot{q}}\right]\Big\} - \frac{1}{\Phi\Psi}\dot{q}^T\frac{\partial\mathcal{F}}{\partial\dot{q}}.\end{aligned} \tag{6.31}$$

Note that the matrices $[\Phi\Psi\mathcal{D} + \mathcal{L}\Phi P]$ and $\mathcal{D}$ are both positive definite and thus have well-conditioned inverses for all $\tilde{q}, \dot{q} \in \mathcal{S}$. As a consequence, the proposed feedback control (6.24) is well-defined for all $\tilde{q}, \dot{q} \in \mathcal{S}$. Substituting (6.24) into (6.31) yields

$$\dot{V} = \frac{-1}{\Psi\Phi}\dot{q}^T\frac{\partial\mathcal{F}}{\partial\dot{q}} - \frac{\dot{q}^T K_D\dot{q}}{\Phi\Psi} \leq 0. \tag{6.32}$$

It follows from (6.32) that

$$V(t) \leq V(0). \tag{6.33}$$

As the desired joint position q_d lies properly inside $\mathcal{S}$ from Assumption 6.8, it follows that

$\mathcal{L}$ is strictly positive on the constraint boundary $\partial\mathcal{S}$. From (6.19), the functions Φ and Ψ are identically zero on $\partial\mathcal{S}$. The cLf V is therefore unbounded (to positive infinity) on $\partial\mathcal{S}$. However, (6.33) guarantees that V remains upper-bounded and together with Assumption 6.8 ensures that the closed-loop trajectories remain inside the admissible constraint set $\mathcal{S}$ for all time.

Application of Lyapunov's direct method [68] to (6.20) and (6.32) guarantees that $\dot{q} \to 0$. From (6.32), it follows that $\dot{V} = 0$ if and only if $\dot{q} = \ddot{q} = 0$. By examining (6.1) and (6.24), it is straightforward to verify that at the equilibrium condition $\dot{q} = \ddot{q} = 0$, the closed-loop dynamics is given by

$$g(q) = g(q) + \mathcal{D}(q)\Big[\Phi(q)\Psi(q,0)\mathcal{D}(q) + \mathcal{L}(\tilde{q},0)\Phi(q)P(q,\dot{q})\Big]^{-1} \Big[-\Phi(q)\Psi(q,0)K_P\tilde{q} + \mathcal{L}(\tilde{q},0)\left\{\Psi(q,0)a_\phi(q) + \Phi(q)a_\psi(q,0)\right\}\Big].$$

Cancelling $g(q)$ and pre-multiplying both sides by $[\Phi(q)\Psi(q,0)\mathcal{D} + \mathcal{L}(\tilde{q},0)\Phi(q)P(q,0)]\,\mathcal{D}^{-1}$ results in the following equality

$$\Phi(q)\Psi(q,0)K_p\tilde{q} = \mathcal{L}(\tilde{q},0)\left[\Psi(q,0)a_\phi(q) + \Phi(q)a_\psi(q,0)\right]. \tag{6.34}$$

Application of Lasalle's Invariance Principle [68] yields the conclusion that all closed-loop trajectories converge to the forward invariant set defined by (6.34). Furthermore, as $\mathcal{L}(q_d,0) = 0$, it follows from (6.34) that the set-point $[q = q_d, \dot{q} = 0]^T$ lies inside this invariant set. □

6.3.1 Asymptotic stability

In general, application of Theorem 6.9 cannot guarantee closed-loop asymptotic stability for robot manipulators subject to arbitrary constraints. This is due to the possibility of local minima being introduced into the cLf (6.20) by the constraint functions Φ and Ψ. However, there are specific cases in which asymptotic stability of the closed-loop system at the set-point $[q = q_d, \dot{q} = 0]^T$ is guaranteed. In what follows we will apply Theorem 6.9 to three such special cases and prove asymptotic stability of the closed-loop system.

Case 1: Pure symmetric joint velocity constraints

Consider the case where the system (6.1) is subjected to M pure symmetric joint velocity constraints. By pure symmetric joint velocity constraints we mean that each of these joint velocity constraints are bounded in norm by a constant. That is, the system

(6.1) is subjected to constraints which can be expressed as follows

$$|\dot{q}(t)_j| \leq B_j, \quad j = 1, ..., M, \quad \forall t \geq 0, \tag{6.35}$$

where $B_j \in \mathbb{R}_+$ is a positive constant. Choosing $\Omega_j = B_j^2/2$, the above constraints can be rewritten as

$$\frac{1}{2}\dot{q}_j(t)^2 = \frac{1}{2}\dot{q}^T e_j e_j^T \dot{q} \leq \Omega_j, \quad j = 1, ..., M, \quad \forall t \geq 0, \tag{6.36}$$

where e_j denotes the unit vector in the j'th direction. The constraint function Ψ is defined as follows

$$\Psi(\dot{q}) = \prod_{j=1}^{M} \psi_j(\dot{q}), \quad \psi_j(\dot{q}) = \Omega_j - \frac{1}{2}\dot{q}^T e_j e_j^T \dot{q}, \quad j = 1, \ldots, M. \tag{6.37}$$

The admissible constraint set is thus the set of states contained in

$$\mathcal{S} = \{(\tilde{q}, \dot{q}) \in \mathbb{R}^n \times \mathbb{R}^n \mid \Psi(\dot{q}) > 0\}, \tag{6.38}$$

whose boundary is given by

$$\partial\mathcal{S} = \{(\tilde{q}, \dot{q}) \in \mathbb{R}^n \times \mathbb{R}^n \mid \Psi(\dot{q}) = 0\}. \tag{6.39}$$

Let us select the following as the candidate cLf

$$V(\tilde{q}, \dot{q}) = \frac{\mathcal{L}}{\Psi} = \frac{1}{2\Psi}\left[\dot{q}^T \mathcal{D}\dot{q} + \tilde{q}^T K_P \tilde{q}\right]. \tag{6.40}$$

Taking the time-derivative of (6.40) yields

$$\dot{V} = \frac{\dot{\mathcal{L}}\Psi - \mathcal{L}\dot{\Psi}}{\Psi^2}. \tag{6.41}$$

The function $\dot{\mathcal{L}}$ is given by (6.27), and

$$\dot{\Psi} = -\langle P_\psi \mathcal{D}^{-1}\left[\tau - C\dot{q} - g - \frac{\partial \mathcal{F}}{\partial \dot{q}}\right], \dot{q}\rangle, \tag{6.42}$$

where

$$P_\psi = \sum_{s=1}^{m}\left(\prod_{j\neq s}^{m} \psi_j(\dot{q})\right) e_s e_s^T, \tag{6.43}$$

which is a positive definite matrix for all $\dot{q} \in \mathcal{S}$. Substituting for $\dot{\mathcal{L}}$ and $\dot{\Psi}$ in (6.41) and

applying Properties 6.2 and 6.3 yields

$$\dot{V} = \frac{\dot{q}^T}{\Psi^2}\left\{[\Psi\mathcal{D} + \mathcal{L}P_\psi]\,\mathcal{D}^{-1}\tau + \Psi\,[K_P\tilde{q} - g] - \mathcal{L}P_\psi\mathcal{D}^{-1}\left[C\dot{q} + g + \dot{q}^T\frac{\partial\mathcal{F}}{\partial\dot{q}}\right]\right\} - \frac{1}{\Psi}\dot{q}^T\frac{\partial\mathcal{F}}{\partial\dot{q}}. \tag{6.44}$$

Let the torque input be

$$\tau = g + \mathcal{D}\,[\Psi\mathcal{D} + \mathcal{L}P_\psi]^{-1}\left[-\Psi\,(K_P\tilde{q} + K_D\dot{q}) + \mathcal{L}P_\psi\mathcal{D}^{-1}\left(C\dot{q} + \dot{q}^T\frac{\partial\mathcal{F}}{\partial\dot{q}}\right)\right]. \tag{6.45}$$

Then $\dot{V}$ is rendered

$$\dot{V} = -\frac{1}{\Psi}\dot{q}^T\frac{\partial\mathcal{F}}{\partial\dot{q}} - \frac{\dot{q}^T K_D\dot{q}}{\Psi} \leq 0, \tag{6.46}$$

which implies that $\dot{q} \to 0$. By examining (6.1) and (6.45), it follows that at the equilibrium condition $\dot{q} = \ddot{q} = 0$, the closed-loop dynamics is given by

$$\Psi(0)K_P\tilde{q} = 0. \tag{6.47}$$

From (6.37), it is clear that $\Psi(0) > 0$ within the admissible constraint set $\mathcal{S}$, which is given by (6.38), and since K_P is chosen to be positive definite (see Theorem 6.9), the equality (6.47) is true if and only if $\tilde{q} = 0$. It follows from Lasalle's Invariance Principle that the closed-loop system is asymptotically stable at the set-point $[q = q_d, \dot{q} = 0]^T$.

Case 2: Joint position constraints

In this section, we explore the case where system (6.1) is subjected to N symmetric joint position constraints. The application of PBC to asymptotically stabilise robot manipulators subject to joint position constraints is not new, and is presented here as an illustration of the usefulness of Theorem 6.9. The idea has been exposed in [150] where the authors also proposed a barrier function-like cLf to achieve boundedness of the joint positions. However, the structure of the barrier function introduced in [150] is very different to ours, and is more restrictive in the sense that joint velocity constraints and obstacle constraints can not be accommodated.

We consider the type of joint position constraints that can be expressed as follows

$$|q(t)_i| \leq X_i, \quad i = 1, ..., N, \quad \forall t \geq 0, \tag{6.48}$$

where $X_i \in \mathbb{R}_+$ is a constant. Choosing $\Delta_i = X_i^2/2$, the above constraints can be re-

written as

$$\frac{1}{2}q_i(t)^2 = \frac{1}{2}q^T e_i e_i^T q \leq \Delta_i, \quad i = 1, ..., N, \quad \forall t \geq 0, \tag{6.49}$$

where e_i denotes the unit vector in the i'th direction. The constraint function Φ is thus defined as

$$\Phi(q) = \prod_{i=1}^{N} \phi_i(q), \quad \phi_i = \Delta_i - \frac{1}{2}q^T e_i e_i^T q, \quad i = 1, ..., N, \tag{6.50}$$

where e_i denotes the unit vector in the i'th direction. The admissible constraint set in this case is the set of states contained in

$$\mathcal{S} = \{(\tilde{q}, \dot{q}) \in \mathbb{R}^n \times \mathbb{R}^n \mid \Phi(q) > 0\}, \tag{6.51}$$

whose boundary is given by

$$\partial\mathcal{S} = \{(\tilde{q}, \dot{q}) \in \mathbb{R}^n \times \mathbb{R}^n \mid \Phi(q) = 0\}. \tag{6.52}$$

Motivated by the concept of gradient re-centred barrier function exposed in [152] (cf. Definition 2.1 and Lemma 2.1), the candidate cLf is selected as follows

$$V(\tilde{q}, \dot{q}) = \frac{1}{2}\dot{q}^T \mathcal{D}\dot{q} + f(q) - f(q_d) - \nabla f(q_d)^T \tilde{q}, \tag{6.53}$$

where

$$f(q) = \frac{q^T K_P q}{2\Phi(q)}. \tag{6.54}$$

Before proceeding any further, we require the following lemma.

Lemma 6.10. *The function $f(q)$ is strictly convex for all $q \in \mathcal{S}$.*

Proof. The function $q^T K_P q$ is strictly convex for all $q \in \mathbb{R}^n$, and has a global minimum at the origin because the matrix K_P is chosen to be constant, diagonal, and positive definite (see Theorem 6.9). The function $\frac{1}{2\Phi(q)}$ is positive, is a barrier function in $\mathcal{S}$ (cf. Definition 2.1), is symmetric about $q = 0$, and its minimum lies on $q = 0$. The function $f(q) = \frac{q^T K_P q}{2\Phi(q)}$ is therefore a barrier function in $\mathcal{S}$, which is strictly convex for all $q \in \mathcal{S}$ by definition. □

It follows from Lemma 6.10 that $\nabla^2 f(q) > 0$, $\forall q \in \mathcal{S}$. This fact will be used later to establish the convexity of the proposed cLf (6.53).

The term $\nabla f(q_d)$ denotes the gradient of the function $f(q)$ at $q = q_d$. The gradient

$\nabla f(q) = \frac{\partial f}{\partial q}(q)$ is given by

$$\nabla f(q) = \frac{1}{\Phi(q)^2}\left[\Phi(q)K_P q + \frac{1}{2}q^T K_P q P_\phi(q) q\right], \tag{6.55}$$

where

$$P_\phi(q) = \sum_{s=1}^{n}\left(\prod_{i\neq s}^{n}\phi_i(q)\right) e_s e_s^T,$$

and is a positive definite matrix for all $q \in \mathcal{S}$.

Differentiating (6.53) with respect to time and applying Properties 6.2 and 6.3 yields

$$\dot{V} = \dot{q}^T\left\{\tau - g + \frac{1}{\Phi^2}\left[\Phi K_P q + \frac{1}{2}q^T K_P q P_\phi q\right] - \nabla f(q_d)\right\} - \dot{q}^T\frac{\partial \mathcal{F}}{\partial \dot{q}}. \tag{6.56}$$

Choosing the input torque to be

$$\tau(\tilde{q},\dot{q}) = g - K_D\dot{q} - \frac{1}{\Phi^2}\left[\Phi K_P q + \frac{1}{2}q^T K_P q P_\phi q\right] + \nabla f(q_d) \tag{6.57}$$

renders

$$\dot{V} = -\dot{q}^T\frac{\partial \mathcal{F}}{\partial \dot{q}} - \dot{q}^T K_D \dot{q} \leq 0. \tag{6.58}$$

This implies that $\dot{q} \to 0$. By inspecting (6.1) and (6.57), it follows that all closed-loop trajectories converge to the following invariant set

$$-\Phi K_P q - \frac{1}{2}q^T K_P q P_\phi q + \Phi(q)^2 \nabla f(q_d) = 0. \tag{6.59}$$

From (6.6), we have $q = \tilde{q} + q_d$. Substituting for q in (6.59) and expanding gives

$$\begin{aligned} &-\Phi(\tilde{q}+q_d)K_P[\tilde{q}+q_d] - \frac{1}{2}[\tilde{q}+q_d]^T K_P[\tilde{q}+q_d]P_\phi(\tilde{q}+q_d)[\tilde{q}+q_d] \\ &\quad + \Phi(\tilde{q}+q_d)^2\left\{\frac{1}{\Phi(q_d)^2}\left[\Phi(q_d)K_P q_d + \frac{1}{2}q_d^T K_P q_d P_\phi(q_d) q_d\right]\right\} = 0. \end{aligned} \tag{6.60}$$

When $\tilde{q} = 0$, the terms on the first line of (6.60) exactly cancel out those on the second line. Thus the set-point $[q_d, 0]^T$ is contained in the forward invariant set expressed by (6.59).

To prove asymptotic stability of the closed-loop system, it is sufficient to establish that the cLf (6.53) is convex in $\tilde{q}$ in $\mathcal{S}$. Checking second-order condition yields

$$\frac{\partial^2 V}{\partial \tilde{q}^2} = \nabla^2 f(q) > 0, \quad \forall \tilde{q} \in \mathcal{S},$$

since we have established in Lemma 6.10 that $f(q)$ is convex for all $q \in \mathcal{S}$, which means that $\nabla^2 f(q) > 0, \forall q \in \mathcal{S}$. Thus, $\tilde{q} = 0$ is the only minimum of $V(\tilde{q}, \dot{q})$ inside the constraint admissible set $\mathcal{S}$. Consequently, all closed-loop trajectories asymptotically converge to the set-point $[q = q_d, \dot{q} = 0]^T$.

The asymptotic stability result proved in this section is predictable given the structure of the chosen cLf (6.53). The barrier function $f(q)$ is convex in $\mathcal{S}$ with the minimum point at $q = 0$. The presence of the constant term $-f(q_d)$ and the linear term $-\nabla f(q_d)\tilde{q}$ serves to relocate the minimum point (re-centre) from the origin to the desired link position q_d [152]. These two terms do not contribute to the second partial derivative of the cLf (6.53) with respect to $\tilde{q}$, and therefore have no effect on its convexity property. The linear term $-\nabla f(q_d)\tilde{q}$ however, changes the gradient of the cLf, which governs the convergence rate of the closed-loop system.

Case 3: Joint position plus joint velocity constraints

It is straightforward to see that in the case where both symmetric joint position and pure symmetric joint velocity constraints are present, asymptotic stability of the closed-loop system can be achieved with the following candidate cLf

$$V(\tilde{q}, \dot{q}) = \frac{1}{2\Psi}\dot{q}^T \mathcal{D}\dot{q} + f(q) - f(q_d) - \nabla f(q_d)^T \tilde{q}, \tag{6.61}$$

where $f(q)$ and $\nabla f(q)$ are as defined by (6.54) and (6.55), respectively. Taking the time-derivative of (6.61) yields

$$\begin{aligned}\dot{V} = \dot{q}^T \Bigg\{ \frac{1}{\Psi^2} \Bigg[\left(\Psi\mathcal{D} + \frac{1}{2}\dot{q}^T \mathcal{D}\dot{q} P_\psi \right) \mathcal{D}^{-1}\tau - g(q) - \frac{1}{2}\dot{q}^T \mathcal{D}\dot{q} P_\psi \mathcal{D}^{-1} \left(g + C\dot{q} + \frac{\partial \mathcal{F}}{\partial \dot{q}} \right) \Bigg] \\ + \frac{1}{\Phi^2} \left[\Phi K_P q + \frac{1}{2} q^T K_P q P_\phi q \right] - \nabla f(q_d) \Bigg\} - \frac{1}{\Psi}\frac{\partial \mathcal{F}}{\partial \dot{q}}.\end{aligned} \tag{6.62}$$

Choosing the input torque

$$\begin{aligned}\tau = g(q) + \mathcal{D} \left[\Psi\mathcal{D} + \frac{1}{2}\dot{q}^T \mathcal{D}\dot{q} P_\psi \right]^{-1} \Bigg[-\Psi K_D \dot{q} + \frac{1}{2}\dot{q}^T \mathcal{D}\dot{q} P_\psi \mathcal{D}^{-1} \left\{ C\dot{q} + \frac{\partial \mathcal{F}}{\partial \dot{q}} \right\} \\ - \frac{\Psi^2}{\Phi^2} \left\{ \Phi K_P q + \frac{1}{2} q^T K_P q P_\phi q \right\} + \Psi^2 \nabla f(q_d) \Bigg]\end{aligned} \tag{6.63}$$

renders

$$\dot{V} = -\frac{1}{\Psi} \left[\dot{q}^T K_D \dot{q} + \dot{q}^T \frac{\partial \mathcal{F}}{\partial \dot{q}} \right] \leq 0, \tag{6.64}$$

which ensures that $\dot{q} \to 0$. Inspection of (6.1) and (6.63) leads to the conclusion that all closed-loop trajectories asymptotically converge to

$$0 = -\Phi K_P q - \frac{1}{2} q^T K_P q P_\phi q + \Phi^2(q) \nabla f(q_d), \tag{6.65}$$

which is exactly the same as (6.59), and therefore contains the set-point $[q_d, 0]$ as proved in case 2. Similarly, since the second partial derivative of the cLf (6.61) with respect to $\tilde{q}$ is exactly the same as that of case 2, the cLf (6.61) is convex for all $\tilde{q} \in \mathcal{S}$. Consequently, all closed-loop trajectories asymptotically converge to the set-point $[q_d, 0]$.

6.3.2 Joint velocity constraints expressed as kinetic energy bound

Another special case that is of practical interest is when the joint velocity constraints are expressed as a bound on the kinetic energy of the system,

$$\Psi(q, \dot{q}) = \Omega - \frac{1}{2} \dot{q}^T \mathcal{D}(q) \dot{q}, \tag{6.66}$$

where $\Omega > 0$ is a constant. In this particular case there is no direct bound on any single joint velocity, however, the overall kinetic energy of the system is upper bounded by the constant Ω.

Corollary 6.11. *Consider the dynamics (6.1) for a serial manipulator. Given general configuration constraints $\Phi(q)$ satisfying Assumption 6.4, a single velocity constraint $\Psi(q, \dot{q})$ of the form (6.66), and the admissible constraint set $\mathcal{S}$ as defined by (6.18). Define $\mathcal{L}(q, \dot{q})$ according to (6.7) and $a_\phi(q)$ according to (6.21). Choose the torque input to be*

$$\tau(\tilde{q}, \dot{q}) = g(q) + \frac{\Psi}{\Phi(\Psi + \mathcal{L})} \left(-\Phi \left[K_P \tilde{q} + K_D \dot{q}\right] + \mathcal{L} a_\phi\right), \tag{6.67}$$

where the control gain matrices $K_P, K_D \in \mathbb{R}^{n \times n}$ are constant, diagonal, and positive definite. Then for any initial condition $[q_0, \dot{q}_0]^T$ and desired link position q_d satisfying Assumption 6.8, all trajectories of the closed-loop system remain inside the admissible constraint set $\mathcal{S}$ for all time, and converge to the invariant set characterised by the following equality

$$K_P \tilde{q} = \frac{\mathcal{L}(\tilde{q}, 0)}{\Phi(q, 0)} a_\phi(q), \tag{6.68}$$

which contains the set point $[q = q_d, \dot{q} = 0]^T$.

Proof. The proof is analogous to the proof of Theorem 6.9. The key difference is that the passivity properties of the system can now be exploited in the time derivative of Ψ as

follows

$$\begin{aligned}\dot{\Psi} &= -\frac{1}{2}\dot{q}^T\dot{\mathcal{D}}\dot{q} - \dot{q}^T\mathcal{D}\ddot{q} \\ &= -\frac{1}{2}\dot{q}^T\left[\dot{\mathcal{D}} - 2C(q,\dot{q})\right]\dot{q} + \dot{q}^T\frac{\partial\mathcal{F}}{\partial\dot{q}} - \dot{q}^T\left[\tau - g(q)\right] \\ &= \dot{q}^T\frac{\partial\mathcal{F}}{\partial\dot{q}} - \dot{q}^T\left[\tau - g(q)\right].\end{aligned}$$

Substituting the above expression into (6.26) results in

$$\dot{V} = -\frac{(\Psi + \mathcal{L})}{\Phi\Psi^2}\dot{q}^T\frac{\partial\mathcal{F}}{\partial\dot{q}} - \frac{\dot{q}^T K_D\dot{q}}{\Phi\Psi} \leq 0.$$

Following verbatim the proof of Theorem 6.9 right after (6.32) leads to the result. Note that the term $\dot{q}^T\frac{\partial\mathcal{F}}{\partial\dot{q}}$ coming from the time derivative of Ψ is left as a general dissipation term in this case, whereas it was required to be explicitly cancelled in the proof of Theorem 6.9. □

The advantage of Corollary 6.11 is that the control law (6.67) is a modified Proportional-Derivative (PD) controller. This type of control is very desirable as a low-level stabilisation technique due to its simplicity and robustness with respect to modeling errors in the inertia matrix $\mathcal{D}(q)$, the Coriolis-centrifugal matrix $C(q,\dot{q})$, and the Rayleigh dissipation function $\mathcal{F}(\dot{q})$. That is, those terms do not appear in the control law (6.67). The velocity constraint expressed as a bound on the kinetic energy is physically intuitive. The final complexity of the control law is dependent on the complexity of the configuration constraint function Φ, or more precisely, its partial derivative a_ϕ.

Remark 6.12. *Given a kinetic energy bound on the robot then any single joint could, in theory, have a velocity $\dot{q}_j(t)$ up to the bound given by*

$$|\dot{q}_j(t)| \leq \sqrt{\Omega/I_j},$$

where I_j is the minimum inertia configuration for that joint j. The normal action of the energy bound will constrain the joint velocities that correspond to large values of kinetic energy. If there is a large amount of kinetic energy in a single joint then the action of the energy bound will be to naturally redistribute this energy among all joints of the robot, at the same time as reducing the overall kinetic energy. The situation that is most dangerous is when there are sensitive low inertia links with velocity constraints on the end of heavier arms with high inertia. In this case it is necessary to individually bound the velocities of the low inertia links.

The function $V(\tilde{q},\dot{q})$ defined by (6.20) is only one of the many functions whose derivative along the trajectories of system (6.1) can be rendered negative semi-definite by the

above constrained control design procedure. A class of such functions of practical interest is

$$V(\tilde{q},\dot{q}) = \frac{\mathcal{L}(\tilde{q},\dot{q})}{\alpha(\Phi\Psi)} = \frac{1}{2\alpha(\Phi\Psi)}\left[\dot{q}^T\mathcal{D}(q)\dot{q} + \tilde{q}^T K_P \tilde{q}\right],$$

where $\alpha(.)$ is a non-negative function and $\alpha(0) = 0$. If it is desired to have no effect from the barrier function outside of a neighborhood of size δ of the boundary of the admissible constraint set, then it is simply a case of choosing $\alpha(.)$ to be monotonic non-decreasing, $\alpha(0) = 0$, $\alpha(x) = 1$ for all $x > \delta$, and such that α is smooth on $x > 0$. An example of an analytic barrier function with localised boundary effect is

$$V = \frac{\mathcal{L}(\tilde{q},\dot{q})}{\tanh(\sigma\Phi\Psi)},$$

where $\sigma \in \mathbb{R}_+$ is a constant. Choosing σ large will limit the effect of the barrier function to the immediate vicinity of the barrier itself, and vice versa.

Remark 6.13. *The proposed control design does not bound the demanded torque input. It is physically impossible to have arbitrary configuration, velocity, and torque bounds. A counter-example can be constructed by choosing initial conditions close to a configuration constraint with non-zero velocity. The torque required to stop the robot before the constraint is reached can be infinitely large.*

In general, however, if the initial conditions are not 'too close' to the boundary and the constraint functions Φ and Ψ are not 'too aggressive' then it is expected that the behaviour of the closed-loop system will share the nice energy minimising properties of PBC designs.

6.4 Simulation results

The experiment setup is a 2-link planar robot manipulator moving horizontally in the Cartesian xy-coordinates (see Figure 6.1). The joint positions are absolute link angles. The dynamics of the system is ([131], pg. 150)

$$\begin{bmatrix} d_{11} & d_{12} \\ d_{12} & d_{22} \end{bmatrix}\begin{bmatrix} \ddot{q}_1 \\ \ddot{q}_2 \end{bmatrix} + \begin{bmatrix} 0 & -h\dot{q}_2 \\ h\dot{q}_1 & 0 \end{bmatrix}\begin{bmatrix} \dot{q}_1 \\ \dot{q}_2 \end{bmatrix} = \begin{bmatrix} \tau_1 \\ \tau_2 \end{bmatrix} \tag{6.69}$$

where

$$\begin{aligned} d_{11} &= m_1 l_{c1}^2 + m_2 l_1^2 + I_1 \\ d_{12} &= m_2 l_1 l_{c2}\cos(q_2 - q_1) \\ d_{22} &= m_2 l_{c2}^2 + I_2 \\ h &= m_2 l_1 l_{c2} sin(q_2 - q_1) \end{aligned}$$

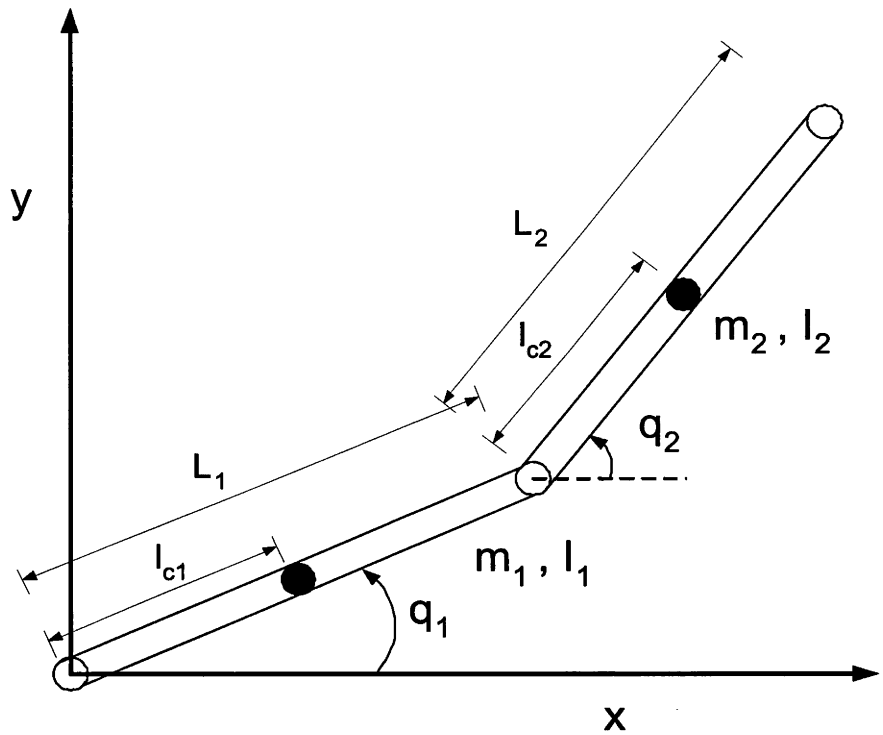

Figure 6.1: Two-link revolute joint manipulator

The parameters m_i denotes the mass of link i, l_i denotes the length of link i, l_{ci} denotes the distance from the previous joint to the centre of mass of link i, and I_i denotes the moment of inertia of link i about an axis normal to the page, passing through the centre of mass of link i. In this experiment, $m_1 = m_2 = 1\text{kg}$, $l_1 = l_2 = 1\text{m}$, $l_{c1} = l_{c2} = 0.5\text{m}$, and $I_1 = I_2 = 1\text{kgm}^2$.

There is a circular obstacle with a radius of 0.5m centred at the coordinates $[x_0, y_0]^T = [0, 2]^T$ (see Figure 6.4). The desired link position is $q_d = [\pi, \frac{2\pi}{3}]^T$, and the commanded set-point is $[q = q_d, \dot{q} = 0]^T$. The initial condition of the manipulator is set at $q_0 = [0, 0]^T$ and $\dot{q}_0 = [0, 0]^T$. To prevent the manipulator from going through itself, the position of the second link relative to the first link is restricted to the range $\pm\frac{17}{18}\pi$. In addition, we further desire that the angular velocity of each link to be constrained, with link 1 to remain below 0.3rad/s and link 2 below 0.2rad/s.

To demonstrate its effectiveness, we compare the simulation results from the proposed constrained passivity-based control (CPBC) design with those from the Proportional-Derivative (PD) controller. The PD-controller used in the simulations has the usual form

$$\tau_{PD} = -K_P\tilde{q} - K_D\dot{q}$$

with $\tilde{q} = q - q_d$. To design the CPBC-controller, we select the following candidate cLf

$$V(\tilde{q}, \dot{q}) = \frac{\mathcal{L}(\tilde{q}, \dot{q})}{(\Phi\Psi)^\alpha},$$

where the constant parameter $\alpha \in \mathbb{R}_+$ is employed to control the shape of the candidate cLf $V(\tilde{q}, \dot{q})$, which directly governs how close to the obstacle the robot's links are allowed to come and how close to their bounds the links' velocities are allowed to reach. The smaller α is chosen to be, the closer to the obstacle the robot's links are allowed to approach, and the closer to their bounds the links' velocities are allowed to get. In this experiment, α is chosen to be 0.2.

The function $\mathcal{L}(\tilde{q}, \dot{q})$ is as defined by (6.7), and

$$\Phi = \phi_1\phi_2,$$

where

$$\phi_1 = [\cos(q_1) + \cos(q_2) - x_0]^2 + [\sin(q_1) + \sin(q_2) - y_0]^2 - 0.5^2$$
$$\phi_2 = \left(\frac{17}{18}\pi\right)^2 - (q_2 - q_1)^2$$

and

$$\Psi = \frac{1}{4}(0.3^2 - \dot{q}_1^2)(0.2^2 - \dot{q}_2^2).$$

Such choices yield the following control law

$$\begin{aligned}\tau_{CPBC} = \mathcal{D}\left[(\Phi\Psi)^\alpha\mathcal{D} + \mathcal{L}\alpha(\Phi\Psi)^{\alpha-1}\Phi P\right]^{-1}\big[&-(\Phi\Psi)^\alpha\left(K_P\tilde{q} + K_D\dot{q}\right)\\ &+\mathcal{L}\alpha(\Phi\Psi)^{\alpha-1}\left(\Psi a_\phi + \Phi a_\psi\right)\\ &+\mathcal{L}\alpha(\Phi\Psi)^{\alpha-1}\Phi P\mathcal{D}^{-1}\mathcal{C}\dot{q})\big].\end{aligned} \tag{6.70}$$

To allow for an accurate comparison, the control gains are set to be $K_P = 4$ and $K_D = 20$ for both controllers. The simulation results are generated by the Planar Manipulators Toolbox [160].

From Figure 6.2, it is straightforward to see that both controllers asymptotically stabilise the manipulator to the desired set-point $[q = q_d, \dot{q} = 0]^T = [(\pi, \frac{2\pi}{3})^T, (0,0)^T]^T$. Figure 6.3 shows that with the PD-controller, link 1 reaches a maximum velocity of approximately 0.585rad/s. For link 2, the maximum velocity reached is around 0.39rad/s. With the CPBC-controller, our objective of restricting the velocity of link 1 to 0.3rad/s and link 2 to 0.2rad/s is successfully achieved. Figure 6.4 illustrates that obstacle avoidance is achieved with the CPBC-controller.

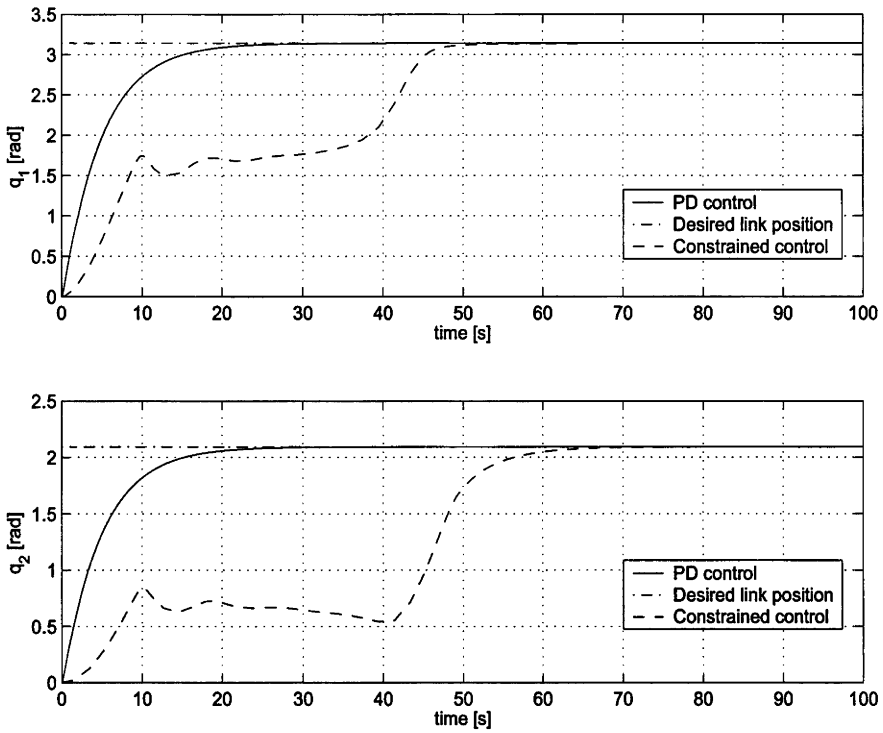

Figure 6.2: Joint positions

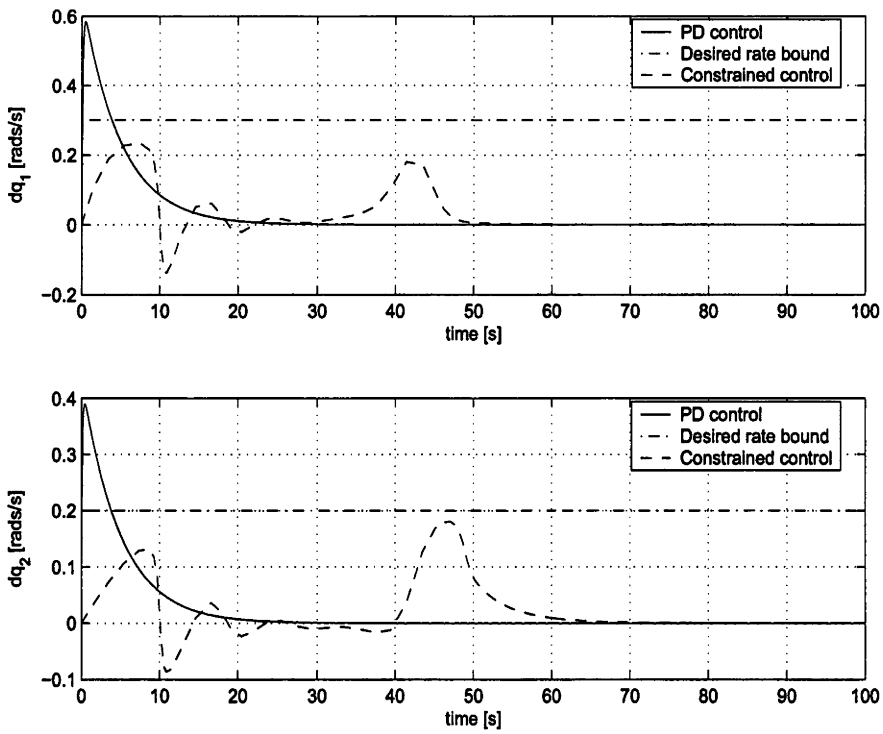

Figure 6.3: Joint rates

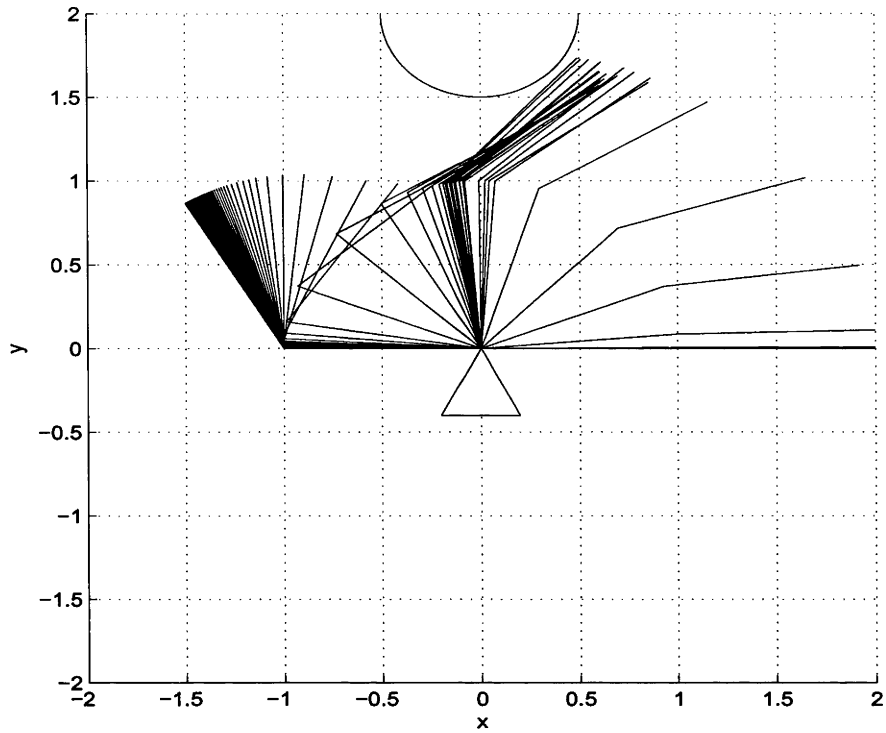

Figure 6.4: Constrained control: Manipulator trajectory in xy-coordinates

6.5 General Euler-Lagrange systems

Although we have focussed on robot manipulators, the control design proposed in this chapter is equally applicable to any state constrained, n-degrees of freedom, fully-actuated Euler-Lagrange systems whose dynamics can be expressed by (6.1), and satisfy Properties 6.1-6.3. Furthermore, if the state constraints are of the same form as those exposed in Section 6.3.1, then asymptotic stability of the closed-loop system is guaranteed.

6.6 Chapter summary

In this chapter we have addressed the problem of autonomous obstacle avoidance for robot manipulators subject to hard constraints on joint positions and joint velocities. These control objectives are achieved simultaneously by combining the ideas of passivity-based control and artificial potential field methods. Although asymptotic stability of the closed-loop system cannot be achieved in general for arbitrary constraints due to the possible presence of local minima in the proposed cLf structure, the key advantages of the proposed control design lie in its simplicity and its basis in energy-based stabilisation, leading to simple and effective stabilising control laws that strictly satisfies configuration and velocity constraints for all time. Furthermore, asymptotic stability is ensured when the

only constraints in effect are pure joint position and joint velocity constraints. Even though we have focussed mainly on the autonomous obstacle avoidance problem for general robot manipulator systems, the results exposed in this chapter can readily be applied to any state-constrained Euler-Lagrange system whose dynamics satisfies the stated properties and assumptions. The validity and effectiveness of the proposed control design are verified through simulations on a 2-link planar manipulator.

Chapter 7

Bounded torque control for robot manipulators with joint velocity constraints

The general tracking problem of robot manipulators in particular, and Euler-Lagrange systems in general, has elegantly been solved by the PBC technique. Since its first introduction in the seminal paper [138], PBC has attracted great interest from the robotics community because it rigorously establishes that computationally simple control laws can achieve quite complicated tasks. The resulting controllers are invariably PD-controllers which are simple, intuitive, and can easily be implemented in practice [122].

There are however, two weaknesses associated with the classical PBC approach. The first is the implicit assumption that the manipulator actuators are able to provide joint torques of any magnitude. This assumption is expensive in practice, and in certain applications, not feasible as all actuators have saturation limits. If these constraints are not taken into consideration, problems such as degraded link position tracking and system failure, will occur [29]. Secondly, classical PBC does not consider the problem of state constraints. Hard constraints on joint positions and joint velocities are a commonly encountered problem. If the problem is not accounted for in the control design, mechanical failure will ultimately ensue. PBC designs with bounded torque input have been addressed in such works as [29,65,66,119]. However, a review of the literature reveals that the set-point regulation problem of robot manipulators with bounded torque inputs subject to state constraints has not been considered in the framework of PBC.

In the last chapter, we extended the PBC methodology to address the problem of autonomous obstacle avoidance for general robot manipulators subject to hard constraints on the robot's joint positions and joint velocities. We however, implicitly assumed that the robot's motors can deliver any demanded torque. This assumption is expensive in practice due to the fitting of highly powerful motors, and in certain applications, may not be at all feasible. In this chapter, we extend the PBC methodology in a different direction to address the problem of set-point regulation for robot manipulators subject to torque

and joint velocity limits. The proposed control design involves shaping and incorporating barrier function characteristics into the cLf. The underlying ideas behind the modified cLf are reminiscent of those employed in the artificial potential field method [76]. We differ from the earlier works by directly integrating the constraint equation into the cLf to derive a unified control law that is bounded in norm, respects joint velocity constraints, and achieves asymptotic stabilisation of the closed-loop system.

The chapter consists of five sections. Section 7.1 states the control problem. Section 7.2 details the main results. Simulation results are presented in Section 7.3. Remarks on extending the proposed control design to general Euler-Lagrange systems and the chapter summary are contained in Sections 7.4 and 7.5, respectively.

7.1 Robot dynamics and problem formulation

7.1.1 Robot dynamics

Consider rigid and fully-actuated n-link revolute robot manipulators with no external forces, that is, no end-effector contacts with the environment, and no external disturbances. Assuming that static friction is negligible, the dynamics of such systems is adequately described by [7,79]

$$\mathcal{D}(q)\ddot{q} + \mathcal{C}(q,\dot{q})\dot{q} + g(q) + F_d\dot{q} = \tau \tag{7.1}$$

where we use the following notation

$q \in \mathbb{R}^n$	generalised joint coordinates
$\mathcal{D}(q) \in \mathbb{R}^{n\times n}$	generalised inertia matrix,
$\mathcal{C}(q,\dot{q}) \in \mathbb{R}^{n\times n}$	Coriolis-centrifugal matrix,
$g(q) \in \mathbb{R}^n$	gravitational torques,
$F_d \in \mathbb{R}^{n\times n}$	joint viscous friction coefficient matrix,
$\tau \in \mathbb{R}^n$	applied input torques.

The following properties hold for (7.1).

Property 7.1. *The inertial matrix $\mathcal{D}(q)$ is symmetric and positive definite. That is,*

$$\mathcal{D}(q)^T = \mathcal{D}(q) > 0, \quad \forall q \in \mathbb{R}^n. \tag{7.2}$$

Property 7.2. *The time derivative of the inertia matrix $\dot{\mathcal{D}}(q)$ and the Coriolis-centrifugal matrix $\mathcal{C}(q,\dot{q})$ satisfy the following "skew-symmetric" relationship*

$$\dot{q}^T[\dot{\mathcal{D}} - 2\mathcal{C}]\dot{q} = 0, \quad \forall q, \dot{q} \in \mathbb{R}^n, \tag{7.3}$$

Property 7.3. *The viscous and/or dynamic friction coefficient matrix F_d satisfies*

$$\dot{q}^T F_d \dot{q} \geq 0, \quad \forall \dot{q} \in \mathbb{R}^n. \tag{7.4}$$

In addition to the above properties, the following assumptions are valid for revolute-joint robot manipulators [79].

Assumption 7.4. *The Coriolis-centrifugal matrix $C(q, \dot{q})$ is linear in $\dot{q}$, and its dependence on q is bounded such that*

$$||C(q, \dot{q})|| \leq \zeta_c ||\dot{q}||, \quad \forall q, \dot{q} \in \mathbb{R}^n. \tag{7.5}$$

where $\zeta_c \in \mathbb{R}_+$ is a constant.

Assumption 7.5. *The gravitational torque vector $g(q)$ is bounded such that there exists a finite constant $\xi_g \in \mathbb{R}_+$ satisfying*

$$||g(q)|| \leq \zeta_g, \quad \forall q \in \mathbb{R}^n. \tag{7.6}$$

Assumption 7.6. *The viscous friction coefficient matrix F_d is bounded such that*

$$||F_d|| \leq \zeta_f, \tag{7.7}$$

where $\zeta_f \in \mathbb{R}_+$ is a constant.

7.1.2 Joint velocity constraints

Each and every individual joint velocity is bounded as follows

$$|\dot{q}_i(t)| \leq B_i, \quad t \geq 0, \quad i = 1, ..., n, \tag{7.8}$$

where $B_i \in \mathbb{R}_+$ is a constant. Choosing $\Omega_i = B_i^2/2$, the above velocity constraints can be expressed as

$$\frac{1}{2}\dot{q}_i(t)^2 = \frac{1}{2}\dot{q}^T e_i e_i^T \dot{q} \leq \Omega_i, \quad t \geq 0, \quad i = 1, ..., n, \tag{7.9}$$

where e_i denotes the unit vector in the i'th direction.

7.1.3 Problem statement

Let the vector $[\tilde{q}, \dot{q}]^T$ define the system state, where

$$\tilde{q} = q - q_d \tag{7.10}$$

represents the error between the actual, q, and the desired, q_d, joint position. The control problem is to design a controller such that:

- The set point $[q = q_d, \dot{q} = 0]^T$ is asymptotically stable.
- The joint velocities are bounded as defined by (7.8).
- The demanded torque input τ is bounded in norm for all time, irrespective of the initial condition.

7.2 Bounded control design

This section proposes a modification to the "classical" PBC design for robot manipulators, (see Section 6.2 for a brief overview), to incorporate actuator bounds as well as hard constraints on joint velocities.

To simplify the subsequent development, we introduce the following notation

$$\Psi(\dot{q}) = \prod_{i=1}^{n} \psi_i(\dot{q}), \quad \psi_i(\dot{q}) = \Omega_i - \frac{1}{2}\dot{q}^T e_i e_i^T \dot{q}, \tag{7.11}$$

for $i = 1, \ldots, n$, and let the vector $\tanh(.) \in \mathbb{R}^n$ denote

$$\tanh(x) = [\tanh(x_1), \tanh(x_2), \ldots, \tanh(x_n)]^T, \tag{7.12}$$

where $x = [x_1, x_2, ..., x_n]^T \in \mathbb{R}^n$.

Let us define the admissible constraint set as follows

$$\mathcal{S} = \{(q, \dot{q}) \mid \Psi(\dot{q}) > 0\} \tag{7.13}$$

whose boundary is given by

$$\partial\mathcal{S} = \{(q, \dot{q}) \mid \Psi(\dot{q}) = 0\}. \tag{7.14}$$

Motivated by the pioneering work in [65,66], we consider the following positive definite and radially unbounded function as the candidate cLf

$$V(\tilde{q}, \dot{q}) = \frac{1}{\Psi(\dot{q})}\left[\frac{1}{2}\dot{q}^T \mathcal{D}(q)\dot{q} + \sum_{i=1}^{n} \frac{1}{\xi_i} K_{P_i} \ln(\cosh(\xi_i \tilde{q}_i))\right], \tag{7.15}$$

where the control gain matrix $K_P \triangleq \text{diag}\{K_{P_i}\} \in \mathbb{R}^{n\times n}$ is constant and positive definite, and the constants ξ_i, for $i = 1, ..., n$, are strictly positive real numbers. The constraint function $\Psi(\dot{q})$ is identically zero on the constraint boundary $\partial\mathcal{S}$. Consequently, the value of $V(\tilde{q}, \dot{q})$ is asymptotically infinite on $\partial\mathcal{S}$. The proposed candidate cLf is similar to the

barrier functions used in optimisation methods and the underlying idea is closely linked to the artificial potential field methods. The advantage of this approach is that the function $V(\tilde{q}, \dot{q})$ can be thought of as a shaped energy function for the constrained system. The set-point $[q_d, 0]$ is the unique minimum of $V(\tilde{q}, \dot{q})$ corresponding to the minimal kinetic and (shaped) potential energy.

Theorem 7.7. *Consider the dynamics (7.1) for a serial manipulator. Given joint velocity constraints of the form (7.8) and the constraint function Ψ as defined by (7.11). Define*

$$P(\dot{q}) = \sum_{s=1}^{n} \left(\prod_{i \neq s}^{n} \psi_i(\dot{q}) \right) e_s e_s^T, \tag{7.16}$$

which is diagonal and positive definite in $\mathcal{S}$. Choose the torque input to be

$$\tau(\tilde{q}, \dot{q}) = g(q) + \mathcal{D}(q) \Big[\Psi \mathcal{D}(q) + \mathcal{L} P \Big]^{-1} \Big[-\Psi \left\{ K_P \tanh(\Xi \tilde{q}) + K_D \tanh(\Gamma \dot{q}) \right\} + \mathcal{L} P \mathcal{D}(q)^{-1} \left\{ C\dot{q} + F_d \dot{q} \right\} \Big], \tag{7.17}$$

where the control gain matrices $K_P, K_D \in \mathbb{R}^{n \times n}$ are constant, diagonal, and positive definite, $\Xi = diag\{\xi_i\} \in \mathbb{R}^{n \times n}$, $\Gamma = diag\{\gamma_i\} \in \mathbb{R}^{n \times n}$, and the constants ξ_i, γ_i are strictly positive real. Then for any initial velocity $\dot{q}_0 \in \mathcal{S}$, the system (7.1) in closed-loop with control (7.17) is asymptotically stable at the set point $[q = q_d, \dot{q} = 0]^T$. Moreover, the joint velocities are bounded as defined by (7.8), and the control torque τ is bounded in norm for all time, regardless of the initial condition.

To simplify the notation, in the following development, functions are written without their arguments except where confusion may arise. Furthermore, let us define

$$\mathcal{L}(\tilde{q}, \dot{q}) = \frac{1}{2} \dot{q}^T \mathcal{D}(q) \dot{q} + \sum_{i=1}^{n} \frac{1}{\xi_i} K_{P_i} \ln(\cosh(\xi_i \tilde{q}_i)). \tag{7.18}$$

Proof. Consider the cLf given by (7.15) which can now be re-written as

$$V(\tilde{q}, \dot{q}) = \frac{\mathcal{L}(\tilde{q}, \dot{q})}{\Psi(\dot{q})} \tag{7.19}$$

where $\mathcal{L}(\tilde{q}, \dot{q})$ is as defined in (7.18). Differentiating (7.19) with respect to time yields

$$\dot{V} = \frac{\dot{\mathcal{L}}\Psi - \mathcal{L}\dot{\Psi}}{\Psi^2}$$

whenever $V(\tilde{q}, \dot{q})$ is well-defined, and bounded at every $t \geq 0$. Taking the time derivatives

of $\mathcal{L}$ and Ψ gives

$$\dot{\mathcal{L}} = \frac{1}{2}\dot{q}^T\left[\dot{\mathcal{D}} - 2\mathcal{C}\right]\dot{q} - \dot{q}^T F_d\dot{q} + \dot{q}^T\left[\tau - g(q) + K_P\tanh(\Xi\tilde{q})\right]$$
$$\dot{\Psi} = -\langle P\mathcal{D}^{-1}\left[\tau - \mathcal{C}\dot{q} - g(q) - F_d\dot{q}\right], \dot{q}\rangle,$$

respectively, where $\langle\cdot,\cdot\rangle$ denotes the inner product. Substituting $\dot{\mathcal{L}}$ and $\dot{\Psi}$ into the expression for $\dot{V}$ yields

$$\dot{V} = \frac{\Psi}{\Psi^2}\left\{\frac{1}{2}\dot{q}^T\left[\dot{\mathcal{D}} - 2\mathcal{C}\right]\dot{q} - \dot{q}^T F_d\dot{q} + \dot{q}^T\left[\tau - g(q) + K_P\tanh(\Xi\tilde{q})\right]\right\}$$
$$- \frac{\mathcal{L}}{\Psi^2}\left\{-\langle P\mathcal{D}^{-1}\left[\tau - \mathcal{C}\dot{q} - g(q) - F_d\dot{q}\right], \dot{q}\rangle\right\}. \tag{7.20}$$

Recalling that $\dot{q}^T[\dot{\mathcal{D}} - 2\mathcal{C}]\dot{q} = 0$ for all $q, \dot{q} \in \mathbb{R}^n$ and $\dot{q}^T F_d\dot{q} \geq 0$ (see Properties 7.2 and 7.3), and collecting like terms together, one obtains

$$\dot{V} = \frac{\dot{q}^T}{\Psi^2}\left\{\left[\Psi\mathcal{D} + \mathcal{L}P\right]\mathcal{D}^{-1}\tau + \Psi\left[K_P\tanh(\Xi\tilde{q}) - g(q)\right] - \mathcal{L}P\mathcal{D}^{-1}\left[\mathcal{C}\dot{q} + g(q) + F_d\dot{q}\right]\right\}$$
$$- \frac{\dot{q}^T F_d\dot{q}}{\Psi}. \tag{7.21}$$

Note that the matrices $[\Psi\mathcal{D} + \mathcal{L}P]$ and $\mathcal{D}$ are both positive definite and thus have well-conditioned inverses for all $\tilde{q}, \dot{q} \in \mathcal{S}$. As a consequence, the proposed feedback control (7.17) is well-defined for all $\tilde{q}, \dot{q} \in \mathcal{S}$. Substituting (7.17) into (7.21) yields

$$\dot{V} = -\frac{\left[\dot{q}^T F_d\dot{q} + \dot{q}^T K_D\tanh(\Gamma\dot{q})\right]}{\Psi} \leq 0. \tag{7.22}$$

Application of Lyapunov's direct method [68] to (7.15) and (7.22) guarantees that $\dot{q} \to 0$. It also follows from (7.22) that $\dot{V} = 0$ only if $\dot{q} = \ddot{q} = 0$. By examining the system dynamics (7.1) and the chosen control law (7.17), it is straightforward to verify that at the equilibrium condition $\dot{q} = \ddot{q} = 0$, the closed-loop dynamics is given by

$$g(q) = g(q) + \mathcal{D}(q)\left[\Psi(0)\mathcal{D}(q) + \mathcal{L}(\tilde{q}, 0)P(0)\right]^{-1}\left\{\Psi(0)\left[-K_P\tanh(\Xi\tilde{q})\right]\right\} \tag{7.23}$$

Cancelling $g(q)$ and pre-multiplying both sides by $[\Psi(0)\mathcal{D}(q) + \mathcal{L}(\tilde{q}, 0)P(0)]\,\mathcal{D}^{-1}$ yields

$$\Psi(0)K_P\tanh(\Xi\tilde{q}) = 0 \tag{7.24}$$

Since $\Psi(0) > 0$ inside $\mathcal{S}$, and Ξ, K_P are positive definite, it follows that the equality (7.24) is true if and only if $\tilde{q} = q - q_d = 0$. Thus, by Lasalle's Invariance Principle, all closed-loop trajectories asymptotically converge to the set-point $[q = q_d, \dot{q} = 0]^T$.

It follows from (7.18) that the function $\mathcal{L}$ is non-zero on the constraint boundary $\partial\mathcal{S}$. Thus, the cLf V escapes to positive infinity as the system state approaches $\partial\mathcal{S}$. However, from (7.22), it follows that V remains upper-bounded since

$$V(t) \leq V(0), \quad \forall t \geq 0. \tag{7.25}$$

Given that the initial velocity $\dot{q}_0 \in \mathcal{S}$, the closed-loop system will remain inside $\mathcal{S}$ for all time. Consequently, the joint velocities are bounded as defined by (7.8) for all time by virtue of (7.11) and (7.13).

To prove the boundedness of the control law (7.17), we invoke the well-known matrix inversion lemma [12]

$$\begin{aligned}(A+B)^{-1} &= A^{-1} - A^{-1}(B^{-1}+A^{-1})^{-1}A^{-1} \\ &= B^{-1} - B^{-1}(A^{-1}+B^{-1})^{-1}B^{-1}\end{aligned}$$

for invertible matrices A and B. Applying the above to the term $(\Psi\mathcal{D}+\mathcal{L}P)^{-1}$ in (7.17) gives

$$(\Psi\mathcal{D}+\mathcal{L}P)^{-1} = (\Psi\mathcal{D})^{-1} - (\Psi\mathcal{D})^{-1}[(\Psi\mathcal{D})^{-1}+(\mathcal{L}P)^{-1}]^{-1}(\Psi\mathcal{D})^{-1}, \tag{7.26}$$

which can be re-written as follows

$$(\Psi\mathcal{D})^{-1} = (\Psi\mathcal{D}+\mathcal{L}P)^{-1} + (\Psi\mathcal{D})^{-1}[(\Psi\mathcal{D})^{-1}+(\mathcal{L}P)^{-1}]^{-1}(\Psi\mathcal{D})^{-1}. \tag{7.27}$$

Since all matrices in (7.27) are positive definite as $\mathcal{D}$ and P are symmetric and positive definite, see Assumptions 7.1 and (7.16), it follows that

$$(\Psi\mathcal{D})(\Psi\mathcal{D}+\mathcal{L}P)^{-1} \leq I_n, \tag{7.28}$$

where I_n denotes the $n \times n$ identity matrix. A similar argument can be used to show that

$$(\Psi\mathcal{D}+\mathcal{L}P)^{-1}(\mathcal{L}P) \leq I_n. \tag{7.29}$$

The control law (7.17) can be re-written as

$$\begin{aligned}\tau = g(q) &- \Psi\mathcal{D}\left[\Psi\mathcal{D}+\mathcal{L}P\right]^{-1}\left[K_P\tanh(\Xi\tilde{q}) + K_D\tanh(\Gamma\dot{q})\right] \\ &+ \mathcal{D}\left[\Psi\mathcal{D}+\mathcal{L}P\right]^{-1}\mathcal{L}P\mathcal{D}^{-1}\left[C\dot{q}+F_d\dot{q}\right].\end{aligned} \tag{7.30}$$

Taking the norm of (7.30) and applying the results from (7.28) and (7.29) yields

$$||\tau|| \leq ||g(q)|| + ||K_P\tanh(\Xi\tilde{q})|| + ||K_D\tanh(\Gamma\dot{q})|| + ||C\dot{q}|| + ||F_d\dot{q}||. \tag{7.31}$$

Since $|\tanh(x)| \leq 1$ for all $x \in \mathbb{R}$, $|\dot{q}_i(t)| \leq B_i$, and applying Assumptions 7.4-7.6, we obtain the following explicit upper bound on the norm of the demanded torque input

$$||\tau|| \leq \zeta_g + \lambda_{max}\{K_P\} + \lambda_{max}\{K_D\} + \zeta_c||B||^2 + \zeta_f||B||, \tag{7.32}$$

where the vector $B = [B_1, ..., B_n]^T$, and the constants $B_1, ..., B_n$ are as defined in (7.8). □

A case that is of practical interest is when the joint velocity constraints are expressed as a bound on the kinetic energy of the system

$$\Psi(q, \dot{q}) = \Omega - \frac{1}{2}\dot{q}^T\mathcal{D}(q)\dot{q}, \tag{7.33}$$

where $\Omega \in \mathbb{R}_+$ is a constant. In this particular case there is no direct bound on individual joint velocity, however, the overall kinetic energy of the system is upper bounded by the constant Ω.

Corollary 7.8. *Consider the dynamics (7.1) for a serial manipulator. Given a single velocity constraint $\Psi(q, \dot{q}) > 0$ of the form (7.33), the admissible constraint set $\mathcal{S}$ and constraint boundary $\partial\mathcal{S}$ as defined by (7.13) and (7.14), respectively. Consider the candidate cLf $V(\tilde{q}, \dot{q})$ as defined by (7.19), where $\mathcal{L}(\tilde{q}, \dot{q})$ is as defined by (7.18). Choose the torque input to be*

$$\tau(\tilde{q}, \dot{q}) = g(q) - \frac{\Psi}{\Psi + \mathcal{L}}\left[K_P \tanh(\Xi\tilde{q}) + K_D \tanh(\Gamma\dot{q})\right], \tag{7.34}$$

where the control gain matrices $K_P, K_D \in \mathbb{R}^{n\times n}$ are constant, diagonal, and positive definite, $\Xi = diag\{\xi_i\} \in \mathbb{R}^{n\times n}$, $\Gamma = diag\{\gamma_i\} \in \mathbb{R}^{n\times n}$, and the constants ξ_i, γ_i are strictly positive real. Then for any initial velocity $\dot{q}_0 \in \mathcal{S}$, the system (7.1) in closed-loop with control (7.34) is asymptotically stable at the set point $[q = q_d, \dot{q} = 0]^T$. Moreover, the system's kinetic energy is bounded as follows

$$\frac{1}{2}\dot{q}^T\mathcal{D}(q)\dot{q} \leq \Omega, \tag{7.35}$$

and the control torque τ is bounded in norm for all time, regardless of the initial condition.

Proof. The key difference between this proof and the proof of Theorem 7.7 is that the passivity properties of the system can now be exploited in the time derivative of Ψ as follows

$$\begin{aligned}
\dot{\Psi} &= -\frac{1}{2}\dot{q}^T\dot{\mathcal{D}}\dot{q} - \dot{q}^T\mathcal{D}\ddot{q} \\
&= -\frac{1}{2}\dot{q}^T\left[\dot{\mathcal{D}} - 2C(q, \dot{q})\right]\dot{q} + \dot{q}^T F_d\dot{q} - \dot{q}^T\left[\tau - g(q)\right] \\
&= \dot{q}^T F_d\dot{q} - \dot{q}^T\left[\tau - g(q)\right]
\end{aligned}$$

Substituting the above expression into (7.20) results in

$$\dot{V} = -\frac{(\Psi + \mathcal{L})}{\Psi^2}\dot{q}^T F_d \dot{q} + \frac{1}{\Psi^2}\dot{q}^T \Big\{ (\Psi + \mathcal{L})\,\tau - (\Psi + \mathcal{L})\,g(q) + \Psi K_P \tanh(\Xi \tilde{q}) \Big\}, \tag{7.36}$$

which in closed-loop with feedback (7.34) yields

$$\dot{V} = -\frac{(\Psi + \mathcal{L})}{\Psi^2}\dot{q}^T F_d \dot{q} - \frac{1}{\Psi}\dot{q}^T K_D \tanh(\Gamma \dot{q}) \leq 0. \tag{7.37}$$

Application of Lyapunov's direct method to (7.15) and (7.37) ensures that $\dot{q} \to 0$. It also follows from (7.37) that $\dot{V} = 0$ if and only if $\dot{q} = \ddot{q} = 0$. By examining (7.1) and (7.34), it is straightforward to verify that at the equilibrium set $\dot{q} = \ddot{q} = 0$, the closed-loop dynamics is given by

$$K_P \tanh(\Xi \tilde{q}) = 0. \tag{7.38}$$

Since Ξ and K_P are positive definite by way of design, the above equality is only true if $\tilde{q} = q - q_d = 0$. Application of Lasalle's Invariance Principle guarantees that the closed-loop dynamics is asymptotically stable at the set-point $[q = q_d, \dot{q} = 0]^T$.

It follows from (7.33) that $\dot{q}$, hence $\mathcal{L}$, is non-zero on the constraint boundary $\partial\mathcal{S}$. Consequently, the cLf V escapes to positive infinity as the system state approaches $\partial\mathcal{S}$. However, from (7.37), V remains upper-bounded since

$$V(t) \leq V(0), \quad \forall t \geq 0. \tag{7.39}$$

Given that the initial velocity $\dot{q}_0 \in \mathcal{S}$, the closed-loop system will remain inside $\mathcal{S}$ for all time. As a result, the system's kinetic energy is bounded as defined by (7.35) for all time by virtue of (7.13) and (7.33).

Since $|\tanh(x)| \leq 1$, $\forall x \in \mathbb{R}$, and using Assumption 7.5, we obtain the following explicit upper bound on the norm of the demanded torque input

$$||\tau|| \leq \zeta_g + \lambda_{max}\{K_P\} + \lambda_{max}\{K_D\}. \tag{7.40}$$

This concludes the proof. □

The advantage of Corollary 7.8 is that the control law (7.34) is a slightly modified PD-plus-gravity-compensation controller. This type of control is very desirable as a low-level stabilisation technique due to its simplicity and robustness with respect to modeling errors in the inertia matrix $\mathcal{D}(q)$, the Coriolis-centrifugal matrix $\mathcal{C}(q, \dot{q})$, and the Rayleigh dissipation function $\mathcal{F}(\dot{q})$. That is, those terms do not appear in the control law (7.34). The velocity constraint expressed as a bound on the kinetic energy is physically intuitive. Furthermore, the bound on the norm of the demanded torque input (7.40) is interesting

because it recovers exactly the bounds obtained in [65, 66] where just the problem of bounded torque control is considered.

Remark 7.9. *Given a kinetic energy bound on the robot then any single joint could, in theory, have a velocity $\dot{q}_j(t)$ up to the bound given by*

$$|\dot{q}_j(t)| \leq \sqrt{\Omega / I_j},$$

where I_j is the minimum inertia configuration for that joint j. The normal action of the energy bound will constrain the joint velocities that correspond to large values of kinetic energy. If there is a large amount of kinetic energy in a single joint then the action of the energy bound will be to naturally redistribute this energy among all joints of the robot, at the same time as reducing the overall kinetic energy. The situation that is most dangerous is when there are sensitive low inertia links with velocity constraints on the end of heavier arms with high inertia. In this case it is necessary to individually bound the velocities of the low inertia links.

Remark 7.10. *The parameters ξ_i and γ_i are not related to the stability of the closed-loop dynamics nor the boundedness of the demanded torque input. They, however, affect the transient response of the closed-loop system. It has been established in [66] that the parameters ξ_i affect the steady-state positioning bias due to the presence of static friction in the robot joints. Choosing ξ_i large reduces the bias. The parameters γ_i, on the other hand, affect the damping of the closed-loop system. Choosing γ_i large improves the damping of the closed-loop system, and vice versa.*

The function $V(\tilde{q}, \dot{q})$ defined by (7.19) is only one of the many cLfs whose derivative along the trajectories of system (7.1) can be rendered negative semi-definite by the constrained control design procedure presented above. A class of such functions of practical interest is

$$V(\tilde{q}, \dot{q}) = \frac{\mathcal{L}(\tilde{q}, \dot{q})}{\alpha(\Psi)},$$

where $\alpha(.)$ is a non-negative function and $\alpha(0) = 0$. If it is desired to have no effect from the barrier function outside of a neighborhood of size δ of the boundary of the admissible constraint set, then it is simply a case of choosing $\alpha(.)$ to be monotonic non-decreasing, $\alpha(0) = 0$, $\alpha(x) = 1$ for all $x > \delta$, and such that α is smooth on $x > 0$. An example of an analytic barrier function with adjustable boundary effect is

$$V = \frac{\mathcal{L}(\tilde{q}, \dot{q})}{\tanh(\sigma \Psi)},$$

where $\sigma > 0$ is a constant. Choosing σ large will limit the effect of the barrier function to the immediate vicinity of the barrier itself, and vice versa.

7.3 Simulation results

The experiment setup is a 2-link planar robot manipulator moving horizontally in the Cartesian xy-coordinates (see Figure 6.1). The joint positions are absolute link angles. The dynamics of the system is ([131], pg. 150)

$$\begin{bmatrix} d_{11} & d_{12} \\ d_{12} & d_{22} \end{bmatrix} \begin{bmatrix} \ddot{q}_1 \\ \ddot{q}_2 \end{bmatrix} + \begin{bmatrix} 0 & -h\dot{q}_2 \\ h\dot{q}_1 & 0 \end{bmatrix} \begin{bmatrix} \dot{q}_1 \\ \dot{q}_2 \end{bmatrix} = \begin{bmatrix} \tau_1 \\ \tau_2 \end{bmatrix} \tag{7.41}$$

where

$$\begin{aligned} d_{11} &= m_1 l_{c1}^2 + m_2 l_1^2 + I_1 \\ d_{12} &= m_2 l_1 l_{c2} \cos(q_2 - q_1) \\ d_{22} &= m_2 l_{c2}^2 + I_2 \\ h &= m_2 l_1 l_{c2} sin(q_2 - q_1) \end{aligned}$$

The parameters m_i denotes the mass of link i, l_i denotes the length of link i, l_{ci} denotes the distance from the previous joint to the centre of mass of link i, and I_i denotes the moment of inertia of link i about an axis normal to the page, passing through the centre of mass of link i. In this experiment, $m_1 = m_2 = 1\text{kg}$, $l_1 = l_2 = 1\text{m}$, $l_{c1} = l_{c2} = 0.5\text{m}$, and $I_1 = I_2 = 1\text{kgm}^2$.

The desired link position is $q_d = [\pi, \pi]^T$, and the commanded set-point is $[q = q_d, \dot{q} = 0]^T$. Two sets of initial conditions are simulated. The first simulation scenario has the initial condition $q_0 = [0, 0]^T$ and $\dot{q}_0 = [0, 0]^T$, and the second simulation scenario has the initial condition $q_0 = [0, 0]^T$ and $\dot{q}_0 = [-0.2, -0.1]^T$. In all cases, we desire that the angular velocity of each link to be constrained, with link 1 to remain below 0.3rad/s and link 2 below 0.2rad/s.

To demonstrate its effectiveness, we compare the proposed bounded passivity-based control (BPBC) design with the PD-controller. The PD-controller used in the simulations has the usual form

$$\tau_{PD} = -K_P \tilde{q} - K_D \dot{q}$$

with $\tilde{q} = q - q_d$. To design the BPBC-controller, we select the following candidate cLf

$$V(\tilde{q}, \dot{q}) = \frac{\mathcal{L}(\tilde{q}, \dot{q})}{\Psi(\dot{q})^\alpha},$$

where the constant parameter $\alpha \in \mathbb{R}_+$ is employed to control the shape of the candidate cLf $V(\tilde{q}, \dot{q})$, which directly governs how close to their bounds the links' velocities are allowed to get. The smaller α is chosen to be, the closer to their bounds the links' velocities are allowed to get, resulting in a faster convergence rate. In this experiment, α is chosen to be 0.2. The function $\mathcal{L}$ is as defined by (7.18) and the constraint function $\Psi(\dot{q})$ is defined as follows

$$\Psi = \frac{1}{2}(0.3^2 - \dot{q}_1^2)(0.2^2 - \dot{q}_2^2).$$

Such choices give rise to the following control law

$$\tau_{BPBC} = \mathcal{D}\left[\Psi^{\alpha}\mathcal{D} + \mathcal{L}\alpha\Psi^{\alpha-1}P\right]^{-1}\left[-\Psi^{\alpha}\left\{K_P \tanh(\Xi\tilde{q}) + K_D \tanh(\Gamma\dot{q})\right\} + \mathcal{L}\alpha\Psi^{\alpha-1}P\mathcal{D}^{-1}\mathcal{C}\dot{q})\right].$$

To allow for an accurate comparison, the control gains are set to be $K_P = \text{diag}\{2, 10\}$ and $K_D = \text{diag}\{4, 20\}$ for both controllers. Those values are selected to ensure good convergence properties. For the BPBC-controller, the parameter matrices Ξ and Γ are chosen to be $\Xi = \Gamma = I_2$ for simplicity. The upper bound on the norm of the torque input for this experiment is

$$\begin{aligned} ||\tau|| &\leq \lambda_{max}\{K_P\} + \lambda_{max}\{K_D\} + \zeta_c||B||^2 \\ &\leq 10 + 20 + (0.5)(0.13) \\ &\leq 30.065\text{Nm}, \end{aligned} \tag{7.42}$$

where $B = [0.3\ 0.2]^T$. The simulation results are generated by the Planar Manipulators Toolbox [160].

Figures 7.1 - 7.3 summarise the results from the first simulation scenario. Figure 7.1 shows that both controllers asymptotically stabilise the manipulator to the commanded set-point. From Figure 7.2, we can observe that with the PD-controller, link 1 reaches a maximum velocity of approximately 1.2rad/s, for link 2, the maximum velocity reached is 1.4rad/s. With the BPBC-controller, our objective of constraining the velocity of link 1 to 0.3rad/s and link 2 to 0.2rad/s is achieved. From Figure 7.3, it is clear that the torque demanded by the BPBC-controller is less than the calculated bound given by (7.42), whereas the torque demanded by the PD-controller reaches a maximum of approximately 31.5Nm.

Figures 7.4 - 7.6 depict the results of the second simulation scenario. Once again, asymptotic stability of the closed-loop system is achieved by both controllers as shown by Figure 7.4. For the BPBC-controller, the joint velocities remain within the imposed bounds. It is interesting to note that the maximum torque demanded by the PD-controller

in this simulation scenario has increased to 33.4Nm whilst the torques demanded by the BPBC-controller is still within the calculated bound of 30.065Nm.

Remark 7.11. *From the simulation results, it is quite clear that the maximum torque demanded by the BPBC-controller is much smaller than the predicted bound of 30.065Nm given by (7.42). This raises the possibility that the arguments used in deriving the absolute bound on the norm of the demanded torque input may be too conservative. It would be interesting, and recommended for future research, to investigate whether a less conservative estimate of the bound on the magnitude of the demanded torque input can be obtained.*

7.4 General Euler-Lagrange systems

Although we have considered only the dynamics of robot manipulators in this chapter, the proposed control design is applicable to any n-degrees of freedom fully-actuated Euler-Lagrange system with no external forces, whose dynamics is given by

$$\mathcal{D}(q)\ddot{q} + \mathcal{C}(q,\dot{q}) + g(q) + \frac{\partial \mathcal{F}}{\partial \dot{q}}(\dot{q}) = \tau,$$

where q, $\dot{q}$, τ, $\mathcal{D}$, $\mathcal{C}$, $g(q)$, and $\frac{\partial \mathcal{F}}{\partial \dot{q}}(\dot{q})$ are as defined in Chapter 6, and satisfies Properties 6.1-6.3, Assumptions 7.4, 7.5 and

$$\left\| \frac{\partial \mathcal{F}}{\partial \dot{q}}(\dot{q}) \right\| \leq \zeta_f,$$

where $\zeta_f \in \mathbb{R}_+$ is a constant.

7.5 Chapter summary

In this chapter, we have proposed a controller design to solve the set-point regulation problem for revolute-joint robot manipulators subject to bounded torque and joint velocity constraints. By combining the ideas of passivity-based control and artificial potential field methods, asymptotic stabilisation of the closed-loop system is guaranteed and all joint velocity constraints are strictly satisfied for all time. Furthermore, the demanded torque input is bounded in norm, irrespective of the initial condition. The resulting controllers are modified PD-controllers, which are intuitive, robust, and can easily be implemented in practice. Although we have only considered the dynamics of robot manipulators, the proposed control design is applicable to any Euler-Lagrange system that satisfies the stated properties and assumptions. The validity and effectiveness of the proposed control design are illustrated through simulations on a 2-link planar manipulator.

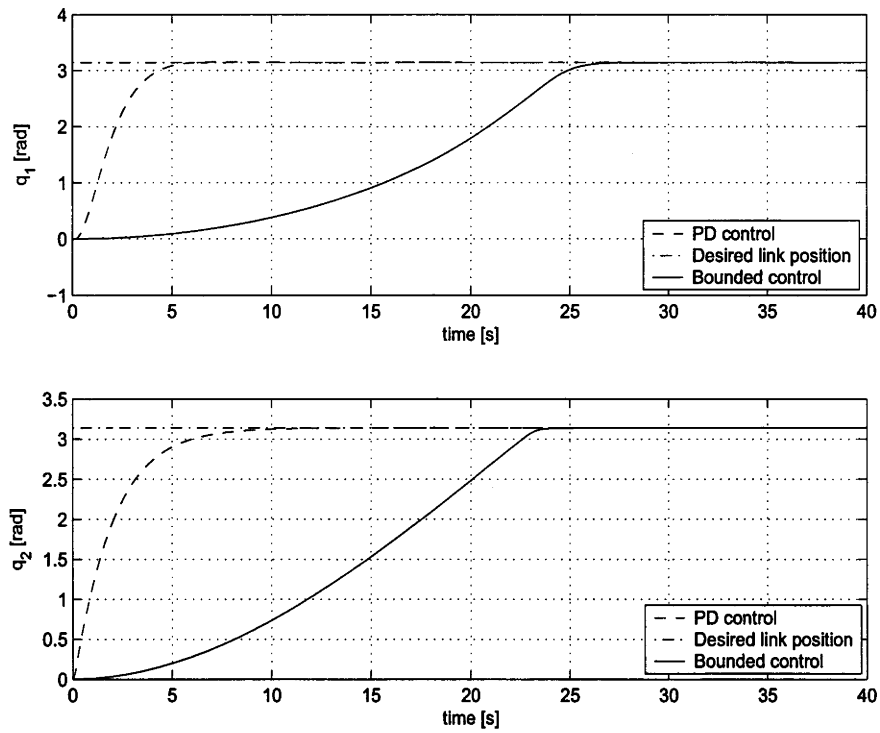

Figure 7.1: Joint positions - initial condition $q_0 = [0,0]^T$, $\dot{q}_0 = [0,0]^T$

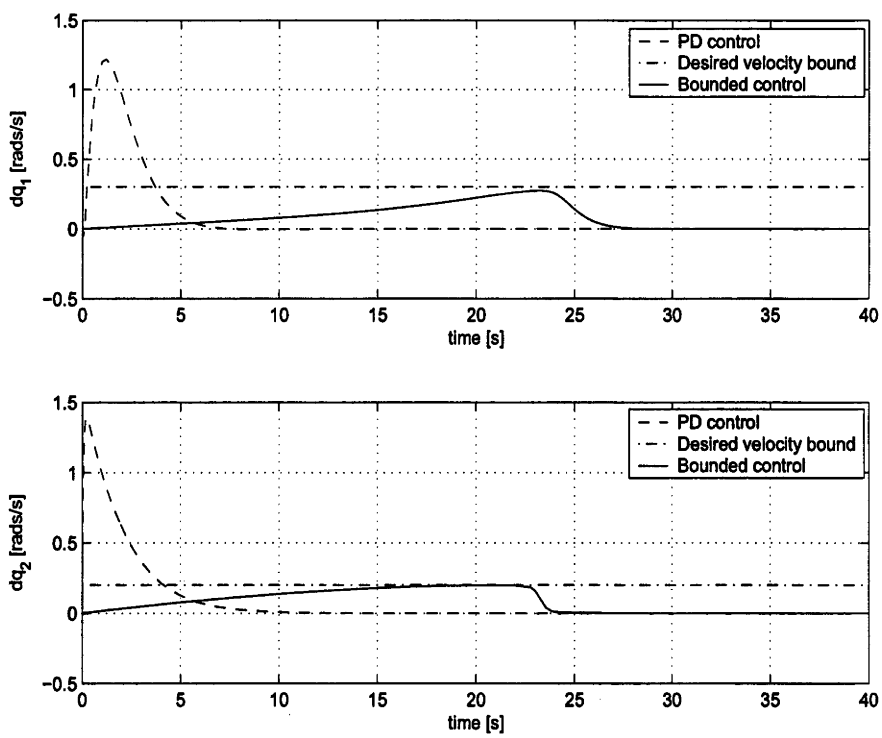

Figure 7.2: Joint velocities - initial condition $q_0 = [0,0]^T$, $\dot{q}_0 = [0,0]^T$

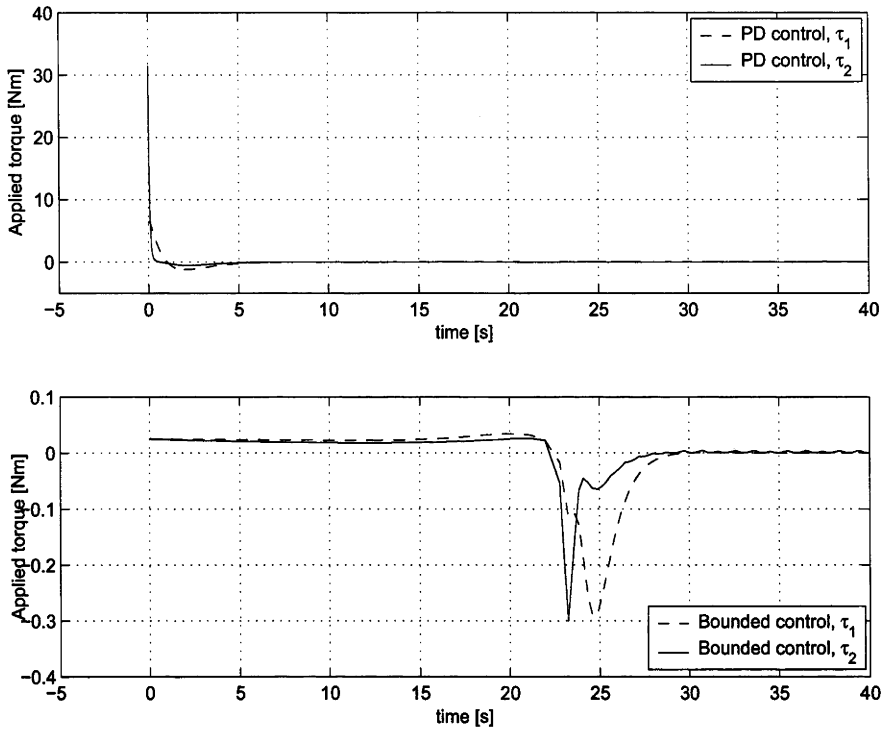

Figure 7.3: Applied torques - initial condition $q_0 = [0, 0]^T$, $\dot{q}_0 = [0, 0]^T$

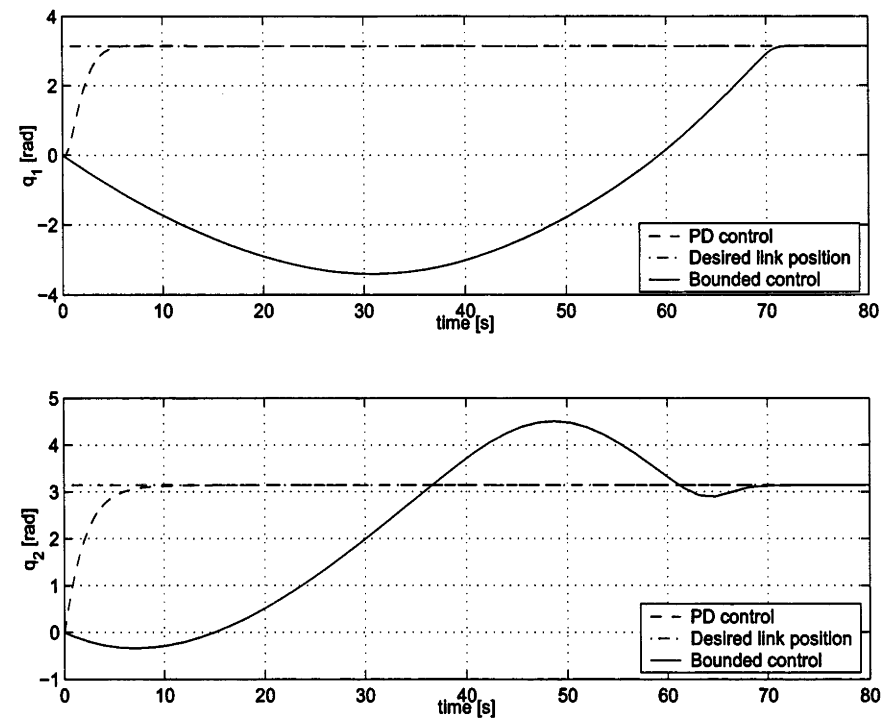

Figure 7.4: Joint positions - initial condition $q_0 = [0, 0]^T$, $\dot{q}_0 = [-0.2, -0.1]^T$

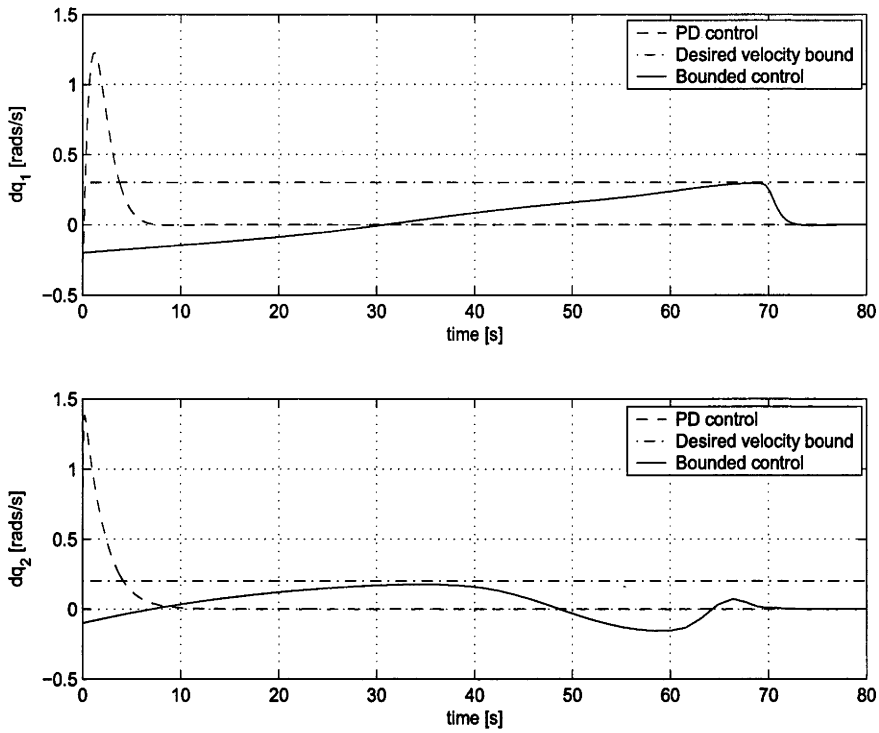

Figure 7.5: Joint velocities - initial condition $q_0 = [0, 0]^T$, $\dot{q}_0 = [-0.2, -0.1]^T$

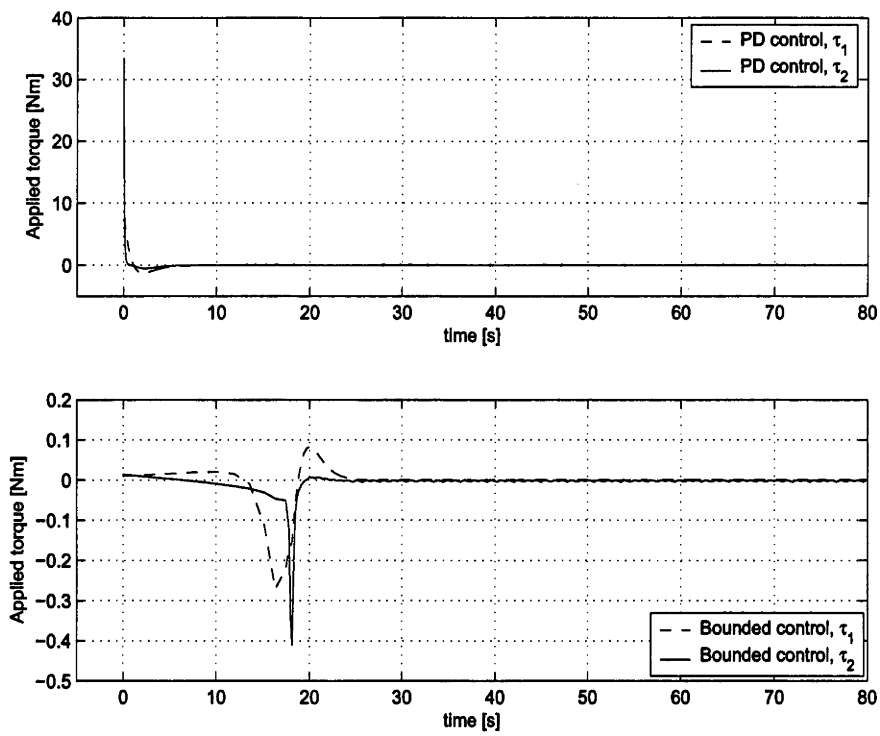

Figure 7.6: Applied torques - initial condition $q_0 = [0, 0]^T$, $\dot{q}_0 = [-0.2, -0.1]^T$

Chapter 8

Conclusions and future research

In this thesis, we have developed constructive nonlinear control design procedures to address the stabilisation problem for constrained nonlinear systems, and applied these procedures to solve practical engineering problems in the fields of aerospace and robotics. The focus was principally on state constraints, which can arise from performance limitations, such as aerodynamic stall in aircraft, or spatial limitations, such as a robot manipulator operating in a cluttered environment. The constraints are incorporated into the design procedures in a natural manner by modifying the energy function of the system to include barrier function characteristics at the constraint boundaries.

In Chapter 3, the main problem considered is the stabilisation of certain classes of non-affine, nonlinear systems subject to a single or two consecutively constrained states. Two design procedures, which are based on the backstepping methodology, were proposed. The first approach, or the "non-strict" approach, assumes that no strict cLfs are available, and involves imposing bounds on the stabilising functions and the error variables pertinent to the constrained states and propagating those boundedness properties through each step of the backstepping methodology. These modifications are seamlessly integrated into the backstepping framework. One disadvantage associated with the approach is that it produces comparatively more complicated control laws for high-order systems due to the presence of barrier function-like terms in the structure of the proposed cLfs. Each time these terms are differentiated, the number of terms in the final control law significantly increases. The second approach, or the "ISS" approach, generally leads to simpler control laws but requires the construction of ISS-cLfs, a typically much harder task than the construction of non-strict, non-ISS-cLfs. Consequently, the applicability of the second approach is more limited than the first. Furthermore, only symmetric constraints can be accommodated using the "ISS" approach. The "non-strict" approach was then applied to design asymptotically stabilising controllers for two practical systems, the active car suspension system subject to suspension travel limits, and the Reaction Wheel Pendulum subject to angular velocity and torque input limits. Closed-loop simulations demonstrated that the proposed control design procedures are valid, and yield effective controllers.

In Chapter 4, we extended the design procedures developed in Chapter 3 to address the problem of multiple state constraints. The adaptation of the "ISS" approach to ac-

commodate multiple state constraints is simple as the only additional ingredient required is the assumption that all nonlinearities in the system's dynamic model and their time derivatives are bounded in norm. Once again, the applicability of the approach to practical systems is limited due to the requirement to construct ISS-cLfs.

For the "non-strict" design procedure, the extension is more complicated. The traditional backstepping approach of cancelling the cross-terms does not work because the cross-terms escape to infinity close to the constraint boundaries. Consequently, we adopted an approach that employed domination rather than cancellation of the cross-terms. The outcome of the proposed design procedure is a set of constraints on the controller parameters. Satisfying these constraints ensures that the closed-loop system is asymptotically stable, and the states are bounded in norm. From these constraints, nonlinear bounds for the stabilising functions and error variables, and ultimately, for the system states, in terms of the controller parameters were computed. Together, the constraints on the controller parameters, the computed bounds on the system states, and the prescribed state bounds provide the ingredients for a multi-criteria constrained optimisation routine to tuning the controller parameters. The result is a set of controller parameters which guarantees that the closed-loop system is asymptotically stable, and yields the maximum possible constraint admissible region given the prescribed state bounds and the constraints imposed by the proposed design procedure. There remains a distinct possibility, due to the worst-case arguments employed in deriving some of the constraints on the controller parameters, that in certain cases, the optimisation routine is ill-conditioned. Two alternative methods were then proposed to tuning the controller parameters, a gain-scheduling approach and a manual approach. The validity of the manual tuning approach was demonstrated via closed-loop simulations of a 4^{th}-order integrator cascade. Due to time limitations, the feasibility and performance of the proposed gain-scheduling approach could not be examined.

In Chapter 5, we proposed backstepping-based controllers to regulate the altitude of the Aerosonde UAV. It was found that application of traditional backstepping results in a very aggressive controller which demands elevator deflections that are proportional to the magnitude of the altitude change command. When the magnitude of the altitude change command is sufficiently large, the resultant elevator deflection demands from the controller will lead to stall. To remedy this problem, we imposed a hard bound on the climb rate of the aircraft. The controller was re-designed using the results developed in Chapter 3. Closed-loop simulations on a fully nonlinear, 6-DOF dynamic model of the Aerosonde UAV demonstrated that the constrained backstepping controller design provides excellent tracking command, and achieves our objective of limiting the climb rate, and ultimately the elevator deflections, thus preventing stall from occurring, irrespective of the magnitude of the altitude change commands. In addition, the controller can be tuned to provide an almost time-optimal command tracking response, given the imposed constraint on the

climb rate.

Chapters 6 and 7 were devoted to developing control laws to stabilise constrained robot manipulators. The proposed controller designs are based on the PBC framework, with modifications made to both the kinetic and potential energy terms in the cLf in classical PBC. The modifications can be thought of as a form of energy shaping, and the structure of the proposed cLfs closely resembles those used in the artificial potential field method. In Chapter 6, the general problem of autonomous, or online, obstacle avoidance of robot manipulators subject to joint position and joint rate constraints was addressed. For arbitrary constraints, closed-loop asymptotic stability can not be guaranteed due to the possible presence of local minima in the structure of the proposed cLfs. However, in special cases where the active constraints possess certain convexity properties, asymptotic stability of the closed-loop system is assured.

In Chapter 7, we extended the literature in a different direction and solved the stabilisation problem of robot manipulators subject to joint velocity and input torque limits. The resulting controllers are modified PD-controllers, which are simple and can easily be implemented in practice. The validity and effectiveness of the proposed controller designs were illustrated via closed-loop simulations on a 2-link planar manipulator.

The attractiveness of the controller designs exposed in Chapters 6 and 7 lies in their simplicity and their basis in the concept of energy-based stabilisation, leading to simple and effective control laws that satisfy all imposed state constraints for all time.

8.1 Future research

Further research can be pursued in the following three directions:

- There exists a distinct possibility, due to the worst-case arguments employed in deriving some of the constraints on the controller parameters, that in certain cases, the optimisation routine associated with the "non-strict" design procedure proposed in Chapter 4 is ill-conditioned. Although two alternative methods were proposed, which are gain-scheduling and manual tuning, the issue of whether the gain-scheduling approach provides better performance and robustness than the "global" approach and manual tuning is unresolved. A detailed analysis into the gain-scheduling approach should therefore be considered. However, it should be noted that the proposed approach is highly complex, and leads to complicated control laws. It is therefore unlikely that such an approach would be suitable for implementation on practical systems such as commercial UAVs.

- In Chapter 6, we have identified that for arbitrary constraints, asymptotic stability may not be attainable due to the possibility of local minima in the structure of the proposed cLfs. An investigation into means to overcome the local minima problem is

recommended. A plausible and direct approach is to manipulate the constraint functions, for example, by introducing artificial constraints that shape the cLf to avoid the creation of local minima. This method is however, mathematically involved, and is highly problem-dependent. A more pragmatic approach would be to try and integrate methods from the artificial potential field literature such as random walk into the control design process.

- In Chapter 7, simulation results indicate that there is a possibility that the arguments used in deriving the explicit upper bound for the demanded torque input are too conservative. It would be interesting to investigate whether a more accurate estimate of the bound on the norm of the demanded torque input can be obtained.

Appendix A

A.1 Proof of Lemma 3.3, pg. 29

Proof. Since the functions 2, $\frac{s}{\sigma+s}$, and $\frac{s}{\beta-s}$ are continuous in the set $\mathcal{S} = \{s \in \mathbb{R} \mid -\sigma < s < \beta\}$, $y(s)$ is continuous in the same set $\mathcal{S}$ as a direct result. To prove that $y(s)$ is positive in $\mathcal{S}$, we use calculus to establish that $y(s)$ has one and only one minimum in $\mathcal{S}$, and that the value of $y(s)$ at this minimum is positive. Differentiating $y(s)$ with respect to s once gives

$$\frac{dy}{ds} = \frac{-\sigma}{(\sigma+s)^2} + \frac{\beta}{(\beta-s)^2}. \tag{A.1}$$

Equating $\frac{dy}{ds} = 0$ yields

$$s_1 = \frac{\beta\sqrt{\sigma} - \sigma\sqrt{\beta}}{\sqrt{\sigma}+\sqrt{\beta}}, \quad s_2 = \frac{\beta\sqrt{\sigma} + \sigma\sqrt{\beta}}{\sqrt{\sigma}-\sqrt{\beta}}. \tag{A.2}$$

Next, we test for which of s_1, s_2, or whether both lie in $\mathcal{S}$. Case s_1

$$\begin{aligned} s_1 = \frac{\beta\sqrt{\sigma} - \sigma\sqrt{\beta}}{\sqrt{\sigma}+\sqrt{\beta}} &< \beta \\ \implies 0 &< \beta + \sigma, \quad \forall \sigma, \beta \in \mathbb{R}_+, \end{aligned} \tag{A.3}$$

and

$$\begin{aligned} s_1 = \frac{\beta\sqrt{\sigma} - \sigma\sqrt{\beta}}{\sqrt{\sigma}+\sqrt{\beta}} &> -\sigma \\ \implies \beta + \sigma &> 0, \quad \forall \sigma, \beta \in \mathbb{R}_+, \end{aligned} \tag{A.4}$$

which is in $\mathcal{S}$ since

$$-\sigma < \frac{\beta\sqrt{\sigma} - \sigma\sqrt{\beta}}{\sqrt{\sigma}+\sqrt{\beta}} < \beta, \quad \forall \sigma, \beta \in \mathbb{R}_+. \tag{A.5}$$

Case s_2

$$s_2 = \frac{\beta\sqrt{\sigma} + \sigma\sqrt{\beta}}{\sqrt{\sigma} - \sqrt{\beta}} < \beta$$
$$\Longrightarrow \beta + \sigma \not< 0, \quad \forall \sigma, \beta \in \mathbb{R}_+, \tag{A.6}$$

which is not in $\mathcal{S}$. Differentiating $y(s)$ with respect to s twice yields

$$\frac{d^2y}{ds^2} = \frac{2\sigma}{(\sigma + s)^3} + \frac{2\beta}{(\beta - s)^3} > 0, \quad \forall s \in (-\sigma, \beta), \quad \forall \sigma, \beta \in \mathbb{R}_+. \tag{A.7}$$

From (A.5), (A.6), and (A.7), we can conclude that $y(s)$ has one and only one minimum in $\mathcal{S}$ at $s = \frac{\beta\sqrt{\sigma} - \sigma\sqrt{\beta}}{\sqrt{\sigma} + \sqrt{\beta}}$. Substituting $s = \frac{\beta\sqrt{\sigma} - \sigma\sqrt{\beta}}{\sqrt{\sigma} + \sqrt{\beta}}$ back into $y(s)$ and simplifying yields

$$y\left(\frac{\beta\sqrt{\sigma} - \sigma\sqrt{\beta}}{\sqrt{\sigma} + \sqrt{\beta}}\right) = 1 + \frac{2\sqrt{\sigma\beta}}{\sigma + \sigma} > 0, \quad \forall \sigma, \beta \in \mathbb{R}_+. \qquad \square$$

A.2 Proof of Lemma 3.12, pg. 51

Proof. Since $y(s)$ is a composition of functions which are all continuous in the set $\mathcal{S} = \{s \in \mathbb{R} \mid -\sigma < s < \beta\}$, $y(s)$ is continuous in $\mathcal{S}$. The boundedness of $y(s)$ in $\mathcal{S}$ is established by first proving that the numerator of $y(s)$

$$N(s) = (\sigma + s)(\beta - s) \tag{A.8}$$

is bounded. Using calculus, one can easily obtain

$$0 < N(s) \leq \frac{1}{4}(\sigma + \beta)^2, \quad \forall s \in (-\sigma, \beta), \quad \forall \sigma, \beta \in \mathbb{R}_+. \tag{A.9}$$

We also established in the proof of Lemma 3.3 that the denominator of $y(s)$

$$D(s) = 2 - \frac{s}{\sigma + s} + \frac{s}{\beta - s} \tag{A.10}$$

is lower bounded by

$$D(s) \geq 1 + \frac{2\sqrt{\sigma\beta}}{\sigma + \beta}, \quad \forall s \in (-\sigma, \beta), \quad \forall \sigma, \beta \in \mathbb{R}_+. \tag{A.11}$$

From (A.9) and (A.11), we can conclude that

$$0 < y(s) \leq \frac{\frac{1}{4}(\sigma + \beta)^3}{\sigma + \beta + 2\sqrt{\sigma\beta}}, \quad \forall s \in \mathbb{R}_+, \quad \forall \sigma, \beta \in \mathbb{R}_+. \qquad \square$$

Bibliography

[1] In Frank Allgöwer and Alex Zheng, editors, *Nonlinear Model Predictive Control.* Birkhäuser, 2000.

[2] In Basil Kouvaritakis and Mark Cannon, editors, *Non-linear Predictive Control: Theory and Practice.* The Institution of Electrical Engineers, London, 2001.

[3] K. J. Åström and L. Rundqwist. Integrator windup and how to avoid it. In *Proceedings of the 1989 American Control Conference*, 1989.

[4] R. Akmeliawati. *Nonlinear Control for Automatic Flight Control Systems.* PhD thesis, University of Melbourne, Melbourne, Australia, June 2001.

[5] C. H. An, C. G. Atkeson, J. D. Griffiths, and J. M. Hollerbach. Experimental evaluation of feedforward and computed torque control. *IEEE Transactions on Robotics and Automation*, 5(3):368–373, June 1989.

[6] M. Arcak, M. Seron, J. Braslavsky, and P. Kokotovic. Robustification of backstepping against input unmodeled dynamics. *IEEE Transactions on Automatic Control*, 45(7):1358–1363, July 2000.

[7] M. A. Arteaga and R. Kelly. Robot control without velocity measurements: new theory and experimental results. *IEEE Transactions on Robotics and Automation*, 20(2):297–308, April 2004.

[8] V. Balakrishnan and A. L. Tits. Numerical optimization-based design. In W. S. Levine, editor, *The Control Handbook*, Electrical Engineering Handbook Series, pages 749–758. CRC Press, 1996.

[9] J. Barraquand, B. Langlois, and J.C. Latombe. Numerical potential field techniques for robot path planning. *IEEE Transactions on Systems, Man, and Cybernetics*, 22(2):224–240, March/April 1992.

[10] A. Bemporad, F. Borelli, and M. Morari. Model predictive control based on linear programming - the explicit solution. *IEEE Transactions on Automatic Control*, 47(12):1974–1985, 2002.

[11] A. Bemporad, A. Casavola, and E. Mosca. Nonlinear control of constrained linear systems via predictive reference management. *IEEE Transactions of Automatic Control*, 42(3):340–349, March 1997.

[12] D. S. Bernstein. *Matrix Mathematics: Theory, Facts, and Formulas with Application to Linear Systems Theory.* Princeton University Press, New Jersey, 2005.

[13] D. S. Bernstein and A. N. Michel. A chronological bibliography on saturating actuators. *International Journal of Robust Nonlinear Control*, 5:375–380, 1995.

[14] F. Blanchini. Set invariance in control. *Automatica*, 35(11):1747–1769, 1999.

[15] F. Blanchini and M. Sznaier. Robust control of constrained systems via convex optimization. *International Journal of Nonlinear and Robust Control*, 5:441–460, August 1995.

[16] S. P. Boyd and C. H. Barratt. *Linear Controller Design: Limits of Performance.* Prentice-Hall, New Jersey, 1991.

[17] J. S. Brinker and K. A. Wise. Stability and flying qualities robustness of a dynamic inversion aircraft control law. *AIAA Journal of Guidance, Control, and Dynamics*, 19(6):1270–1277, 1996.

[18] R. A. Brooks. Planning collision-free motions for pick-and-place operations. In *Proceedings of the First International Robotics Research Symposium*, number 4, pages 5–38, 1984.

[19] C. I. Byrnes and A. Isidori. New results and examples in nonlinear feedback stabilization. *Systems and Control Letters*, 12:437–442, 1989.

[20] A. J. Calise and R. T. Rysdyk. Nonlinear adaptive flight control using neural networks. *IEEE Controls Systems Magazine*, 18(6), December 1998.

[21] E. F. Camacho and C. Bordons. *Model Predictive Control.* Advanced Textbooks in Control and Signal Processing. Springer-Verlag, London, 2004.

[22] T. F. Chan and R. V. Dubey. A weighted least-norm solution based scheme for avoiding joint limits for redundant manipulators. *IEEE Transactions on Robotics and Automation*, 11(2):286–292, April 1995.

[23] J.-L. Chen and J.-S. Liu. Avoidance of obstacles and joint limits for end-effector tracking in redundant manipulators. In *Proceedings of the Seventh International Conference on Control, Automation, Robotics, and Vision*, pages 839–843, Singapore, December 2002.

[24] S. I. Choi and B. K. Kim. Obstacle avoidance control for redundant manipulators using collidability measure. *Robotica*, 18:143–151, 2000.

[25] C. G. Cullen. *Linear Algebra and Differential Equations.* PWS-Kent Publishing Company, Boston, Massachusetts, 1991.

[26] M. A. Dahleh and J. B. Pearson. L_1-optimal compensators for continuous-time systems. *IEEE Transactions on Automatic Control*, 32(10):889–895, 1987.

[27] P. Dassanayake, K. Watanabe, and K. Izumi. Robot manipulator task control with obstacle avoidance using fuzzy behavior-based strategy. *Journal of Intelligent and Fuzzy Systems*, 10(3-4):139–158, 2001.

[28] Z. Ding. Adaptive control of triangular systems with nonlinear parameterization. *IEEE Transactions on Automatic Control*, 46(12):1963 –1968, December 2001.

[29] W. E. Dixon, M. S. de Queiroz, F. Zhang, and D. M. Dawson. Tracking control of robot manipulators with bounded torque inputs. *Robotica*, 17:121–129, 1999.

[30] I. Fantoni and R. Lozano. *Non-linear Control for Underactuated Mechanical Systems*. Springer-Verlag, London, 2002.

[31] J. A. Farrell, M. M. Polycarpou, and M. Sharma. Adaptive backstepping with magnitude, rate, and bandwidth constraints: aircraft longitude control. In *Proceedings of the 2003 American Control Conference*, pages 2557–2562, 2003.

[32] B. Faverjon. Obstacle avoidance using an octree in the configuration space of a manipulator. In *Proceedings of the IEEE International Conference on Robotics*, Atlanta, GA, March 1984.

[33] R. Findeisen, F. Imsland, L. Allgwer, and B.A. Foss. State and output feedback nonlinear model predictive control: An overview. *European Journal of Control*, 9(2-3):190–207, 2003.

[34] M. Forti and P. Nistri. Global convergence of neural networks with discontinuous neuron activations. *IEEE Transactions on Circuits and Systems*, 50(11):1421–1435, November 2003.

[35] R. Freeman and L. Praly. Integrator backstepping for bounded controls and control rates. *IEEE Transactions of Automatic Control*, 43(2):258–262, February 1998.

[36] R. A. Freeman and P. V. Kokotovic. Backstepping design of robust controllers for a class of nonlinear systems. In *Preprints of second IFAC nonlinear control systems design symposiums*, pages 307–312, Bordeaux, France, 1992.

[37] R. A. Freeman and P. V. Kokotovic. Design of softer robust nonlinear control laws. *Automatica*, 29:1425–1437, 1993.

[38] R. A. Freeman and P. V. Kokotovic. *Robust Nonlinear Control Design*. Birkhäuser, Boston, 1996.

[39] E. G. Gilbert and K. T. Tan. Linear systems with state and control constraints: The theory and application of maximal output admissible sets. *IEEE Transactions on Automatic Control*, 36(9):1008–1020, 1991.

[40] M. A. C. Gill and A. Y. Zomaya. A cell decomposition-based collision avoidance algorithm for robot manipulators. *Cybernetics and Systems*, 29(2):113–135, March 1998.

[41] T. D. Gillespie. *Fundamentals of Vehicle Dynamics.* Society of Automotive Engineers International, Warrendale, PA, 1992.

[42] A. H. Glattfelder and W. Schaufelberger. Stability analysis of single loop control systems with saturation and antireset-windup circuits. *IEEE Transactions on Automatic Control*, 28:1074–1081, 1983.

[43] A. H. Glattfelder and W. Schaufelberger. *Control Systems with Input and Output Constraints.* Advanced Textbooks in Control and Signal Processing. Springer-Verlag, London, 2003.

[44] F. Grognard. *Control of constrained systems: closed-loop, open-loop, and hybrid solutions.* PhD thesis, Université Catholique de Louvain, Belgium, 2001.

[45] F. Grognard, R. Sepulchre, G. Bastin, and L. Praly. Nested linear low-gain designs for semi-global stabilization of feedforward systems. In *Proceedings of the 4^{th} IFAC Nonlinear Control Systems Design Symposium*, pages 829–834, Enschede, the Netherlands, July 1998.

[46] O. Härkegård and S. T. Glad. A backstepping design for flight path angle control. In *Proceedings of the 39^{th} Conference on Decision and Control*, pages 3570–3575, 2000.

[47] J. M. Hollerbach. Dynamic scaling of manipulator trajectories. A. I. Memo 700, Massachusetts Institute of Technology, January 1983.

[48] T. Hu and Z. Lin. *Control Systems With Actuator Saturation : Analysis and Design.* Birkhäuser, Boston, 2001.

[49] T. Hu and Z. Lin. *Control Systems with Actuator Saturation: Analysis and Design.* Birkhäuser, Boston, USA, 2001.

[50] T. Hu and Z. Lin. On improving the peroformance with bounded continuous feedback laws. *IEEE Transactions on Automatic Control*, 47(9):1570–1575, 2002.

[51] H. H. Jr. Hurt. *Aerodynamics for Naval Aviators.* Aviation Supplies and Academics, Washington, 1992.

[52] A. Isidori. *Nonlinear Control Systems.* Springer-Verlag, London, 3^{rd} edition, 2002.

[53] M. Jankovic, R. Sepulchre, and P. V. Kokotovic. Constructive lyapunov stabilization of nonlinear cascade systems. *IEEE Transactions on Automatic Control*, 41(1723-1736), 1996.

[54] Z.-P. Jiang. Private communication between the author and Professor Zhong-Ping Jiang. 2004.

[55] Z. P. Jiang and I. Mareels. A small gain control method for nonlinear cascaded systems with dynamic uncertainties. *IEEE Transactions on Automatic Control*, 42(3):292–308, 1997.

[56] Z. P. Jiang and L. Praly. Design of robust adaptive controllers for nonlinear systems with dynamic uncertainties. *Automatica*, 34(7):825–840, July 1998.

[57] Z. P. Jiang, A. Teel, and L. Praly. Small-gain theorem for iss systems and applications. *Mathematics of Control, Signals and Systems*, 7(2):95–120, 1994.

[58] L. Jin, P.N. Nikiforuk, and M.M. Gupta. Global equilibrium stability of discrete-time analog neural networks. In *Proceedings of 1995 IEEE International Conference on Fuzzy Systems*, pages 1949–1953, 1995.

[59] I. Kanellakopoulos, P. V. Kokotovic, and A. S. Morse. Systematic design of adaptive controllers for feedback linearizable systems. *IEEE Transactions on Automatic Control*, 36:1241–1253, 1991.

[60] N. Kapoor, A. R. Teel, and P. Daoutidis. An anti-windup design for linear systems with input saturation. *Automatica*, 34:559–574, 1998.

[61] N. Karlsson. *Constructive Methods for Nonlinear Control of Finite and Infinite Dimensional Systems.* PhD thesis, University of California (Santa Barbara), March 2002.

[62] N. Karlsson, A. Teel, and D. Hrovat. A backstepping approach to control of active suspensions. In *Proceedings of the 40^{th} IEEE Conference on Decision and Control*, pages 4170–4175, Orlando, USA, 2001.

[63] N. Kawarazaki and K. Taguchi. Collision-free path planning for a manipulator using free form surface. In *Proceedings of the IEEE International Conference on Intelligent Robots and Systems*, pages 130–137, 1995.

[64] C. Y. Kaya and J. L. Noakes. Computations and time-optimal controls. *Optimal Control Applications and Methods*, 17:171–185, 1996.

[65] R. Kelly and V. Santibáñez. A class of global regulators with bounded control actions for robot manipulators. In *Proceedings of the 35th IEEE Conference on Decision and Control*, pages 3382–3386, Kobe, Japan, December 1996.

[66] R. Kelly, V. Santibáñez, and H. Berghuis. Point-to-point robot control under actuator constraints. *Control Engineering Practice*, 5(11):1555–1562, 1997.

[67] R. Kelly, V. Santibáñez, and A. Loría. *Control of Robot Manipulators in Joint Space.* Advanced Textbooks in Control and Signal Processing. Springer-Verlag, London, 2005.

[68] H. K. Khalil. *Nonlinear Systems.* Prentice Hall, 3rd edition, 2002.

[69] O. Khatib. Real-time obstacle avoidance for manipulators, and mobile robots. *International Journal of Robotic Research*, pages 90–98, 1986.

[70] P. Khosla and T. Kanade. Real-time implementation and evaluation of the computed-torque scheme. *IEEE Transactions on Robotics and Automation*, 5(2):245–253, April 1989.

[71] P. V. Kokotovic and H. J. Sussmann. A positive real condition for global stabilization of nonlinear systems. *Systems & Control Letters*, 19:177–185, 1989.

[72] M. V. Kothare, M. Morari, P. J. Campo, and C. N. Nett. A unified framework for the study of anti-windup designs. *Automatica*, 30:1869–1883, 1994.

[73] K. Kreutz. On manipulator control by exact linearization. *IEEE Transactions on Automatic Control*, 34:763–767, 1989.

[74] M. Krstic, I. Kanellakopoulos, and P. Kokotovic. *Nonlinear and Adaptive Control Design.* Wiley, New York, 1995.

[75] G. J. Lastman. A shooting method for solving two-point boundary-value problems arising from non-singular bang-bang optimal control processes. *International Journal of Control*, 27:513–524, 1978.

[76] J. C. Latombe. *Robot Motion Planning.* Kluwer Academic Publishers, Norwell, MA, 1990.

[77] D. Lawrence and W. Rugh. Gain scheduling dynamic linear controllers for a nonlinear plant. *Automatica*, 31:381–390, 1995.

[78] T. Lee and Y. Kim. Nonlinear adaptive flight control using backstepping and neural networks controller. *AIAA Journal of Guidance, Control, and Dynamics*, 24(4):693–699, 2001.

[79] F. Lewis, C. Abdallah, and D. Dawson. *Control of Robot Manipulators.* MacMillan, New York, 1993.

[80] C-L. Lin. Adaptive fuzzy gain scheduling in guidance system design. *Journal of Guidance, Control, and Dynamics*, 24(4):683–692, July-August 2001.

[81] J-S. Lin and I. Kanellakopoulos. Nonlinear design of active suspensions. *IEEE Control Systems*, pages 45–58, June 1997.

[82] Z. Lin and A. Saberi. Semi-global exponential stabilization of linear discrete-time systems subject to 'input saturation' via linear feedbacks. *Systems & Control Letters*, 24:125–132, 1995.

[83] Z-L. Lin. Semi-global stabilization of linear systems with position and rate-limited actuators. *Systems and Control Letters*, 30(1):1–11, 1997.

[84] Z.-L. Lin and A. Saberi. Semiglobal exponential stabilization of linear systems subject to input saturation via linear feedbacks. *Systems and Control Letters*, 21(3):225–239, 1993.

[85] T. Lozano-Perez. A simple motion-planning algorithm for general robot manipulators. *IEEE Journal of Robotics and Automation*, 3(3):224–238, June 1987.

[86] J. M. Maciejowski. *Predictive control with constraints.* Prentice-Hall, New Jersey, 2002.

[87] J. Mareczek, M. Buss, and M. W. Spong. Invariance control for a class of cascade nonlinear systems. *IEEE Transactions on Automatic Control*, 47(4):636–640, April 2002.

[88] R. Marino and P. Tomei. Robust stabilization of feedback linearizable time-varying uncertain systems. *Automatica*, 29:181–189, 1993.

[89] R. Marino and P. Tomei. *Nonlinear Control Design: Geometric, Adaptive, & Robust.* Prentice-Hall, London, 1995. Out of print.

[90] H. J. Marquez. *Nonlinear Control Systems.* Wiley, New Jersey, USA, 2003.

[91] D. Q. Mayne, J. B. Rawlings, C. V. Rao, and P. O. M. Scokaert. Constrained model predictive control: Stability and optimality. *Automatica*, 36(6):789–814, 2000.

[92] F. Mazenc and A. Iggidr. Backstepping with bounded feedbacks. *Systems and Control Letters*, 51:235–245, 2004.

[93] F. Mazenc and L. Praly. Adding integrations, saturated controls and stabilization for feedforward systems. *IEEE Transactions on Automatic Control*, 41:1559–1578, 1996.

[94] J. B. Mdebe, X. Huang, and M. Wang. Robust neuro-fuzzy sensor-based motion control among dynamic obstacles for robot manipulators. *IEEE Transactions on Fuzzy Systems*, 11(2):249–261, April 2003.

[95] A. Megretski. l^2 bido output feedback stabilization with saturated control. In *Proceedings of IFAC World Congress*, 1996.

[96] P. Menon, M. Badgett, and R. Walker. Nonlinear flight test trajectory controllers for aircraft. *Journal of Guidance, Control, and Dynamics*, 10(1):67–72, 1987.

[97] P. Menon, M. Yousefpor, T. Lam, and M. Steinberg. Nonlinear flight control system synthesis using genetic programming. In *Proceedings of AIAA Guidance, Navigation, and Control Conference*, pages 461–470, 1995.

[98] P. Miotto. *Fixed Structure Methods for Flight Control Analysis and Automated Gain Scheduling.* PhD thesis, MIT, 1997.

[99] R. R. Mohler. *Bilinear Control Processes.* Prentice Hall, New Jersey, 1973.

[100] R. R. Mohler. *Nonlinear Systems Volume II, Applications to Bilinear Control.* Prentice Hall, New Jersey, 1991.

[101] F. Morabito, A. R. Teel, and L. Zaccarian. Nonlinear antiwindup applied to euler-lagrange systems. *IEEE Transactions on Robotics and Automation*, 20(3):526–537, 2004.

[102] A. G. O. Mutambara. A framework for a supervisory expert system for robotic manipulators with joint-position limits and joint-rate limits. Technical Memorandum 208845, NASA, December 1998.

[103] K. B. Ngo, R. Mahony, and Z. P. Jiang. Integrator backstepping design for motion systems with velocity constraint. In *Proceedings of the 5^{th} Asian Control Conference 2004*, pages 141–146, Melbourne, Australia, July 2004.

[104] K. B. Ngo, R. Mahony, and Z.-P. Jiang. Integrator backstepping using barrier functions for systems with multiple state constraints. In *Proceedings of the 44^{th} IEEE Conference on Decision and Control and European Control Conference 2005*, Seville, Spain, December 2005.

[105] M. Niculescu. The aerosim blockset version 1.2. www.u-dynamics.com.

[106] H. Nijmeijer and A. J. van der Schaft. *Nonlinear Dynamical Control Systems.* Springer-Verlag, New York, 1990.

[107] R. Olfati-Saber. *Nonlinear Control of Underactuated Mechanical Systems with Application to Robotics and Aerospace Vehicles.* PhD thesis, Massachusetts Institute of Technology, 2001.

[108] M. Oosterom, G. Schram, R. Babuska, and H. B. Verbruggen. Automated procedure for gain scheduled flight control law design. *AIAA*, 2000.

[109] R. Ortega, A. Loria, P. J. Nicklasson, and H. Sira-Ramirez. *Passivity-based Control of Euler-Lagrange Systems: Mechanical, Electrical and Electromechanical Applications.* Springer-Verlag, London, 1998.

[110] A. Ostroff and M. Proffitt. Longitudinal-control design approach for high-angle-of-attack aircraft. Technical report, NASA, February 1993.

[111] J. D. Paduano. *Automated Gain Scheduling of Flight Control Laws.* PhD thesis, MIT, 1992.

[112] M. Perhenschi. A modified genetic algorithm for the design of an autonomous helicopter control system. In *Proceedings of AIAA Guidance, Navigation, and Control Conference*, pages 1183–1192, 1997.

[113] J. Reilly. *Development and Analysis of a Nonlinear Dynamic Inverse Control Strategy.* PhD thesis, The University of Maryland, 1996.

[114] E. Rimon and D. Koditschek. Exact robot navigation using artificial potential functions. *IEEE Transactions on Robotic Automation*, 8(5):501–518, October 1992.

[115] L. Rundqwist. *Anti-reset windup for PID controllers.* PhD thesis, Lund Institude of Technology, Lund, Sweden, 1991.

[116] A. Saberi, J. Han, and A. Stoorvogel. Constrained stabilization problems for linear plants. *Automatica*, 38(4):639–654, April 2002.

[117] A. Saberi, Z. Lin, and A. R. Teel. Control of linear systems with saturating actuators. *IEEE Transactions on Automatic Control*, 41(3):368–378, June 12 1996. Actuator saturations; Linear system.

[118] A. Saberi, A. A. Stoorvogel, G. Shi, and P. Sannuti. Semi-global stabilization of linear systems subject to non-right invertible constraints. *International Journal of Robust and Nonlinear Control*, 14(5):1087–1103, September 2004.

[119] V. Santibáñez, R. Kelly, and F. Reyes. A new set-point controller with bounded torques for robot manipulators. *IEEE Transactions on Industrial Electronics*, 45(1):126–133, February 1998.

[120] S. Sastry, J. Hauser, and P. Kokotovic. Zero dynamics of regularly perturbed systems may be singularly perturbed. *Systems & Control Letters*, 13:299–314, 1989.

[121] S. S. Sastry. *Nonlinear Systems: Analysis, Stability and Control.* Springer Verlag, New York, 1999.

[122] L. Sciavicco and B. Siciliano. *Modelling and Control of Robot Manipulators.* Springer-Verlag, London, second edition, 2003.

[123] R. Sepulchre, M. Jankovic, and P. V. Kokotovic. *Constructive Nonlinear Control.* Springer-Verlag, London, 1997.

[124] J. S. Sharma and K. Tu. Output feedback control for systems with constraints and saturations: scalar control case. *Systems & Control Letters*, 35:1–11, 1998.

[125] M. Sharma and D. G. Ward. Flight-path angle control via neuro-adaptive backstepping. In *Proceedings of the American Control Conference*, Anchorage, AK, May 2002.

[126] S. Singh and M. Steinberg. Adaptive control of feedback linearizable nonlinear systems with application to flight control. *AIAA Journal of Guidance, Control, and Dynamics*, 19(4):871–877, July 1996.

[127] J.-J. Slotine and W. Li. *Applied Nonlinear Control.* Prentice Hall, New Jersey, 1991.

[128] S. A. Snell, D. F. Enns, and W. L. Jr. Garrard. Nonlinear inversion flight control for a supermaneuverable aircraft. *Journal of Guidance, Control, and Dynamics*, 15(4):976–984, 1992.

[129] E. D. Sontag. Smooth stabilization implies coprime factorization. *IEEE Transactions on Automatic Control*, 34:435–443, 1989.

[130] M. Spong, P. Corke, and R. Lozano. Nonlinear control of the reaction wheel pendulum. *Automatica*, 37:1845–1851, 2001.

[131] M. W. Spong and M. Vidyasagar. *Robot Dynamics and Control.* Wiley, Canada, 1989.

[132] J. E. Steck and K. Rokhasz. Use of neural networks in control of high alpha maneuvers. In *Proceedings of the AIAA Aerospace Design Conference*, Irvine, CA, 1992.

[133] M. L. Steinberg. Comparison of intelligent, adaptive, and nonlinear flight control laws. *Journal of Guidance, Control, and Dynamics*, 24(4):693–699, July-August 2001.

[134] B. Stevens and F. Lewis. *Aircraft Control and Simulation (Second Edition).* Wiley, New Jersey, 2003.

[135] T. Sugie, K. Fujimoto, and K. Yutaka. Obstacle avoidance of manipulators with rate constraints. *IEEE Transactions on Robotics and Automation*, 19(1):168–174, February 2003.

[136] H. J. Sussman and Y. Yang. On the stabilizability of multiple integrators by means of bounded feedback controls. In *Proceedings of the 30^{th} IEEE Conference on Decision and Control*, pages 70–72, 1991.

[137] H. J. Sussmann, E. D. Sontag, and Y. Yang. A general result on the stabilization of linear systems using bounded controls. *IEEE Transactions on Automatic Control*, 39:2411–2425, December 1994.

[138] M. Takegaki and S. Arimoto. A new feedback method for dynamic control of manipulators. *ASME Journal of Dynamic Systems, Measurement, and Control*, 103:119–125, 1981.

[139] A. Teel. Semiglobal stabilizability of linear null controllable systems with input nonlinearities. *IEEE Transactions on Automatic Control*, 40(1):96–100, 1995.

[140] A. R. Teel. *Feedback Stabilization: Nonlinear Solutions to Inherently Nonlinear Problems.* PhD thesis, University of California, Berkeley, 1992a.

[141] A. R. Teel. Global stabilization and restricted tracking for multiple integrators with bounded controls. *Systems and Control Letters*, 18:165–171, 1992b.

[142] A. R. Teel. Using saturation to stabilize a class of single-input partially linear composite systems. In *Preprints of the second IFAC nonlinear control systems design symposium*, pages 224–229, Bordeaux, France, 1992c.

[143] A. R. Teel. A nonlinear small gain theorem for the analysis of control systems with saturation. *IEEE Transactions on Automatic Control*, 41(9):1256–1270, September 1996.

[144] A. R. Teel and N. Kapoor. Uniting local and global controllers. In *Proceedings of European Control Conference*, 1997.

[145] K. L. Teo, C. J. Goh, and K. H. Wong. *A Unified Computational Approach to Optimal Control Problems.* Longman Scientific and Technical, Essex, 1991.

[146] R. Toogood, H. Hao, and C. Wong. Robot path planning using genetic algorithms. In *Proceedings of the IEEE International Conference on Systems, Man, and Cybernetics*, pages 489–494, 1995.

[147] J. Tsinias. Sufficient lyapunov-like conditions for stabilization. *Mathematics of Control, Signals, and Systems*, pages 343–357, 1989b.

[148] J. Tsinias. Existence of control lyapunov functions and applications to state feedback stailizability of nonlinear systems. *SIAM Journal of Control and Optimization*, 29:457–473, 1991.

[149] J. Wen and A. A. Desrochers. An algorithm for obtaining bang-bang control laws. *Journal of Dynamic Systems, Measurement, and Control*, (109):171–175, 1987.

[150] J. T. Wen and D. S. Bayard. New class of control laws for robotic manipulators. part 1: Non-adaptive case. *International Journal of Control*, 47(5):1361–1385, 1988.

[151] T. S. Wikman and W. S. Newman. A fast, on-line collision avoidance method for a kinematically redundant manipulator based on reflex control. In *Proceedings of the IEEE International Conference on Robotics and Automation*, pages 261–266, 1992.

[152] A. Wills. *Barrier Function Based Model Predictive Control.* PhD thesis, The University of Newcastle, 2003.

[153] A. G. Wills and W. P. Heath. Barrier function-based model predictive control. *Automatica*, 40(8):1415–1422, August 2004.

[154] J. Wolff and M. Buss. Invariance control design for nonlinear control affine systems under hard state constraints. In *Proceedings of the Symposium on Nonlinear Control Systems*, Stuttgart, Germany, 2004.

[155] J. Wolff and M. Buss. Invariance control design for constrained nonlinear systems. In *Proceedings of the 16^{th} IFAC World Congress*, 2005.

[156] W. M. Wonham and C. D. Johnson. Optimal bang-bang control with quadratic performance index. *Transactions of the ASME Series D*, 86:107–115, 1964.

[157] G. F. Wredenhagen and P. R. Belanger. Piecewise-linear lq control for systems with input constraints. *Automatica*, 30(3):403–416, 1994.

[158] S.X. Yang and M. Meng. Neural network approaches to dynamic collision-free trajectory generation. *IEEE Transactions on Systems, Man, and Cybernetics*, 31(3):302–318, June 2001.

[159] Y. Zhang, C. Wen, and Y. C. Soh. Adaptive backstepping control design for systems with unknown high-frequency gain. *IEEE Transactions on Automatic Control*, 45(12):2350 –2354, December 2000.

[160] L. Zlajpah. *Planar Manipulators Toolbox.* Jozef Stefan Institute, http://www2.ijs.si/ leon/planman.html, 2000.